NANYANG TECHNOLOGICAL UNIVERSITY

DROUGHT RISK ANALYSIS AND RAINFALL INDEX INSURANCE MODEL DEVELOPMENT

CHEN WEN

SCHOOL OF CIVIL AND ENVIRONMENTAL ENGINEERING

2015

DROUGHT RISK ANALYSIS AND RAINFALL INDEX INSURANCE MODEL DEVELOPMENT

CHEN WEN

School of Civil and Environmental Engineering

A thesis submitted to the Nanyang Technological University

in partial fulfilment of the requirement for the degree of

Doctor of Philosophy

2015

ACKNOWLEDGEMENTS

I would like to express my deep gratitude to my supervisor, Prof Tiong Lee Kong, for his patient guidance of my research work, kind mentoring, and constant encouragement over the past five years.

My sincere thanks to Dr Roman Hohl from Asia Risk Centre, whose exclusive knowledge of index-based insurance has helped me overcome many obstacles in the progress of the research.

Many thanks to my colleagues from School of Civil and Environmental Engineering (CEE), including Roshan, Shao Zhe and Du Bo, for reading my report and offering valuable advice, and Mansi, staff member from Asia Risk Centre (ARC), for suggestions and corrections regarding my practical knowledge of statistics and insurance.

And, finally, I can never express enough thanks to my dear parents and Rex, for your understanding and endless love.

TABLE OF CONTETNS

SUMMARY

Drought has been identified as the main threat to agriculture production and people's lives, due to its long-term social and economic impact. The frequency analysis of drought risk plays an important role in helping insurers to (a) identify the spatial distribution of risk in the insured area, (b) make decisions about risk pooling, and (c) calculate the potential extreme losses. This research project is the first in the field of Standardized Precipitation Index (SPI)–based drought-risk studies to use diffusion kernel density estimation (DKDE) to estimate the bivariate probability density functions (PDFs) and the joint return period (RP). Historical daily rainfall data collected from 19 weather stations in China's Shandong province was used to assess the DKDE for the drought-risk frequency analysis in this thesis. The results show that the DKDE method is capable of producing an index that can consider multiple factors with higher accuracy, and of eliminating the unwanted probability shifts that occur in the existing estimation method, at a lower computation cost. The utilization of the DKDE function for drought-risk analysis also provides a reference for identifying regional agricultural drought, and offers important technological support for drought-risk management.

Agriculture insurance plays an important role in compensating farmers for revenue loss due to adverse weather events. Rainfall index insurance, based on the assumption that crop productivity and income from farmers are highly correlated with precipitation in the crop-growth phases, has attracted the attention of researchers and institutions for its relatively lower transaction cost, faster loss adjustment, and faster payout. A rainfall index insurance model was developed for this research based on

the statistical analysis of the relationship between rainfall per corn phenological growth phase and yield reduction. This model distinguishes itself from the existing approaches by independently considering the characteristics of each growth phase in different insured areas for correlation development. The Probable Maximum Loss (PML) caused by drought was estimated through calculating the drought severity extreme return level at *r*-return period using DKDE. The cumulative rainfall (CR) index insurance model was established for five counties of Shandong province with historical daily rainfall data (1981–2011) and corn-yield data (1985–2011). The results of premium and premium rate pricing suggest that rainfall index insurance is a viable product to complement the existing indemnity-based, government-supported corn insurance program in Shandong province. Furthermore, rainfall indices could be a developed into a possible product to insure farmers against drought in regions where no insurance coverage is currently available, due to high historical drought-caused yield losses.

Key Words: Basis Risk, Cumulative Rainfall Index, Diffusion Kernel Density Estimation, Drought Duration, Drought Intensity, Gaussian Kernel Density Estimation, Premium, Premium Rate, Probable Maximum Loss, Rainfall Index Insurance, Risk Premium, Standardized Precipitation Index, Thiessen Polygon

LIST OF TABLES

LIST OF FIGURES

LIST OF SYMBOLS

CDF: Cumulative Density Function

CIRC: Chinese Insurance Regulatory Commission

CMI: Crop Moisture Index

DM: Drought Monitor

DKDE: Diffusion Kernel Density Estimation

GKDE: Gaussian Kernel Density Estimation

EP: Effective Precipitation

MPCI: Multi Perils Crop Insurance

PDF: Probability Density Function

PICC: People's Insurance Company of China

PML: Probable Maximum Loss

PSDI: Palmer Drought Severity Index

SMDI: Soil Moisture Deficit Index

SPI: Standardized Precipitation Index

VCI: Vegetation Condition Index

WTP: Weighted Thiessen Polygon

CHAPTER 1

INTRODUCTION

The resilience of rural households is challenged by the uncertainties of climate risks such as drought and flood (Barnett and Mahul, 2007; Hellmuth *et al.*, 2009; Nieto *et al.*, 2010; Trærup, 2012). The IPCC fifth report (Field *et al.*, 2014) has shown that drought-prone regions will be exposed to higher drought risks as the regional-to-global soil moisture ratio worsens towards the end of this century. The report also emphasizes that more unforeseen rainfall patterns will occur, reducing the well-being of farming households and exacerbating food security problems all around the world.

Drought is recognized as the major threat to agriculture production and farmers' livelihoods due to its long-term social and economic impact. In the past ten years, out of all natural perils, drought-related disasters alone have caused widespread damage across over 50% of the total area affected by natural disasters in China. In 2010, more than two million people were plunged back into poverty as a result of the impact of the drought in southwest China (Sivakumar, 2010). In 2011, the cumulative drought-affected area in China encompassed 30 million hectares, and the direct agricultural economic loss was about 16 billion USD.

Rural households can choose to invest in drought-resistant crops, fertilizers, irrigation systems, and crop-variety diversification to mitigate the impact of weather risks. However, these mitigation measures are not always feasible or cost effective (Barnett and Mahul, 2007), and so risk-averse rural households are not always willing to invest. In order to overcome poverty, households can also alleviate financial stress through

income diversification and the financial market. Although the physical impact of natural disasters cannot be reduced through financial instruments such as insurance. Nevertheless income pressure of the farmers' can be substantially alleviated through risk transfer in the insurance market.

1.1 Background of Weather Index Insurance

Agriculture insurance plays a key role in compensating farmers for revenue loss due to adverse weather events. Conventional indemnity-based agriculture insurance, such as Multiple Peril Crop Insurance (MPCI), is widely available in developed markets for large farms with well-established loss adjustment systems (Skees *et al.*, 2009). However, conventional agriculture insurance is not always available and feasible in developing countries due to: i) the high transaction cost; ii) moral hazard and adverse selection caused by asymmetric information between farmers and insurers; iii) high exposure to correlated risk; iv) the lacking of distribution channels and farm-based loss-adjustment capacities.

As an alternative, index-based crop insurance is being developed at an increasing rate in emerging markets. This is a result of growing interest from policymakers in helping small rural households to mitigate the risk of natural disasters, and therefore secure their livelihoods and alleviate poverty (Collier *et al.*, 2009; Hellmuth *et al.*, 2009). Under the coverage of index insurance, farmers in a pre-defined area are insured by the same index and will receive the same amount of payout per surface unit in case of a loss. Unlike the traditional MPCI, whose insured areas are normally large and payout amount is static across an insured area, index insurance can provide farmers

with more reasonable payouts without the need of loss adjustment. Index-based crop insurance is usually categorized into: (i) weather index insurance, for which the indemnity development is based on realizations of specific weather parameters measured over a pre-specified period of time at a particular weather station (Deng *et al.*, 2007); (ii) yield index insurance, based on the calculation of the loss between the actual yield of a certain area and its average expected yield. As the loss adjustment is bypassed in index insurance, it is then superior to conventional indemnity-based insurance in terms of higher cost efficiency, better control of moral hazards, adverse selection and faster payouts (Deng *et al.*, 2007; Sarris, 2013).

One of the main constraints of index insurance is the basis risk caused by the imperfect correlation between the index and the underlying loss in terms of production shortfall at farm level (Barnett and Mahul, 2007). There are three categories of basis risk depending on the causes: (i) spatial basis risk, which is caused by the physical distance between the index location and the weather stations. The accuracy of the index will decrease as the distance increases; (ii) technological basis risk, which is caused by the underlying index hedging imperfectly against its risk exposure; (iii) temporal basis risk, caused by the temporal misalignment between the badly designed insurance phases and the intended crop-growth stages (Wang *et al.*, 2011).

As mentioned above, agricultural activities in developing countries are mostly small-farmer-centric. The development of index insurance can therefore better help millions of farmers overcoming weather-risk difficulties in comparison to the large-farm-

oriented MPCI. To maintain the accuracy of the index, a standardized model of index development should be followed to minimize possible basis risks.

1.2 Background of Drought Risk Analysis

Drought is ranked as the number one natural disaster in terms of worldwide crop losses (Keyantash and Dracup, 2002; He *et al.*, 2013), which is a concern for governments, NGOs, and scientists from hydrology, agriculture, and climate studies (Mishra and Singh, 2010).

The precise definition of drought varies in different applications (Palmer, 1965; Tate and Gustard, 2000; Mishra and Singh, 2010). Its general definition is a condition of moisture deficit (e.g. of precipitation, streamflow, soil moisture) in a specific time period (McKee *et al.*, 1993; Kao and Govindaraju, 2009). In practice, there are four categories of drought: (i) Meteorological drought, the precipitation shortage over a period of time; (ii) Hydrological drought, the deficiency in stream flow; (iii) Agricultural drought, which results in insufficient soil moisture to support the demands of crop growth; and (iv) Socio-economic drought, the failure of the water supply to meet the water demand (Mishra and Singh, 2010).

Yevjevich (1969) established the fundamental drought-risk computation theory by considering multiple variables, including drought duration, drought intensity and drought severity. This theory has been widely used in hydrology studies in recent years (Dalezios *et al.*, 2000; Kim *et al.*, 2006; Shiau *et al.*, 2007; Mishra and Singh, 2009). To further increase the effectiveness of drought-risk assessment, recent studies tend to analyse drought from multivariate aspects (Michele *et al.*, 2013), which leads

to discussions about estimating the multivariate probability density functions (PDFs) by parametric or non-parametric methods for the multiple risk variables (duration, intensity and severity) (Santhosh and Srinivas, 2013). Parametric analysis of the density function assumes that the available sample follows the population of a parameterized probability density function. On the other hand, non-parametric analysis of the density function requires no underlying frequency distribution, and makes no assumptions about the density functions of the sample variables. In the field of hydrology studies, there are no universally accepted distributions (Kim *et al.*, 2003), and as pointed out by Santhosh and Srinivas (2013), non-parametric PDF estimation is more reliable for analyzing hydrological risk from multiple perspectives, while parametric models are only recommended when the underlying variable density is known.

Of the various ways to estimate the PDF using non-parametric functions, kernel density estimation has gained the most recognition (Santhosh and Srinivas, 2013), and has been widely adopted in the frequency analysis of flood and drought (Dalezios *et al.*, 2000; Kim and Heo, 2002; Kim *et al.*, 2006; Moon *et al.*, 2010; Kannan and Ghosh, 2013; Parviz *et al.*, 2013). Among the different kernel density estimation methods, the standardized kernel function is known for its relatively straightforward computation steps, the boundary-leakage problem (Santhosh and Srinivas, 2013) that generates a biased PDF for the left-skewed variable, and PDF shape-shifting due to bandwidth selection (Kannan and Ghosh, 2013). To improve on the shortcomings of the standardized kernel function, an alternative non-parametric method – the diffusion-based kernel density estimation (DKDE), has been proposed by Botev *et al.*

(2010). The DKDE has been shown to be an effective and viable option in terms of avoiding the boundary-leakage and shape-shifting problems that exist in the standardized kernel function.

1.3 The Agriculture Insurance Market in China

Back in the 1950s, when agriculture insurance was firstly introduced, the idea of insuring crops was not so popular. However, the Chinese government has then realized the importance of agriculture to the sustainable development of the economy, and has given priority to agriculture insurance since the issue of an official document known as "The Three Dimensional Rural Issues" in 2004, in which the risk transfer of crop losses through the insurance market is emphasized. According to corporate statistical data from the People's Insurance Company of China (PICC), the agriculture insurance premiums collected have grown significantly since the Central Committee of the Communist Party of China (CPC) approved 1 billion RMB (roughly 13 million USD in 2007) to fund agriculture insurance subsidies in 2007. The central and provincial governments are currently subsidizing up to 80% of the premiums to make agriculture insurance affordable for farmers in China. Currently, four main crops (rice, wheat, corn, and cotton) are subsidized by the central government, while some provincial governments provide further subsidies for extended crop coverage (rapeseed, sugarcane).

By 2010, the new agriculture insurance program was expanded to 25 provinces and autonomous regions (Yang *et al.*, 2010; Wang *et al.*, 2011). Figure 1-1 below shows the premium incomes and indemnity payouts of agriculture insurance from the PICC

in the last ten years (Yearbook, 2002-2011). The total agriculture insurance premiums in China increased from 100 million USD in 2006 to 5 billion USD in 2013 (CIRC, 2014). Further growth is expected as a result of increasing insurance penetration, higher sums insured, and extended crop coverage.

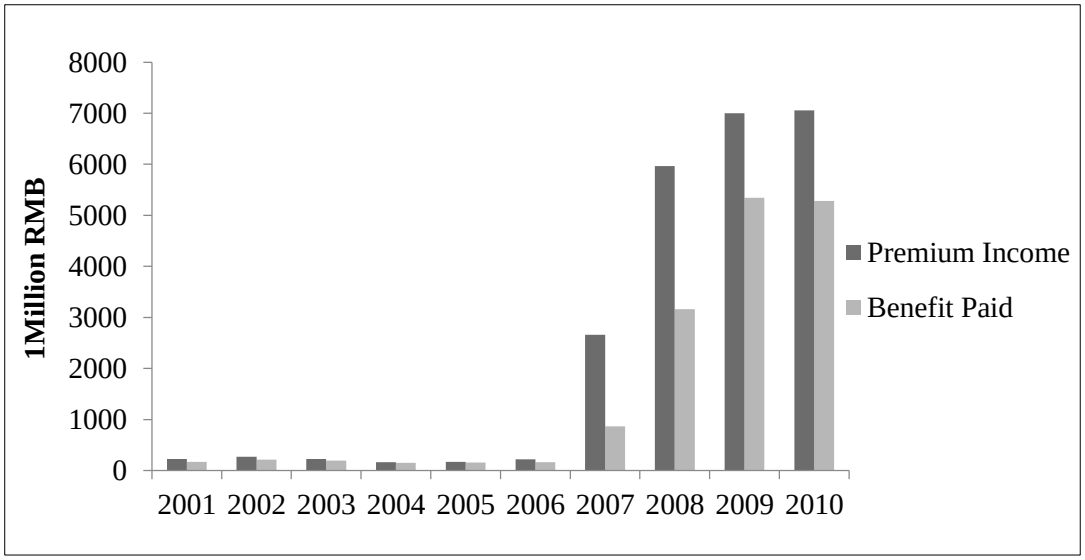

Figure 1-1 Corporate statistics of agriculture insurance of the People's Insurance Company of China (PICC) (2001–2010) (Source: Yearbooks of China's Insurance 2002–2011)

Despite the rapid development of the agriculture insurance market, the weather index insurance market in China is still underdeveloped. The agriculture insurance market remains dominated by the traditional MPCI. MPCI provides farmers with coverage for perils such as drought, flood, frost, hail/wind, and typhoon, with peril-specific franchises and deductibles. For a given crop type, a fixed premium rate is applied to every farm within one province, and is normally up to 6% of the sum insured (300 RMB/mu or 50 USD/mu). Nonetheless, in the highly drought-prone provinces of Shanxi, Gansu, Hebei, and Shandong, MPCI products do not cover drought due to

the high drought risk in these provinces. In the provinces of Sichuan, Hubei, and Henan, high franchises are applied for the drought coverage.

In China, the development and research of weather index insurance has just started. The China Insurance Regulatory Commission (CIRC) (2012) has encouraged the research and development of index insurance by providing more opportunities for researchers to evaluate weather index insurance as an alternative to indemnity-based agriculture insurance. Some feasibility studies of index-based crop insurance in China have been conducted over the years. Lou et al. (2009) investigated the feasibility of a frost index for damage to citrus production in Zhejiang province, based on county-level yield-loss data. In the same province, Wu (2010) developed a yield index for rice by correlating yield reductions with weather parameters for each county. In Anhui province, a rainfall–temperature index per growth phase has been used by rice farmers since 2009 (Zhu, 2011). Yang et al. (2013) developed several weather indices for drought, late spring frost, dry hot wind events, and continuous overcast rain for winter wheat in one county. Heimfarth and Musshoff (2011) conducted research on the development of a rainfall deficit index for corn and wheat, based on province-level yield and rainfall data from 23 weather stations in Shandong province. The use of high-resolution crop-yield data (township level) and weather-station data (county level) in this research provides a new assessment of the feasibility of compensating for drought losses via rainfall index insurance in China.

1.4 Objectives of Research

The objectives of this research are development of two models based on the following two aspects:

1.4.1 Bivariate Drought-Risk Model

The diffusion kernel density estimation (DKDE) shows better performance than the standardized kernel density estimation in terms of improving asymptotic bias, reducing computational cost and avoiding the boundary-leakage problem in estimating the PDF for left-skewed variables (e.g. precipitation). The first step in the development of the bivariate drought-risk model is to compute the Standardized Precipitation Index (SPI) from the weather data collected. The bivariate PDF is then estimated with the DKDE method, based on the computed SPI. Following this, the joint return period is estimated, and finally the drought-risk model is established. This established risk model will then provide a reference for identifying regional agricultural drought, and offer important technological support for drought planning and management based on the return level of drought risk under difference conditions. As discussed above, the development of the model consists of two major parts:

- Standardized Precipitation Index (SPI)-based drought-risk variables: Drought risk is estimated from multiple variables, including the drought duration and drought intensity in the model, based on the theory of runs. The SPI is computed to define the drought duration and drought intensity. The phenological growth cycle of corn (Emergence phase, Jointing phase, Anthesis phase, Grain Filling

phase, and Maturity phase) is used as the time-scale interval of the SPI at different growth stages.

- Diffusion kernel density estimator (DKDE): The DKDE is used to estimate the bivariate probability density and the joint return period of SPI-based drought risk. The estimations provide a better understanding of the occurrence frequency and severity of drought risk per growth phase of corn. Combined with GIS spatial analysis techniques, the drought duration and drought intensity are presented to reveal the spatial and temporal variation of agricultural droughts.

1.4.2 **Rainfall Index Insurance Development Model**

The advantages of index insurance over conventional indemnity-based insurance have been previously discussed with regard to cost efficiency, moral hazard control, adverse selection, and fast payouts. The rainfall index insurance development model focuses on standardizing the development of rainfall index insurance, so that the standardized method can be adopted by institutes and reapplied to develop index-based insurance for drought-prone regions. This model contributes to the existing rainfall-index development approach in the following respects:

- Reducing temporal basis risk caused by temporal misalignment of insurance phases with crop-growth stages. From time to time, farmers change their farming practices, such as seeding time, fertilizer application, and mitigation methods, based on their experience and observations of weather conditions. However, the insurance-developing institutes normally deduce crop growth and insurance phases based on fixed and outdated farming-practice information. Therefore, to

maintain data consistency between the farmers and institutes, a questionnaire was designed and distributed to the farming households directly, to acquire accurate data such as corn-growth phases, commercial prices, and production costs.

- Reducing technical basis risk caused by hedging the index imperfectly against risk exposure. The yield data and weather data have to have the same geographical coverage to produce an accurate index describing the risk exposure. To ease the process of matching the geographical coverage of data, high-resolution yield data (township level) and weather data (county level) were used in the development of the indices.
- Reducing spatial basis risk caused by a lack of rainfall and yield-data locality. Spatial basis risk occurs at the areas remotely located from the weather stations, and can be reduced by increasing the weather-data locality. For this model, the weighted Thiessen polygon method was adopted for areas located outside the effective radius of a weather station, to increase the weather-data locality.
- Developing a statistical approach to set payout functions (trigger and exit) for the index. This model distinguishes itself from the existing approaches by independently considering the characteristics of each growth phase and insured area for correlation development. Hence it is able to provide high accuracy in the computation of the respective triggers and exits. This approach also provides a valuable alternative to the usage of water-requirement levels.
- Calculating the probable maximum loss, via drought-severity PDF estimation with univariate DKDE, which will help financial institutions and governments

capture the potential extreme losses and compensate for the probable maximum loss caused by extreme drought events.

1.5 Organization

This thesis is organized to address the previously mentioned objectives as follows:

Chapter 2 provides literature reviews of previous works covering the impact of climate change on agriculture, the theoretical method and pilot development of weather index insurance, and drought-risk analysis. The advantages of weather index insurance over the conventional MPCI are reviewed from different aspects. The studies of drought risk are analyzed from parametrical and non-parametrical perspectives based on the theory of runs. The applications and limitations of non-parametric analysis kernel-density estimation are reviewed and compared with the DKDE.

Chapter 3 provides an explanation of the methodology for designing rainfall index insurance, including hazard analysis, drought-risk analysis and insurance policy analysis. The questionnaire for the prefeasibility study of index insurance is provided. The drought-risk analysis is explained regarding the SPI, theory of runs, parametric density estimation and diffusion kernel-density estimation. A detailed rainfall index insurance model is developed based on the correlation analysis between yield reduction and rainfall per corn-growth period.

Chapter 4 provides a detailed account of the application of bivariate diffusion kernel density estimation for drought risk. The DKDE approach was adopted to estimate the

bivariate frequency and joint return level of SPI-based drought risk. A brief description of the best-fitted bivariate PDF of drought risk in four corn-growth phases, with daily precipitation data collected from 19 weather stations in Shandong province from 1951 to 2006, is presented. In addition, a comparison between the bivariate Gaussian kernel estimation with rule of thumb bandwidth selection and the diffusion kernel density estimator will be made and discussed.

Chapter 5 provides a detailed development model of a rainfall index for corn in five counties in Shandong province, with high-resolution yield and weather data. The viability of the product from an insurance point of view is also evaluated.

Chapter 6 provides a frequency estimation of drought severity by univariate DKDE in the insured areas of Shandong province, with historical daily rainfall data from 1981 to 2011. Rainfall pattern is analyzed by comparing four commonly used parameterized density functions. The Probable Maximum Loss (PML) for extreme drought-risk levels for a 100-year return period is also calculated. Finally, the premiums, including pure premiums and risk premiums, are calculated based on the loss-cost analysis of Chapter 5 and the PML analysis.

Chapter 7 provides the conclusion and discusses the limitations of the thesis. Recommendations are also made for future studies in the fields of drought-risk research and index insurance development.

CHAPTER 2

REVIEW OF THEORY AND PREVIOUS WORKS

Chapter 2 consists of three parts: 1) The impact of climate change on financial attitudes and farming activities; 2) The advantages of weather index insurance over other risk-mitigation measures, especially indemnity-based agriculture insurance, and the development of the methodologies applied in designing rainfall index insurance; 3) The development of drought risk analysis by parametric analysis and nonparametric analysis.

2.1 Impact of Climate Change on Farming Households

Studies have identified climate change as one of the important factors affecting farming practice (Gornall *et al.*, 2010; Skoufias, 2012), in addition to severe weather events such as drought and flood. Highly unpredictable rainfall pattern is one of the new threats to small-scale farmers and will expose the farmers to more frequent drought events in the context of global warming (Solomon, 2007; Stocker *et al.*, 2013). Li (2009) discovered that drought can cause productivity reduction of about 60–75% for barley, maize, rice, and wheat by correlating the yield reduction of major crops and drought hazard, based on the Palmer Drought Severity Index (PDSI) (Palmer, 1965). He also predicted that crop-yield reduction resulting from drought will be 1.5 to 1.9 times higher in 2060 than in 2010.

In the face of global warming and its consequences, the development level of a country has an important role to play in sustaining the livelihood of farmers. In

comparison with developed countries, rural households in developing countries rely much more on weather conditions, and easily suffer asset losses from climate-change-related events (Hess *et al.*, 2002). Carter *et al.* (2005) described the relationship between natural hazards and the asset levels of households by comparing the different asset situations of two representative households, Household A and Household B. Both households have an increasing trend in asset levels in the beginning and Household A has more valuable assets (Figure 2-1). It is assumed that Household A represents a household from a developed country, where Household B represents a household in a transient group between poverty and non-poverty from a developing country. The asset levels of both households fall immediately after a natural hazard occurrence. However, compared with the rather quick recovery of Household A, Household B recovers much more slowly, or does not recover at all as its initial poverty has retarded its ability to recover and escape further poverty. Therefore, as climate change intensifies, having a better understanding of disaster risks will help financial institutions and governments in developing countries to capture the potential extreme losses more accurately, and better compensate for the uncertainties of probable maximum loss caused by extreme drought events.

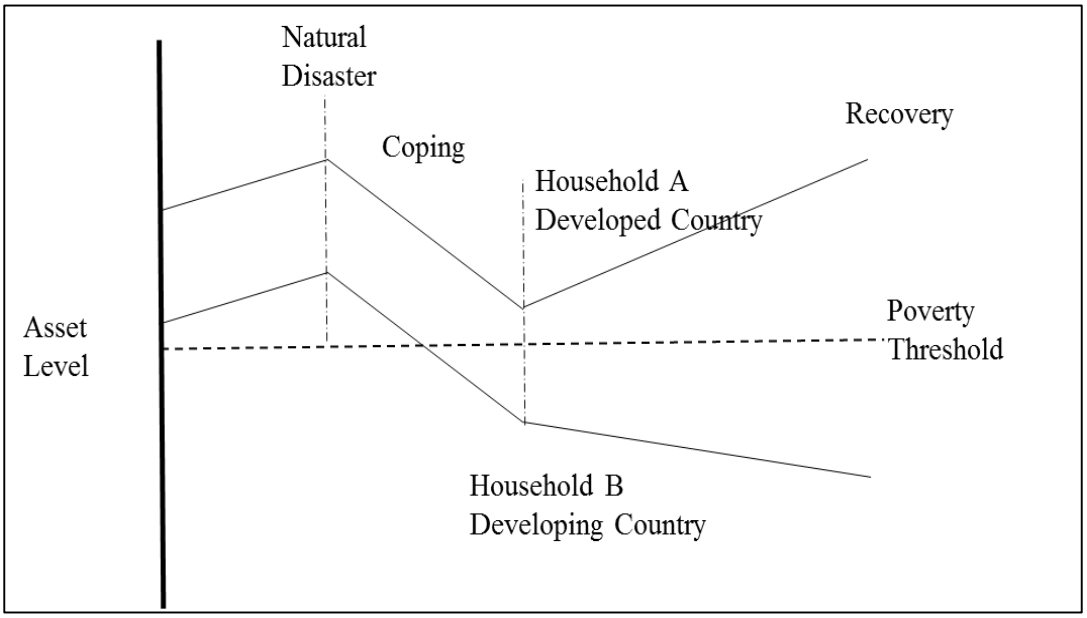

Figure 2-1 Reactions of different households from developing and developed countries after natural disaster impact (Carter *et al.*, 2005)

2.1.1 **Mitigation Measures**

Studies have analyzed the mitigation measures of rural households and communities to reduce natural disaster risks, as shown in Table 2-1 below (Hess *et al.*, 2002; Skees *et al.*, 2002; Carter *et al.*, 2005; Skees and Barnett, 2006; Barnett and Mahul, 2007; Nieto *et al.*, 2010). In general, the mitigation measures can be divided into three categories: i) households and communities; ii) government; iii) credit market.

- Households and Communities

Crop diversification and inter-cropping strategies are stated to be the most common strategies for rural households to reduce crop loss due to adverse weather events (Hess, 2007). However, these strategies will not be beneficial if they require the

farmers to change their farming practices too much and finally get diverged from the most productive practices (Nieto *et al.*, 2010).

A number of studies have shown that small-scale farmers can deal with idiosyncratic (non-correlated) shocks through community risk sharing under informal networks. However, covariate (correlated) shocks, such as the impact of drought, can easily break down the entire network as all members of the community will usually be simultaneously affected (Linnerooth-Bayer *et al.*, 2005; Trærup, 2012; Sarris, 2013).

- Government Intervention and Credit Market

Muamba (2010) points out that public intervention, such as investments in irrigation systems to alleviate crop vulnerability to droughts, can encourage rural households to invest more in high-yield varieties. In situations of harvest failure due to extreme weather events, small-scale farmers in emerging markets often have to rely entirely on government ad-hoc disaster payments, since private-sector financial solutions such as insurance are hardly available. In markets where financial instruments are available, the impacts of natural disasters may discourage rural households from accessing the credit market and taking adverse risks, due to the fear of not receiving a payout (Hill *et al.*, 2013).

Risk transfer through insurance has been identified as an effective measure to (i) provide farmers with a safety net against the impacts of extreme weather events; (ii) contribute to the stability of government ad-hoc disaster budgets (Skees *et al.*, 2006; Hertel and Rosch, 2010; Turvey and Kong, 2010; Skoufias, 2012); (iii) speed up the recovery of food production by providing a collateral for farmers to take loans from

banks to invest in the next crop-growth cycle immediately after the disaster and access higher-quality input supplies (Karlan *et al.*, 2011). With growing insurance penetration in rural household communities, agriculture insurance should ultimately lead to higher crop production and contribute to the alleviation of food-security concerns in some of the world's key production regions.

Table 2-1 Risk-coping strategies from the perspectives of households and community, government, and credit market

	Mitigation Measures	**Remarks**
Rural Households and Community	Saving and borrowing	Savings and borrowing from informal institutions or relatives and community members can allow households to purchase assets providing high returns, ensure smooth consumption between low and high revenue periods, and reduce the liquidation of productive assets after natural disasters (Skees and Barnett, 2006).
	Income diversification	E.g. crop trades, food manufacture, and transportation.
	Crop diversification	E.g. crop inter-cropping strategies
	Selling assets	Households liquidate productive assets to smooth consumption following natural disasters, but this incurs a net loss.
	Risk aversion	Households adopt low-return options rather than higher-return options like productivity-enhancing technologies, which require additional investments.
Government	Infrastructure construction	The building of new infrastructure projects such as irrigation systems.
	Financial assistance	Governments provide ex post free disaster assistance to households after natural disasters, or make public investments in agricultural risk-sharing markets, e.g. providing subsidies for the agriculture insurance market to protect households against productivity and revenue loss.
Credit market		Includes agriculture loans and agriculture insurance products.

2.1.2 **Impact of Natural Risks on Agriculture in China**

China is one of the largest agriculture producers that also supply most of their own domestic food needs. In 2011, the revenue from agriculture production accounted for 13% of China's annual GDP and the agriculture industry engaged 41% of the total labor force. Over half of China's population is based in rural areas with small tracts of farmland per household. Hence Chinese farmers are more vulnerable to natural hazards than large farm households in developed countries.

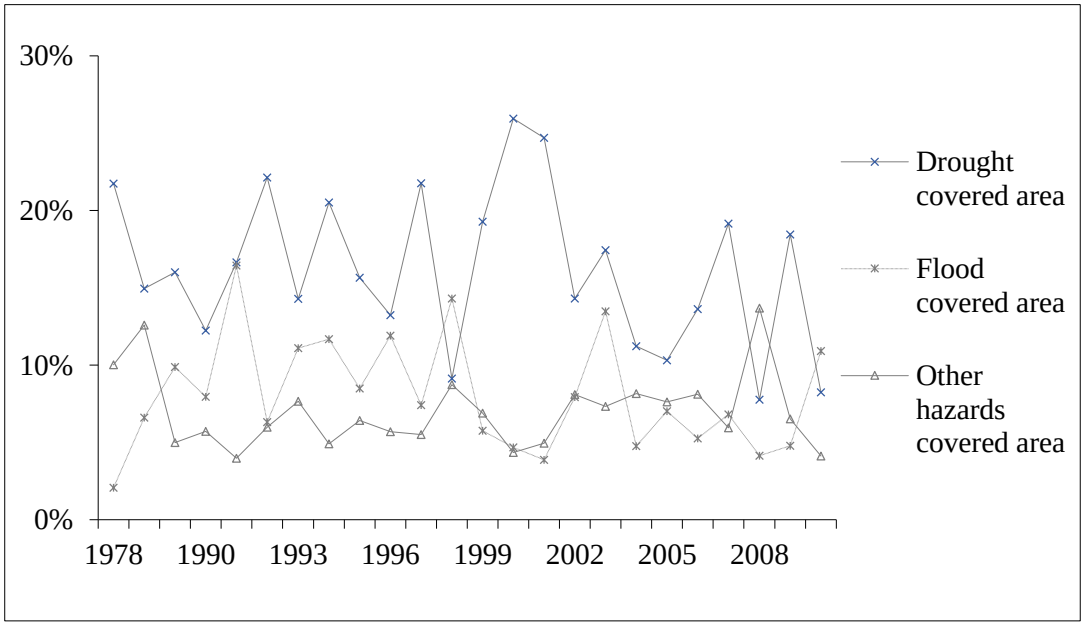

Figure 2-2 Farmland affected by natural disasters in China, 1978–2010, for key perils (Yearbook, 2011)

Figure 2-2 shows the farmland affected by natural disasters in China from 1987 to 2010 (Yearbook, 2011). Out of all perils, drought caused the most widespread damage, which accounts for more than 50% of the total affected area nationwide. In 2010, more than two million people were plunged back into poverty because of

drought in southwest China (Sivakumar, 2010). The cumulative drought-affected area in 2011 was 30 million Mu, with the direct economic loss of the agriculture industry about 16 billion USD.

2.2 Rainfall Index Insurance

Under index insurance, farmers in a pre-defined area are insured by the same index and obtain the same payout per surface unit in case of a loss. The indemnity development of weather index insurance is based on realizations of specific weather parameters measured over a pre-specified period of time at a particular weather station (Deng *et al.*, 2007). Figure 2-3 shows an example of rainfall index insurance, indemnity payments will start if the underlying rainfall index drops below the trigger value during the coverage period and incrementally accumulate with defined incremental payments until the limit is reached. The limits is set by considering the high cost of protection against extreme losses occurring in the long tail of risk distribution, where the ambiguity is high.

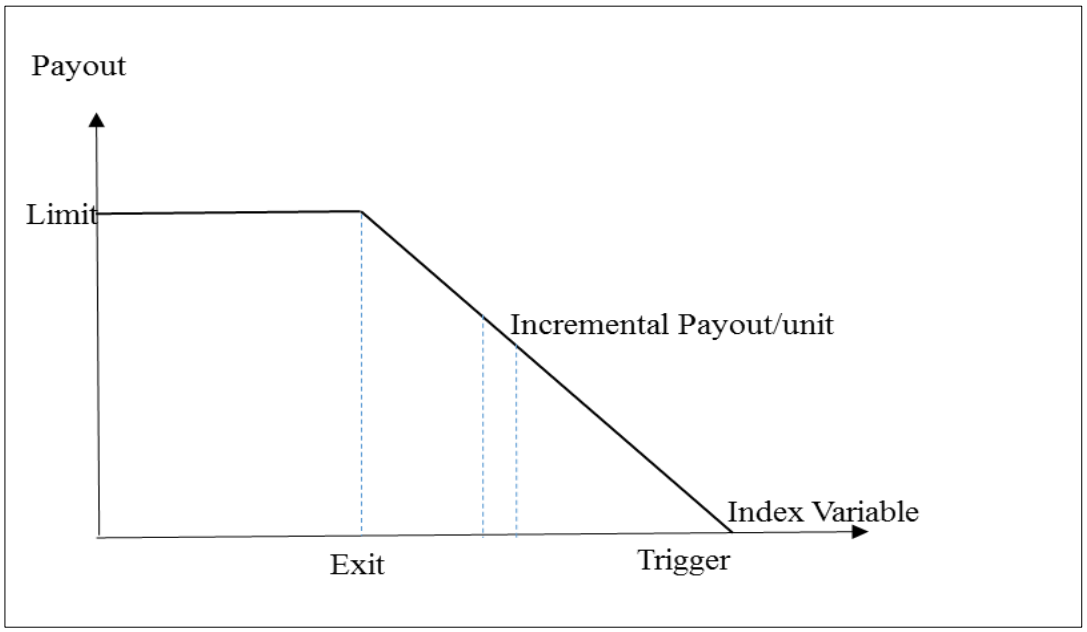

Figure 2-3 Contract parameters of weather index insurance: Trigger, Exit, Limit, and Incremental payout

Given the advantages of index insurance over MPCI products, there has been growing interest in implementing weather index insurance programs in countries with small-scale farming systems, including Indonesia (Stoppa and Manuamorn, 2010), Malawi (Hess and Syroka, 2005), Morocco (Skees, 2001), Ethiopia (Dinku *et al.*, 2009), and India (Manuamorn, 2005; Lev and Iames, 2012). India introduced weather index insurance in 2003. It is the first country to introduce weather index insurance to the agriculture insurance market and its index insurance covers the most number of farmers to date (Antoine and Philippe, 2011). Table 2-2 provides the summary of the index insurance pilots developed in countries with small-scale farming systems recent years.

Table 2-2 Examples for successful weather index insurance schemes around the world

Country	Risk	Index	Crop	Year	Remarks
Ethiopia	Drought	Rainfall	Wheat, millet, cowpea, and maize	2006	The project was initiated by the World Food Program, with technical assistance from the Food and Agricultural Organization (FAO). The Ethiopia Drought Index is based on the cumulative rainfall, determined by data from 26 weather stations from a national meteorological agency, as well a crop-water-balance model. Remote sensing is used in case rainfall data is tampered with, and to cover areas without weather stations.
				2007	Limited weather data is compensated for by a combination of satellite data, rainfall simulator, and statistical tools, and basis risk is reduced by determining the maximum distance between farm and weather station.
			Haricot	2009	The contract is based on a simplified Water Requirement Satisfaction Index (WRSI), assuming the soil water holding capacity is zero, and measuring the balance between rainfall and water demand of crops during growing season (germination and vegetative phase, flowering phase, and seed formation and ripening phase). The rainfall deficit of each phase is calculated by summing up all the deficits in each dekad within the phase.
Malawi	Drought	Rainfall	Groundnut	2005	

			Maize	2006	The project is offered with a package for loans with agricultural inputs. Data from weather stations in Malawi are used to determine the Water Requirement Satisfaction Index, on which the national maize yield assessment model of the Malawi government is based. The low density of automated rainfall stations has limited the extension of this project in Malawi.
			Tobacco	2007	
Mexico	Drought and excessive rainfall	Rainfall	Maize, sorghum, barley, and bean	2002-2008	The rainfall index is based on cumulative rainfall for different growth stages.
Central America	Drought and rainfall	Rainfall	Groundnut and rice	2007	The contract combines three weather risks: excess rainfall at sowing, drought during growth, and excess rainfall during harvest.
Brazil	Drought, flooding	Area yield	Maize	2001	Triggers are set at 10% deviation of average yield in 2001.
India	Drought	Rainfall	Groundnut and castor	2003	India introduced weather index insurance in 2003, and is the first country to introduce weather index insurance to the agriculture insurance market. It is also the country that covers the highest number of farmers (Antoine and Philippe, 2011).

2.2.1 **Advantages and Limitations of Weather Index Insurance**

- Advantages

Rather than depending on the loss inspector to assess farm-level losses, the payout from weather index insurance depends on the public data published by the meteorological bureau. The payout is triggered by meteorological parameter variables, which cannot be influenced by the behavior of households. This also significantly reduces the costs of controlling moral hazard and adverse selection.

- Limitations

Basis risk is the main challenge to the implementation of weather index insurance. It is caused by the imperfect correlation between the index and the underlying loss in terms of production shortfall at farm level (Barnett and Mahul, 2007). There are three types of basis risk: (i) spatial basis risk, which refers to the fact that the index defined at a given weather station will become unable to accurately deduce the weather at a location remote from the station; (ii) technical basis risk, which is caused by the underlying index being an imperfect hedge against risk exposure; (iii) temporal basis risk, the result of the implementation of badly designed insurance phases which are not temporally aligned with the intended crop-growth stages (Wang *et al.*, 2011).

The interaction between clients and insurance experts or local farmers is the key to solving temporal and technical basis risk. In Eastern Indonesia (Skees, 2011), a questionnaire is distributed among farmers to gather crop-growth information, risk

information and financial information. In Ethiopia (Hellmuth *et al.*, 2009), the method known as the "farmer-centric approach" is introduced to identify weather risk and growth information about underlying crops. To reduce the spatial basis risk, the weather index should only cover an area within a radius of 20–30 km from the weather station (Hellmuth *et al.*, 2009). The more homogeneous the area, the lower the spatial basis risk, and the more effectively the index insurance can interpolate weather data (Skees *et al.*, 2006).

2.2.2 **Development of Weather Index Insurance**

The concept of index insurance, methodologies for developing indices and benefits of index insurance comparing with indemnity-based insurance have been widely discussed (Barnett and Mahul, 2007; Dinku *et al.*, 2009; Skees *et al.*, 2009; Hazell *et al.*, 2010; Turvey and Kong, 2010; Clarke, 2011; Norton *et al.*, 2013). As determined by previous pilots, there are two basic components in building weather index insurance:

1. Identify the potential pilot area and quantify the weather exposure of crops through prerequisite surveys, including: (i) identifying the weather station reflecting risk; (ii) identifying the period during which risk is prevalent; (iii) identifying the weather index that is the best proxy for the risk exposure (Hartell *et al.*, 2006).
2. Design the index that can enable farmers to get reasonable payouts when adverse weather events occur, including: (i) quantification of the financial impact of risk on farmers' revenues and production cost; (ii) measurement of

index parameters; (iii) identification of trigger and limit; (iv) pricing of premium and premium rate.

2.3 Drought-Risk Analysis

Yevjevich (1969) was the first to propose the theory of runs, which is the continuous period that the drought variable is below the truncation level of moisture, to identify drought risks. As illustrated in Figure 2-4, the duration, intensity and severity of drought risk are expressed by the truncation level (Yevjevich, 1969; Kim *et al.*, 2006). Drought duration *D* is the continuous period in which the drought variable is below the threshold, drought severity *M* is the cumulative deficiency of the drought variable during the drought period and drought intensity *I* is the average moisture deficiency, which equals to *M/D*. The theory of runs has been widely used in the study of the identification of drought risks (Dalezios *et al.*, 2000; Kim *et al.*, 2006; Shiau *et al.*, 2007; Mishra and Singh, 2009). In this research, the theory of runs is adopted for the drought-risk analysis.

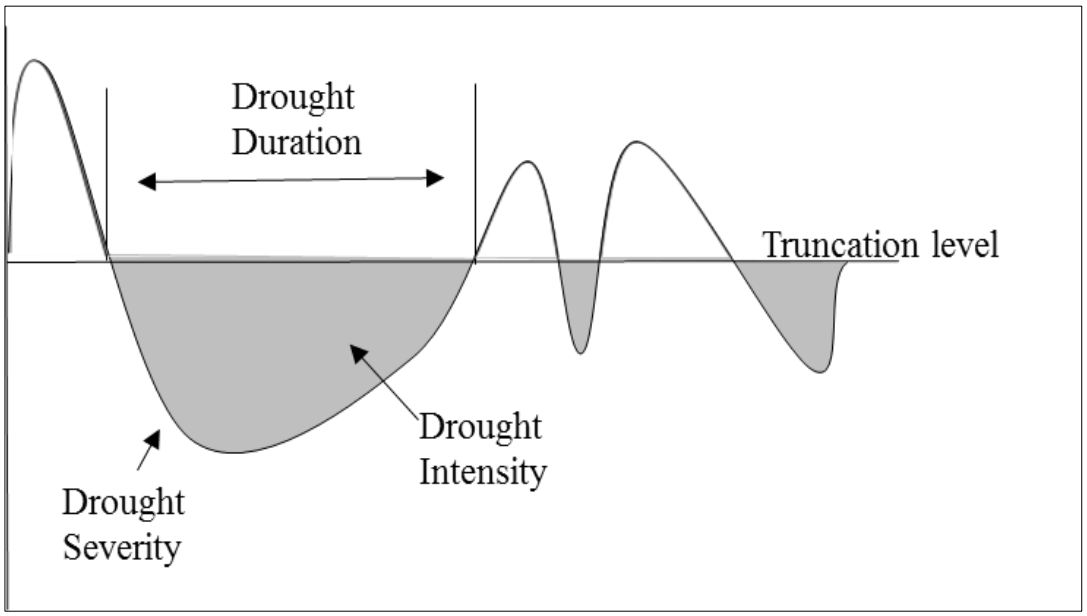

Figure 2-4 Theory of runs for identification of drought risk: Truncation level and Drought duration, intensity, and severity

2.3.1 **Drought Index**

The agricultural drought risk can be identified through agricultural system modeling and drought indices. Agricultural system modeling is a valuable tool that reflects the interactions between crop and weather parameters, soil moisture, planting practices and crop physiology in actual farming practice (Barnett, 2009). The Decision Support System for Agro-technology Transfer (DAAST) is a commonly used agricultural system model in index insurance development. The DSSAT cropping-management system simulates the biological process of crop growth from germination to harvest under consideration of more variables than simple water variability in the estimation of crop yields; some of these additional variables include farming practices, soil pattern, and weather parameters (daily solar radiation, temperatures, and precipitation) (Osgood *et al.*, 2007). However, the detailed information-based models can also lead

to serious basis risk. Osgood *et al.* (2007) concludes that the index insurance product needs a model to reflect the drought stress for different planting practice patterns within a region, but the detailed model is too sensitive with standardized parameter assumptions that varies among farmers. He recommends that a more detailed process-based model shall be developed as an evaluator for indices and assessment of the robustness of the contract design.

Commonly used indicators for drought (Mishra and Singh, 2010) include the Standardized Precipitation Index (SPI) (McKee *et al.*, 1993), Palmer Drought Severity Index (PSDI) (Palmer, 1965), Crop Moisture Index (CMI) (Palmer, 1968), Surface Water Supply Index (SWSI) (Shafer and Dezman, 1982), Vegetation Condition Index (VCI) (Kogan, 1995), Effective Precipitation (EP) (Byun and Wilhite, 1999), and Soil Moisture Deficit Index (SMDI) (Narasimhan and Srinivasan, 2005). Numerous literatures have encompassed comparisons of the available drought indices for studying different aspects of droughts (Alley, 1984; Guttman, 1998; Heim Jr, 2002; Keyantash and Dracup, 2002; Mishra and Singh, 2010).

McKee (1998) developed the Standardized Precipitation Index (SPI) to monitor drought events; this index was firstly used as an experimental drought-monitoring tool in Colorado back in 1992. The SPI was designed to quantify precipitation anomalies in terms of severity, magnitude and frequency in small and non-homogeneous areas (Sadat Noori *et al.*, 2012). The computation of the index is based on the cumulative probability function of long-term precipitation data in the absence of other meteorological parameters. The SPI has been widely applied in the identification and monitoring of drought severity around the world (Narasimhan and

Srinivasan, 2005; Łabędzki, 2007; Livada and Assimakopoulos, 2007; Manatsa *et al.*, 2010). More than forty countries have adopted the SPI as an indicator of drought risk (Wu and Wilhite, 2004). Keyantash and Dracup (2002) concluded that the SPI appears to be a powerful drought analytical index among the most prominent drought estimators by assessing it in six criteria (robustness, tractability, transparency, sophistication, extendibility, and dimensionality). A study conducted by Noori (2012) in Hamadan showed that the SPI can have a prominent role in the early prediction of crop yield when climate parameters (evapotranspiration and temperature) and the one-month SPI are combined, which can explain 89% of the temporal variability of wheat production. Wu and Wilhite (2004) developed an agricultural drought-risk model by combining the SPI and Crop Specific Drought Index (CSDI) to evaluate the impact of drought on the critical phenological phases of corn and soybean in the USA. This model shows that the SPI can be applied to a wide time scale to indicate the duration, intensity, and distribution of rainfall before and during the growth stages of crops. Hence the SPI is superior to other drought indices in terms of flexibility of time scale and geography. As a result it is chosen to monitor drought risk in multiple periods in this research.

2.3.2 Parametric Analysis and Nonparametric Analysis

Natural disasters like drought and flooding are categorized as events with low frequency but high financial loss risk. By understanding the occurrence frequency and severity of drought better, financial institutions and governments will be able to more accurately capture the potential extreme losses and compensate for the uncertainties of the probable maximum loss caused by extreme drought events.

The aim of frequency analysis is to find the best-fitted PDF of the risk variables and investigate the severest risk at a specific return level. For effective evaluation, the drought risk should be analysed considering multivariate aspects, including drought severity, drought intensity and drought duration via the theory of runs (Yevjevich, 1969). The essence of the approach is to develop a multivariate PDF with parametric or nonparametric methods for the multiple risk variables (Santhosh and Srinivas, 2013).

Parametric analysis of the density function assumes that the available sample will follow a population with a parameterized probability density function. However, nonparametric analysis makes no assumption about the density function. In the past several decades, parametric density function distributions such as Lognormal, Gamma, Generalized Extreme Value (GEV), Generalized Pareto and Weibull have been extensively considered in hydrology studies (Hiemstra *et al.*, 1976; Singh and Singh, 1991; Kim *et al.*, 2003; Indrani and Abir, 2011; Vicent *et al.*, 2011; Fischer *et al.*, 2012; Acharya *et al.*, 2013). In the field of hydrology, there is no universally accepted probability density function. For example, Fischer (2012) compared the Generalized Extreme Value (GEV), Gamma III, Generalized Pareto and Wakeby distribution for precipitation extremes. He found that the GEV was the most reliable and robust distribution for estimating precipitation pattern on a basin scale in Zhujiang River of China. Later, Zhang (2013) added two more candidate distributions (Lognormal and Pearson III distribution) in a study of drought-risk evaluation in Pearl River of China. The results indicated that the Weibull distribution works better than other candidates for the estimation of drought duration series.

There are several commonly adopted methods in estimating the parameters for parameterized density functions, such as Maximum Likelihood (Akaike, 1998) and L-moment (Hosking, 1990). Using different parameter-estimation methods may result in different quantile estimates (Fischer *et al.*, 2012). The Maximum Likelihood method can be used for a larger variety of estimations, while the L-moment is superior to other methods when dealing with small sample sizes and heavy tail distributions (Delicado and Goria, 2008). Suppose independent variables $x_1, x_2, \dots, x_i, \dots x_n$ have joint distribution and the likelihood function is denoted by (Akaike, 1998):

$$\mathrm{lik}(\theta) = \prod_{i=1}^{n} f(x_i|\theta) \qquad 2\text{-}1$$

where,

θ: the vector of parameters belonging to the assumed distribution family.

The Bayesian Information Criterion (BIC) proposed by Gideon E. Schwarz (1978) and Akaike's Information Criterion (AIC) proposed by Akaike (1974) are the commonly adopted methods for choosing the best-fitted parametric functions. If the residuals of the data points from fitted lines follow a normal distribution, the BIC and AIC are given by:

$$\mathrm{BIC} = k * \ln(n) - 2\ln(L) \qquad 2\text{-}2$$

$$\mathrm{AIC} = 2k - 2\ln(L) \qquad 2\text{-}3$$

where,

n: number of data points;

L : the likelihood function;

k: the number of free parameters to be estimated.

Nonparametric analysis for the estimation of the density function was at first introduced by Fix and Hodeges (1951). It illustrates the discrimination of sample variables without an assumed density function. Kim (2003) compared the density function of three parameterized distributions (Lognormal, Gumble, and Pearson III) with the nonparametric density function by using kernel estimator for drought risks. He proofed that the nonparametric density function has a better estimation of drought intensity than the parameterized density functions with result of Absolute Relative Bias (ARB). Parviz (2013) compared nonparametric kernel estimation with eight parameterized density functions for annual precipitation in Iran; the results showed that the nonparametric way is better than the parametric way. More details of the limitations of parametric density analysis can be found in the research of Santhosh and Srinivas (2013).

2.3.3 **Bivariate Kernel Density Estimation**

Among the various ways to estimate the PDF by nonparametric functions, Kernel density estimation has gained recognition (Santhosh and Srinivas, 2013) and been widely adopted in Hydrology studies (Dalezios *et al.*, 2000; Kim and Heo, 2002; Kim *et al.*, 2003; Kim *et al.*, 2006; Moon *et al.*, 2010; Kannan and Ghosh, 2013; Parviz *et al.*, 2013).

Let $(x_1, x_2, \dots, x_n)$ denote the n random variables; the kernel density function is then given by:

$$\hat{f}_h(x) = \frac{1}{nh}\sum_{i=1}^{n} K\left(\frac{x-x_i}{h}\right) \quad 2\text{-}4$$

where,

h: the bandwidth of random variables, which is also the smoothing parameter;

K: the kernel function. Table 2-3 below shows the commonly used Kernel density functions in the study of hydrology.

Table 2-3 Example of kernel function (Kim *et al.*, 2003)

Kernel Function	**K(t)**
Epanechnikov	K(h)=0.75(1-t^2), |t|≤1; otherwise, K(t)=0
Triangular	K(t)=1-|t|, |t|≤1; otherwise, K(t)=0
Gaussian	K(t)=$(2\pi)^{-1/2}e^{-(t^2)/2}$
Rectangular	K(t)=0.5, |t|≤1; otherwise, K(t)=0

The Kernel density estimation can be extended to the multivariate density function as follows:

$$\hat{f}_{h_1,h_2\dots h_n}(x, x_{i1}, x_{i2} \dots x_{in}) = \frac{1}{nh_1h_2\dots h_n}\sum_{i=1}^{n} K\left(\frac{x_1-x_{i1}}{h_1}\right) \dots K\left(\frac{x_n-x_{in}}{h_n}\right) \quad 2\text{-}5$$

where,

n: the number of observations $(x_{i1}, x_{i2} \ldots x_{in})$, for the bivariate density function, *n*=2; $h_1 h_2 \ldots h_n$: the bandwidth for $(x_{i1}, x_{i2} \ldots x_{in})$.

2.3.4 **Bandwidth Selection**

The value of the bandwidth in the process of estimating the PDF is very important. Changing the bandwidth may drastically modify the shape of the PDF (Kannan and Ghosh, 2013). A larger *h* will result in lower variance, but important features may be smoothed away and increase the bias of $\hat{f}(x)$ with respect to the target density (over-smooth); a lower *h* will result in higher variance, but the function will be too rough (under-smooth). The way to select the best bandwidth is to minimize the mean integrated square error (MISE) or asymptotic mean integrated square error (AMISE) between the kernel estimated density and target density, denoted by (Kim and Heo, 2002):

$$\mathrm{MISE} = \mathrm{E}\left(\int \left[\widehat{\mathrm{f_h}}(\mathrm{x}) - \mathrm{f}(\mathrm{x})\right]^2 \mathrm{dx}\right)$$

$$= \frac{1}{4}\mathrm{h}^4 \alpha^{\,2} \mu + \frac{1}{\mathrm{n}}\beta \qquad 2\text{-}6$$

$$\mathrm{AMSIE} = \frac{1}{\mathrm{nh}}\beta + \mathrm{h}^4 \left(\frac{\alpha}{2!}\right)^2 \mu \qquad 2\text{-}7$$

where,

$\alpha = \int \mathrm{x}^2 \mathrm{K}(\mathrm{x})\mathrm{dx}$;

$\beta = \int \mathrm{K}^2(\mathrm{x})\mathrm{dx}$;

$\mu = \int \mathrm{f}''(\mathrm{x})^2 \mathrm{dx}$.

The MISE and AMISE cannot be used directly to get the optimal bandwidth because of the unknown function f, so data-based methods have been developed to select the optimal bandwidth. There are several commonly adopted techniques such as the Rule of thumb (Silverman, 1986) and the Plug-in method (Park and Marron, 1990; Sheather and Jones, 1991). Kim and Heo (2002) compared seven bandwidth selection methods, including Rule of thumb, Cross validation (Least square cross validation, Smoothed cross validation (Hall *et al.*, 1992)), Bandwidth factorized cross validation (Jones *et al.*, 1996), Biased cross validation (Scott and Terrell, 1987) and Plug-in method (Park and Marron, 1990). They concluded that the Sheater and Jones Plug-in method showed the smallest integrated square error in the estimation of flood quintiles in the Han River basin of Korea.

Silverman's Rule of thumb assumes that the underlying true density is normally distributed and aims to minimize the AMISE (Silverman, 1986) (2-8). However the normal assumption will lead to biased estimation and over-smooth the data (Kim and Heo, 2002; Santhosh and Srinivas, 2013).

$$\mathrm{h} = \left(\frac{\beta}{\alpha^2 \mu \mathrm{n}}\right)^{\frac{1}{5}} \qquad 2\text{-}8$$

When the Gaussian function is adopted for multivariate data, only function f'' is unknown; it is assumed to be the normally distributed with a mean of zero and the standard deviation of *h*. The optimal bandwidth h is given by:

$$\mathrm{h_d} = \left[\frac{4}{\mathrm{n(p+2)}}\right]^{\frac{1}{\mathrm{p+4}}} \sigma_\mathrm{d} \qquad 2\text{-}9$$

where,

p: the number of dimensions;

σ_d: the standard deviation of distribution in dimension d;

The Plug-in method is refined based on the Rule of thumb. It states that the function f'' will be also estimated via a nonparametric method to minimize the MISE (Park and Marron, 1990) (2-10). The P-M Plug-in method has been proven to be simple and shows good performance. However it may generate a negative value when the bandwidth is small (Kim and Heo, 2002; Härdle, 2004).

$$\hat{f}_g''(x) = \frac{1}{ng^3}\sum_{i=1}^{n} K''\left(\frac{x-x_i}{g}\right) \qquad 2\text{-}10$$

2.3.5 **Kernel Density Estimation via Diffusion**

One concern about the standardized kernel function is the boundary leakage problem (Santhosh and Srinivas, 2013), which may generate a biased PDF in the case of large bandwidth or a left-skewed variable. For instance, Kim (2003) estimated the return period of drought in arid regions in the Conchos river basin in Mexico via univariate and bivariate kernel estimation. He obtained negative value for the drought variable because the Gaussian kernel function does not take the domain of data into account. The standardized kernel functions such as the Gaussian kernel, lack of local adaptivity and only suitable for the unbounded variables. Extensive studies have been performed to deal with boundary bias and developed various tools including the reflection kernel (Silverman, 1986; Nelson *et al.*, 1992; Karunamuni and Alberts, 2005), transformation kernel (Buch-Larsen *et al.*, 2005; Swanepoel and Van Graan, 2005; Gustafsson *et al.*, 2009) and special kernels such as the beta kernel (Chen, 1999;

Bouezmarni and Rolin, 2003), gamma kernel (Chen, 2000; Ali *et al.*, 2008), boundary kernel (Cowling and Hall, 1996; Jones and Foster, 1996) and adaptive kernel (Van Kerm, 2003; Botev *et al.*, 2010; Santhosh and Srinivas, 2013). However most of techniques will result in a biased density function or be unable to accommodate variable bandwidths (Botev *et al.*, 2010; Ramsey, 2014).

Botev *et al.* (2010) proposed diffusion-based kernel density estimation (DKDE). It is an effective and viable option to avoid the disadvantages of standardized kernel functions in estimating the PDF of left-skewed variables. Santhosh and Srinivas (2013) studied the potential of the D-kernel in the estimation of flood frequency. Their results indicated that the D-kernel is more effective than the conventional Gaussian kernel in solving the boundary leakage problem. The DKDE can also be applied in the study of crop-yield density estimation in the agriculture insurance field. Ramsey (2014) determined the crop premium rate based on the crop-yield density estimated from the DKDE without generation of negative crop yield.

Given the DKDE shows better performance compared to the standardized kernel density estimation on the aspects of improving asymptotic bias, reducing computational cost and avoiding the boundary leakage problem in estimating the PDF for left-skewed variables (e.g. precipitation), it is chosen to estimate the bivariate probability density and the joint return period of drought risk in this study. The estimations provided a different way to study the occurrence frequency and severity of drought risk from multiple perspectives and to estimate the probable maximum loss caused by extreme drought events.

CHAPTER 3

METHODOLOGY

The rainfall index insurance designing model consists of four main blocks: Hazard analysis, Exposure analysis, Vulnerability analysis and Insurance policy analysis (Figure 3-1): i) Hazard analysis is conducted through a pre-requisite study questionnaire. The information obtained through questionnaire includes the identification of drought risk in drought prone region, the crop phenological growth phases, the market price and the production cost of crop in recent years; ii) Exposure analysis is deduced based on the calculated sum of insured. In order to lower the basis risk and increase the accuracy of the sum of insured, high resolution data such as crop yield at township level and daily rainfall data at county level for the period of 1981-2011 are used; iii) Vulnerability analysis of the drought risk is conducted by studying the standardized predication index (SPI) based bivariate drought risk using diffusion kernel density estimator (DKDE); iv) Insurance policy analysis covers essential steps of the Cumulative Rainfall (CR) index insurance policy development, including: a) the definition of insurance area; b) investigation of trigger and exits value based on the index and yield loss; c) estimation of premium and premium rate using historical burn analysis (HBA) and univariate diffusion kernel estimated probable maximum loss. Details of the Hazard and Exposure analysis will be discussed in Chapter 3.1, Vulnerability analysis will be discussed in Chapter 3.2 and the Insurance policy analysis will be discussed in Chapter 3.3.

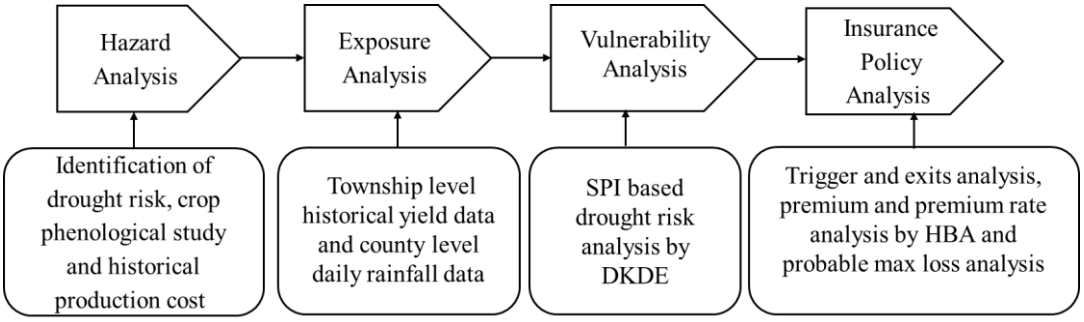

Figure 3-1 Conceptual model for rainfall index insurance

3.1 Hazard and Exposure Analysis of Drought Risk

3.1.1 Questionnaire

In order to identify the impact of weather risks on crop production, problems such as the complexity of determining crop-growth phases and the vulnerability of crop yields to multiple risks, have firstly to be resolved. Having a better understanding of local crop and weather history is the key to reduce the uncertainty in determining growth phases and the influence of risk composition on crop yield.

To help gathering the information from the farmers, a questionnaire was designed and directly distributed to the farming households to acquire accurate data. The questionnaire is translated into Chinese for the understanding of local farmers. The questionnaire was designed to collect: (i) relative information, including historical yield-loss events and causes of the yield loss. The relative information was used to identify the dominating risks impacting the crop yield and reduce the statistical noise caused by other trivial risks; (ii) phenological information about corn such as growth periods, the length of growth phases, the start and the end dates of each growth phase.

The phenological information has a tendency to vary among different farming regions due to different geographical characteristics, so getting localized information from the farmers was the best way to increase the accuracy of growth-phase determination. In addition, it is also important to reduce the spatial basis risk caused by misalignment between the crop-growth phase and insurance phase; iii) information about the historical production costs and commercial value of corn, which will be the basis for the development of the total sum insured in future work; iv) information about historical drought events and drought-risk mitigation measures, which is gathered for stakeholders such as the credit market, insurance market and government policies to better evaluate the risk factors.

Questionnaire

The questionnaire was designed to collect information about corn growth and the impact of historical drought events for the design of rainfall index insurance in the prefecture-level city of Tai'an, in Shandong province, China.

General information
Date
County
Crop tyepe
Other information

Corn information

1. What is the variety of corn planted?
2. What is the size (mu) of your corn farmland?

3. How long is the growth period for corn?
4. When is the earliest planting date of corn?
5. When is the latest planting date of corn? Please provide more information about the growth calendar of corn.
6. What is the average corn-production cost in your county? What is the total cost of input per hectare, including the seed, fertilizer, chemicals, equipment, and rent? Please fill in the corresponding cost for each growing phase:

Phenological phases	**Date**	**Length**	**Production inputs (RMB/ha)**					**Rainfall (mm)**
			Seeds	Fertilizer	Chemical	Equipment	Total	
Sowing								
Jointing								
Flowering								
Grain Filling								
Maturation								

7. How is the irrigation system in your county? Please provide the level of irrigation coverage and state when you started to use the irrigation.
8. What is the highest historical yield in your county?
9. What is the average yield in your county?
10. Who is the main buyer of corn – market traders or the government? Is there any forward contract for corn?
11. What has the market price of corn (RMB/kg) been in recent years?

Risk

1. What are the primary risks to corn production?

Pests	
Diseases	
Weather events	
Inputs supply	
Others	

2. What are the specific weather risks that impact the production of corn?

Droughts	
Excess rainfall	
Frost	
Hail	

3. How do you judge whether the rainfall is sufficient for the growth of corn and how do you mitigate the drought risk?

4. How frequently is crop-yield loss caused by drought?

5. In which years do you recall having the best/worst yields, in the past 30 years? Please specify the details, including year, farm size, and yield.

Phases	**Year**				
Planting					
Establishment					
Vegetative					
Flowering					
Maturation					

6. In which growth phase does the occurrence of drought cause the most reduction in yield?

7. Does the rainfall data provided by local weather stations indicate the rainfall pattern of your county? Is there any weather data advisory and crop loss prevention information available for you to access?

3.1.2 **Detrending Method**

In the presence of high technical basis risk, the relationship between yield loss and the index can be blurred (Dick *et al.*, 2011). High technical basis risk complicates the process of analyzing the index. In order to reduce the technical basis risk caused by hedging the index imperfectly against risk exposure, the yield data and weather data have to possess the same geographical coverage to produce an accurate index describing the risk exposure. To ease the process of matching the geographical coverage of data, high-resolution yield data (township level) and weather data (county level) are used in the development of the indices.

Technical basis risk can also increase as the length of the historical data increases. This is because of the influence of unwanted statistical noise stacks as the time series increases, which makes the impact of the dominant factor unidentifiable. However, the formulation of the future premium pricing requires at least 20 years of historical weather data, which makes the presence of technical basis risk unavoidable. Hence, a method of detrending is then introduced to reduce the technical basis risk in the lengthy historical data while keeping the influence of the dominant factor.

Crop-yield data often contain trends that arise from new planting technologies, such as the adoption of high-yield varieties and changes of fertilizers. Therefore it is necessary to remove such noises to identify the conclusive changes in variables and

to show the actual structural trend through statistical regression. The crop yield is assumed to be stationary in industry practice (Hartell *et al.*, 2006). Additionally, detrending is performed on the yield to fulfill the assumption of constant farming practice and same seeds are adopted in the historical years. The linear detrending method (Hartell *et al.*, 2006) is to decompose the yield data set $y(t)$ into forecasted yield and noises $\varepsilon(t)$, which follows the normal distribution with a mean of 0 and standard deviation σ (3-1).

$$y(t_i) = m_0 + m_i t \ + \varepsilon(t) \qquad 3\text{-}1$$

where,

t: time unit;

m_0, m_i: intercept and slope.

The decision on the existence of the linear trend is made based on the statistical significance of the linear slope at a given confidence level and coefficient of determination R^2, which measures the proportion of variability explained by the fitted linear model.

By comparing the values for R^2 and the statistical significance of m_1 at a given confidence level, the detrended dataset is given by:

$$y^*(t) = \varepsilon(t) + y(t_n), i = 1, \dots, n \qquad 3\text{-}2$$

where,

n: the most recent year.

3.2 Vulnerability Analysis of SPI-Based Drought-Risk and Diffusion Kernel Density Estimator

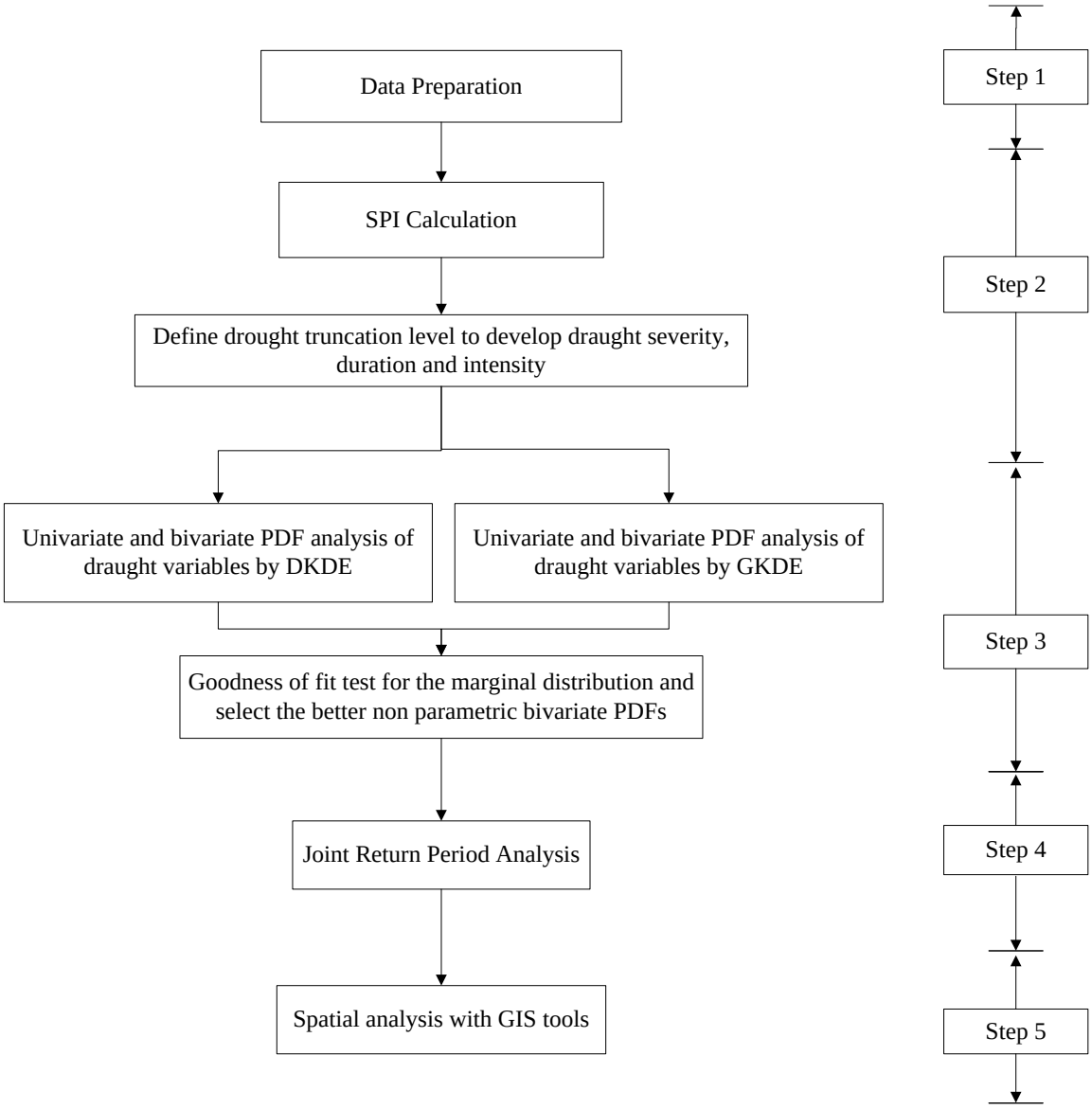

Figure 3-2 Framework for the development of SPI-Based Drought-Risk model with Diffusion Kernel Density Estimator

The key steps in the development of the SPI-based drought-risk model are shown in Figure 3-2 above, and elaborated with a case study in Chapter 4. A summary of each step is as follows:

1. *Data Preparation*

   At least 30 years of historical daily rainfall data of each weather station were prepared for the calculation of the cumulative rainfall per predefined time-scale interval. The rainfall data is interpolated with Thiessen Polygons according to the location of weather stations in the study area. The cumulative rainfall data per time-scale interval is detrended by the linear detrending method to eliminate the factors caused by artificial impacts.

2. *Standardized Precipitation Index-Based Drought-Variables Analysis*

   Each phenological growth stage of the crop is defined as a time-scale interval of the SPI. Based on the theory of runs, SPI per growth phase is converted into the drought duration, severity, and intensity.

3. *Bivariate PDFs Analysis*

   The PDFs of drought risk are estimated from univariate and bivariate aspects. The PDFs estimated by the Diffusion Kernel Density Estimator (DKDE) and Gaussian Kernel Density Estimator (GKDE) are compared with empirical distributions using the K-S test. The estimations provide a better understanding of the occurrence frequency and severity of droughts per growth phase, from the bivariate perspective.

4. *Joint Return Period Analysis*

The return period *r* is derived from the bivariate cumulative probability function (CPF) by integrating PDF constructed by DKDE.

5. *Spatial Analysis*

   The GIS spatial analysis tool shows the spatial distribution of the drought-risk return levels at different drought intensities and drought durations, for the whole study region.

3.3 Development of Index Insurance Policy

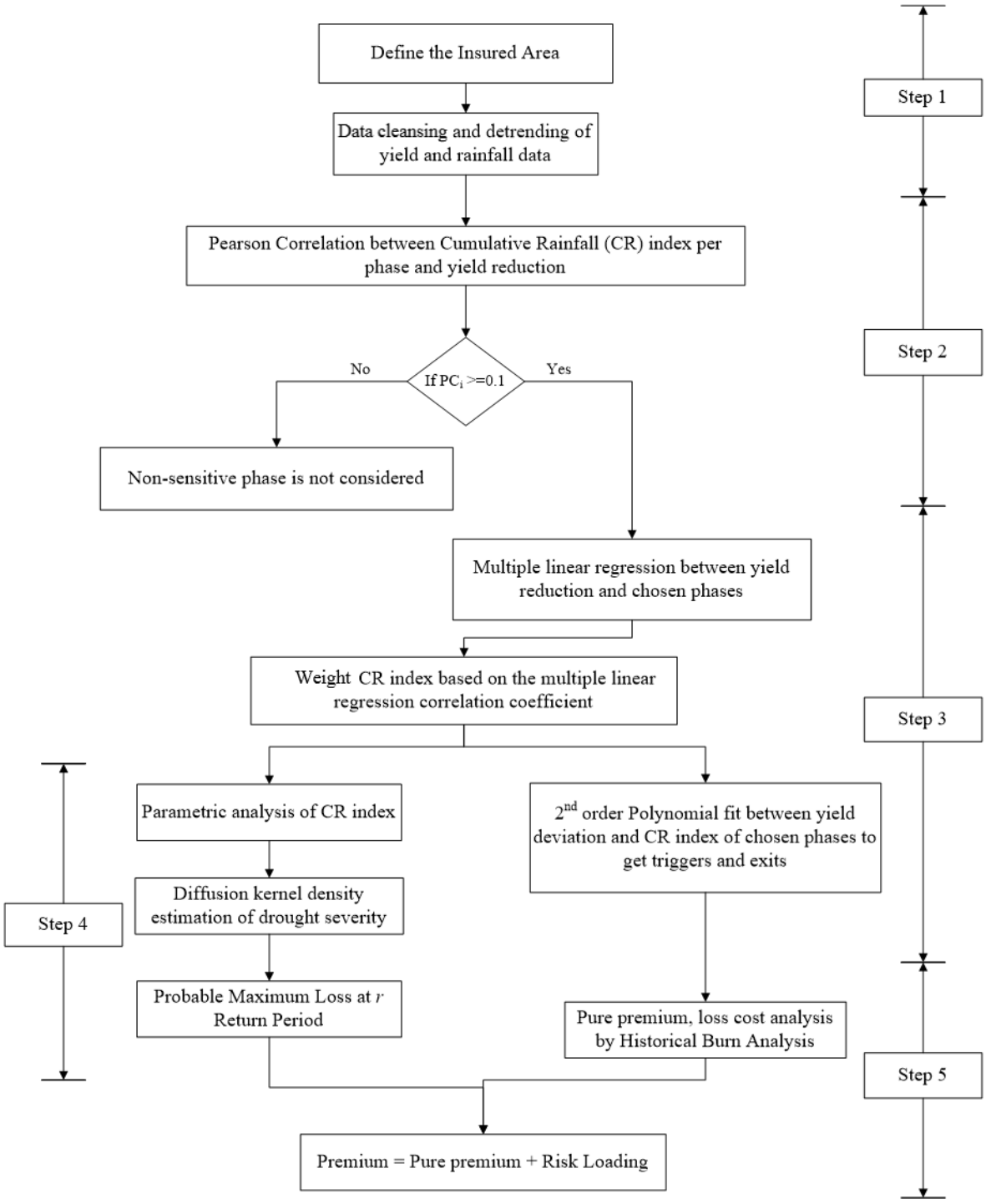

Figure 3-3 Framework of the development of rainfall index insurance model

There are five basic steps in the development of rainfall index insurance model (as laid out in Figure 3-3):

1. *Definition of the Insured Area and Data Preparation*

   An Area is defined as the region covered by a circle with a 25-km radius and the center at a specific weather station. Areas outside the 25-km radius are treated separately by interpolating rainfall data with Thiessen Polygons and named as Special Areas.

2. *Analysis of Rainfall and Yield Data*

   Pearson correlation analysis is used to determine the correlation between the detrended cumulative rainfall per growth phase and the yield loss. The growth phase that has a high correlation with the yield loss is then chosen to compute the index in the next step.

3. *Design of the Rainfall Indices including Triggers and Exits*

   A polynomial fitting between yield loss and cumulative rainfall index per growth phase is used to determine the levels of the triggers and exits.

4. *Probable Maximum Loss Analysis*

   A diffusion kernel estimator is adopted to investigate the extreme drought event at *r* return period and the probable maximum loss for the insurance company caused by the extreme events.

5. *Payout Analysis*

   Payout analysis involves calculating the indices risk premium rates, computing the payout frequency and the amount analysis using Historical Burn Analysis.

CHAPTER 4

DIFFUSION KERNEL DENSITY ESTIMATION BASED DROUGHT RISK ANALYSIS IN SHANDONG, CHINA

4.1 Introduction

Drought is defined as the occurrence of insufficient soil moisture during the crop phenological phases. In the Chapter 1 and 2 high crop drought exposure in China had been discussed. In order to overcome the addressed problems, the Standardized Precipitation Index (SPI) has been chosen to model the drought events considered its flexibility in data time scale and tolerance in data geographical coverage. In Chapter 4 a SPI based drought risk analysis is constructed with historical daily rainfall data of 19 weather stations from 1951 to 2006 in Shandong province.

Yevjevich (1969) proposed the theory of runs to identify drought risk in a continuous period by setting a truncation level of moisture. The theory of runs method is adopted in this chapter to define the SPI based drought duration and drought intensity. One of the nonparametric probability density estimation methods, the Diffusion kernel density estimation (DKDE) (Botev *et al.*, 2010) is adopted to estimate the joint probability density function (PDFs) of drought variables. After the estimation of joint distribution of drought variables, the analysis of joint return period of different drought events are discussed in the later part of Chapter 4. In the analysis a comparison between the bivariate standard kernel estimation with the rule of thumb bandwidth selection and diffusion kernel density estimator are conducted. Hence, this

chapter concludes by proposing the methodology of utilizing the DKDE function for analyzing agricultural drought. Combined with GIS spatial analysis techniques, the drought duration and the drought intensity are presented to reveal the spatial and temporal variation of agricultural droughts for corn in Shandong province. The results of in this chapter provide a reference for identifying regional agricultural drought and offer an important technological support for drought risk management.

4.2 Study Area and Data

4.2.1 Shandong Province

Shandong province is a part of the Northern China Plain located in the region between longitudes 34°N to 38°N and latitudes 114°E to 122°E (Figure 4-1). It lies between the humid subtropical and continental zones and has four distinct seasons, which is optimal for the grain production and makes it the third largest grain-producing province in China with a 10% contribution to the overall national grain production in 2012.

Annual precipitation in Shandong is 550 to 950 millimeters and the majority of the rainfall occurs over the period from June to September (Figure 4-2). Generally, the precipitation in spring (March to May) is 50–140 mm, accounting for 10 to 15 % of the annual precipitation. The precipitation in summer (June to August) is 400–560 mm, which accounts for nearly 80% of the total annual rainfall and the average rainfall in autumn (September to November) is 100–150 mm. The precipitation in

summer demonstrates great volatility, which may cause the total rainfall to vary from -60% to 50% of the average rainfall level (Figure 4-3).

In despite of its reputation in grain production, the province is also known as one of the most drought prone regions in China. Xue (2004) identified drought as the key peril for crop production in Shandong. It is confirmed by analyzing the size of area with over 30% yield loss caused by natural disasters. The result shows that in Shandong, 64% of the affected area was hit by drought over the period 1978–2011(Yearbook, 1979-2012) (Figure 4-4).

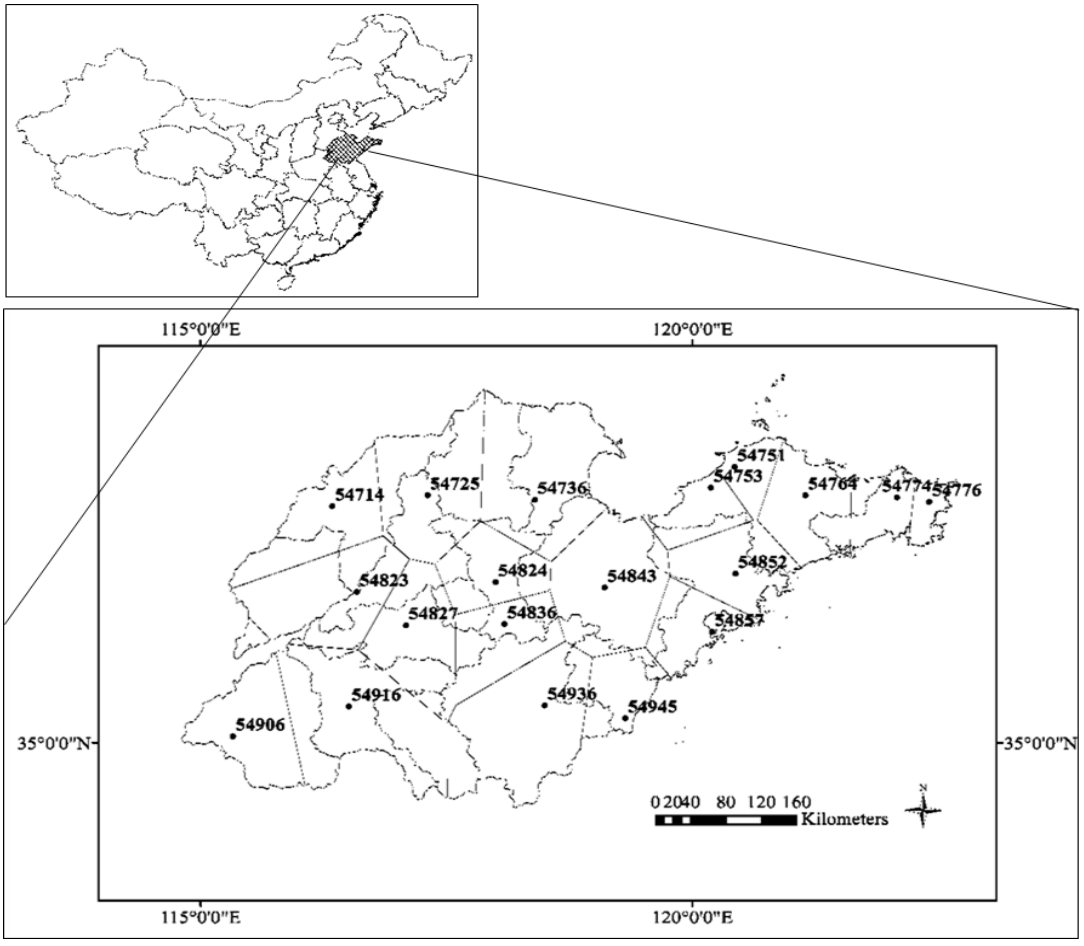

Figure 4-1 Location of Shandong province in China (top), Shandong province (below) with 19 weather stations (points) and Insured Areas by Thiessen polygons

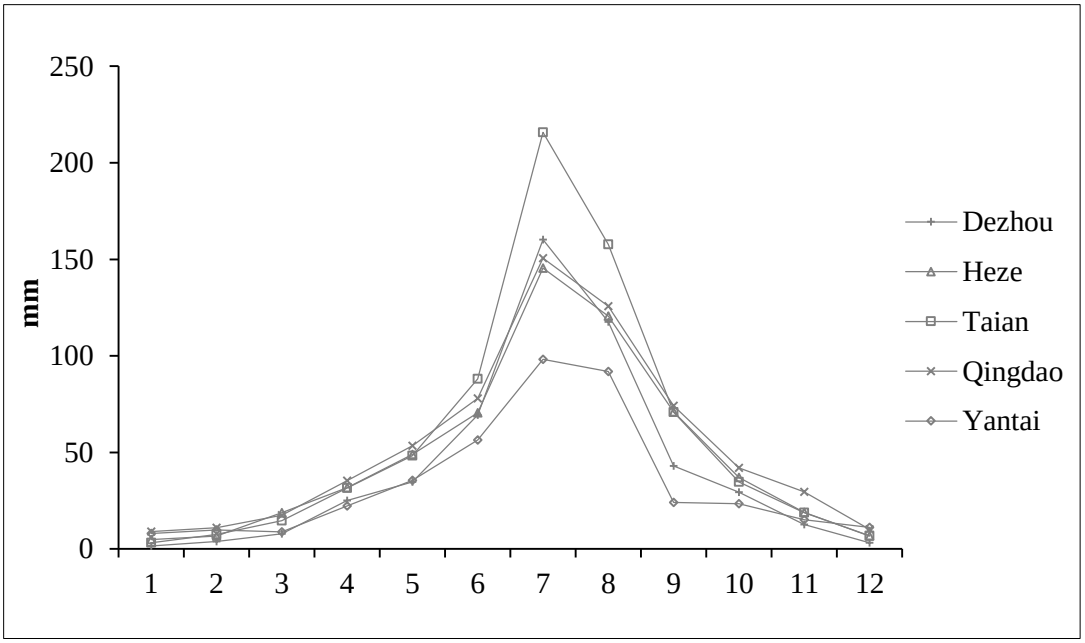

Figure 4-2 Distribution of the average monthly rainfall (1961–2006) for selected weather stations in Shandong

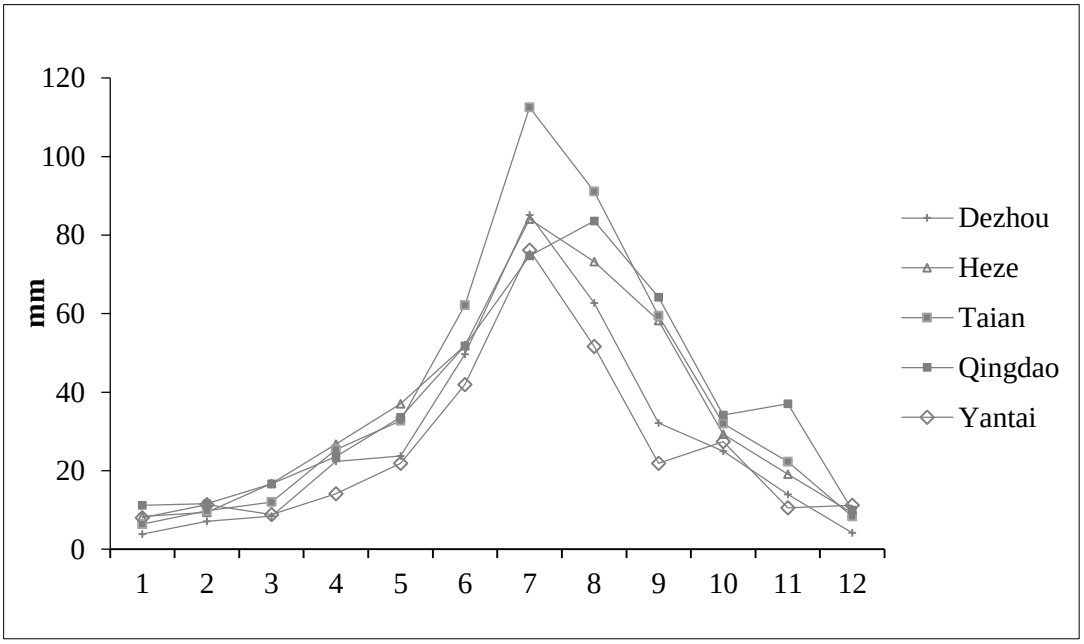

Figure 4-3 Standard deviation of average monthly rainfall (1961–2006) for selected weather stations in Shandong

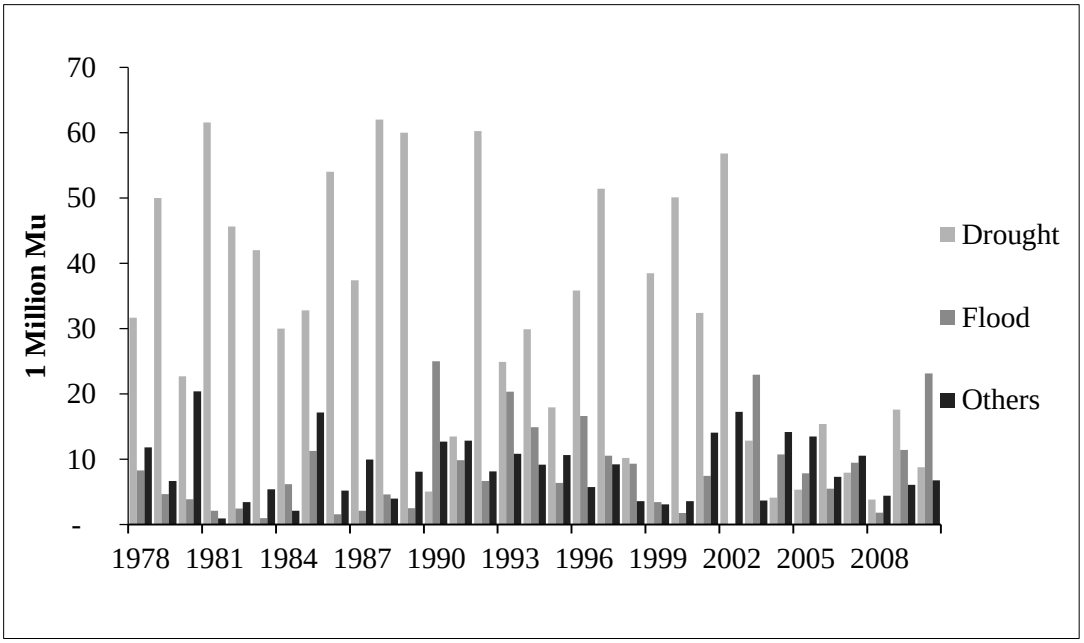

Figure 4-4 Sown agricultural area affected by drought, flood, and other perils in Shandong province from 1978 to 2011

4.2.2 **Data Preparation**

In this study, daily precipitation data of 19 weather stations from 1951 to 2006 from National Meteorological Information Center (NMIC) is collected for the corn drought risk assessment (Table 4-1). Thiessen Polygons Method is applied to interpolate historical daily rainfall data collected from 19 weather stations that covers the entire Shandong province (Figure 4-1). Thiessen Polygon defines the area around a preselected seed point, in this study the seed point is the weather station. The inference is that all points in the polygon are closer to the seed point of the particular polygon than to all the other seed points (Thiessen, 1911).

Growth Stages	**Emergence**	**Jointing**	**Anthesis**	**Graining Filling**	**Maturity**
Dates	6 Jun – 13 Jun	14 Jun – 15 Jul	16 Jul – 1 Aug	2 Aug – 22 Aug	23 Aug – 13 Sep
Duration	8 days	32 days	17 days	21 days	22 days

Figure 4-5 Corn phenological growth stages in Shandong province

Corn is the predominant crop normally planted in June and harvested in September (Figure 4-5). The sowing time of corn in Shandong starts around 6th of June. Therefore, in this study the start of sowing date is set on the 6th of June. Growth periods is phenologically divided into Emergence (Phase I: 6 June -13 June), Jointing (Phase II: 14 June -15 July), Anthesis (Phase III: 16 July- 1 August), Grain Filling (Phase IV: 2 August – 22 August) and Maturity (23 August – 13 September) (Figure 4-5). Phase I is not involved in the study of the indexing. Because, firstly due to the importance of pre-sowing soil moisture for germination the farmers will assess soil moisture very carefully before planting. Secondly, excessive rainfall in Phase I will impact the germination and emergence rate of corn, hence hinder the development of root system and make corn planted more vulnerable to drought in the following growth phases. As a result considering Phase I in indexing will imply negative correlation between the rainfall and corn yield, which complicates the accuracy of indexing and does not realistically reflect the risk exposure since the farmers can

totally minimize the Phase I related loss based on their experience. Thus Phase I is not taken into account for the development of the index.

Table 4-1 Locations and rainfall records of 19 weather stations in Shandong province

	Station ID	Latitude	Longitude	Remarks
1	54714/54715	37.2	116.3	Data before 1995 is collected from 57414
2	54725	37.3	117.3	
3	54736	37.3	118.4	
4	54751	37.6	120.4	
5	54753	37.4	120.2	
6	54764/57465	37.3	121.2	Data before 1992 is collected from 54764
7	54774	37.3	122.1	
8	54776	37.2	122.4	
9	54823	36.4	116.6	
10	54824/54830	36.5	118.0	Data before 1995 is collected from 54824
11	54827	36.1	117.1	
12	54836	36.1	118.1	
13	54843	36.5	119.1	
14	54852	36.6	120.4	
15	54857	36.0	120.2	
16	54906/54909	35.1	115.3	Data before 1995 is collected from 54906
17	54916	35.3	116.5	
18	54936	35.4	118.5	
19	54945	35.2	119.3	

4.3 Methodology

For this study, a five-step approach as elaborated in Chapter 3 is adopted to construct the SPI based drought risk analysis for corn in Shandong province:

4.3.1 Data Cleansing and Detrending

Meteorological data may contain trends caused by artificial influence such as relocation of weather station (Hartell *et al.*, 2006). In this study, the historical rainfall records of stations 57415/57465/54830/54909 suffers from the impacts of relocation in the 1990s. Therefore, detrending is conducted to remove the relocation caused noise in rainfall in prior to future risk analysis. The conclusive changes in rainfall will be identified with statistical regression to show the actual structural trend (Hartell *et al.*, 2006). The rainfall data is assumed to be stationary in a long time series. The linear detrending method (Hartell *et al.*, 2006) is adopted to decompose the rainfall data set $r(t)$ into linear trend and noises $\varepsilon(t)$ to test the statistical significant trend with student *T*-test (4-1). The noise is assumed to be normally distributed with a mean of 0 and standard deviation σ.

$$r(t) = m_0 + m_1 t + \varepsilon(t) \qquad 4\text{-}1$$

where,

m_0, m_1: intercept and slope of the linear trend line.

By comparing values for R^2 and the statistical significance of slope m_1 at a given confidence level under the hypothesis that m_1 is zero, the detrended rainfall can be obtained with the following function:

$$r^*(t) = \varepsilon(t) \ + R(t_n) \quad \text{4-2}$$

where,

$r^*(t)$: the detrended rainfall;

$R(t_n)$: the data of most recent yield.

The detrended rainfall will be used to compute the SPI in the following step.

4.3.2 **Standardized Precipitation Index (SPI)**

The calculation of SPI is based on the probability density estimation of rainfall in a given time period. Mathematically, at least 30 years of continuous precipitation data is required for the calculation (McKee *et al.*, 1993). The precipitation time series can be well fitted by a Gamma distribution as shown in the existing literatures (McKee *et al.*, 1993).

Firstly, the accumulated rainfall over a chosen period of time for each insured area is fitted with a gamma distribution (McKee *et al.*, 1993) (4-3). The shape and scale parameters are estimated by Maximum Likelihood (Akaike, 1998). Hence, the rainfall amount less than a defined amount can be determined based on the probability density. Following the method provided in the previous section, the precipitation data of each of the 19 weather stations for the continuous period from year 1951 to year 2006 are cleansed and detrended. In this study, the length of each phenological corn growth stages are chosen to be the time scale interval (Figure 4-5). The following equations show the steps of fitting the rainfall data of the region into gamma distribution:

$$g(x) = \frac{1}{\beta^{\alpha}\Gamma(\alpha)} x^{\alpha-1} e^{-x/\beta} \quad 4\text{-}3$$

$$\Gamma(\alpha) = \int_0^{\infty} y^{\alpha-1} e^{-y}\, dy \quad 4\text{-}4$$

where,

$\alpha > 0, \alpha$ is a shape parameter;

$\beta > 0, \beta$ is a scale parameter;

$x > 0, x$ is the cumulative rainfall per time scale interval;

$\Gamma(\alpha)$: the gamma function;

Secondly, due to the rainfall pattern difference of each region, the gamma distribution computed possess different mean and standard deviation. And the difference will result in different drought characteristics. Hence, the magnitude of drought events are incomparable across different regions directly. In order to compare the drought severity across different regions, the gamma cumulative distribution function is transformed to the standardized normal cumulative distribution function with a mean of zero and standard deviation of unity (4-5) (Guttman, 1999; Sadat Noori *et al.*, 2012). The value of the rainfall amount in the gamma distribution will then be given a new value with same probability in the normal distribution, which is the SPI. Positive SPI indicates greater rainfall amount than median, while negative values indicate less rainfall than median. The resulting SPI is now independent from geographical and topographical difference (Manatsa *et al.*, 2010), and normalized for temporal and spatial comparison. And can be used to compare the magnitude of drought events across different regions.

$$SPI = \frac{(x-\hat{\mu})}{\hat{\sigma}} \quad 4\text{-}5$$

where,

$\hat{\mu}$: the sample estimate of the population mean;

$\hat{\sigma}$: the sample estimate of the population standard deviation.

Theoretically, SPI represents how much the observed precipitation data departs from the mean with regards to gamma density function. The degree of the departing precipitation data has been quantified and express as the "z-score" representing numbers of standard deviation from mean in normal distribution. For example, the cumulative probability of one negative standard deviation (SPI=-1) is 0.159 and two (SPI=-2) is 0.023. Table 4-2 illustrates a dry spell expressed in SPI, in which a SPI ≤-2 is extremely dry, a SPI between -2 to -1.5 is severely dry, a SPI between -1.5 to -1 is moderately dry and a SPI between -1 to 0 is nearly normal (McKee *et al.*, 1993).

Table 4-2 Drought Categories based on Standardized Precipitation Index

SPI Values	**Drought Categories**
SPI≤-2	Extremely Dry
-2≤SPI≤-1.5	Severely Dry
-1.5≤SPI≤-1	Moderately Dry
-1≤SPI≤1	Near Normal
1≤SPI≤1.5	Moderately Wet
1.5≤SPI≤2	Severely Wet
SPI≥2	Extremely Wet

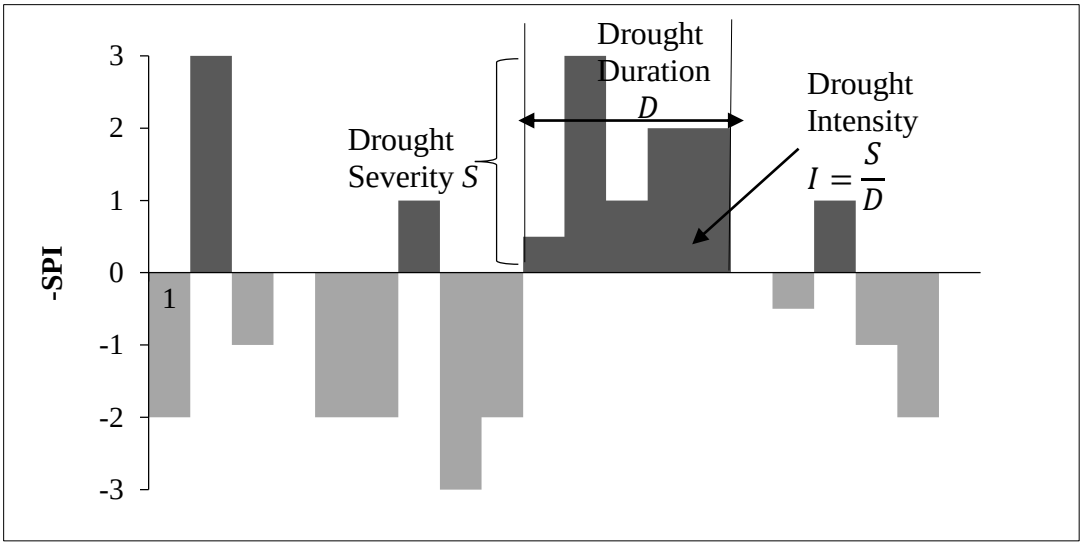

Figure 4-6 Standardized Precipitation Index (SPI) based drought duration D, intensity I and severity S

Figure 4-6 explains the SPI based drought parameters including drought events, drought duration D, intensity I and severity S:

- The drought duration D is the period when the SPI is below truncation level. The effect of drought on crop yield is an accumulative process. Hence the occurrence of normal rainfall (-1<SPI <0) at some points of the crop growth period, does not change the fact that the accumulated shortage of rainfall during the same period has already demonstrated drought occurrence. It is shown in the figure (Figure 4-6) due to the accumulated rainfall shortage at each growth period the crop yield is already impacted. Therefore the SPI=0 is marked as the truncation level.
- Drought severity S is the negative sum of the SPI in drought duration D:

$$S = -\sum_{1}^{D} SPI_i \qquad 4\text{-}6$$

- The drought intensity I is the average SPI below the truncation during the drought duration D, calculated by dividing the drought severity S by the drought duration D.

4.3.3 Gaussian Kernel Density Estimation and Diffusion Kernel Density Estimation

To quantify the drought risk during a corn growth period, the drought risk will be assessed from multiple aspects by analysing the univariate and bivariate PDFs of multi drought variables (duration, severity and intensity) defined by SPI in previous step. The univariate and bivariate PDFs estimated by DKDE and GKDE will be compared with empirical distributions by K-S test in the step. This section provides a detailed calculation process of GKDE and DEKE.

- **Standardized Kernel Density Estimation**

Kernel density estimation is firstly introduced by Rosenblatt (1956) and the general form is given by Härdle (1991):

Let $(x_1, x_2, \dots, x_n)$ denote the random variables, the density function is given by:

$$\hat{f}(x,h) = \frac{1}{nh}\sum_{i=1}^{n} K\left(\frac{x-x_i}{h}\right) \quad 4\text{-}7$$

where,

h: the bandwidth of random variables, which is also the smoothing parameter;

n: number of observations;

K: kernel function. Gaussian kernel is mathematically expressed as:

$$K(t)=(2\pi)^{-1/2}e^{-(t^2)/2} \quad 4\text{-}8$$

The density estimation can be extended to bivariate density function as the following:

$$\hat{f}(x,h)=\frac{1}{nh_1h_2}\sum_{i=1}^{n}K\left(\frac{x_1-x_{i1}}{h_1}\right)K\left(\frac{x_2-x_{i2}}{h_2}\right) \quad 4\text{-}9$$

where,

h_1h_2: the bandwidth for observations (x_{i1}, x_{i2});

K: the kernel function.

Upon determining the kernel, the bandwidth has to be chosen in the next step. Rule of thumb assumes that the underlying true density is normally distributed and targets to minimize the asymptotic mean integrated square error (AMISE) between kernel estimated density and target density (Silverman, 1986). When the Gaussian function is adopted for multivariate data, the optimal bandwidth h_d at dimension with GKDE is given by:

$$h_d=\left[\frac{4}{n(p+2)}\right]^{\frac{1}{p+4}}\sigma_d \quad 4\text{-}10$$

where,

p: the number of dimension;

σ_d: the standard deviation of distribution in dimension d;

- **Univariate Diffusion Kernel Density Estimation (DKDE)**

To estimate the density function by DKDE, the variable should be firstly rescaled to be in the domain [0,1]. Let the rescaled SPI based drought variables $x = (x_1, x_2, \dots, x_n)$ denote the series of random variables, t is defined as the bandwidth parameter h^2 and Gaussian kernel is given by:

$$\varphi(x, x_i; t) = \frac{1}{\sqrt{2\pi t}} e^{(-\frac{(x-x_i)^2}{2t})} \quad 4\text{-}11$$

which satisfies the Kolmogorov backward equation:

$$\frac{\partial}{\partial t}\hat{f}(x;t) = \frac{1}{2}\frac{\partial^2}{\partial x^2}\hat{f}(x;t) \quad 4\text{-}12$$

Therefore, the model builds on the smoothing property of linear diffusion process based on a linear partial differential equation L:

$$\frac{\partial}{\partial x}\hat{f}(x;t) = L\hat{f}(x;t) \quad 4\text{-}13$$

$$L = \frac{1}{2}\frac{d}{dx}(\alpha(x)\frac{d}{dx}(\frac{\cdot}{\rho(x)})) \quad 4\text{-}14$$

where,

α *and* ρ: arbitrary positive function on x with bounded second derivatives.

The initial condition $\hat{f}(x;0)=\Delta(x) = \frac{1}{n}\sum_{i=1}^{n}\delta(x - x_i)$, which is the empirical density of data set$x$. The Neumann boundary condition (4-15) ensures that the $\frac{d}{dh}\int \hat{f}(x;t)dx = 0$ when x ∈ [0,1].

$$\frac{\partial}{\partial x}\hat{f}(x;t)|_{x=1} = \frac{\partial}{\partial x}\hat{f}(x;t)|_{x=0} = 0 \quad 4\text{-}15$$

The analytical solution of the partial differential equation is given by:

$$\hat{f}(x;h) = \frac{1}{n}\sum_{i=1}^{n}\frac{1}{\sqrt{2\pi t}}e^{(-\frac{(x-x_i)^2}{2t})} \stackrel{\text{def}}{=} \frac{1}{n}\sum_{i=1}^{n}K(x,x_i,t)\,, x \in [0,1] \quad 4\text{-}16$$

where, the diffusion kernel K is estimated by discrete cosine transform and is defined by:

$$k(x,x_i,t) = \sum_{j=-\infty}^{+\infty}K(x,2j+x_i;t) + K(x,2j-x_i;t), x \in [0,1] \quad 4\text{-}17$$

- **Bivariate Diffusion Kernel Density Estimation**

The rescaled SPI based drought variables (duration and intensity) are denoted by $x = (x_1, x_2, \dots, x_n)$ and $y = (y_1, y_2, \dots, y_n)$. The bivariate histogram of x and y is converted by discrete cosine transform and bivariate diffusion kernel density function is given as:

$$\hat{f}(x,y) = \sum_{i=1}^{m}\sum_{j=1}^{m}\frac{1}{2\sqrt{t_x t_y}}e^{-(\frac{(x-x_i)^2}{2t_x}+\frac{(y-y_i)^2}{2t_y})} \quad 4\text{-}18$$

An improved plug-in bandwidth selection method is introduced by Botev *et al.* (2010) with a parameter t^* given by:

$$\hat{t}^* = (2\pi n(\psi_{0,2} + \psi_{2,0} + 2\psi_{1,1}))^{-1/3} \quad 4\text{-}19$$

where, $\psi_{i,j}$ is digamma function of order i through j evaluate by $\hat{t}_{i,j}$:

$$\psi_{i,j} = (-1)^{i+j}\int(\frac{\partial^{(i+j)}}{\partial x^i \partial y^j}f(x))^2 dx \quad 4\text{-}20$$

$$\hat{t}_{i,j} = (\frac{1+2^{-i-j-1}}{3}\frac{-2q(i)q(j)}{n(\widehat{\psi}_{i+1,j}+\widehat{\psi}_{i,J+1})})^{1/(2+i+j)} \quad 4\text{-}21$$

where,

$$q(l) = \begin{cases} (-1)^l \frac{1\times3\times5\times\ldots\times(2l-1)}{\sqrt{2\pi}}, l \geq 1 \\ \frac{1}{\sqrt{2\pi}} \qquad\qquad\qquad\quad , l = 0 \end{cases} \tag{4-22}$$

$$t_x = \left(\frac{\widehat{\psi}_{0,2}^{3/4}}{4\pi N \widehat{\psi}_{0,2}^{\frac{3}{4}}(\widehat{\psi}_{1,1}+\sqrt{\widehat{\psi}_{2,0}\widehat{\psi}_{0,2}})}\right)^{1/3} \tag{4-23}$$

$$t_y = \left(\frac{\widehat{\psi}_{2,0}^{3/4}}{4\pi N \widehat{\psi}_{0,2}^{\frac{3}{4}}(\widehat{\psi}_{1,1}+\sqrt{\widehat{\psi}_{2,0}\widehat{\psi}_{0,2}})}\right)^{1/3} \tag{4-24}$$

The estimation of t_x and t_y is based on the iteration procedure: compare the difference between $\hat{t}^*$ and $\hat{t}_{i,j}$, if $\hat{t}^* < \hat{t}_{i,j}$, then t_x and t_y are calculated by 4-23 and 4-24. Otherwise, $\hat{t}_{i,j}$ is updated to $\hat{t}^*$ and the previous steps are iterated until $\hat{t}^*=\hat{t}_{i,j}$.

4.3.4 **Return Period Analysis**

After the joint PDFs of drought variables (duration and intensity) are estimated by DKDE and GKDE, the joint return period derived from the bivariate cumulative probability functions (CPFs) by integrating the joint PDFs is calculated for different drought events. The return period *R* is defined as the average time recurrence interval that the magnitude of event has the probability *1/R* of being exceeded. The bivariate return period can be defined by (Li *et al.*, 2013):

$$R_{x,y} = \frac{1}{P(X\geq x_i \text{ or } Y\geq y_i)} = \frac{1}{1-K(F_X(x),F_Y(y))} \tag{4-25}$$

where,

$F(x, y)$: Joint cumulative density function of variable x *and* y;

$K(\cdot)$: the diffusion kernel function.

4.4 **Results and Discussion**

To examine the performance of DKDE and GKDE with rule of thumb bandwidth selection (Silverman, 1986) in estimating univariate and bivariate PDFs, both methods are applied to SPI per growth phase of 19 weather stations in Shandong province. Weather station 57414 is taken as an example (results of other weather stations are shown in Appendix 1). The joint return period of drought duration and drought intensity based on the DKDE are developed for the spatial drought risk analysis in Shandong province. The performance examination between DKDE and GKDE is conducted by comparing the SPI based corn drought risk for all four corn growth phases in two aspects: drought duration and drought intensity.

4.4.1 **Standardized Precipitation Index**

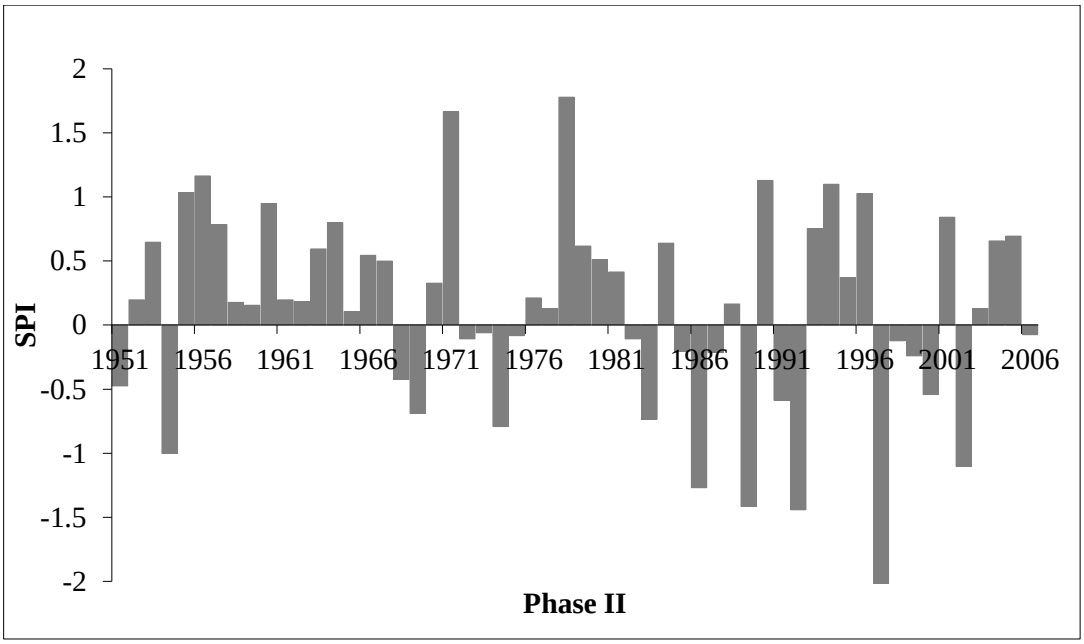

(a)

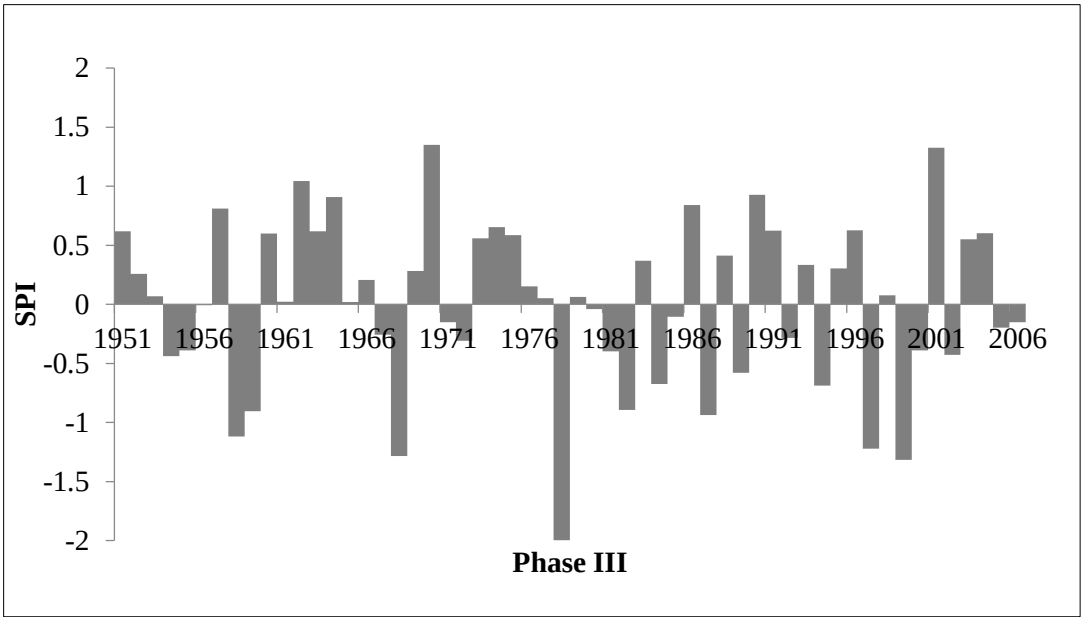
SPI
2
1.5
1
0.5
0
-0.5
-1
-1.5
-2
1951
1956
1961
1966
1971
1976
1981
1986
1991
1996
2001
2006
Phase III

(b)

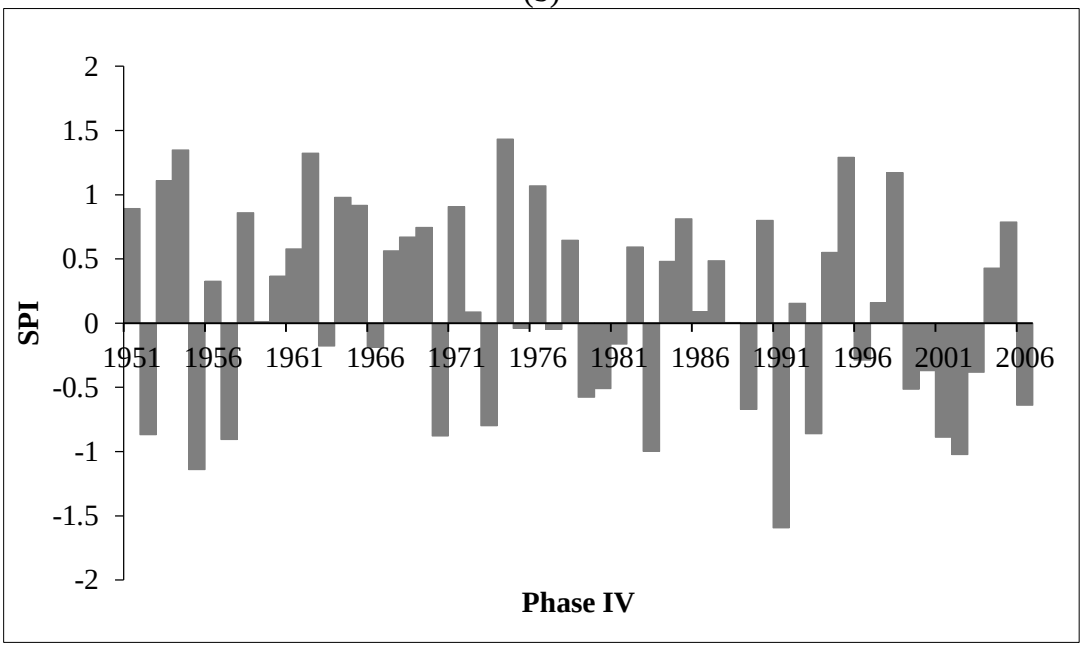
SPI
2
1.5
1
0.5
0
-0.5
-1
-1.5
-2
1951
1956
1961
1966
1971
1976
1981
1986
1991
1996
2001
2006
Phase IV

(c)

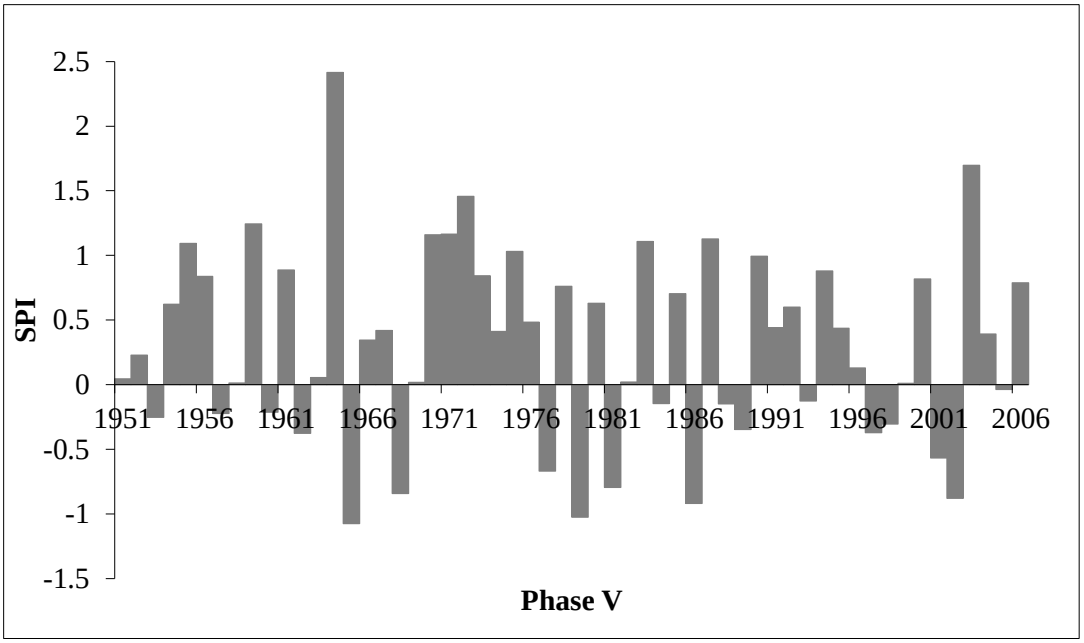

(d)

Figure 4-7 SPI per corn Growth Phase II (a), III (b), IV (c) and V (d) for Weather station 57414, 1951-2006

After cleansing and detrending cumulative rainfall of each corn growth phase per weather station, the data is converted into SPI following the method provided in 4.3. The monthly SPI per year and SPI of Phase II to V of each weather station are separately calculated. The fluctuation of SPI per growth phase (for example weather station 57414) from 1951 to 2006 (Figure 4-7) indicates that the lowest SPI is around -2 in the last 56 years. More drought events occur in Phase III and IV, which is the Anthesis and Grain Filling phase. Lots experiments and literatures have shown that the Anthesis and Grain Filling phases are the most water sensitive phases of the corn growth cycle (Allen *et al.*, 1998). It also indicates that the frequency of drought is more frequent in recent 20 years, especially in Phase II and III.

4.4.2 **Univariate and Bivariate Probability Density Function Analysis**

One thing shows that the DKDE performances better than the GKDE through examining the boundary leakage or boundary bias problem. Figure 4-8 shows the bivariate PDF of drought intensity and duration for Phase II-V estimated by DKDE and GKDE separately. Figure 4-8 (b) shows that the PDF estimated by GKDE results in negative drought intensity, and in Figure 4-8 (c) the left boundary of GKDE marginal PDF estimation extends into the negative region of drought intensity, which all indicates the poor performance of GKDE in avoiding the boundary leakage problem. The Kolmogorov–Smirnov (K-S) test at 95% confidence level shows that DKDE has a better goodness of fit of univariate PDF for drought intensity compared to GKDE. In Table 4-3 it is shown that 92% of P values of K-S test estimated by DKDE are higher than those estimated by GKDE. An overall of 76 drought intensity samples based on SPI for each growth phase and 19 samples for the whole growth period are tested. On top of that, 19 out of 114 samples are rejected by the hypothesis that the drought intensity follows the specified distribution estimated by GKDE and only 6 samples are rejected by the hypothesis that the drought intensity follows the distribution estimated by DKDE. Hence, the DKDE is chosen to be the better candidate for the bivariate PDF analysis of drought risk in the next steps.

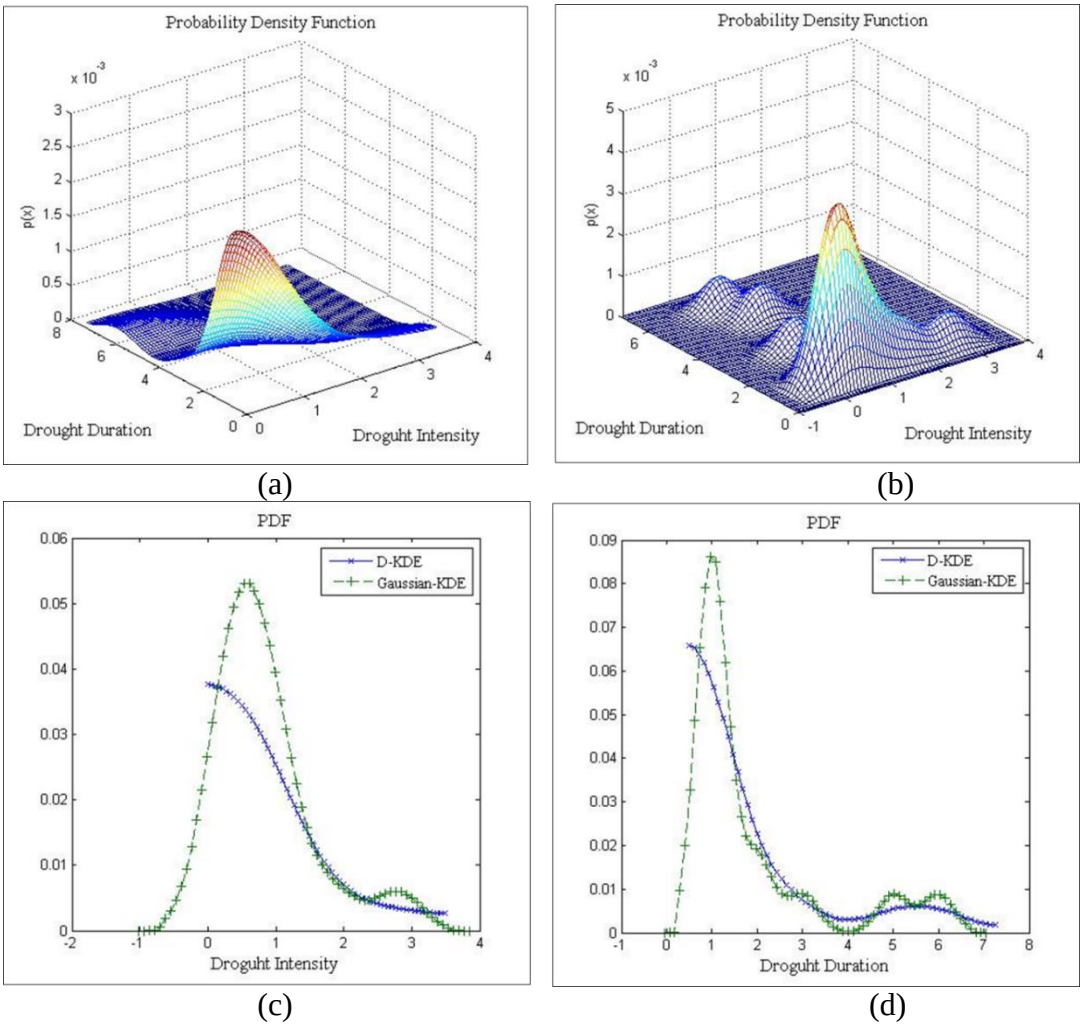

Figure 4-8 Weather station 54714 (a) DKDE estimated bivariate PDF of SPI based drought risk (PII-PV) (b) GKDE estimated bivariate PDF of SPI based drought risk (PII-PV) (c) Comparison of univariate PDF for drought intensity by DKDE and DKDE (d) Comparison of univariate PDF for drought duration by DKDE and GKDE

Table 4-3 K-S test statistics for univariate PDF of drought intensity estimated by DKDE and GKDE

	Drought Intensity											
	DKDE						**GKDE**					
ID	Whole Year	II-IV	II	III	IV	V	Whole Year	II-IV	II	III	IV	V
54714	0.5	0.6	0.2	0.0	0.2	0.9	0.7	0.1	0.2	0.0	0.1	0.7
54725	0.7	0.8	0.8	0.2	0.6	0.1	0.7	0.5	0.7	0.1	0.1	0.0
54736	0.9	0.1	0.0	0.2	0.6	0.2	0.6	0.0	0.1	0.3	0.2	0.0
54741	0.8	0.8	0.1	0.7	0.9	0.5	0.8	0.2	0.1	0.1	0.2	0.1
54753	0.7	0.0	0.8	0.5	0.3	0.2	0.7	0.0	0.1	0.2	0.0	0.0
54764	0.8	0.2	0.4	0.6	0.2	0.4	0.7	0.1	0.1	0.2	0.0	0.5
54774	0.9	0.2	0.9	0.9	0.5	0.9	0.8	0.1	0.3	0.7	0.3	0.3
54776	0.4	0.0	0.6	0.9	0.2	0.9	0.6	0.0	0.2	0.6	0.2	0.5
54823	0.8	0.5	0.9	0.9	0.9	0.8	0.8	0.5	0.3	0.2	0.2	0.3
54824	0.7	0.9	0.5	0.9	0.5	0.2	0.6	0.9	0.1	0.2	0.1	0.0
54827	0.8	0.4	0.9	0.5	0.6	0.2	0.8	0.1	0.2	0.5	0.1	0.5
54836	0.6	0.9	0.2	0.2	0.5	0.5	0.6	0.4	0.2	0.1	0.2	0.2
54843	0.6	0.9	0.9	0.9	0.9	0.8	0.8	0.6	0.3	0.2	0.2	0.3
54852	0.6	0.3	0.2	0.0	0.2	0.8	0.6	0.0	0.2	0.0	0.1	0.2
54857	0.7	0.2	0.4	0.2	0.2	0.2	0.5	0.0	0.1	0.0	0.1	0.0
54906	0.8	0.0	0.2	0.7	0.2	0.2	0.7	0.0	0.2	0.8	0.1	0.0
54916	0.8	0.7	0.5	0.9	0.7	0.1	0.7	0.5	0.0	0.2	0.1	0.0
54936	0.7	0.7	0.8	0.7	0.9	0.8	0.7	0.7	0.1	0.4	0.5	0.2
54945	0.4	0.0	0.9	0.7	0.2	0.1	0.4	0.0	0.9	0.2	0.1	0.0

4.4.3 **Return Period Analysis**

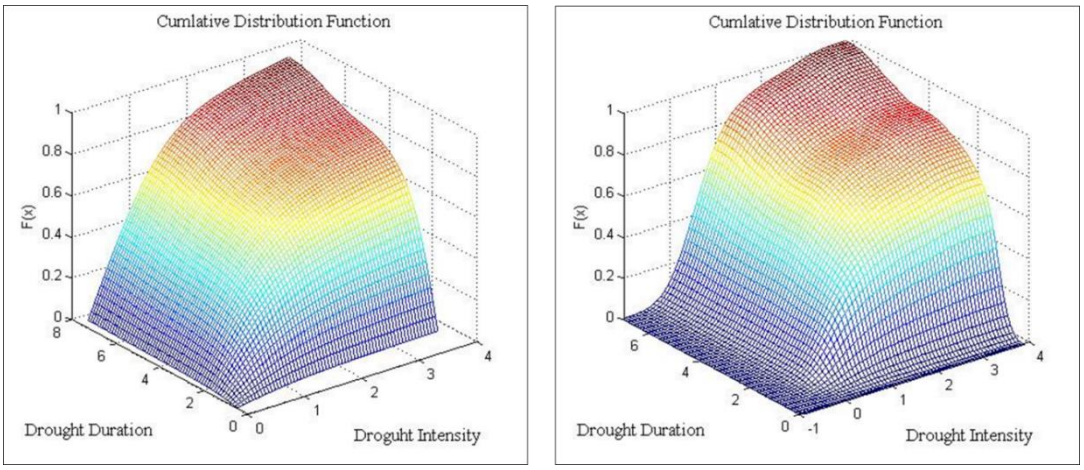

(a) (b)

Figure 4-9 (a) DKDE estimated bivariate CDF of SPI based drought risk (PII-PV) (b) GKDE estimated bivariate CDF of SPI based drought risk (PII-PV)

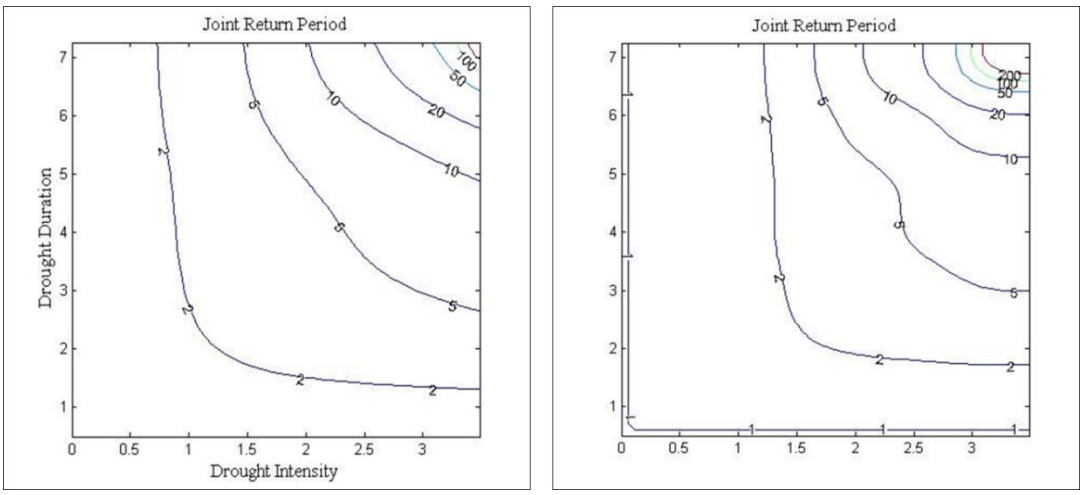

(a) (b)

Figure 4-10 (a) Joint return period of drought duration and drought severity for corn (Phase II-V) estimated by DKDE (b) Joint return period of drought duration and drought severity for corn (Phase II-V) estimated by GKDE (weather station 57414)

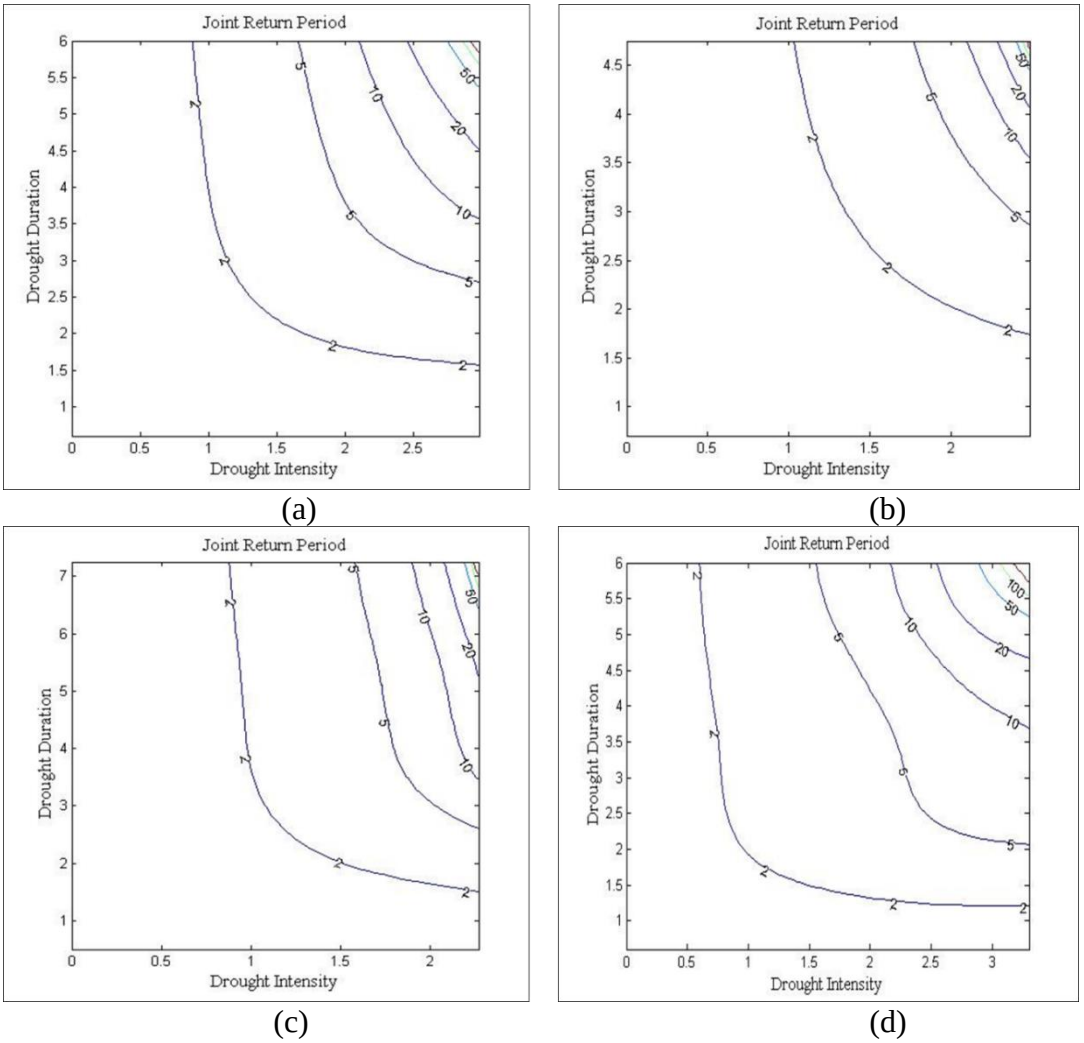

Figure 4-11 Joint return period of drought duration and drought severity for corn growth phase II, III, IV and V (weather station 57414)

The bivariate exceeding probability function is derived from the bivariate cumulative probability function (CPF) (Figure 4-9) by integrating PDF constructed by DKDE and GKDE. The bivariate exceeding probability function is later used to derive the joint return period. Comparison of joint return period estimated by DKDE and GKDE in terms of drought duration and drought intensity is shown in Figure 4-10. It indicates that both of drought duration and drought intensity estimated by Gaussian kernel are higher than the values estimated by DKDE at same joint return period.

Figure 4-11 shows the joint return period of drought duration and intensity in Phase II, III, IV and V estimated by DKDE.

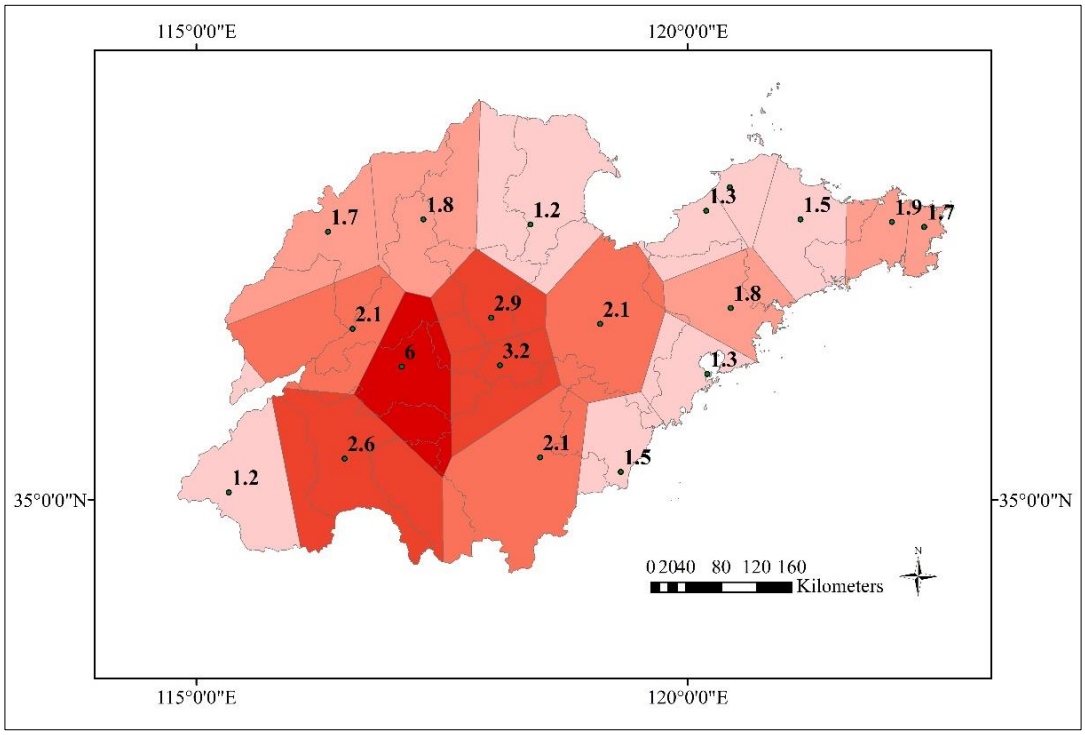

Figure 4-12 Map of Shandong province with joint return period with drought duration of 1 years and drought intensity of 2 for whole growth phases (Phase II-V)

The joint return period by DKDE for whole Shandong is computed under the assumption that drought duration is 1 year and drought intensity is 2. The spatial distribution joint return period for whole growth phases and Phase II, III, IV and V in Shandong are shown separately in Figure 4-12 and Figure 4-13. A higher return period characterized by the given drought duration (1 year) and drought intensity (-SPI= 2) can be observed in central region of the province, and the return period is lower in north east and southeast of the province throughout all the growth phases (Phase II-V). Regions around the weather station 54936 shows the highest return

period (6.7) of drought risk in Phase II among the 19 regions. In Phase III and IV, the average return periods of all regions are approximately 2, while region around weather station 54936 and central region of the province show the highest return period. For Phase V, weather station 54836 locating in the central of Shandong shows the highest return period (5.3). The spatial distribution of joint return period with duration 1 and intensity 2 in Shandong shows a higher return period for the central area, indicating a lower drought risk potential in central region comparing to the other regions.

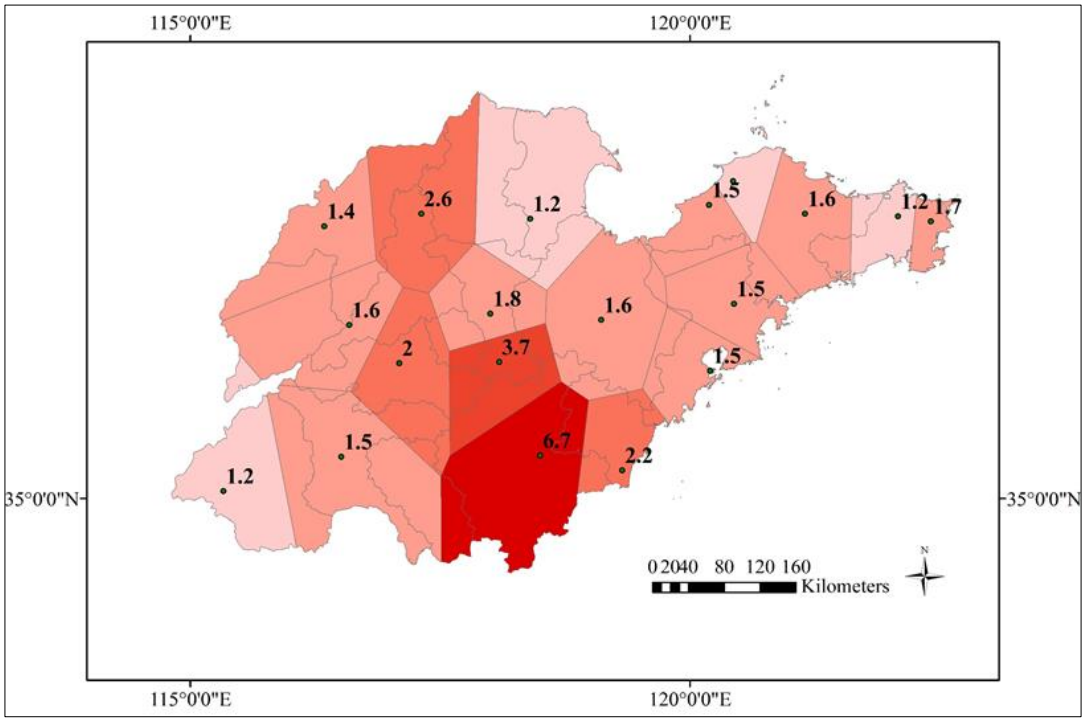

(a)

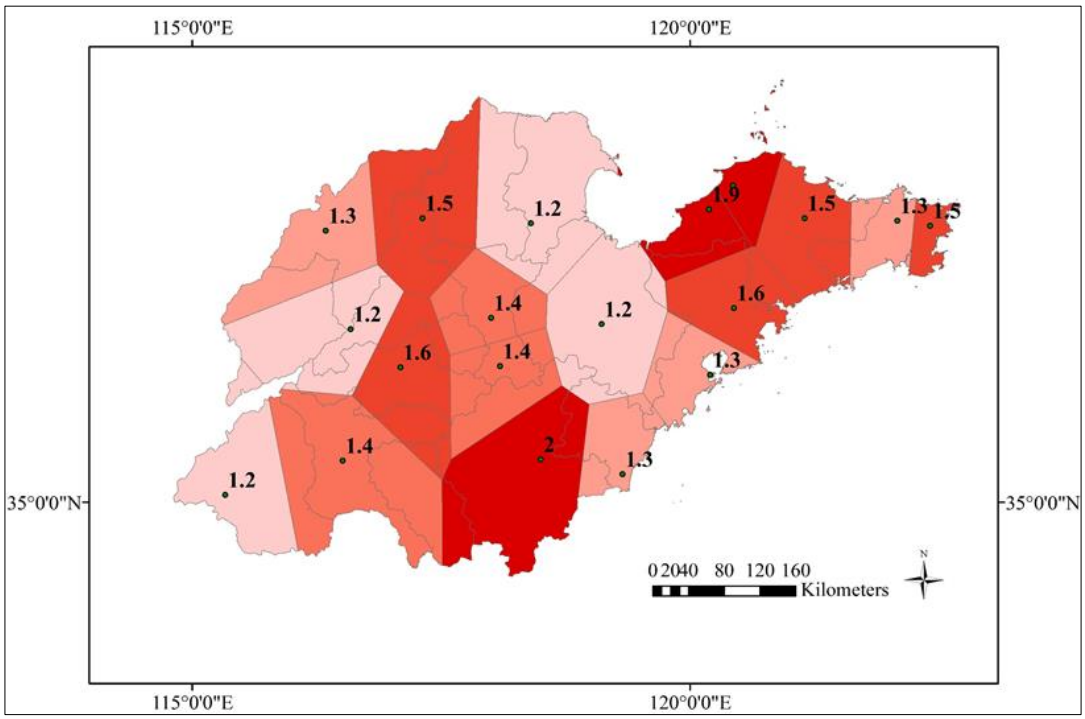
115°0'0"E
120°0'0"E
35°0'0"N
1.3
1.5
1.2
1.9
1.5
1.3
1.5
1.2
1.4
1.2
1.6
1.6
1.4
1.3
1.4
2
1.3
1.2
0 20 40 80 120 160
Kilometers
N

(b)

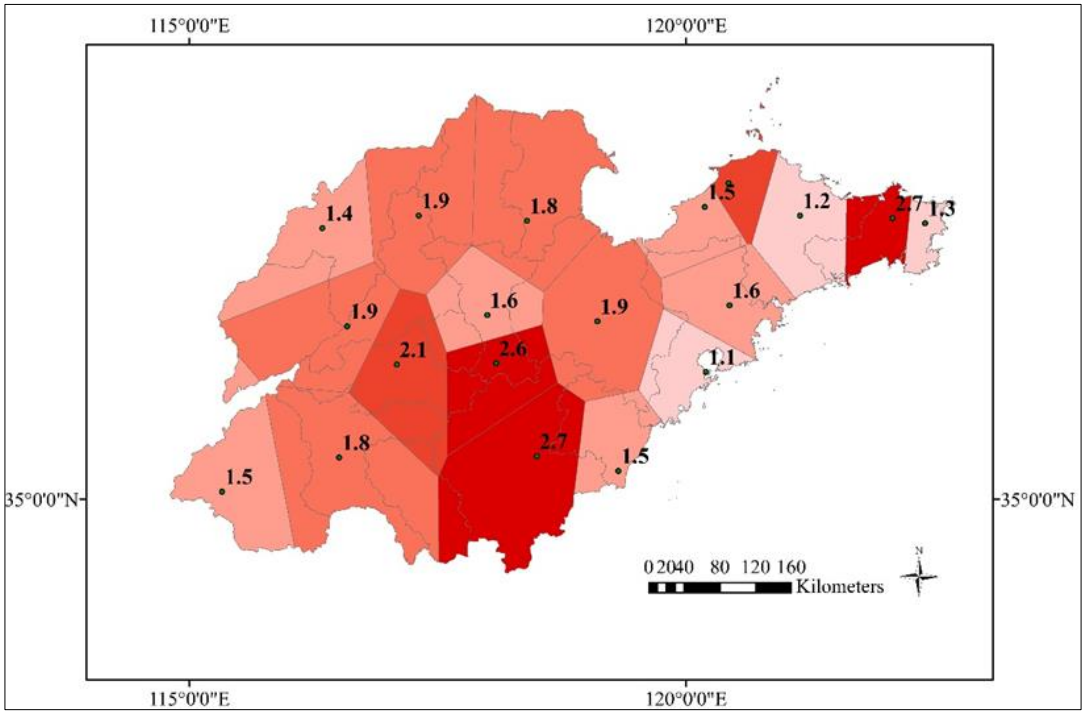
115°0'0"E
120°0'0"E
35°0'0"N
1.4
1.9
1.8
1.5
1.2
2.7
1.3
1.9
1.6
1.9
1.6
2.1
2.6
1.1
1.8
2.7
1.5
1.5
0 20 40 80 120 160
Kilometers
N

(c)

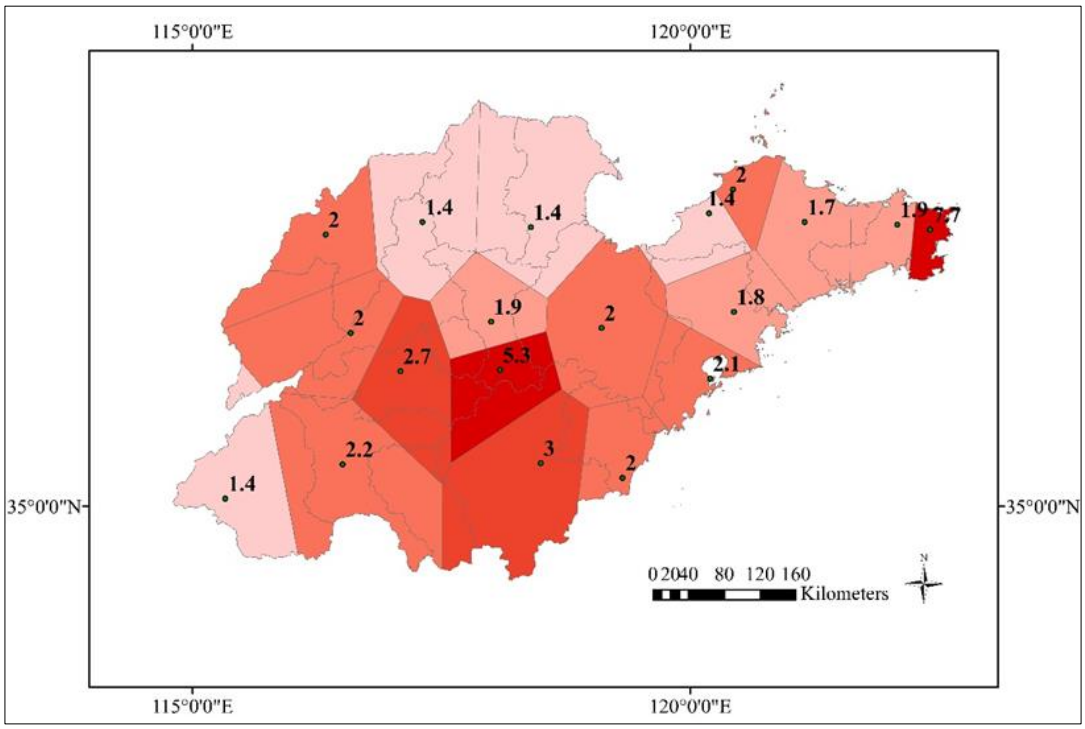

(d)

Figure 4-13 Map of Shandong province with joint return period with drought duration of 1 years and drought intensity of 2 (a) Phase II (b) Phase III (c) Phase IV (d) Phase V

CHAPTER 5

DEVELOPMENT OF RAINFALL INDEX INSURANCE FOR CORN IN SHANDONG, CHINA

5.1 Introduction

The development of rainfall deficit index insurance for distinctive phenology phases reflecting the corn water sensitivity of five counties in the prefecture-level city of Tai'an, in Shandong province, is discussed in detail in this chapter. Given China's severe drought risk exposure and underdeveloped agriculture insurance market, the development of such insurance is arguably essential.

The objectives of this chapter are: (i) to develop a Cumulative Rainfall (CR) index for each individual growth phase and a Total Rainfall (TR) index for the entire growth phase of corn in five counties in Shandong province; (ii) to evaluate the viability of the developed indices from an insurer's point of view.

5.2 Data

5.2.1 Study Area

Shandong province is a part of the Northern China Plain located between longitudes 34°N to 38°N and latitudes 114°E to 122°E (Figure 5-1). Shandong is known to have a flat topography and a temperate climate which makes it the third largest grain-producing province, with a 10% contribution to national grain production in 2012. Corn is the predominant crop, normally planted in June and harvested in September.

Xue (2004) identified drought as the key peril for crop production in Shandong; this is further proven by area-affected data ranked by disaster, which shows that 64% of the area affected by natural disasters was hit by drought (Yearbook, 1979-2012).

Shandong province is one of the earliest provinces to adopt agriculture insurance, back in 1984. The agriculture insurance market in Shandong expanded quickly in the first ten years, but has grown slowly in the last ten years. In order to make crop insurance affordable to farmers, government agencies subsidize the cost of the insurance premium by 80%. With the subsidies from the government, the total premium income of Shandong increased to 170 million USD in 2013. Indemnity-based agriculture insurance has been introduced for the main crop types (corn, wheat, cotton) and normally covers perils including drought, flood, frost, hail and disease. However, drought is not covered for corn in Shandong. For grain crops, insurance issues a flat premium rate, which is 3.3% of the sum insured (300 RMB/mu). The sum insured is meant to cover the farmer's production cost, but unfortunately it is currently only able to make up 40% of the total corn-production market value and cost per surface unit. A study of the agriculture insurance market of China has also found that a majority of farmers feel that the total sum insured is too low to cover the production cost (Gao, 2014).

For this research, five counties in the prefecture of Tai'an (Figure 5-1), with a total number of 78 townships and 191,000 hectares of corn plantation, were selected as the study area for index development. The area has generally flat topography and low irrigation levels, which makes it an ideal territory for the development of a rainfall index product.

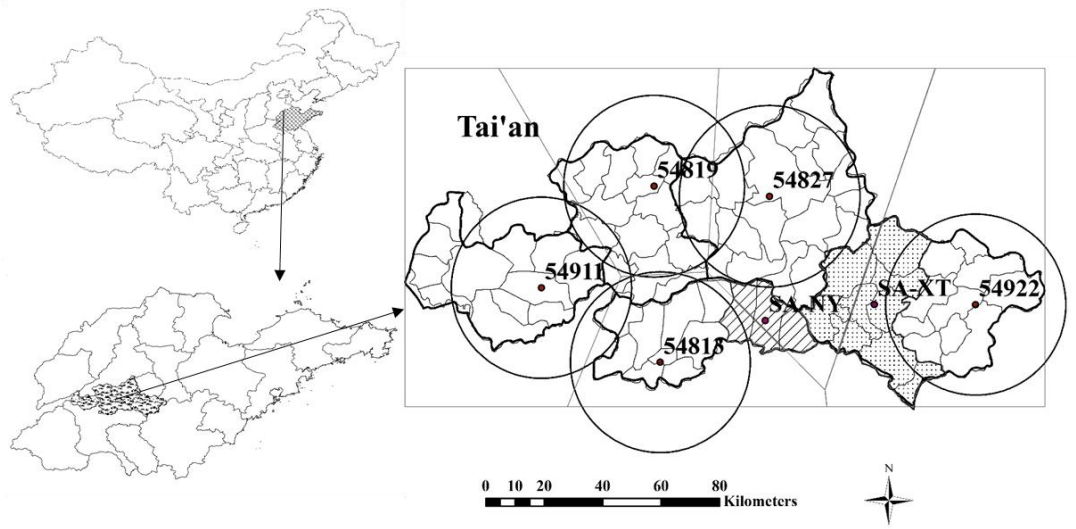

Figure 5-1 Location of Shandong province in China (top left), Tai'an prefecture within Shandong province (bottom right), the study area with five counties (bold outlines) and 78 townships (thin outlines), the locations of weather stations (dots with numbers), and the special study areas of SA-XT (dotted) and SA-NY (striped)

5.2.2 Rainfall Data and Agriculture Production Data

Daily rainfall data is available from five weather stations of the Shandong Meteorological Bureau for the period 1980–2011 and each weather station covers one county (Table 5-1). The weather data does not contain missing values over the corn-growing period, the consistency of the data is ensured. Data on corn-sown areas, production and yield are available at county level and township level from the Statistical Year Books of the relevant counties (Table 5-1) (Yearbook, 1989-2011).

To consolidate the raw data for this research, the author conducted a survey in Daiyue county, interviewed farmers and input suppliers, and approached the Tai'an Bureau of Agriculture to obtain data on: (i) corn-growth phases in Tai'an prefecture; (ii) corn prices per county; (iii) production costs of corn, including the costs of key

components such as seed, fertilizer, land rent, labor and equipment for each corn-growth phase.

Table 5-1 Rainfall and corn-yield data for the five counties and two Special Areas in study area

County	Station ID	Townships (Number)	Daily Rainfall	De-trending Cleansing	Average Yield (kg/mu)
Daiyue	54827	15	1980–2011	Yes	523
Feicheng	54819	14	1980–2011	Yes	513
Xintai	54922	12	1980–2011	Yes	456
Ningyang	54813	12	1980–2011	Yes	494
Dongping	54911	14	1980–2011	Yes	494
Special AreaXT	\	8	1980–2011	Yes	469
Special AreaNY	\	3	1980–2011	Yes	493

	De-trending Cleansing	Weather Station Circle	Township Corn Yield	County Corn Yield
Daiyue	Yes	25 km	1981–2010	1981–2010
Feicheng	Yes	25km	1989–2010	1989–2010
Xintai	No	25km	1986–2010	1986–2010
Ningyang	Yes	25km	1989–2010	1989–2010
Dongping	Yes	25km	\	1989–2010
SA-Xintai	Yes	\	1986–2010	1986–2010
SA-Ningyang	Yes	\	1989–2010	1989–2010

**Average Yield is based on the last 5 seasons' yield for the townships within the defined 25-km circle around the weather stations and the townships within the special area polygons*
**15 mu equals 1 hectare*

After the results of the survey in Daiyue county were obtained, individual corn-growth phases were defined for the study area as follows: Sowing (Phase I, 6–13 June), Jointing (Phase II, 14 June–15 July), Anthesis (Phase III, 16 July–1 August), Grain Filling (Phase IV, 2–22 August), and Maturity (Phase V, 23 August–13 September).

The corn price of 2012, as obtained from the survey, was 2.2 RMB/kg (0.36 USD/kg) (Table 5-2). The commercial production value of corn is county dependent, computed using the corn price and five-year average yield. The production cost, which indicates the farmer's investments in corn production to calculate the total sum insured under the index insurance, is set at 65% of the commercial production value. The sub-sum insured per growth phase was set at: 10% (Phase I), 30% (Phase II), 50% (Phase III), 70% (Phase IV), and 100% (Phase V) of the total sum insured based on the cumulative production costs in each phase.

Table 5-2 Market value and production cost of corn for farmers in Shandong in 2012 (Yearbook, 2013)

Total Value	**Corn Yield**	**Market Price**	**Profit**
RMB/mu	*kg/mu*	*RMB/kg*	*RMB/mu*
1101	501	2.2	277
Production Cost	**Fertilizers**	**Equipment**	**Rent**
RMB/mu	*RMB/mu*	*RMB/mu*	*RMB/mu*
824	186	115	131
	Seeds	**Chemicals**	**Labor**
	49	16	321

**Production cost=seeds + chemicals + fertilizers+ equipment + rent + labor + others*

**Market price=summer corn yield × market price per mu=production cost + profit*

5.3 Methodology

Numerous approaches to determining rainfall indices have been developed over the years, which are described and summarized in (Dinku *et al.*, 2009; Skees *et al.*, 2009; Stoppa and Manuamorn, 2010; Skees, 2011). For this research, a three-step approach was adopted to develop a different rainfall index for each growth phase and an overall rainfall deficit index for the entire growth phase: (i) definition of the insured area and data preparation, which includes trend and correlation analysis; (ii) index development, including the determination of triggers, exits and ticks; (iii) payout analysis, which involves the calculation of premium rates for indices risk, payout frequency and amount analysis using Historical Burn Analysis (HBA).

5.3.1 Definition of the Insured Area and Data Preparation

As mentioned in previous chapters, the correlation between the actual yield loss and insurance payout must be kept at an acceptable level in order to maintain a minimum basis risk. Ideally, the rainfall indices should be developed at high resolution to account for the spatial variability of rainfall and topography. Several studies have revealed that an area covered by a rainfall index needs to be within an effective radius of 20–30 km from the weather station to maintain an acceptable level of spatial basis risk (Hellmuth *et al.*, 2009; Skees *et al.*, 2009). For this study, an effective radius of 25 km was chosen to develop the indices (Figure 5-1). However, there were three areas located outside the 25-km effective radius of any of the five weather stations. These areas were thus treated as Special Areas (SAs). Only two of these non-covered areas, SA Xintai (SA-XT) and SA Ningyang (SA-NY) possessed enough data to develop rainfall indices based on the spatial interpolation of weather data from surrounding weather stations. SA Dongping (SA-DP) was not studied because rainfall data from neighboring counties was unavailable.

An alternative approach to the commonly used inverse distance method (e.g. as employed by Chen and Liu (2012)) to spatially interpolate rainfall is the Weighted Thiessen Polygons (WTP) method. The WTP method considers areal average precipitation values (Teegavarapu and Chandramouli, 2005) and uses the weather station weight as seed points (Sen, 1998; Fiedler, 2003). The weather station weight is calculated by dividing the segment area by the total area of the Thiessen Polygons. For this study, the WTP method was used to determine the daily rainfall (R_{SA}) for SA

Xintai (SA-XT) and SA Ningyang (SA-NY) based on the data from the surrounding weather stations:

$$R_{SA} = \frac{\sum_1^n A_i R_i}{\sum_1^n A_i} \quad 5\text{-}1$$

where,

A_i: the Area segmentation i of the Special Area;

R_i: the daily rainfall of given weather station i; and

n: the number of segmentations in the Special Area.

Different farming practices such as changes in seed types, fertilizer application, irrigation and crop protection may vary over time to cause unwanted trends in the historical data. The unwanted trends will amplify the technical basis risk and hence lower the correlation between the underlying index and risk exposure. Therefore, yield data have to be analyzed to reveal and remove statistically significant trends, in order to achieve meaningful index development. Firstly, yields are calculated for each insured area by aggregating the township-level farming area and the production of that area. In order to remove the statistically significant trends from the total yield, the data should go through the process of de-trending. With reference to existing studies, a linear de-trending methodology with a Student's *T*-test at 95% confidence level (e.g. as employed by (Hartell *et al.*, 2006; Breustedt *et al.*, 2008)) was used for this thesis to determine the significance in trends. According to the results, all areas except Xintai showed a statistically significant positive yield trend (Table 5-1), which was removed for the development of the rainfall indices. In order to relate rainfall

data per corn-growth phase, the de-trended data was used to compute yield deviations with a three-year moving average.

In the next step, the rainfall amount of each corn-growth phase (Phases I–V) was correlated to yield the deviation for each insured area and historical time series to perform a Pearson correlation analysis. The value of the correlation coefficient denotes the level of influence of rainfall per growth phase on the overall yield volatility. In the cases where the correlation coefficient is less than 0.1, the rainfall of the specific growth phase is meant to be only responsible for less than 10% of the overall yield volatility. As a result the relevant growth phase will not be considered for the development of the indices.

5.3.2 **Index Development**

The development of a rainfall deficit index for insurance purposes involves the determination of the following key components: (i) definition of index; (ii) the Trigger, i.e. the threshold rainfall amount – the index pays out if the rainfall amount falls below it; (iii) the Tick, which is the monetary payout per rainfall unit (e.g. RMB/mm); (iv) the Payout Function, which defines the way of the payout, either linear (constant payout) or digital (the entire payout is made as soon as the Trigger is reached); (v) the Exit, which is the rainfall amount that stops the index from paying once is beneath. The index only pays out if the actual rainfall measured at a weather station for the relevant phases is below the Trigger and above the Exit.

The Trigger is often determined by the water requirement levels for each growth phase, which is available from government resources. The water requirement defines

the amount of water required by a crop in a given time period to compensate for evapotranspiration loss under field conditions (Allen *et al.*, 1998). The term 'water requirement' encompasses water-related elements such as rainfall, evapotranspiration, irrigation, soil-water holding capacity and non-water-related elements like crop characteristics. The existing rainfall deficit index studies were only based on the lacking of rainfall and such studies normally assign a fixed index for all insured areas throughout the year. This study attempts to improve the index accuracy by using an alternative approach, in which Triggers and Exits are statistically determined for each insured area and corn-growth phase. The CR index is determined based on total rainfall amount in each growth phase.

Firstly, to derive the weighted coefficient for a given growth period, a multiple linear regression analysis is carried out between the yield reduction and rainfall amount of each growth phase. The correlation coefficient W_m for a given phase is then weighted by division of the sum of the correlation coefficients:

$$N_m = \frac{W_m}{\sum_1^n W_m} \qquad 5\text{-}2$$

Secondly, it is assumed that yield reductions and rainfall are non-linearly correlated following a 2nd order polynomial distribution (Zaw and Naing, 2008). The hypothesis is tested using an ANOVA regression and an F-test at 90% confidence level:

$$YL_{ei} = a_o + a_1 * N_m * CR_{mi} + a_2 * (\mathrm{N_m} * \mathrm{CR_{mi}})^2 \qquad 5\text{-}3$$

where,

YL_{ei}: the estimated yield reduction of year i;

N_m: the weighted coefficient for a given growth phase m;

CR_{mi}: the CR index for a given growth phase m in year i;

a_o, a_1, and a_2: intercepts and coefficients.

Thirdly, the Trigger and Exit analysis reveals the relative frequency of the yield reduction for a certain rainfall amount per growth phase. Trigger and Exit of payout is derived from the combination of parametric analysis of historical yield loss at township level and polynomial regression analysis of yield loss against the weighted cumulative rainfall per growth phase:

(i) The probability density function estimation of the yield reduction at township level with the Maximum Likelihood method and Kolmogorov–Smirnov (K–S) test can provide the relative frequency curve of corn-yield reduction in the region.

(ii) The Trigger (τ_m) is derived from the polynomial function, where the independent value is the mean of the yield reduction.

(iii) The Exit (μ_m) is computed when the cumulative relative frequency of the yield reduction is 10%. The limit is computed by substituting the Exit (μ_m) rainfall value into the payout function.

(iv) The Tick T_m is calculated by dividing the sum insured for each growth phase by the difference between the Trigger and the Exit of each growth phase.

In the study, a linear payout function is applied which is explained in the next section. The same procedure was used over the entire growth phase for the Total Rainfall (TR)

Index, which is defined as the sum of the weighted total rainfall amount per growth phase in the following equation:

$$TR = \sum W_m * CR_m \qquad 5\text{-}4$$

5.3.3 **Payout Analysis**

To analyze the payouts of the deficit rainfall indices over time, a rainfall data series was run against the indices for each insurance area, using the Historical Burn Analysis (HBA) method. The HBA assumes that the historical index time series is statistically consistent and independent from other historical indices (Jewson and Brix, 2005). It derives the historical payout of the index over the past *n* years under today's conditions by using the same Trigger and Exit to establish the annual expected loss. This provides an effective illustration of the distribution of historical insurance payouts (Alexandridis and Zapranis, 2012). In order to quantify the performance of the index, a correlation analysis is undertaken between the payouts over the growth phases and yield reductions for each year and insured area. The payout *(P)* for a given growth phase and deficit rainfall index is calculated as

$$P = \min(\sum_1^n min\left(max\left(\frac{(CR_m - \mu_m)}{(\tau_m - \mu_,)}, 0\right) * T_m, M_m\right), T), \tau > \mu \qquad 5\text{-}5$$

where,

CR_m: the cumulative rainfall per growth phase m;

μ_m: the Exit per growth phase m;

τ_m: the Trigger per growth phase m;

T_m: the Tick per growth phase m;

M_m: the Sum Insured per growth phase m;

T: the Total Sum Insured for the insurance contract.

It should be noted that the total payout is limited to a pre-defined amount, referred to as the Total Sum Insured, which is normally pre-agreed in a rainfall index insurance contract. This allows the insurer to limit the total payout over the entire growth phase.

The Pure Premium is the mean annual payout and is calculated by aggregating historical payouts throughout a number of years then divided by the number of years. Using the Pure Premium, the insurer typically calculates the Commercial Premium by adding (i) the costs of distributing and administrating the index product; (ii) a catastrophe loading to account for the fact that large loss events might not have occurred in the historical time series; (iii) a data-uncertainty loading based on the Central Limit Theorem with an upper-bound uncertainty level (90%), to reflect the uncertainty about the quality and length of the underlying weather data. For this study, Risk Premium with only data uncertainty was calculated, following the methodology of the World Bank (2011):

$$Risk\ Premium = \frac{\sum_1^k \sum_1^n P_{im}}{k} + \alpha * \frac{\sigma}{\sqrt{k}} \quad 5\text{-}6$$

where,

P_{im}: the payout per growth phase m in year i;

n: the number of growth phases;

k: the number of years with available daily rainfall data;

α: an uncertainty loading at 90% confidence level;

σ: the standard deviation of the total payout of the index of the past years.

5.4 Results and Discussion

For this study, the CR Index for five counties and two Special Areas was developed. The results are discussed with regard to three aspects: (i) the relationship between the CR index and yield; (ii) the correlation between the index payouts and yield reductions for basis risk indication; (iii) a general comparison between the index insurance and the existing MPCI corn insurance policy. The county of Daiyue and the Special Area of SA-Xintai are taken as examples to illustrate the results.

5.4.1 Relationship between Rainfall and Yield

Both CR index over corn growth period (Figure 5-2) and yield levels (Figure 5-3) show similar behavior across the insured areas and time (1985–2011), which is to be expected given the close proximity of the counties. The CR indices over the corn growth season (1 June to 13 September) show a high inter-annual volatility (Figure 5-2). Wang *et al.* (2014), in their study of Shandong, noted the occurrence of drought in 1989, 1992, 1997 and 2002, which is consistent with the findings of this chapter. At first, the corn yield shows an overall increasing trend from 1985 to 2000, with declines in 1989 and 1992. After that, the corn yield shows a decline from 2001 to 2002 and a gradual increase since 2003 (Figure 6-3). The overall increase in corn yield from 1985 to 2000 was a result of the change in farming practices, and hence detrending is required to remove the farming practice improvement trend in order to

identify the impact of drought better. Even without detrending, drought years (reduction in accumulative rainfall) can be spotted in the rainfall data, as well as the yield data in 1989, 1992 and 2002. A high correspondence of rainfall distribution over the corn-growth period with corn yield was noticed at the different weather stations, indicating that the reduced rainfall led to low yield.

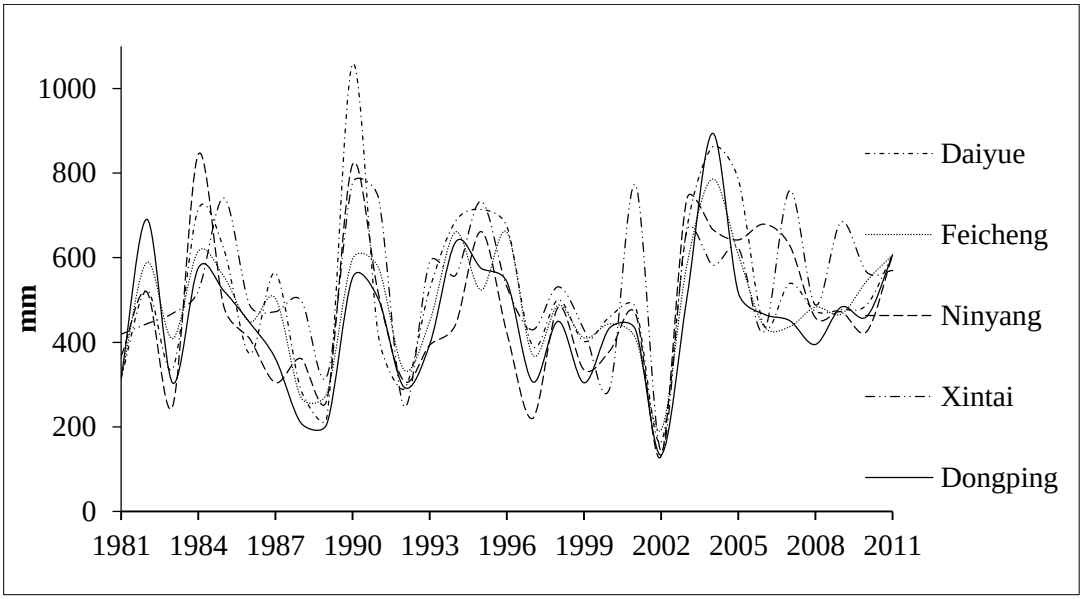

Figure 5-2 Cumulative Rainfall (millimeters) over the corn-growth period (1 June to 13 September) for the five counties in the study area for the period 1981–2011

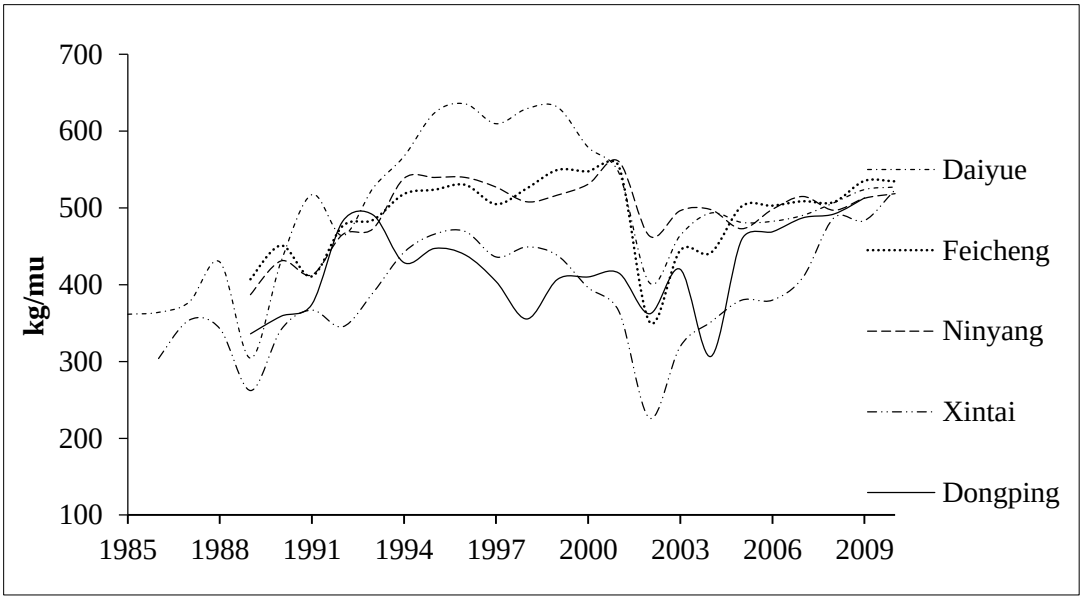

Figure 5-3 Corn yield in the five counties in the study area (1985–2010)

The correlation analysis between CR index per growth phase and yield reduction (Table 5-3) showed the following:

(i) Negative correlations during Phase I (Sowing) in all insured areas except Dongping. Excessive rainfall in Phase I will disrupt the soil moisture content and impact the root development and germination process. The root system will be prevented from growing deeper and the corn will be more vulnerable to drought in subsequent growth phases.

(ii) The highest positive correlation coefficients (0.55–0.69) during Phase II in every insured area. This is because of that Phase II is the Jointing phase, it is the period when the growth of the plant becomes highly dependent on water availability.

(iii) Negative or low correlation between yield reduction and CR index in each growth phase in Dongping, which indicates that it is not an ideal region to

develop the rainfall-based index. This could be because Dongping has the highest irrigation coverage of all the counties, and an inner lake that can further moderate the drought exposure of corn farmland.

Table 5-3 Pearson correlation coefficient between yield reduction and CR index for each corn-growth phase

County	PI	PII	PIII	PIV	PV
Daiyue	-0.37	0.55	0.25	0.38	0.29
Feicheng	-0.33	0.59	0.25	0.15	0.15
Xintai	-0.25	0.59	0.33	0.20	0.43
Ningyang	-0.45	0.64	0.28	0.29	0.51
Dongping	-0.01	-0.1	-0.27	-0.36	0.12
SA-Ningyang	-0.48	0.69	0.24	0.54	0.20
SA-Xintai	-0.35	0.69	0.2	0.32	0.45

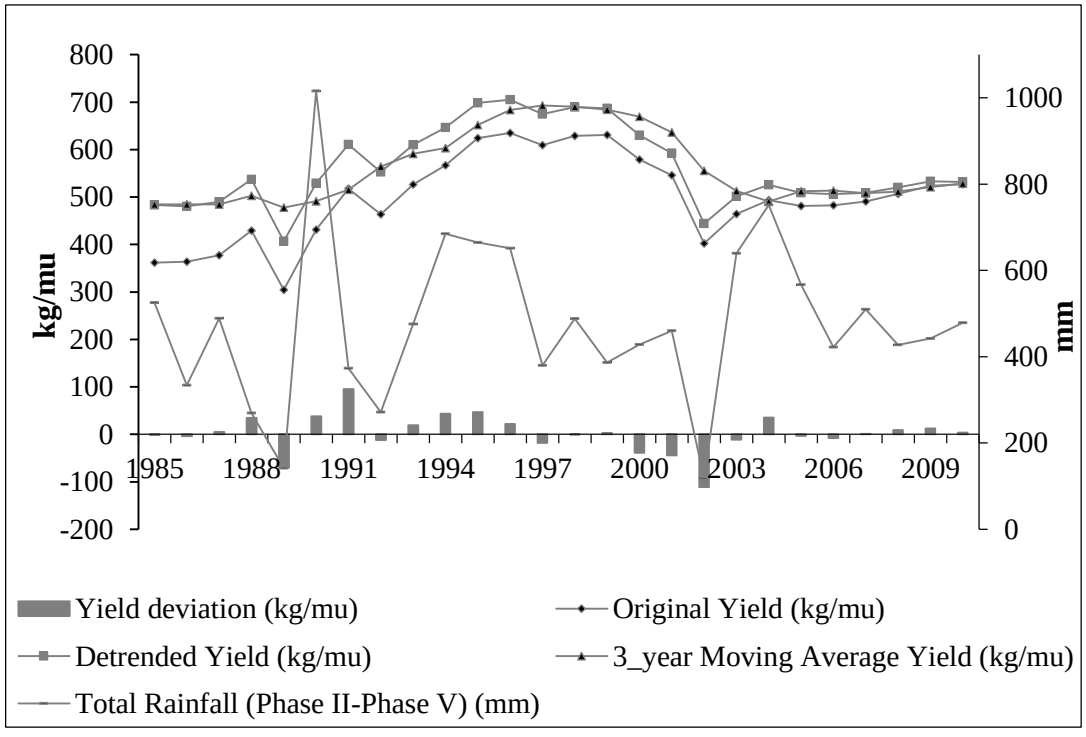

Figure 5-4 Detrended corn yield and cumulative rainfall from Phase II to Phase V in Daiyue county (1985–2010) with yield reduction compared with the 3-year moving average yield

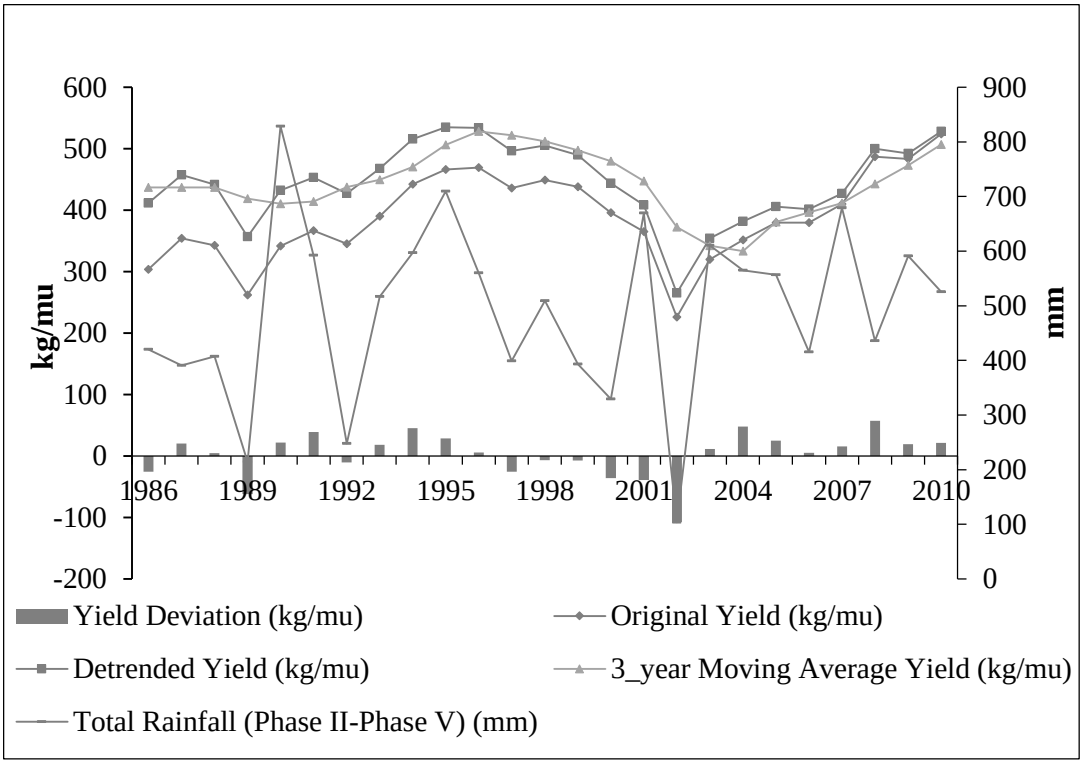

Figure 5-5 Detrended corn yield and cumulative rainfall from Phase II to Phase V in SA-Xintai (1986–2010) with yield reduction compared with 3-year moving average yield

Figure 5-4 and Figure 5-5 show the detrended corn yield with yield reduction, plotted against the CR index for Phase II to Phase V of the corn-growth phases in Daiyue and SA-Xintai. The historical county-level average corn yields in both Daiyue and SA-Xintai show a slightly increasing trend from 1985 to 2010, with huge yield losses in 1989, 2000, 2001 and 2002, and slight yield reduction in 1992, 1997 and 2003. The figures also show that in 1989, 1992 and 2002, huge rainfall deficits occurred. The closely matched years of yield reduction and rainfall deficit indicate that the shortage in rainfall was likely the cause of the reduced corn yield. This explanation can be further extended to explain the statistics of 2000 and 2001, when cumulative rainfall amounts were above average and yield levels were below normal. The

excessive rainfall that occurred during Phase III and Phase IV of 2000 and 2001 probably decreased the corn pollination, leading to the reduced yield. Since the main objective of this chapter was to develop a deficit rainfall index but examine excessive rainfall, such excessive rainfall cases have not been further investigated.

5.4.2 **Index Development**

To derive the Trigger and Exit of every growth phase, the CRD index is at first weighted by the weighted coefficient. The weighted coefficient is deduced based on the multiple linear regression between yield reduction and CRD index per growth phase using the following

$$y_{daiyue} = 0.12 * P_{II} + 0.16 * P_{III,IV} + 0.18 * P_V - 90.8 \quad \text{5-7} y_{saxintai} =$$

$$0.2 * P_{II} + 0.1 * P_{III,IV} + 0.24 * P_V - 78.7 \quad \text{5-8}$$

The rainfalls of Phase III and Phase IV were combined to derive a higher correlation between the predicted yield reduction (regression line) and actual yield reduction (Table 5-4). A high Multiple R was acquired based on the multiple regression analysis of yield reduction and CR index per-phase, which indicates a high correlation between the predicted and actual corn yield loss. Thus the indices are reliable proxies for the yield loss caused by rainfall deficit.

Table 5-4 Weighted coefficients and Mutiple R per growth phase in the insured area

County	PII	PIII	PIV	PV	Multiple R
Daiyue	0.37	0.30		0.33	0.78
Feicheng	0.39	0.33		0.27	0.78
Xintai	0.29	0.18	0.13	0.40	0.84
Ningyang	0.51		0.49		0.69
SA-Ningyang	0.57		0.42		0.66
SA-Xintai	0.37	0.19		0.44	0.85

It results that a 2nd order polynomial function confidently describes yield reduction in function of rainfall deficit which is further confirmed by the ANOVA F-tests (Figure 5-6 and Figure 5-7). Zaw and Naing (2008) came to a similar conclusion in that as rainfall increases, yield will increase before reaching a threshold, above which yield starts decreasing. The results suggest that using 2nd order polynomial functions between deficit rainfall and yield loss is a valuable approach to determine triggers and exit for weather index insurance. This approach has advantages compared to using water requirement level which reflects not only rainfall deficits but also considers soil properties and evapotranspiration of the plant and can hence increase the basis risk.

Figure 5-6 (a) indicates that under the K-S test, the Logistic Distribution can have the relative frequency of the township-level yield loss in Daiyue well fitted, with a mean of 1.75 kg/mu and standard deviation of 51.7 kg/mu. The mean of the relative frequency curve (1.75 kg/mu) was chosen to be the independent value for the polynomial curve between the weighted CR index and yield reduction. In Daiyue county, the Trigger is 50 mm for Phase II with a mean yield loss of 1.75 kg/mu. The

Exit is 5 mm when the cumulative relative frequency is 10 percent and the yield loss is around 60 kg/mu. Despite the close proximities of the insurance areas, it results that the insurance terms associated to the developed CR indices vary among the insured areas (Table 5-5).

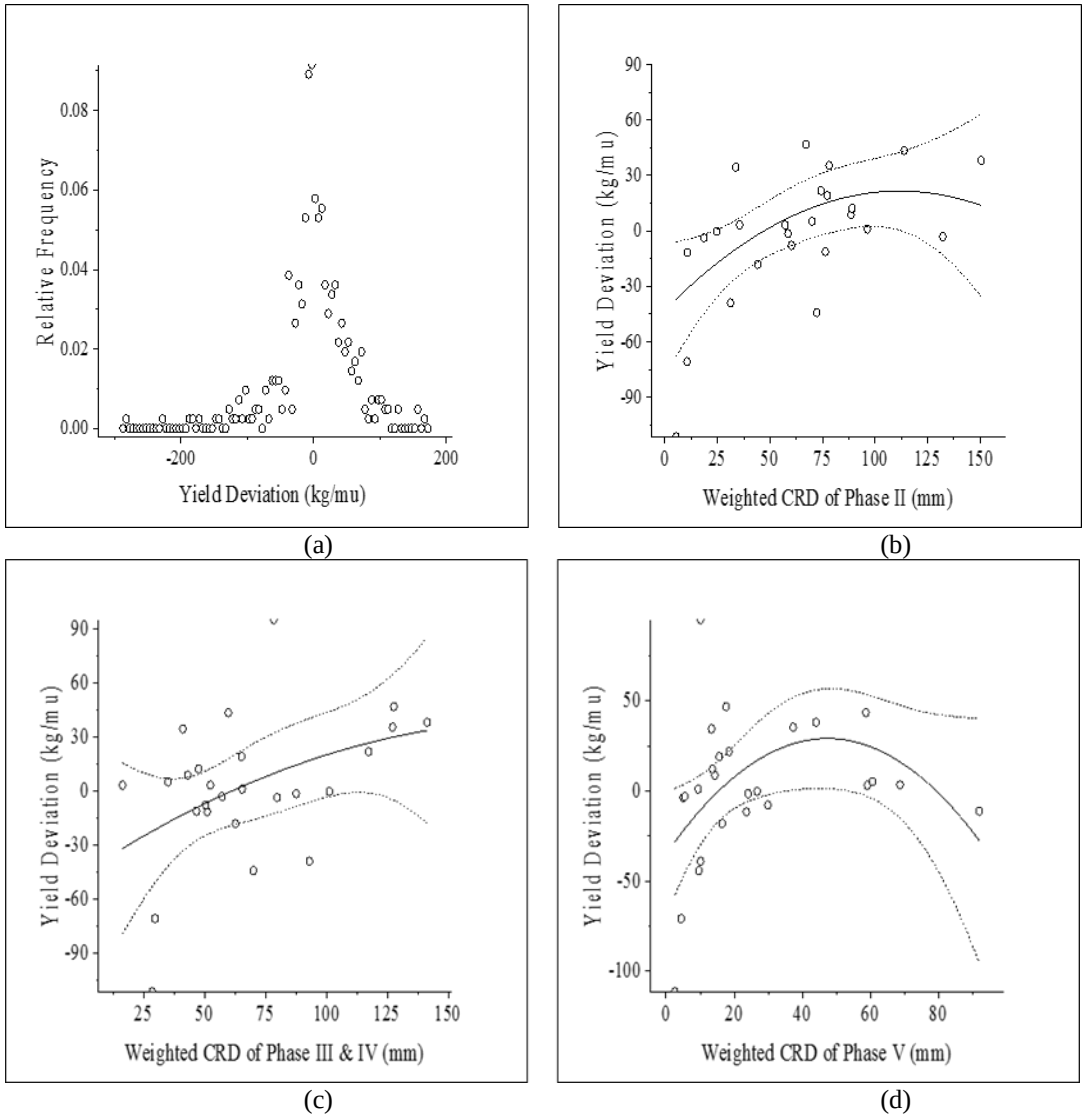

Figure 5-6 Frequency analysis of yield reductions (a) and 2nd order Polynomial curve fitting (solid line) between yield reductions and weighted CR indices of Phase II (b), III & IV (c), and V (d) in Daiyue county (dashed lines reveal the 90% conference level)

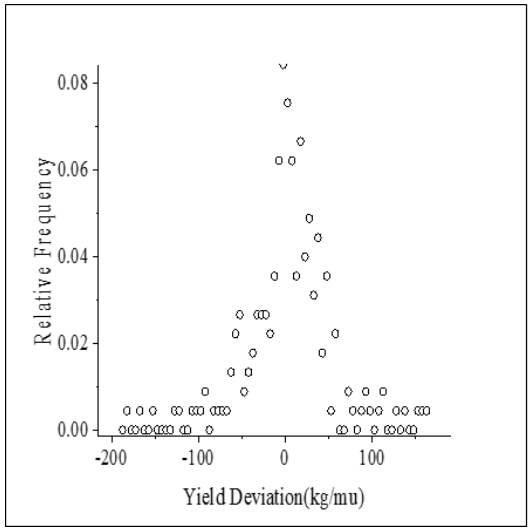
Relative Frequency
0.08
0.06
0.04
0.02
0.00
-200
-100
0
100
Yield Deviation(kg/mu)

(a)

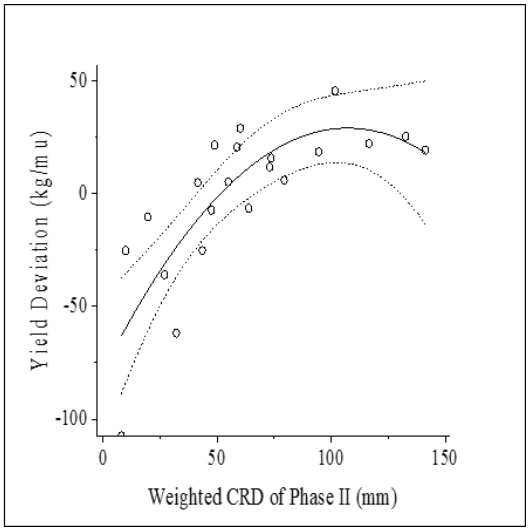
Yield Deviation (kg/mu)
50
0
-50
-100
0
50
100
150
Weighted CRD of Phase II (mm)

(b)

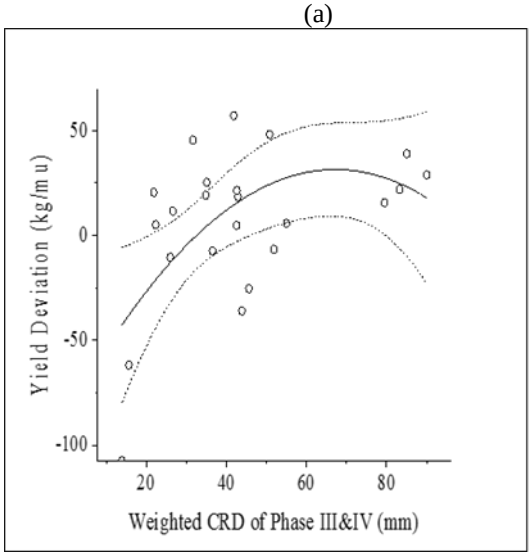
Yield Deviation (kg/mu)
50
0
-50
-100
20
40
60
80
Weighted CRD of Phase III&IV (mm)

(c)

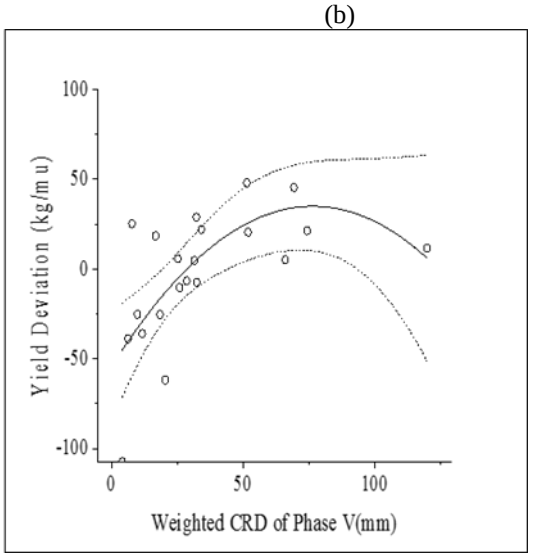
Yield Deviation (kg/mu)
100
50
0
-50
-100
0
50
100
Weighted CRD of Phase V(mm)

(d)

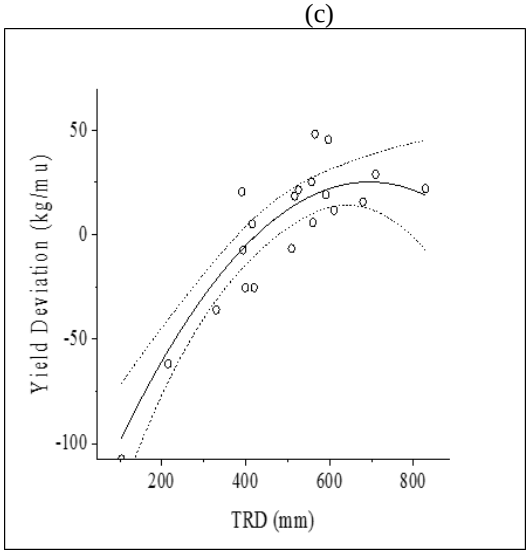
Yield Deviation (kg/mu)
50
0
-50
-100
200
400
600
800
TRD (mm)

(e)

Figure 5-7 Frequency analysis of yield reductions (a) and 2nd order Polynomial curve fitting (solid line) between yield reductions and weighted CR indices of Phase II (b), III & IV (c), and V (d) in SA-Xintai county and 2nd order Polynomial curve fitting (solid line) between yield reduction and weighted TR index (e) in SA-Xintai county (dashed lines reveal the 90% conference level)

Table 5-5 Insurance parameters and loss costs in six regions of Tai'an city

County	Phase	Trigger (mm)	Exit (mm)	Sum Insured (rmb/ mu)	TSI (rmb/ mu)	Mean Payout (rmb/mu)	Loss Cost
Dai Yue	PII	50	5	225	1178	41	3.5%
	PIII,IV	68	10	530			
	PV	15	5	754			
Fei Cheng	PII	78	20	225	1170	48	4.1%
	PIII, IV	71	35	525			
	PV	17	5	750			
Xin Tai	PII	40	5	200	1040	56	5.3%
	PIII	19	3	330			
	PIV	12	5	465			
	PV	20	5	660			
Ning Yang	PII,III	100	20	376	1127	57	5.0%
	PIV,V	50	5	751			
SA-Xintai	PII	47	10	200	1070	64	5.9%
	PII,IV	40	5	478			
	PV	28	5	678			
SA-Ningyang	PII,III	143	40	375	1125	49	4.4%
	PIV,V	65	10	750			

5.4.3 **Analysis of CRD and TRD Indices**

The purpose of crop insurance is to protect farmers against financial losses resulting from adverse weather conditions and compensate for actual production cost. A correlation analysis between the payouts of the CR indices and the yield loss shows the extent to which the indices payout, i.e., the lower the correlation coefficient, the

higher the basis risk in that the index payouts pays out but yield levels were near normal, or on the contrary, the index does not payout but farmers incurred significant yield losses. High basis risk is often been cited as a limiting factor to expand weather index insurance programs and designing indices based on high resolution weather and yield data as well as testing the indices for payouts is essential.

Table 5-6 Mean payout, uncertainty loading, risk premium and correlation between payouts and yield reductions for the insured area

Insured Area	Index	Mean Payout (RMB/mu)	Uncertainty Loading (RMB/mu)	Risk Premium (RMB/mu)	Risk Premium (%)	Correlation
Daiyue	CR	41	24	65	5.6%	0.86
Feicheng	CR	48	22	70	6.0%	0.96
Xintai	CR	56	40	96	9.2%	0.91
Ningyang	CR	57	36	93	8.2%	0.87
SA-Xintai	CR	64	49	131	12.2%	0.71
SA-Ningyang	CR	49	38	87.3	7.8%	0.86
SA-Xintai	TR	128	38	164	15.3%	0.87

The correlation analyses between payouts of the CRD indices and yield losses, reveals the following results (Table 5-6):

(i) All insured areas, expect SA Xintai, have correlation coefficients above 0.85 which is often considered an acceptable level in the development of weather index insurance. This is a satisfying result and shows that CR indices capture yield losses from defict rainfall (drought) reasonably well. Illustrated at the example of Daiyue county (Figure 5-8), the severe yield losses in 1989 and 2002 triggered high payouts

under the CR indices, both per phase and in total (Total Payout). The years 2000 and 2001 show large yield reductions without indemnity from the CR indices, which is explained by the fact that both years revel excess rainfall. In years with small yield reductions such as 2003 and 2006, the CR indices did not trigger a payout as rainfall amounts are deemed sufficient to achieve acceptable yields.

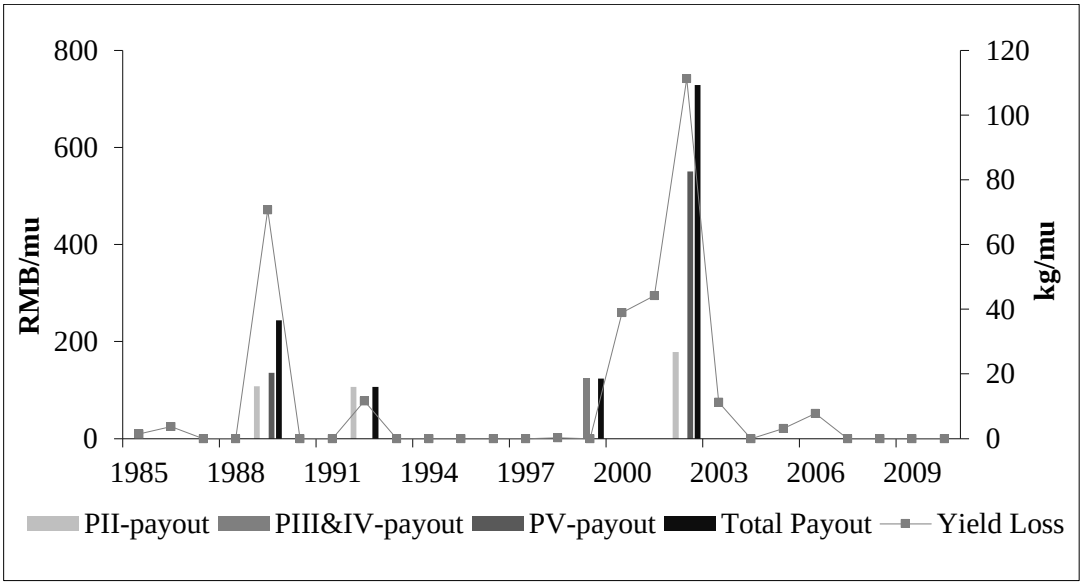

Figure 5-8 Yield reduction and payouts of the indices per phase and in total for Daiyue county (1985-2010)

(ii) The correlation coefficient in SA-Xintai reaches 0.71 indicating a higher level of basis risk than in the other insured areas. Under the CR indices, farmers would have received compensations in 1986, 2000, 2001 and 2002 for yield loss caused by a rainfall deficit in the corresponding growth stage (Figure 5-9). More importantly, the CR indices do not create a payout in 1989 when large yield losses occurred but on the other hand pay out in 2005 when yield levels where at normal level. A majority of the payout of the CR indices occur in Phase IV (maturity).

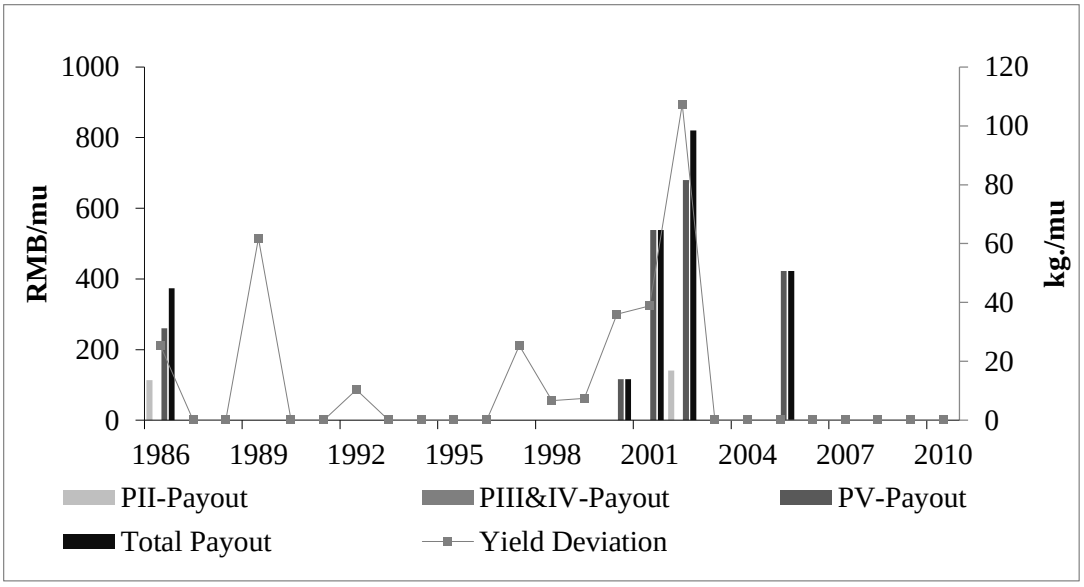

Figure 5-9 Yield reduction and payouts of the indices per phase and in total for SA-Xintai (1986-2010)

The basis risk decreases considerably using a rainfall deficit index over the entire corn growth phase (TR) including Phases II-V with a correlation coefficient of 0.87 (Table 5-6). Compared to the CR indices, the TR index triggers payouts in 1992, 1997 for small yield losses and most importantly the TR index does not trigger a payment in 2005 (Figure 5-10). In this case, the TR index clearly performs better than the CR indices.

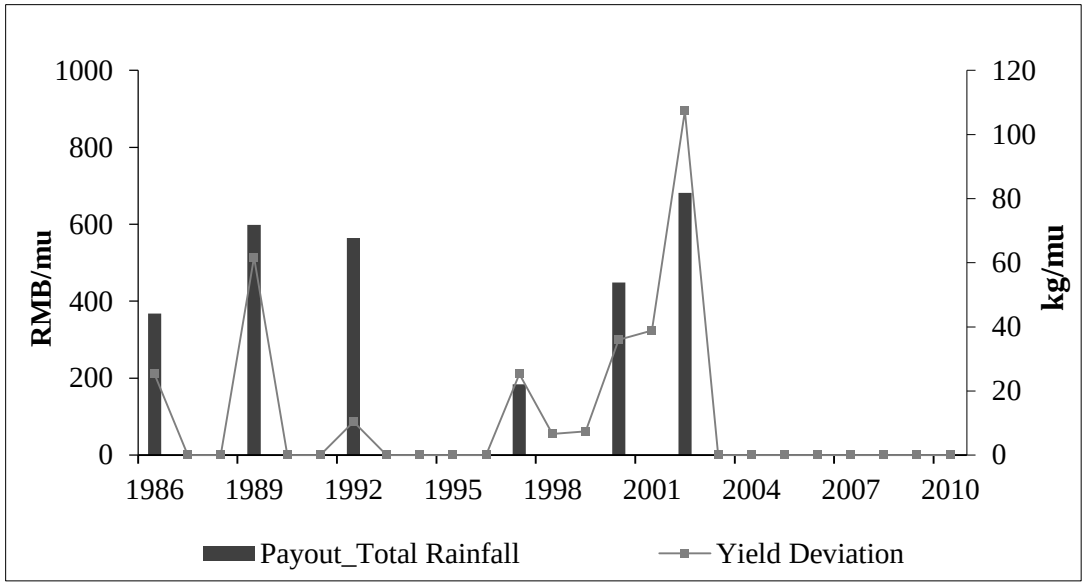

Figure 5-10 Historical Yield Reduction, total payouts of Total Rainfall Index in Special Area Xintai

(iii) The level of the risk premium rate is generally a good indicator of the risk associate to rainfall deficit. Among all insured areas, SA-Xintai has the highest premium rate under the CR indices (12.2%) and the TR index (15.3%). SA-Xintai shows the most volatile rainfall pattern in the insured area, also matching the highest premium rate. The lowest risk premium rates result for Daiyue (5.6%) and Feicheng (6.0%). From the perspective of rainfall pattern, Daiyue and Feicheng are less volatile compared with other regions. Cao et al (2013) developed a drought index for spring wheat for different cities in Shandong and obtained pure insurance rates for different cities in Shandong ranging from 2.4% (RMB 12.2/mu) to 11.4% (RMB 56.9/mu) with pure insurance rates for Tai'an city which corresponds to the study area in this study reaching 4.5% (RMB 22.7/mu). While spring wheat has a different sensitivity to drought and phenology than corn, it is interesting to note that the rates obtained in this study are in the range of the rates calculated for wheat by Cao et al (2013).

Given the high exposure to drought risk in Shandong province, premiums ranging for corn ranging from 5.6% (Daiyue) to 12.2% (SA-Xintai) have to be expected. Under the current MPCI insurance policy, all corn areas are insured for a sum insured of RMB 350/mu at a commercial premium rate of 4.3% which translates to a premium of RMB 15/mu. However, the MPCI policy does not cover drought risk and indemnifies farmers only for losses from flood, wind/hail and frost with a 30% franchise, i.e., only losses above 30% of sum insured are compensated for the insured perils. The risk rates of the CR indices for rainfall deficit (drought) of this st studye higher than the commercial premium rate of the MPCI insurance product for perils excluding drought. Considering the systemic nature of droughts and the frequency and severity of such droughts in Shandong, drought insurance under the MPCI policy would most likely exceed the risk rates obtained in this study.

CHAPTER 6

PROBABLE MAXIMUM LOSS ANALYSIS OF RAINFALL INDEX INSURANCE IN SHANDONG, CHINA

6.1 Introduction

In Chapter 5, it is mentioned that the insurer typically adds three risk loadings to the Pure Premium to calculate the Commercial Premium: (i) the administration cost of the index insurance product; (ii) catastrophe loading to account for the fact that large loss events might not have occurred in the historical time series; (iii) a data-uncertainty loading based on the Central Limit Theorem. The Risk Premium based on the estimation of data-uncertainty loading is calculated to reflect the uncertainty about the quality and length of the underlying rainfall data, as mentioned in Chapter 5. This chapter focuses on the analysis of catastrophe loading to account for the Probable Maximum Loss (PML) of drought events, based on the frequency analysis of drought severity as defined in the rainfall index insurance.

In Chapter 5, the Cumulative Rainfall (CR) index per corn growth phase was designed. As the results show, indemnity payment starts once the CR index drops below the trigger value during the coverage period. However, the sample of drought variables in a paid year was too low for the density analysis to be conducted, due to a lack of historical drought incidents. Fortunately, as shown in Chapter 2, the rainfall patterns are known to follow a family of parameterized probability density functions. Therefore, it is possible to use parameter density estimation to analyze rainfall pattern

per growth phase and generate a historical CR index via simulation. The extreme drought severity in the insured area derived from the simulated CR per growth phase can then be estimated with the univariate diffusion kernel density estimator (DKDE) elaborated on in Chapter 4. Hence the PML derived from the insurance payout for extreme drought-risk levels over a 100-year return period can be better calculated by considering more possible drought variables. Finally, the premium, including pure premium and risk premium, is priced based on the Loss Cost analysis in Chapter 5 and the PML analysis in this chapter.

6.2 Methodology

For this study, a three-step method was adopted to calculate the catastrophe loading to account for the Probable Maximum Loss (PML) of drought events, based on the frequency analysis of the drought variables defined in the rainfall index insurance:

(i) *Parametric Analysis Of Cumulative Rainfall Patterns*

Following the calculation of the CR index per corn-growth phase in each insured area in Chapter 5, the parameter density estimation was conducted to analyze the rainfall pattern of the underlying CR index. Monte Carlo simulation was applied based on the estimated density function for the CR index, to eliminate the problem caused by the lack of drought variable samples. Since insurers compensate for losses on a yearly basis, drought severity in this study is defined as the deviation of the CR from the trigger level if payment is made in the particular year. The drought severity is derived from the simulated cumulative rainfall amount per growth phase.

(ii) *PDF Analysis Of Drought Variables By DKDE*

Univariate DKDE was adopted to estimate the PDF of drought severity and the return level of drought severity at *r* year return period. The probable maximum payout at *r*-year return period for each chosen phase will be calculated by interpolating the trigger and limit with the generated phased drought severity.

(iii) *Premium Pricing*

The Premium with Pure Premium calculated in Chapter 5, and catastrophe loading, are priced.

6.2.1 **Parametric Analysis of Rainfall Patterns**

Four density functions were chosen as candidate distribution functions: Gamma dstribution, Generalized Extreme Value (GEV) distribution, Lognormal distribution, and Weibull distribution. Table 6-1 below presents the mathematical expression of their PDFs, where x is the cumulative rainfall, σ is the shape for Lognormal distribution, μ, ξ, and σ are the location, scale, and shape for GEV distribution, k and θ are the shape and scale of Gamma distribution, and $\boldsymbol{\lambda}$ and k are the scale and shape of Weibull distribution. A Monte Carlo simulation (Binder and Heermann, 2010) was conducted to simulate the CR index 10000 times, based on the chosen PDF candidates.

Table 6-1 Probability density functions for Gamma, GEV, Lognormal, and Weilbull distributions

Distribution	Probability Density Function	Domains
Lognormal	$\frac{1}{x\sqrt{2\pi}\sigma} e^{-\frac{(\ln x-u)^2}{2\sigma^2}}$	σ >0 μ ∈ R x ∈ (0, +∞)
Generalized Extreme Value	$\frac{1}{\sigma} t(x)^{\xi+1} e^{-t(x)}$ $t(x) = \begin{cases} (1+(\frac{x-u}{\sigma}))^{-\frac{1}{\xi}} & if\ \xi \neq 0 \\ e^{-\frac{x-u}{\sigma}} & if\ \xi = 0 \end{cases}$	μ ∈ R ξ ∈ R σ > 0 x ∈ [μ − σ /ξ, +∞) whenξ > 0, x ∈ (−∞, +∞) whenξ = 0, x ∈ (−∞, μ − σ / ξ] when ξ < 0.
Gamma	$\frac{1}{\Gamma(k)\theta^k} x^{k-1} e^{-\frac{x}{\theta}}$	K >0 θ >0 x ∈(0,+∞)
Weibull	$\begin{cases} \frac{k}{\lambda}(\frac{x}{\lambda})^{k-1} e^{-(\frac{x}{\lambda})^k} & if\ x \geq 0 \\ 0 & if\ x = 0 \end{cases}$	$\boldsymbol{\lambda}$ ∈ (0,+∞) k ∈ (0,+∞) x ∈ [0,+∞)

The parameters of the functions are estimated by the Maximum Likelihood method. Assuming that independent CR indices in each growth phase $x_1, x_2 \ldots, x_i, \ldots x_n$ have joint distribution, the likelihood function L is denoted by (Akaike, 1998):

$$L(\theta) = \prod_{i=1}^{n} f(x_i|\theta) \qquad 6\text{-}1$$

where,

θ: the vector of parameters belonging to the assumed distribution family.

Akaike's Information Criterion (AIC) (6-2) proposed by Akaike (1974) were adopted to choose the best fitted parametric functions. A smaller value means better fitting.

$$AIC = 2k - 2 * Ln(L) \quad 6\text{-}2$$

where,

L : the likelihood function;

k: the number of free parameters to be estimated.

6.2.2 **Diffusion Kernel Density Estimator**

To estimate the density function, the CR index per growth phase derived from the Monte Carlo simulation based on the rainfall density function was first converted into drought severity. The drought severity is defined as the deviation of CR from the trigger level. To estimate the frequency of drought severity by DKDE, the variable should first be rescaled to be in the domain [0, 1]. The calculation of univariate DKDE is explained in detail in Chapter 4.

The return period *R* is defined as the average recurrence time interval that the drought severity of event has the probability *1/r* of being exceeded. The PML at *r*-year return period for each chosen phase will be calculated through interpolating the trigger and limit with the generated phased drought severity. The return period *R* is derived from the cumulative density function (CDF) by integrating the PDF, as follows:

$$R = \frac{1}{F(X>x_r)} = \frac{1}{1-F(X<x_r)} \quad 6\text{-}3$$

where,

F(·): the cumulative distribution function of drought variables;

x_r: the drought severity of event with a return period of *r*.

6.2.3 **Premium Pricing**

The methodology of the World Bank (2011) was adopted to calculate the price of the premium as follows:

$$Premium = Pure\ Premium\ +\ Risk\ Loading \tag{6-4}$$

$$Risk\ Loading = \alpha * \frac{\sigma}{\sqrt{k}} +\ \beta * \left(PML - \frac{\sum_1^k \sum_1^n P_{im}}{k}\right) \tag{6-5}$$

$$Premium\ Rate = \frac{Premium}{Total\ Sum\ Insured} \tag{6-6}$$

where,

P_{im}: payout of Phase m in year i;

n: number of chosen phases;

k: number of years for which daily rainfall data are available;

α: Uncertainty loading at 90 percent confidence level;

σ: Standard deviation of total payout in historical time series;

PML: Probable maximum loss of payout simulated over 100 years;

β: The loading for PML over 100 year.

6.3 Results and Discussion

6.3.1 Parametric Analysis

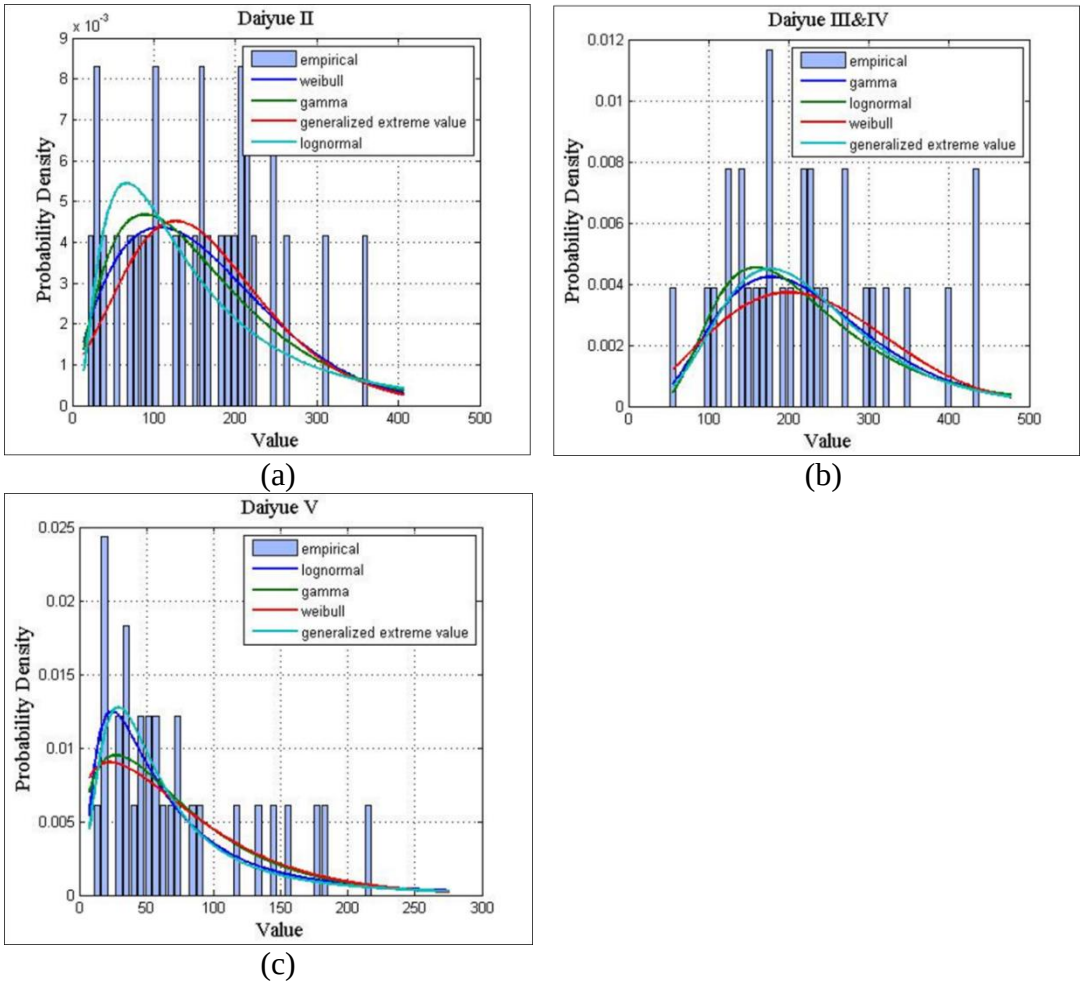

Figure 6-1 Comparison of PDF estimation (Lognormal, Gamma, Weibull, and Generalized Extreme Value) for cumulative rainfall of Phase II (a), Phases III & IV (b), and Phase V (c) in Daiyue county

To conduct the frequency analysis of drought severity through DKDE, the frequency analysis of rainfall amount per growth phase was first conducted to generate more rainfall data. As with Daiyue county, only the year 1999 had a historical burnpayout for Phases III & IV from 1981 to 2011, as shown in Chapter 5 (Figure 5-8), the sample

size was not large enough for extreme drought-severity-level estimation by DKDE. Hence to estimate the rainfall pattern of cumulative rainfall per corn-growth phase in the insured area, the CR index per phase was first fitted by the density function candidates (Gamma, GEV, Lognormal, and Weibull distribution) (Figure 6-1). The results show that for Daiyue county, the Weibull distribution can best fit the rainfall pattern of Phase II, the Gamma distribution can best fit Phases III & IV, and the Lognormal distribution best fits Phase V, based on the value of AIC (Table 6-2). On a prefectural scale, the Weibull distribution is the most reliable distribution for estimating and representing the frequency of the rainfall pattern in the six regions (Appendix 3).

Table 6-2 AIC value for PDF estimation of rainfall in Phase II, III & IV, V

Candidates	**Phase II**	**Phase III&IV**	**Phase V**
Lognormal	377.1	375.9	331.4
Weibull	370.1	376.7	332.3
GEV	374.1	377.5	333.7
Gamma	371.6	375.3	330.3

6.3.2 **Univariate Diffusion Kernel Density Estimation**

The drought-severity level for *r* year return period was derived based on the estimation of the PDF and CDF of drought severity by DKDE. Figure 6-2 and Figure 6-3 illustrate the PDF and CDF of rainfall in Phase II, Phases III & IV, and Phase V with optimized bandwidth. The return period derived by inversing the exceeding probability is illustrated in Figure 6-4 below. The drought-severity levels for a 100-year return period for Phases II, III & IV, and V in Daiyue are 43mm, 41mm, and 10

mm respectively. The return periods of drought severity in the historical burn payout years (1983, 1989, 1992, 1999 and 2002) are shown in Table 6-3 below. The rainfall deficit occurrence in Phase II of 2012 shows the highest return period, which means cumulative rainfall of 14.3 mm in corn-growth phase II occurs only once in 10 years.

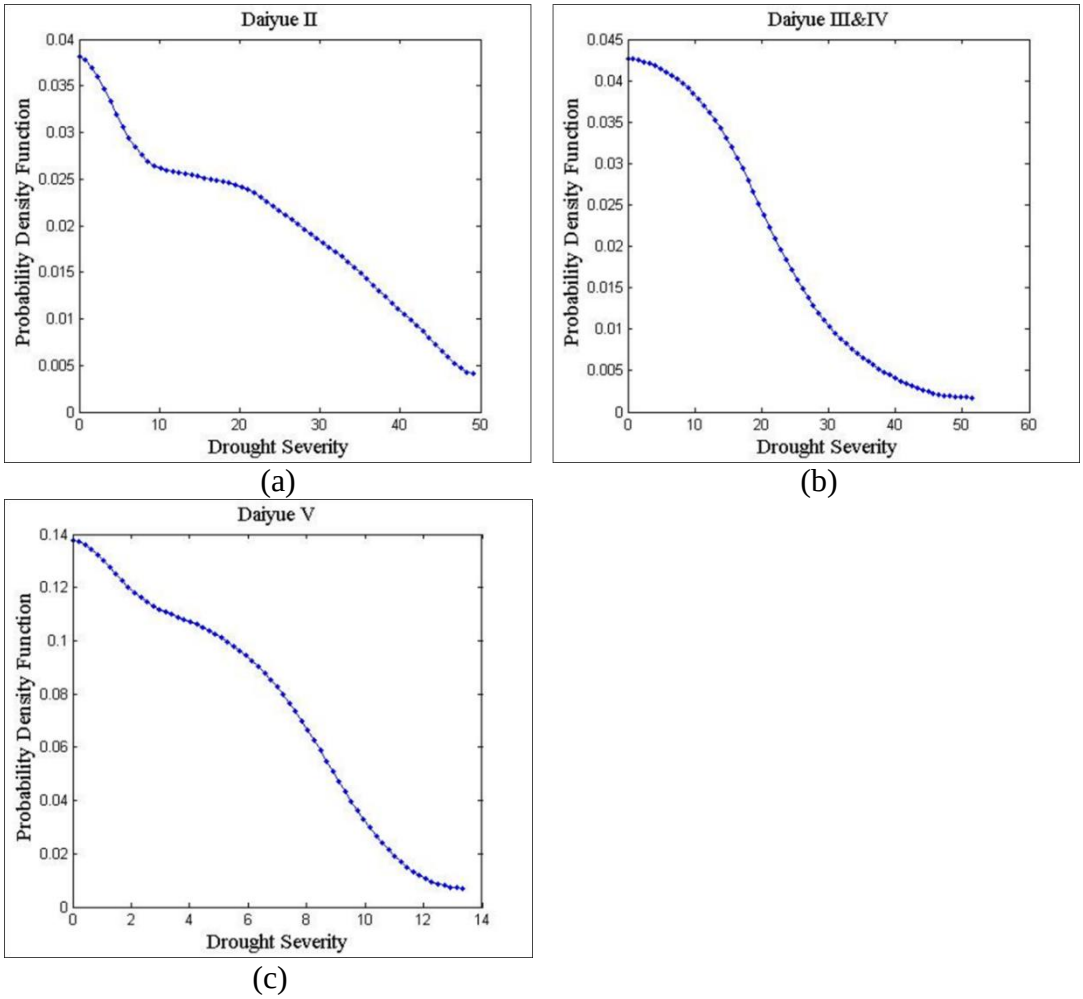

Figure 6-2 PDF of drought severity in Phase II (a), Phases III & IV (b), and Phase V (c) in Daiyue county, estimated by DKDE

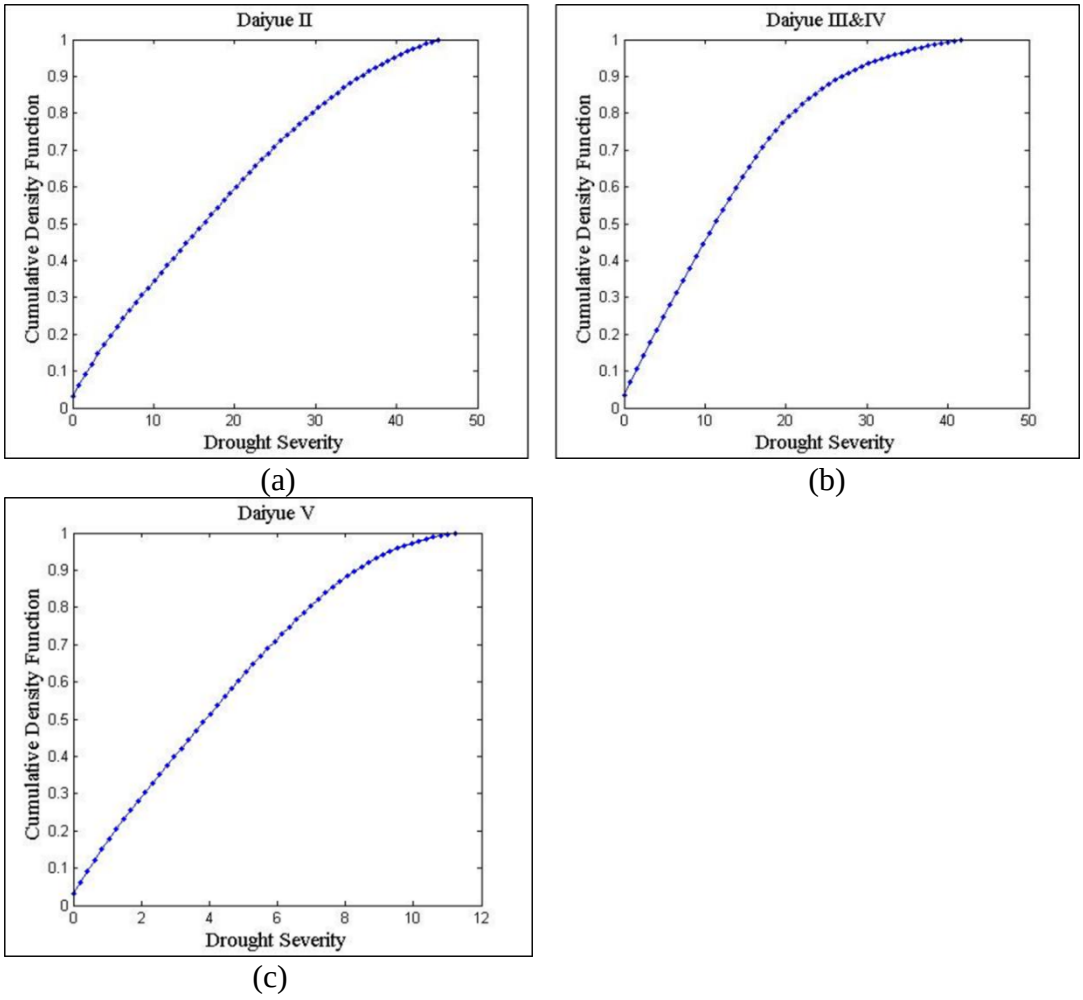

Figure 6-3 CDF of drought severity in Phase II (a), Phases III & IV (b), and Phase V (c) in Daiyue county, estimated by DKDE

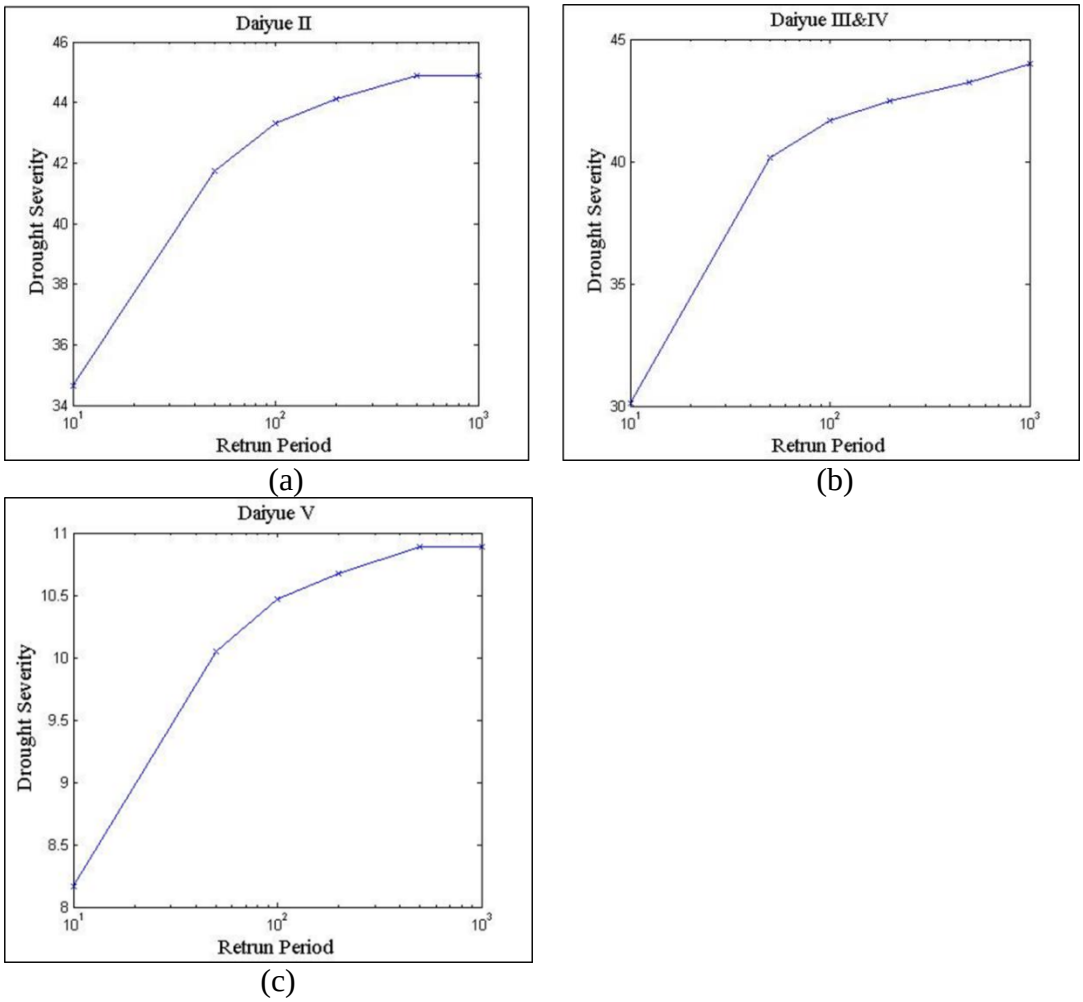

Figure 6-4 Drought-severity return level (50 years, 100 years, 200 years, 500 years, and 1000 years) of Phase II, Phases III & IV, and Phase V in Daiyue county

Table 6-3 Return periods of drought severity in historical payout year in Daiyue county

Year	**Cumulative Rainfall Index (mm)**			**Return Period (Severity) (years)**		
	Phase II	Phases III & IV	Phase V	Phase II	Phases III & IV	Phase V
1983	35.9			1.8		
1989	28.4		13.2	2.7		1.3
1992	28.7			2.7		
1999		55.6			1.4	
2002	14.3		7.7	10		3.5

6.3.3 **Premium Pricing**

Table 6-4 Drought severity for 100-year return period per insured phase, risk premium, and premium rate in six insured regions of Tai'an city

Region	**II** (mm)	**III** (mm)	**IV** (mm)	**V** (mm)	**PML(TSI)** (rmb/mu)
Daiyue	43	41		10	1378(1177)
Feicheng	67	23		10	1220(1171)
Xintai	35	11	10.5	14.5	1534(1039)
Ningyang	81.5		48.5		1127(1178)
SA-Xintai	39	22		22	1255(1070)
SA-Ningyang	92		53		1057(1231)

	Pure Premium (rmb/mu)	**Risk Premium** (rmb/mu)	**Premium** (rmb/mu)	**Premium Rate**
Daiyue	72.2	11.7	83.9	7.1%
Feicheng	70	11.7	82.7	7%
Xintai	95.8	10.4	106.2	10.2%
Ningyang	92.9	11.3	104.2	8.8%
SA-Xintai	131	10.7	141.7	13.2%
SA-Ningyang	87.3	10.5	97.8	7.9%

Table 6-4 provides the drought-severity level for a 100-year return period per insured phase in each region. Corresponding to the payout trigger and exit level per phase, the Probable Maximum Loss per insured phase was calculated by interpolating the drought severity into the proportional equation in Chapter 5 (5-5). In Daiyue county, the total payout based on a 100-year drought severity return level is 1378rmb/mu, which exceeds the Total Sum Insured (TSI) of 1177 rmb/mu. Therefore, the PML for Daiyue over 100 years is 1177 rmb/mu. Xintai county shows the highest drought risk

over the 100-year return period; according to the drought-severity calculation, the total payout is 1534 rmb/mu. According to the setting of the payout limit, the PML should be the limit of the payout in Xintai (1039 rmb/mu).

The PML loading is uniformly taken as 0.1 for all the six regions, because different insurers have different risk loadings, taking other portfolios into account. Feicheng County has the lowest premium rate, 7%, of all the six regions, and its premium is 82.7 rmb/mu. Special Area Xintai has the highest premium, 141.7 rmb/mu, and the highest premium rate, 13.2%.

CHAPTER 7

CONCLUSIONS AND RECOMMENDATIONS

7.1 Conclusion

According to the historical weather data, drought has frequently occurred over the past decades, and the existing literature states that the situation could become much worse by the end of this century (Field et al. 2014). Therefore, risk-transfer measures have a very important role to play in the context of global food security and the wellbeing of farmers. Agricultural insurance has shown the potential to mitigate the impact of weather-related disasters on the farming yield by: (i) reducing economic loss due to extreme weather events; (ii) helping post-disaster recovery without much government intervention; (iii) providing farmers with sufficient funds to not only sustain their livelihoods, but also invest in future agricultural production. However, conventional agriculture insurance is not always available and feasible to implement in developing countries, due to: i) the high transaction cost; ii) moral hazard and adverse selection caused by asymmetric information between farmers and insurers; iii) high exposure to correlated risk; iv) the lack of distribution channels and farm-based loss-adjustment capacities. As an alternative, index-based crop insurance is therefore being developed to meet the needs of small farmers in emerging markets.

The frequency analysis of drought risk plays an important role in helping insurers to (a) identify the spatial distribution of risk in the insured area; (b) make decisions about risk pooling; and (c) calculate the potential extreme losses. Therefore, it is the

duty of the insurance institutions to conduct ample analysis of the related risks beforehand, for the benefit of both the insurer and the insured.

This research has established two models to help the insurance institutes analyze drought risk, for the development of small-farm-centric drought-risk insurance products:

1. Bivariate Drought-Risk Model: this research is the first in the field of Standardized Precipitation Index (SPI)–based drought-risk studies to employ diffusion kernel density estimation (DKDE) for the estimation of bivariate probability density functions (PDFs) and the joint return period (RP). The model is introduced in Chapter 4, and is illustrated with a case study of Shandong province in China. Two nonparametric approaches were tested with regard to the identification of the SPI-based drought risk for corn in the province: the diffusion kernel density estimation (DKDE) and Gaussian kernel density estimation (GKDE). As shown in the results, DKDE is more effective than GKDE in estimating the bivariate PDFs of drought risk in terms of accuracy and the ability to avoid boundary-leakage problems. Using the DKDE function to analyze agricultural drought will eventually help the institutes determine premium pricing by providing a reference for identifying regional drought risk, and offer important technological support for drought management.
2. Rainfall Index Insurance Model: this model is elaborated in Chapter 5 and Chapter 6. The model is established based on the impact of deficit rainfall on the yield of summer corn in five counties and two regions of Shandong

province. Multiple linear regression analysis was conducted to assess the association between the Yield Deviation and Cumulative Rainfall (CR) indexes of the chosen phases. The result shows that the CR index does provide a good proxy for the corn-yield loss caused by drought in the research area. One objective of this model is to eliminate the basis risks that exist in the computation of the index. It has been shown that the model can significantly reduce technical basis risk by utilizing the high-resolution yield data collected, and reduce temporal basis risk by adopting the carefully chosen contract phases determined from the answers to the questionnaire. The model can also minimize the spatial basis risk with the adoption of Weighed Thiessen Polygons for regions located outside the effective regions of the weather stations. By following the approach provided in the model, insurers can extend the insurance coverage to areas previously unreachable without worrying about the influence of excessive basis risks. Furthermore, this model has also demonstrated the advantage of determining the trigger and exit of the payout, via the combination of parametric analysis of historical yield loss and polynomial regression analysis of yield loss against the weighted cumulative rainfall. In conclusion, the results of this study show that rainfall index insurance is a viable alternative product to complement the existing indemnity-based, government-supported corn insurance program in Shandong province. In addition, rainfall indices could be another possible product to insure against drought risk, for farmers in regions where no insurance coverage is currently available, due to high historical losses from drought.

7.2 Innovations and Contributions of the Research

- **Rainfall index coverage area allocating method for insurance institutes**

For insurance institutes, remotely located weather stations are the main cause of basis risk in index insurance products. To help the insurance institutes reducing the technical basis risk, this study brings up the idea of Special Area and creates a rainfall index specific Thiessen polygon methodology. The methodology is used to mitigate weather data error based on the distance and the shape of the monitored region. Accurate weather data can be collected by considering each weather station around the monitored special area is with a weighted average. The result has shown significant reduction in basis risk and is promising to help insurance institutes to extend index insurance coverage to regions remotely located from weather stations.

- **Structured framework of index data cleansing**

Spatial basis risks can be reduced by increasing the resolution of weather and yield data used. However the data is normally archived by individual county level government organizations that varies in resolution and format from time to time. Hence this study constructs a framework to standardize the format of the weather data and yield data to increase the overall data resolution and ease the traditional process of data cleansing. The original data are grouped in township level and arranged according to historical order. Data with lower historical resolution are normalized with a preset weightage value for resolution up scaling. Standardized yield and weather data format logging sheets are developed accordingly for the purpose of easier archiving of government organizations.

- **Farming data quantification and coherence improvement measure**

Insurance products developed based on outdate farming information are insecure for both the insured and the insurer. The farm owners knows better about the variation of crop's seasonal behavior from year to year. It is difficult for the insurers to predict accurate risk without communicating with up to date farming information. The mismatch in farming information is greatly reduced with the help of issuing questionnaires to the farm owners on a yearly basis. As a result, with the periodical updates of data the insurance institutes are able to compute accurate risk and provide the farmers with more coverage and reasonable premiums. This study creates a protocol in setting questionnaires, it ensures the questions set to cover farming aspects those are common for crops in the region as well as the unique behaviors of specific crops in unordinary growth phase.

- **Multivariate drought risk estimation methodology**

The risk estimation in index insurance is normally univariate. The composition of drought risk are often complicate and consist of more than one variable. Hence it is important to establish a method that is able to evaluate the risk probability from analysis of more than one factor. The research is the first in the field of SPI–based drought-risk studies to employ DKDE for the estimation of bivariate probability density functions and the joint return period. The DKDE method shows to be capable of producing index considering multiple factors with higher accuracy and eliminating unwanted probability shifts in the existing estimation method at a lower computation cost. Using the DKDE function to analyze agricultural drought will eventually help

the institutes determine premium pricing by providing a reference for identifying regional drought risk, and offer important technological support for drought management.

7.3 Limitations and Recommendations

The limitations of this research into the bivariate drought-risk model and the development of the rainfall index insurance model, and the recommendations for future research, are as follows:

- The flexible time-scale intervals and geographical coverage have made the SPI widely adopted in the monitoring of drought severity around the world. However, the SPI also has some drawbacks, such as being unable to be applied in the absence of drought variables, and producing erroneous results from weather data containing highly left-skewed distribution. The agricultural impact of drought is a combination of short-term precipitation shortages, temperature anomalies, and soil-water deficits. Hence the SPI alone may not be sufficient to monitor drought risk in all scenarios. The future study of rainfall index insurance should consider employing multiple drought indices to model drought risk. An agricultural drought index that integrates various parameters such as rainfall, temperature, evapotranspiration (ET), runoff, and other water-supply indicators should be adopted to meet the demands of different applications and give a comprehensive picture for decision making. However, more factors to consider means more data limitations and uncertainty, which will in turn result in a reduction of the

transparency of the contracts for policyholders. Therefore, it is important to choose an appropriate and reliable index to evaluate drought severity.

- For this research, the sown date of corn was assumed to be the same every year. However, this varies from year to year in reality, and the growth period of corn also varies depending on seed varieties and other weather elements such as temperature. Hence the growth period should be regarded as dynamic for the future development of rainfall index insurance.

- For this research, drought risk was analyzed in terms of the bivariate aspects. However, it can also be estimated from other variables besides drought duration and drought intensity. In the research, drought variables were based on SPI per growth phase. In the future studies, more drought index can be adopted in the definition of drought variables (e.g. PDSI-drought duration and intensity, SMI-drought duration and intensity) to estimate the drought risk from multiple aspects. A multivariate diffusion kernel density estimation can be considered for use in future drought-risk analysis.

- For the research, the historical daily rainfall data were collected from observation weather stations. The resolution of the data was around 25 km, which is enough for the industry development of index insurance, but not appropriate for study and development of drought risk model. Therefore, higher resolution data such as satellite weather data should be considered for catastrophic risk model development. Besides, the data uncertainty analysis should also be considered in the study of drought risk modelling.

- For this research, data uncertainty loading and catastrophe loading were considered in the calculation of the premium without the estimation of administration costs and premium deductibles. The results of this study should encourage future researchers to compare the administration loading and deductible for the pricing premium with those of the current traditional multi-peril product policies. Hence this study can be used to demonstrate the advantages of weather indices insurance over the traditional MPCI to small farmers in drought-proven regions, and familiarize them with the benefits of this insurance that no other insurance product can provide.

REFERENCES

Acharya, N., Mohanty, U.C., Sahoo, L. (2013), "Probabilistic multi-model ensemble prediction of Indian summer monsoon rainfall using general circulation models: A non-parametric approach", *Comptes Rendus Geoscience*, Vol. 345 No. 3, pp.126-135.

Akaike, H. (1974), "A new look at the statistical model identification", *Automatic Control, IEEE Transactions on*, Vol. 19 No. 6, pp.716-723.

Akaike, H., (1998). *Information theory and an extension of the maximum likelihood principle*. Selected Papers of Hirotugu Akaike. Springer, New York, pp. 199-213.

Alexandridis, A., Zapranis, A.D. (2012), *Weather Derivatives: Modeling and Pricing Weather-related Risk*, Springer Science & Business Media, New York.

Ali, M., Masoom, M.P., Woo, J. (2008), "Skewed reflected distributions generated by reflected gamma kernel", *Pakistan Journal of Statistics*, Vol. 24 No. 1, pp.77.

Allen, R.G., Pereira, L.S., Raes, D., Smith, M. (1998), *Crop evapotranspiration: Guidelines for computing crop water requirements*, FAO.

Alley, W.M. (1984), "The Palmer drought severity index: limitations and assumptions", *Journal of Climate and Applied Meteorology*, Vol. 23 No. 7, pp.1100-1109.

Antoine, L., Philippe, Q. (2011), "Agricultural insurances based on meteorological indices: Realizations, methods and research agenda", *Meteorological Applications*, Vol. 20 No. 1, pp.1-9.

Barnett, B.J. (2009), "Weather index insurance and climate change opportunities and challenges in lower income countries", *The Geneva Papers on Risk and Insurance Issues and Practice*, Vol. 34 No. 3, pp. 401-424.

Barnett, B.J., Mahul, O. (2007), "Weather index insurance for agriculture and rural areas in lower-income countries", *Am J Agr Econ*, Vol. 89 No. 5, pp.1241-1247.

Binder, K., Heermann, D. (2010), *Monte Carlo Simulation in Statistical Physics: an Introduction*, Springer, Berlin Heidelberg.

Botev, Z.I., Grotowski, J.F., Kroese, D.P. (2010), "Kernel density estimation via diffusion", *The Annals of Statistics*, Vol. 38 No. 5, pp.2916-2957.

Bouezmarni, T., Rolin, J.M. (2003), "Consistency of the beta kernel density function estimator", *Canadian Journal of Statistics*, Vol. 31 No. 1, pp.89-98.

Breustedt, G., Bokusheva, R., Heidelbach, O. (2008), "Evaluating the potential of index insurance schemes to reduce crop yield risk in an arid region", *Journal of Agricultural Economics*, Vol. 59 No. 2, pp.312-328.

Buch-Larsen, T., Nielsen, J.P., Guillén, M., Bolancé, C. (2005), "Kernel density estimation for heavy-tailed distributions using the Champernowne transformation", *Statistics*, Vol. 39 No. 6, pp.503-516.

Byun, H.R., Wilhite, D.A. (1999), "Objective quantification of drought severity and duration", *Journal of Climate*, Vol. 12 No. 9, pp.2747-2756.

Carter, M.R., Little, P.D., Mogues, T., Negatu, W. (2005), "Poverty Traps and Natural Disasters in Ethiopia and Honduras", *World Development*, Vol. 35 No. pp.835-856.

Chen, F.W., Liu, C.W. (2012), "Estimation of the spatial rainfall distribution using inverse distance weighting (IDW) in the middle of Taiwan", *Paddy Water Environ*, Vol. 10 No. 3, pp.209-222.

Chen, S.X. (1999), "Beta kernel estimators for density functions", *Computational Statistics & Data Analysis*, Vol. 31 No. 2, pp.131-145.

Chen, S.X. (2000), "Probability density function estimation using gamma kernels", *Annals of the Institute of Statistical Mathematics*, Vol. 52 No. 3, pp.471-480.

CIRC (2012), http://www.circ.gov.cn/tabid/106/InfoID/201902/frtid/3871/Default.aspx.

CIRC (2014), http://www.circ.gov.cn/web/site0/tab5257/info3901864.htm.

Clarke, D.J. (2011), *A Theory of Rational Demand for Index Insurance*, Department of Economics, University of Oxford.

Collier, B., Skees, J., Barnett, B. (2009), "Weather index insurance and climate change: opportunities and challenges in lower income countries", *The Geneva Papers on Risk and Insurance-Issues and Practice*, Vol. 34 No. 3, pp.401-424.

Cowling, A., Hall, P. (1996), "On pseudodata methods for removing boundary effects in kernel density estimation", *Journal of the Royal Statistical Society. Series B (Methodological)*, Vol. 58 No. 3, pp.551-563.

Dalezios, N.R., Loukas, A., Vasiliades, L., Liakopoulos, E. (2000), "Severity-duration-frequency analysis of droughts and wet periods in Greece", *Hydrological Sciences Journal*, Vol. 45 No. 5, pp.751-769.

Delicado, P., Goria, M.N. (2008), "A small sample comparison of maximum likelihood, moments and L-moments methods for the asymmetric exponential power distribution", *Computational Statistics & Data Analysis*, Vol. 52 No. 3, pp.1661-1673.

Deng, X., Barnett, B.J., Vedenov, D.V., West, J.W. (2007), "Hedging dairy production losses using weather-based index insurance", *Agricultural Economics*, Vol. 36 No. 2, pp.271-280.

Dick, W., Stoppa, A., Anderson, J., Coleman, E., Rispoli, F. (2011), *Weather Index based Insurance in Agricultural Development: A Technical Guide*, International Fund for Agricultural Development.

Dinku, T., Giannini, A., Hansen, J.W., Holthaus, E., Ines, A.V.M., Kaheil, Y., Karnauskas, K.B., Lyon, B., Madajewicz, M., McLaurin, M. (2009), *Designing index-based weather insurance for farmers in Adi Ha, Ethiopia*, International Research Institute for Climate and Society.

Fiedler, F.R. (2003), "Simple, practical method for determining station weights using Thiessen polygons and isohyetal maps", *Journal of Hydrologic Engineering*, Vol. 8 No. 4, pp.219-221.

Field, C.B., Barros, V.R., Dokken, D.J., Mach, K.J., Mastrandrea, M.D., Bilir, T.E., Chatterjee, M., Ebi, K.L., Estrada, Y.O., Genova, R.C. (2014), *Climate Change 2014: Impacts, Adaptation, and Vulnerability. Contribution of Working Group II to the Fifth Assessment Report of the Intergovernmental Panel on Climate Change*, Cambridge University Press, Cambridge, United Kingdom and New York, NY, USA.

Fischer, T., Su, B., Luo, Y., Scholten, T. (2012), "Probability distribution of precipitation extremes for weather index-based insurance in the Zhujiang River basin, south China", *Journal of Hydrometeorology*, Vol. 13 No. 3, pp.1023-1037.

Fix, E., Hodges Jr, J.L. (1951), *Discriminatory analysis-nonparametric discrimination: consistency properties*, US Air Force School of Aviation Medicine.

Gao, B. (2014), http://sdny.gov.cn/art/2014/9/15/art_4042_376436.html.

Gornall, J., Betts, R., Burke, E., Clark, R., Camp, J., Willett, K., Wiltshire, A. (2010), "Implications of climate change for agricultural productivity in the early twenty-first century", *Philosophical Transactions of the Royal Society B: Biological Sciences*, Vol. 365 No. 1554, pp.2973-2989.

Gustafsson, J., Hagmann, M., Nielsen, J.P., Scaillet, O. (2009), "Local transformation kernel density estimation of loss distributions", *Journal of Business & Economic Statistics*, Vol. 27 No. 2, pp.161-175.

Guttman, N.B. (1998), "Comparing the palmer drought index and the standardized precipitation index", *Journal of the American Water Resources Association*, Vol. 34 No. 1, pp.113-121.

Guttman, N.B. (1999), "Accepting the SPI: A calculation algorithm", *JAWRA Journal of the American Water Resources Association*, Vol. 35 No. 2, pp.311-322.

Hall, P., Marron, J.S., Park, B.U. (1992), "Smoothed cross-validation", *Probability Theory and Related Fields*, Vol. 92 No. 1, pp.1-20.

Härdle, W. (1991), *Smoothing techniques: with implementation in S*, Springer, New York.

Härdle, W. (2004), *Nonparametric and Semiparametric Models*, Springer, New York.

Hartell, J., Ibarra, H., Skees, J., Syroka, J. (2006), *Risk management in agriculture in natural hazards*, ISMEA, Rome.

Hazell, P., Anderson, J., Balzer, N., Hess, U. (2010), *The potential for scale and sustainability in weather index insurance for agriculture and rural livelihoods*, IFAD / WFP.

He, B., Wu, J., Lü, A., Cui, X., Zhou, L., Liu, M., Zhao, L. (2013), "Quantitative assessment and spatial characteristic analysis of agricultural drought risk in China", *Nat Hazards*, Vol. 66 No. 2, pp.155-166.

Heim Jr, R.R. (2002), "A review of twentieth-century drought indices used in the United States", *Bulletin of the American Meteorological Society*, Vol. 83 No. 8, pp.1149-1165.

Heimfarth, L.E., Musshoff, O. (2011), "Weather index-based insurances for farmers in the North China Plain: an analysis of risk reduction potential and basis risk", *Agricultural Finance Review*, Vol. 71 No. 2, pp.218-239.

Hellmuth, M.E., Osgood, D.E., Hess, U., Moorhead, A., Bhojwani, H. (2009), *Index insurance and climate risk: prospects for development and disaster management*, International Research Institute for Climate and Society.

Hertel, T.W., Rosch, S.D. (2010), "Climate change, agriculture, and poverty", *Applied Economic Perspectives & Policy*, Vol. 32 No. 3, pp.355-385.

Hess, U., (2007). *Weather index insurance for coping with risks in agricultural production*. Managing Weather and Climate Risks in Agriculture. Springer-Verlag, Berlin Heidelberg, pp. 377-405.

Hess, U., Richter, K., Stoppa, A. (2002), *Weather risk management for agriculture and agri-business in developing countries*, International Finance Corporation, London.

Hess, U., Syroka, J. (2005), *Weather-based insurance in Southern Africa: The case of Malawi*, The World Bank.

Hiemstra, L.A.V., Zucchini, W.S., Pegram, G.G.S. (1976), "A method of finding the family of runhydrographs for given return periods", *Journal of Hydrology*, Vol. 30 No. 1, pp.95-103.

Hill, R.V., Hoddinott, J., Kumar, N. (2013), "Adoption of weather-index insurance: Learning from willingness to pay among a panel of households in rural Ethiopia", *Agricultural Economics*, Vol. 44 No. 4-5, pp.385-398.

Hosking, J.R.M. (1990), "L-moments: analysis and estimation of distributions using linear combinations of order statistics", *Journal of the Royal Statistical Society. Series B (Methodological)*, Vol. No. pp.105-124.

Indrani, P., Abir, A.T. (2011), "Assessing seasonal precipitation trends in India using parametric and non-parametric statistical techniques", *Theoretical & Applied Climatology*, Vol. 103 No. 1/2, pp.1-11.

Jewson, S., Brix, A. (2005), *Weather Derivative Valuation: the Meteorological, Statistical, Financial and Mathematical Foundations*, Cambridge University Press.

Jones, C., Marron, J.S., Sheather, S.J. (1996), "Progress in data-based bandwidth selection for kernel density estimation", *Computational Statistics*, Vol. No. 11, pp.337-381.

Jones, M.C., Foster, P.J. (1996), "A simple nonnegative boundary correction method for kernel density estimation", *Statistica Sinica*, Vol. 6 No. 4, pp.1005-1013.

Kannan, S., Ghosh, S. (2013), "A nonparametric kernel regression model for downscaling multisite daily precipitation in the Mahanadi basin", *Water Resources Research*, Vol. 49 No. 3, pp.1360-1385.

Kao, S.C., Govindaraju, R.S. (2009), "A copula-based joint deficit index for droughts", *Journal of Hydrology*, Vol. 380 No. 1, pp.121-134.

Karlan, D., Kutsoati, E., McMillan, M., Udry, C. (2011), "Crop price indemnified loans for farmers: A pilot experiment in rural Ghana", *Journal of Risk and Insurance*, Vol. 78 No. 1, pp.37-55.

Karunamuni, R.J., Alberts, T. (2005), "A generalized reflection method of boundary correction in kernel density estimation", *Canadian Journal of Statistics*, Vol. 33 No. 4, pp.497-509.

Keyantash, J., Dracup, J.A. (2002), "The quantification of drought: An evaluation of drought indices", *Bulletin of the American Meteorological Society*, Vol. 83 No. 8, pp.1167.

Kim, K.D., Heo, J.H. (2002), "Comparative study of flood quantiles estimation by nonparametric models", *Journal of Hydrology*, Vol. 260 No. 1, pp.176-193.

Kim, T.W., Valdes, J.B., Yoo, C. (2006), "Nonparametric approach for bivariate drought characterization using Palmer drought index", *Journal of Hydrologic Engineering*, Vol. 11 No. 2, pp.134-143.

Kim, T.W., Valdés, J.B., Yoo, C. (2003), "Nonparametric approach for estimating return periods of droughts in arid regions", *Journal of Hydrologic Engineering*, Vol. 8 No. 5, pp.237-246.

Kogan, F.N. (1995), "Droughts of the late 1980s in the United States as derived from NOAA polar-orbiting satellite data", *Bulletin of the American Meteorological Society*, Vol. 76 No. 5, pp.655-668.

Łabędzki, L. (2007), "Estimation of local drought frequency in central Poland using the standardized precipitation index SPI", *Irrigation and Drainage*, Vol. 56 No. 1, pp.67-77.

Lev, M., Iames, V. (2012), *Microinsurance: a case study of the Indian rainfall index insurance market*, The World Bank.

Li, N., Liu, X., Xie, W., Wu, J., Zhang, P. (2013), "The return period analysis of natural disasters with statistical modeling of bivariate joint probability distribution", *Risk Analysis*, Vol. 33 No. 1, pp.134-145.

Li, Y., Ye, W., Wang, M., Yan, X. (2009), "Climate change and drought: a risk assessment of crop-yield impacts", *Climate Research*, Vol. 39 No. 1, pp.31-46.

Linnerooth-Bayer, J., Mechler, R., Pflug, G. (2005), "Refocusing disaster aid", *Science*, Vol. 309 No. 5737, pp.1044-1046.

Livada, I., Assimakopoulos, V.D. (2007), "Spatial and temporal analysis of drought in greece using the Standardized Precipitation Index (SPI)", *Theoretical & Applied Climatology*, Vol. 89 No. 3/4, pp.143-153.

Lou, W., Wu, L., Ni, H., Tang, Q., Mao, Y. (2009), "Design of weather claiming index for citrus freezing damage insurance", *Scientia Agricultura Sinica*, Vol. 42 No. 4, pp.1339-1347.

Manatsa, D., Mukwada, G., Siziba, E., Chinyanganya, T. (2010), "Analysis of multidimensional aspects of agricultural droughts in Zimbabwe using the Standardized Precipitation Index (SPI)", *Theoretical & Applied Climatology*, Vol. 102 No. 3/4, pp.287-305.

Manuamorn, O.P. (2005), *Scaling-Up Micro Insurance*, World Bank.

McKee, T.B., Doesken, N.J., Kleist, J. (1993),"The relationship of drought frequency and duration to time scales", in *Proceedings of the 8th Conference on Applied Climatology*, Anaheim, California, Jan 17-22, American Meteorological Society Boston, MA, pp.179-183.

Michele, C., Salvadori, G., Vezzoli, R., Pecora, S. (2013), "Multivariate assessment of droughts: Frequency analysis and dynamic return period", *Water Resources Research*, Vol. 49 No. 10, pp.6985-6994.

Mishra, A.K., Singh, V.P. (2009), "Analysis of drought severity - area - frequency curves using a general circulation model and scenario uncertainty", *Journal of Geophysical Research: Atmospheres (1984 - 2012)*, Vol. 114 No. D6.

Mishra, A.K., Singh, V.P. (2010), "A review of drought concepts", *Journal of Hydrology*, Vol. 391 No. 1-2, pp.201-216.

Moon, Y.I., Oh, T.S., Kim, M.S., Kim, S.S. (2010),"A drought frequency analysis for Palmer Drought Severity Index using boundary kernel function", in *World*

Environmental and Water Resources Congress 2010, Rhode Island, United States, May 16-20, American Society of Civil Engineers, pp.2708-2716.

Narasimhan, B., Srinivasan, R. (2005), "Development and evaluation of Soil Moisture Deficit Index (SMDI) and Evapotranspiration Deficit Index (ETDI) for agricultural drought monitoring", *Agricultural and Forest Meteorology*, Vol. 133 No. 1, pp.69-88.

Nelson, P., Seth, D.L., Vasudevan, R. (1992), "An integrodifferential equation for the two-dimensional reflection kernel", *Applied Mathematics and Computation*, Vol. 49 No. 1, pp.1-18.

Nieto, J.D., Cook, S.E., Laderach, P., Fisher, M.J., Jones, P.G. (2010), "Rainfall index insurance to help smallholder farmers manage drought risk", *Clim Dev*, Vol. 2 No. 3, pp.233-247.

Norton, M.T., Turvey, C., Osgood, D. (2013), "Quantifying spatial basis risk for weather index insurance", *The Journal of Risk Finance Incorporating Balance Sheet*, Vol. 14 No. 1, pp.20-34.

Osgood, D.E., McLaurin, M., Carriquiry, M., Mishra, A., Fiondella, F., Hansen, J.W., Peterson, N., Ward, M.N. (2007), *Designing weather insurance contracts for farmers in Malawi, Tanzania and Kenya: Final report to the Commodity Risk Management Group, ARD, World Bank*, International Research Institute for Climate and Society.

Palmer, W.C. (1965), *Meteorological drought*, Office of Climatology, US Weather Bureau.

Palmer, W.C. (1968), "Keeping track of crop moisture conditions, nationwide: The new crop moisture index", *Weatherwise*, Vol. 21 No. 4, pp.156-161.

Park, B.U., Marron, J.S. (1990), "Comparison of data-driven bandwidth selectors", *Journal of the American Statistical Association*, Vol. 85 No. 409, pp.66-72.

Parviz, H.J., Akhoond-Ali, A.M., Nazemosadat, M.J. (2013), "Nonparametric kernel estimation of annual precipitation over Iran", *Theoretical and Applied Climatology*, Vol. 112 No. 1-2, pp.193-200.

Ramsey, F. (2014),"An application of kernel density estimation via diffusion to group yield insurance", in *2014 AAEA Annual Meeting*, Minneapolis, July 27-29,

Rosenblatt, M. (1956), "Remarks on some nonparametric estimates of a density function", *The Annals of Mathematical Statistics*, Vol. 27 No. 3, pp.832-837.

Sadat Noori, S.M., Liaghat, A.M., Ebrahimi, K. (2012), "Prediction of crop production using drought indices at different time scales and climatic factors to manage drought risk", *Journal of the American Water Resources Association*, Vol. 48 No. 1, pp.1-9.

Santhosh, D., Srinivas, V.V. (2013), "Bivariate frequency analysis of floods using a diffusion based kernel density estimator", *Water Resources Research*, Vol. 49 No. 12, pp.8328-8343.

Sarris, A. (2013), "Weather index insurance for agricultural development: introduction and overview", *Agricultural Economics*, Vol. 44 No. 4-5, pp.381-384.

Schwarz, G. (1978), "Estimating the dimension of a model", *The Annals of Statistics*, Vol. 6 No. 2, pp.461-464.

Scott, D.W., Terrell, G.R. (1987), "Biased and unbiased cross-validation in density estimation", *Journal of the American Statistical Association*, Vol. 82 No. 400, pp.1131-1146.

Sen, Z. (1998), "Average areal precipitation by percentage weighted polygon method", *Journal of Hydrologic Engineering*, Vol. 3 No. 1, pp.69-72.

Shafer, B.A., Dezman, L.E. (1982),"Development of a Surface Water Supply Index (SWSI) to assess the severity of drought conditions in snowpack runoff areas", in *Proceedings of the Western Snow Conference*, Reno, Nevada, April, Western Snow Conference, pp.164-175.

Sheather, S.J., Jones, M.C. (1991), "A reliable data-based bandwidth selection method for kernel density estimation", *Journal of the Royal Statistical Society. Series B (Methodological)*, Vol. No. pp.683-690.

Shiau, J.T., Feng, S., Nadarajah, S. (2007), "Assessment of hydrological droughts for the Yellow River, China, using copulas", *Hydrological Processes*, Vol. 21 No. 16, pp.2157-2163.

Silverman, B.W. (1986), *Density Estimation for Statistics and Data Analysis*, CRC press.

Singh, K., Singh, V.P. (1991), "Derivation of bivariate probability density functions with exponential marginals", *Stochastic Hydrology and Hydraulics*, Vol. 5 No. 1, pp.55-68.

Sivakumar, M.V.K. (2010),"Agricultural drought-WMO perspectives", in *Agricultural Drought Indices: Proceedings of an Expert Meeting*, Murcia, Spain, June 2-4, World Meteorological Organizatio.

Skees, J., Hartell, J., Murphy, A., Collier, B. (2009), *Designing agricultural index insurance in developing countries: A GlobalAgRisk market development model handbook for policy and decision makers*, Global AgRisk, Inc.

Skees, J., Varangis, P., Larson, D., Siegel, P. (2002), *Can financial markets be tapped to help poor people cope with weather risks?*, Department of Agricultural Economics, University of Kentucky，Development Research Group, The World Bank.

Skees, J.R. (2001), *Developing rainfall-based index insurance in Morocco*, World Bank Publications.

Skees, J.R. (2011), *Pre-feasibility: Earthquake risk and index based insurance for Indonesia-Prepared for the Ford Foundation*, GlobalAgRisk.

Skees, J.R., Barnett, B.J. (2006), "Enhancing microfinance using index-based risk-transfer products", *Agricultural Finance Review*, Vol. 66 No. 2, pp.235-250.

Skees, J.R., Barnett, B.J., Hartell, J. (2006),"Innovations in government responses to catastrophic risk sharing for agriculture in developing countries", in *International Association of Agricultural Economists Conference*, Gold Coast, Australia, August 12–18.

Skoufias, E. (2012), *The poverty and welfare impacts of climate change quantifying the effects, identifying the adaptation strategies*, World Bank Publications.

Solomon, S., D. Qin, M. Manning, Z. Chen, M. Marquis, K.B. Averyt, M. Tignor and H.L. Miller (2007), *IPCC Fourth Assessment Report: Climate Change. Contribution of Working Group I to the Fourth Assessment Report of the Intergovernmental Panel on Climate Change*, Cambridge, United Kingdom and New York, NY, USA.

Stocker, T.F., Qin, D., Plattner, G.K., Tignor, M., Allen, S.K., Boschung, J., Nauels, A., Xia, Y., Bex, V., Midgley, P.M. (2013), *Climate Change 2013. The Physical Science Basis. Working Group I Contribution to the Fifth Assessment Report of the Intergovernmental Panel on Climate Change*, Cambridge University Press, UK.

Stoppa, A., Manuamorn, O.P. (2010), *Weather index insurance for maize production in eastern Indonesia*, International Finance Corporation.

Swanepoel, J.W.H., Van Graan, F.C. (2005), "A new kernel distribution function estimator based on a non-parametric transformation of the data", *Scandinavian Journal of Statistics*, Vol. 32 No. 4, pp.551-562.

Tate, E.L., Gustard, A., (2000). *Drought Definition: A Hydrological Perspective*. Drought and Drought Mitigation in Europe. Springer, New York, pp. 23-48.

Teegavarapu, R.S.V., Chandramouli, V. (2005), "Improved weighting methods, deterministic and stochastic data-driven models for estimation of missing precipitation records", *Journal of Hydrology*, Vol. 312 No. pp.191-206.

Thiessen, A.H. (1911), "Precipitation averages for large areas", *Monthly Weather Review*, Vol. 39 No. 7, pp.1082-1089.

Trærup, S.L.M. (2012), "Informal networks and resilience to climate change impacts: a collective approach to index insurance", *Global Environmental Change*, Vol. 22 No. 1, pp.255-267.

Turvey, C.G., Kong, R. (2010), "Weather risk and the viability of weather insurance in China's Gansu, Shaanxi, and Henan provinces", *China Agricultural Economic Review*, Vol. 2 No. 1, pp.5-24.

Van Kerm, P. (2003), "Adaptive Kernel Density Estimation", *Stata Journal*, Vol. 3 No. 2, pp.148-156.

Vicent, A.O., Llasat, M.C., Ferrari, E., Atencia, A., Sirangelo, B. (2011), "Monthly Rainfall Changes in Central and Western Mediterranean Basins, at the End of the 20th and Beginning of the 21st Centuries", *International Journal of Climatology*, Vol. 31 No. 13, pp.1943-1958.

Wang, M., Shi, P., Ye, T., Liu, M., Zhou, M. (2011), "Agriculture Insurance in China: History, Experience, and Lessons Learned", *International Journal of Disaster Risk Science*, Vol. 2 No. 2, pp.10-22.

Wang, X., Hou, X., Li, Z., Wang, Y. (2014), "Spatial and Temporal Characteristics of Meteorological Drought in Shandong Province, China, from 1961 to 2008", *Advances in Meteorology*, Vol. 2014 No.

Wu, H., Wilhite, D.A. (2004), "An operational agricultural drought risk assessment model for Nebraska, USA", *Nat Hazards*, Vol. 33 No. 1, pp.1-21.

Wu, L.Y., Yiping (2010), "Design of products for rice agro-meteorological index insurance: A case in Zhejiang province ", *Scientia Agricultura Sinica* Vol. 43 No. 23, pp.4942-4950.

Xue, X. (2004), *Study on quantificational relation between drought and agriculture yield in Shandong province*, Ocean University of China, Qingdao.

Yang, R., Wang, L., Xian, Z. (2010), "Evaluation on the efficiency of crop insurance in China's major grain-producing area", *Agriculture and Agricultural Science Procedia*, Vol. 1 No. 0, pp.90-99.

Yang, T., Liu, B., Sun, X., Li, D., Xun, S. (2013), "Design and application of the weather indices of winter wheat planting insurance in Anhui province", *Chinese Journal of Agrometeorology*, Vol. 2 No. pp.017.

Yearbook (1979-2012), *Shandong Statistical Yearbook*, China Statistics Press, Beijing.

Yearbook (1989-2011), *Statistic Yearbook of Taian*, China Statistics Press, Beijing.

Yearbook (2002-2011), *Yearbook of China's Insurance (2002-2011)*, China Statistics Press, Beijing.

Yearbook (2011), *China Statistical Yearbook*, China Statistics Press, Beijing.

Yearbook (2013), *Shandong Statistical Yearbook*, China Statistics Press, Beijing.

Yevjevich, V. (1969), "Review: An objective approach to definitions and investigations of continental hydrologic droughts. Fort Collins, Colorado State University, 1967, 19 p. (Hydrology paper no. 23)", *Journal of Hydrology*, Vol. 7 No. pp.353.

Zaw, W.T., Naing, T.T. (2008), "Empirical statistical modeling of rainfall prediction over Myanmar", *International Scholarly and Scientific Research & Innovation*, Vol. 2 No. 10, pp.3418-3421.

Zhang, Q., Xiao, M., Singh, V.P., Chen, X. (2013), "Copula-based risk evaluation of droughts across the Pearl River basin, China", *Theoretical and Applied Climatology*, Vol. 111 No. 1-2, pp.119-131.

Zhu, J. (2011), "Evaluation of an insurance scheme based on the weather index", *Chinese Economy*, Vol. 44 No. 6, pp.56-72.

APPENDIX 1

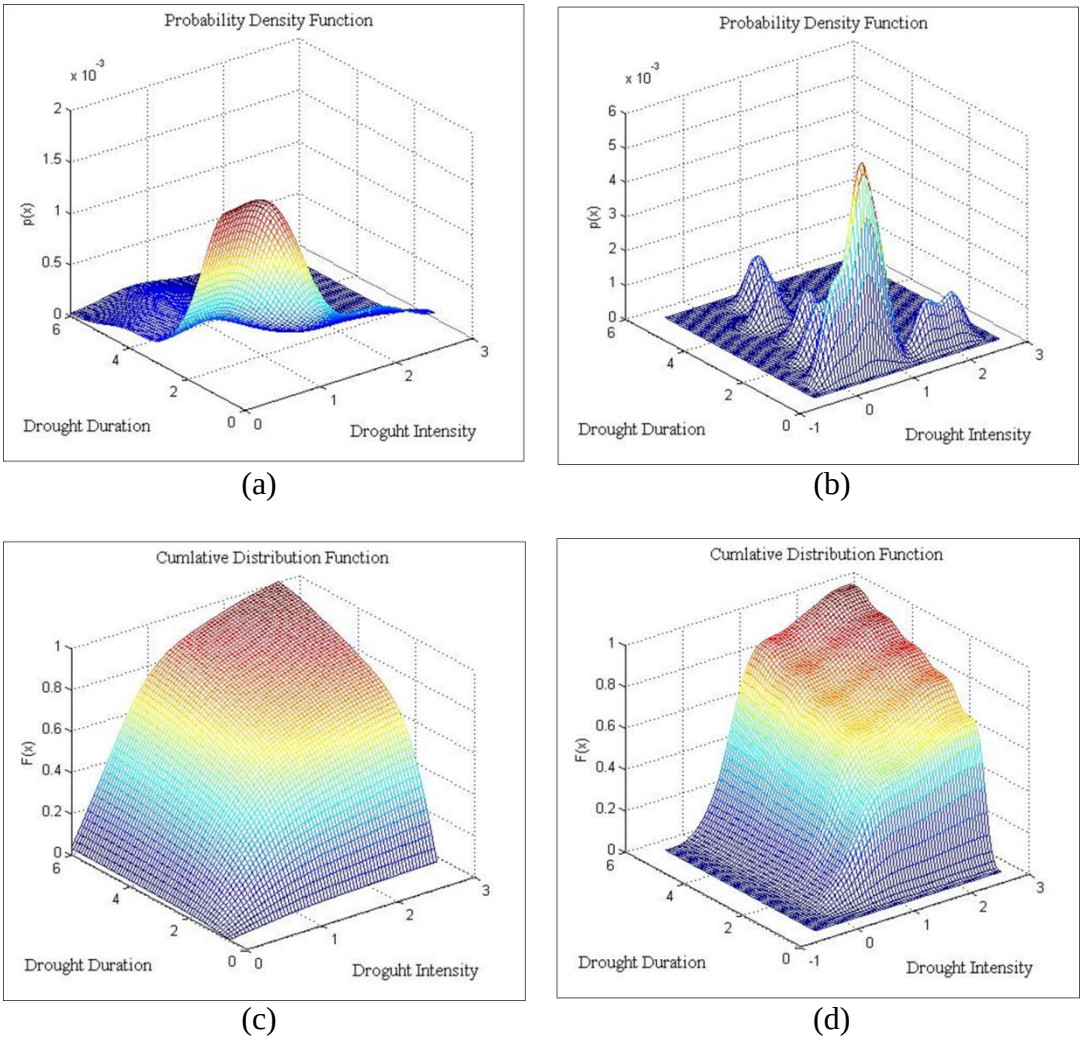

Figure 9-1 Weather station 54725 (a) DKDE estimated bivariate PDF of SPI based drought risk (PII-PV) (b) GKDE estimated bivariate PDF of SPI based drought risk (PII-PV) (c) DKDE estimated bivariate CDF of SPI based drought risk (PII-PV) (d) GKDE estimated bivariate CDF of SPI based drought risk (PII-PV)

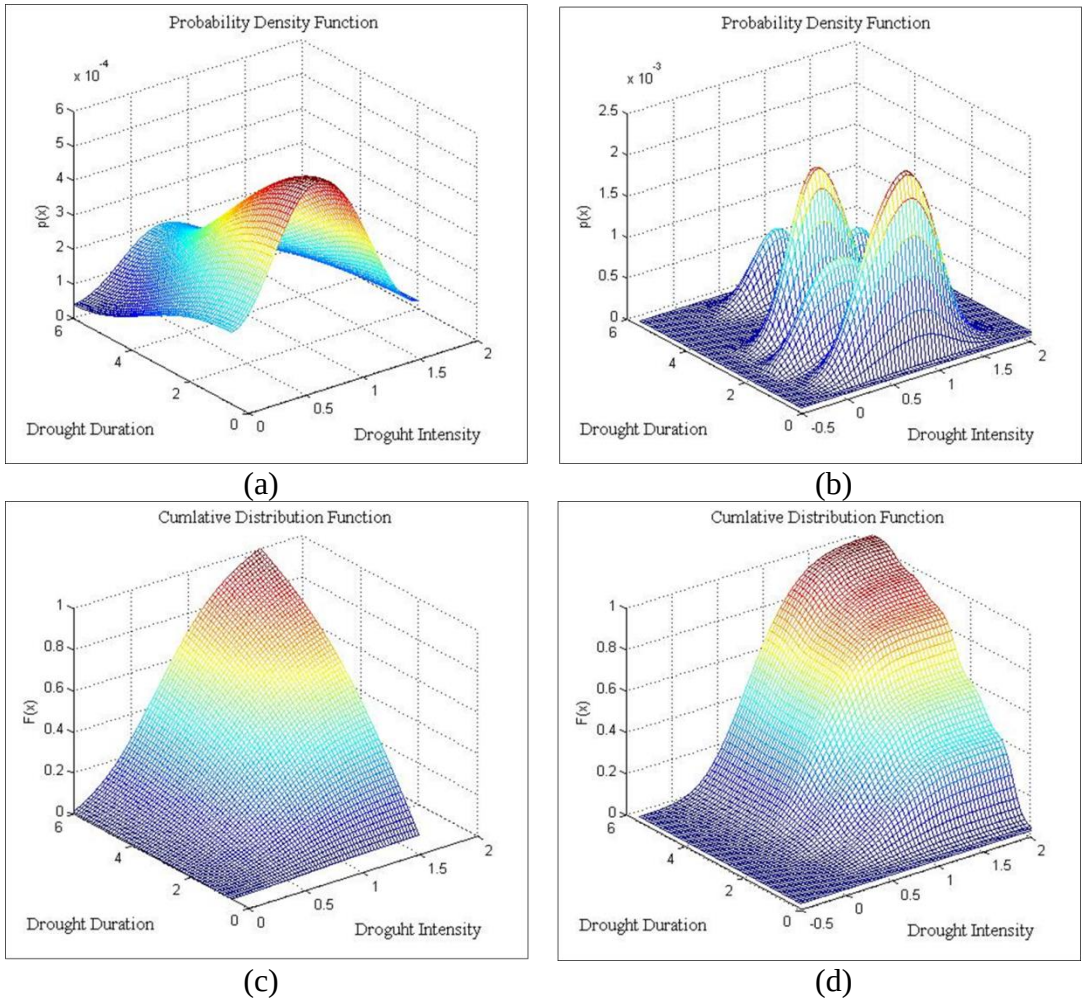

Figure 9-2 Weather station 54736 (a) DKDE estimated bivariate PDF of SPI based drought risk (PII-PV) (b) GKDE estimated bivariate PDF of SPI based drought risk (PII-PV) (c) DKDE estimated bivariate CDF of SPI based drought risk (PII-PV) (d) GKDE estimated bivariate CDF of SPI based drought risk (PII-PV)

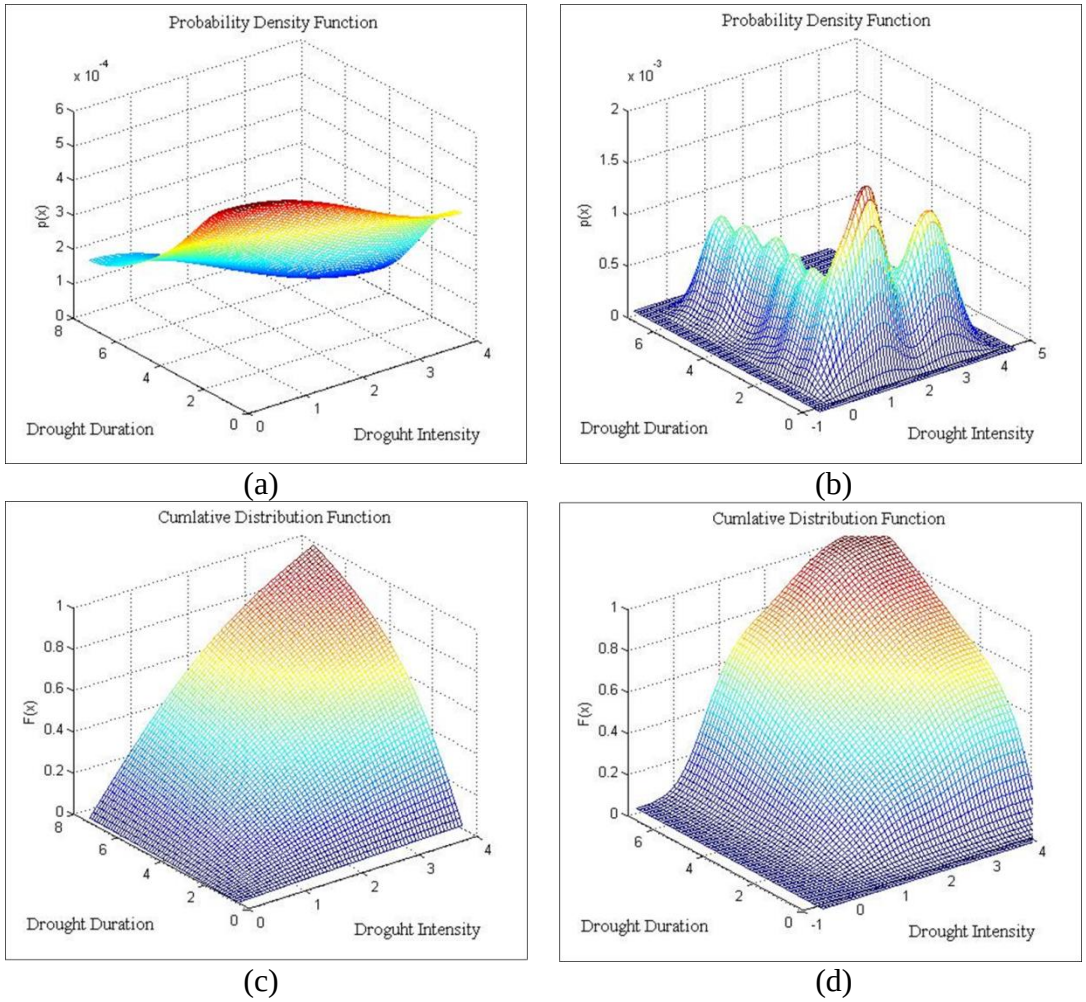

Figure 9-3 Weather station 54741 (a) DKDE estimated bivariate PDF of SPI based drought risk (PII-PV) (b) GKDE estimated bivariate PDF of SPI based drought risk (PII-PV) (c) DKDE estimated bivariate CDF of SPI based drought risk (PII-PV) (d) GKDE estimated bivariate CDF of SPI based drought risk (PII-PV)

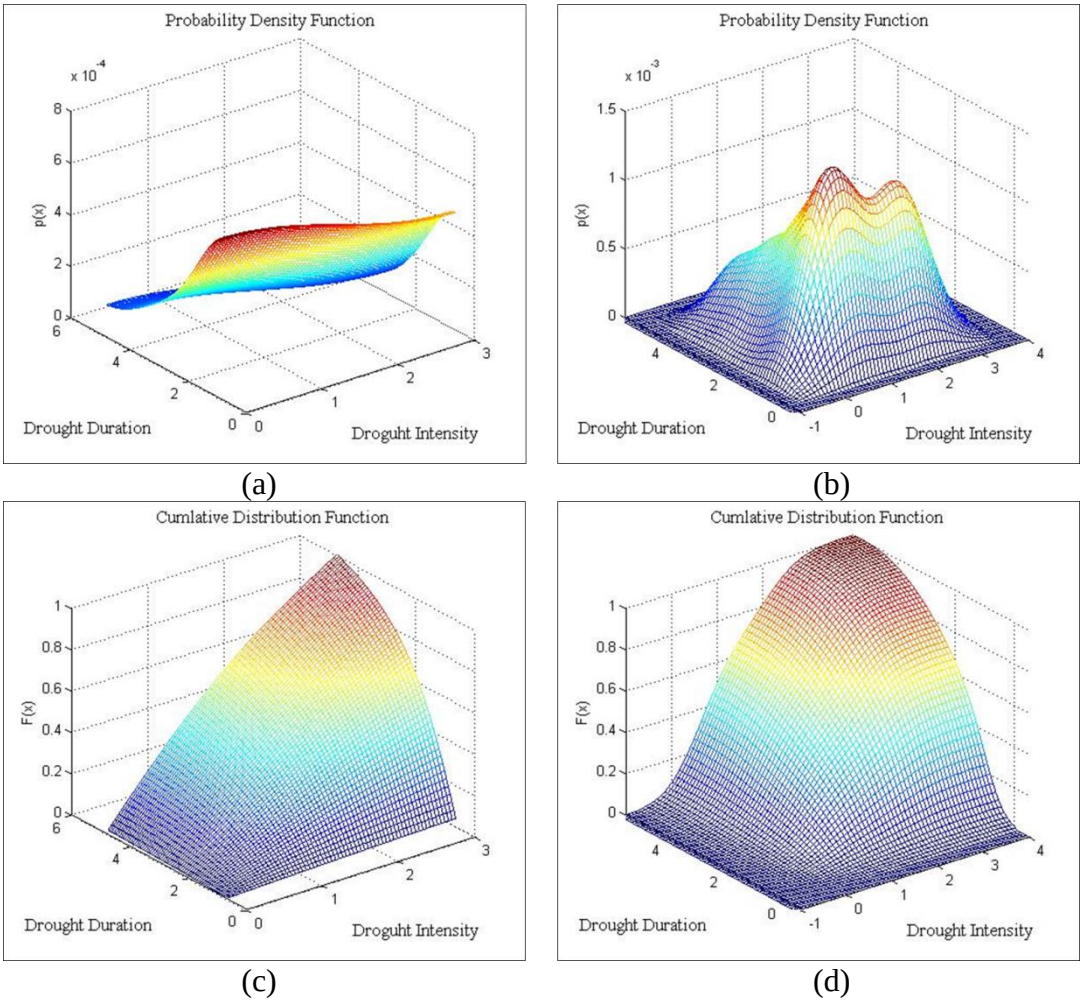

Figure 9-4 Weather station 54753 (a) DKDE estimated bivariate PDF of SPI based drought risk (PII-PV) (b) GKDE estimated bivariate PDF of SPI based drought risk (PII-PV) (c) DKDE estimated bivariate CDF of SPI based drought risk (PII-PV) (d) GKDE estimated bivariate CDF of SPI based drought risk (PII-PV)

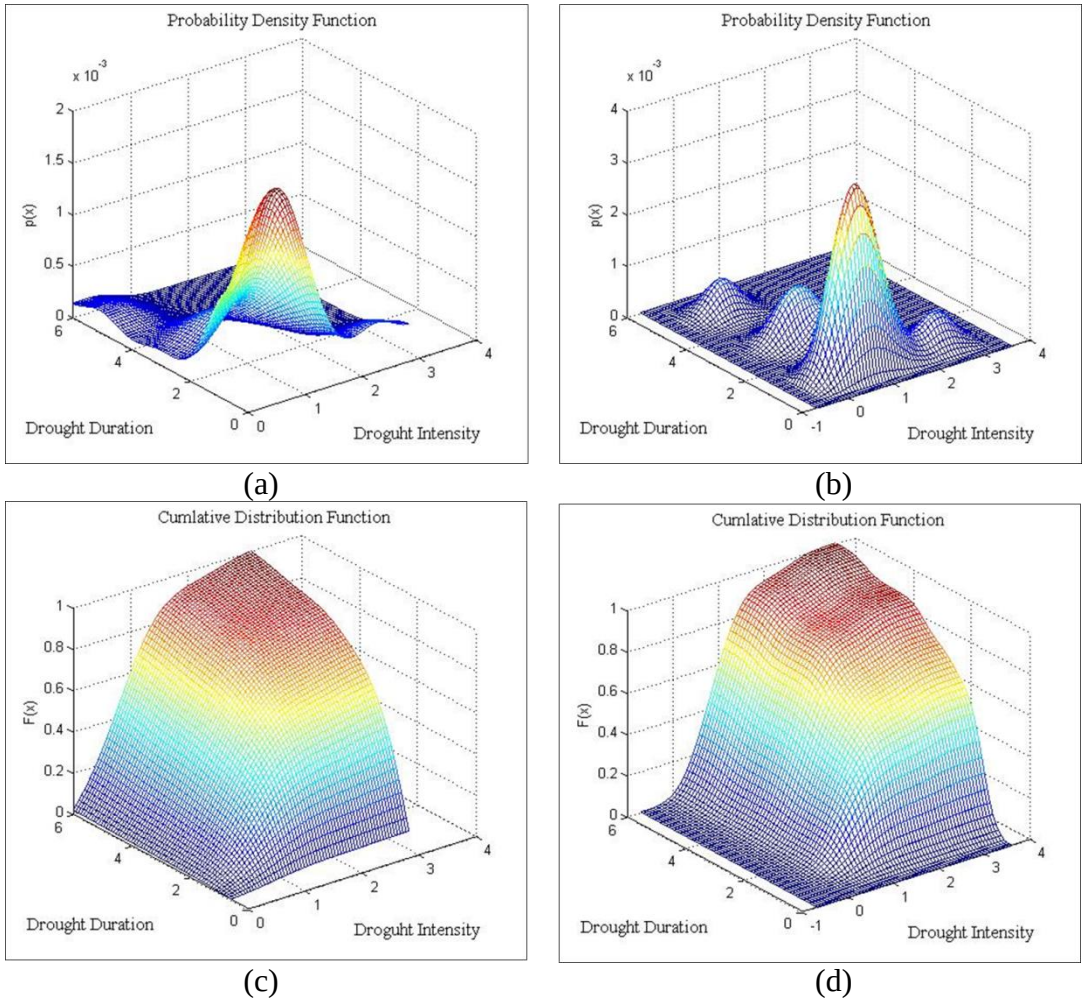

Figure 9-5 Weather station 54764 (a) DKDE estimated bivariate PDF of SPI based drought risk (b) GKDE estimated bivariate PDF of SPI based drought risk (c) DKDE estimated bivariate CDF of SPI based drought risk (d) GKDE estimated bivariate CDF of SPI based drought risk

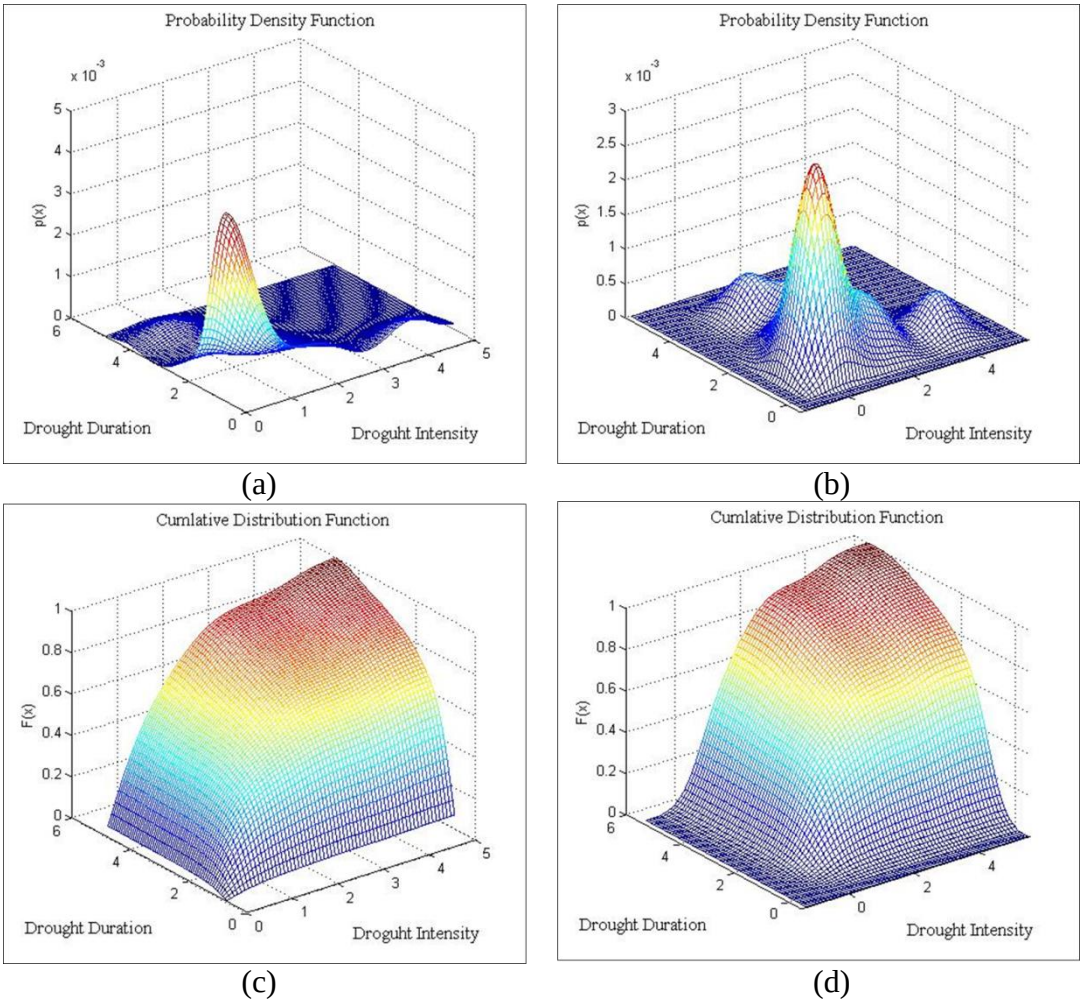

Figure 9-6 Weather station 54774 (a) DKDE estimated bivariate PDF of SPI based drought risk (PII-PV) (b) GKDE estimated bivariate PDF of SPI based drought risk (PII-PV) (c) DKDE estimated bivariate CDF of SPI based drought risk (PII-PV) (d) GKDE estimated bivariate CDF of SPI based drought risk (PII-PV)

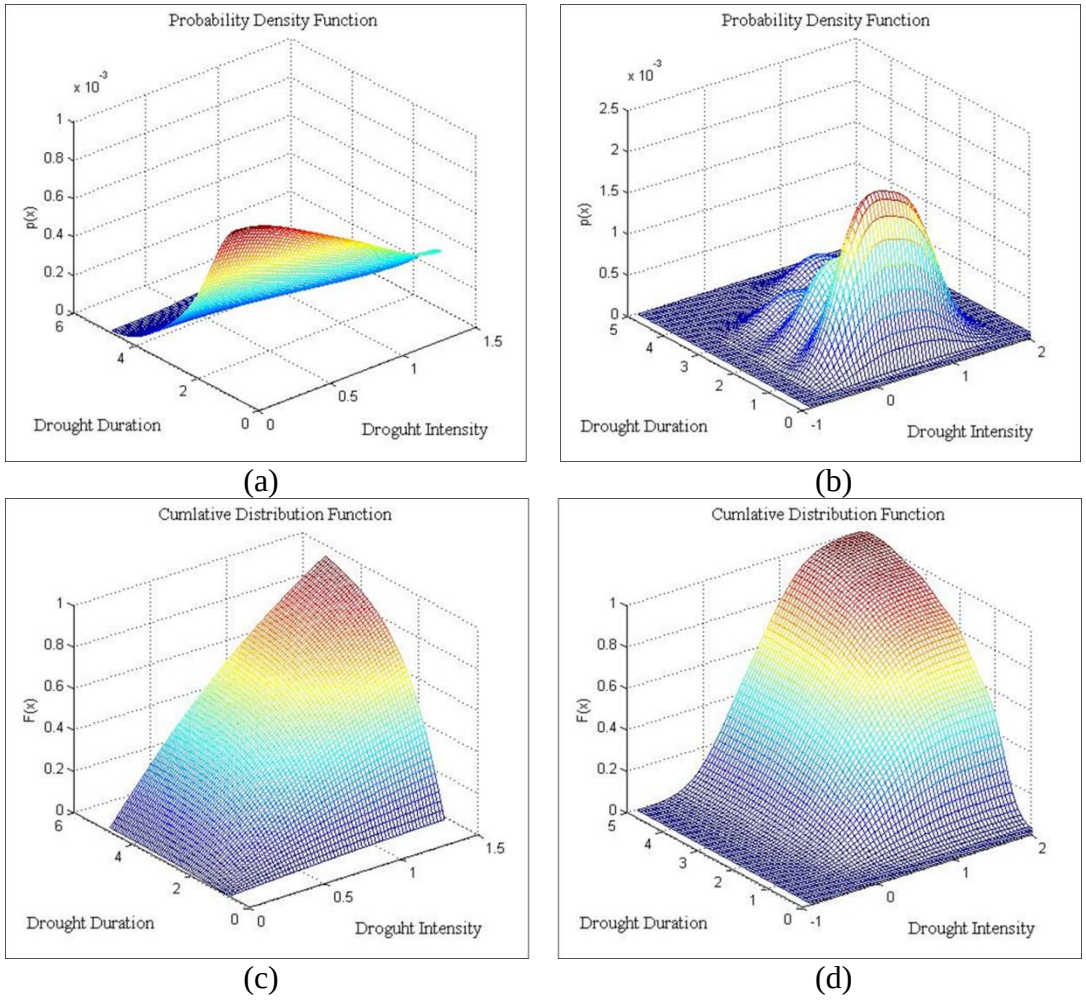

Figure 9-7 Weather station 54776 (a) DKDE estimated bivariate PDF of SPI based drought risk (PII-PV) (b) GKDE estimated bivariate PDF of SPI based drought risk (PII-PV) (c) DKDE estimated bivariate CDF of SPI based drought risk (PII-PV) (d) GKDE estimated bivariate CDF of SPI based drought risk (PII-PV)

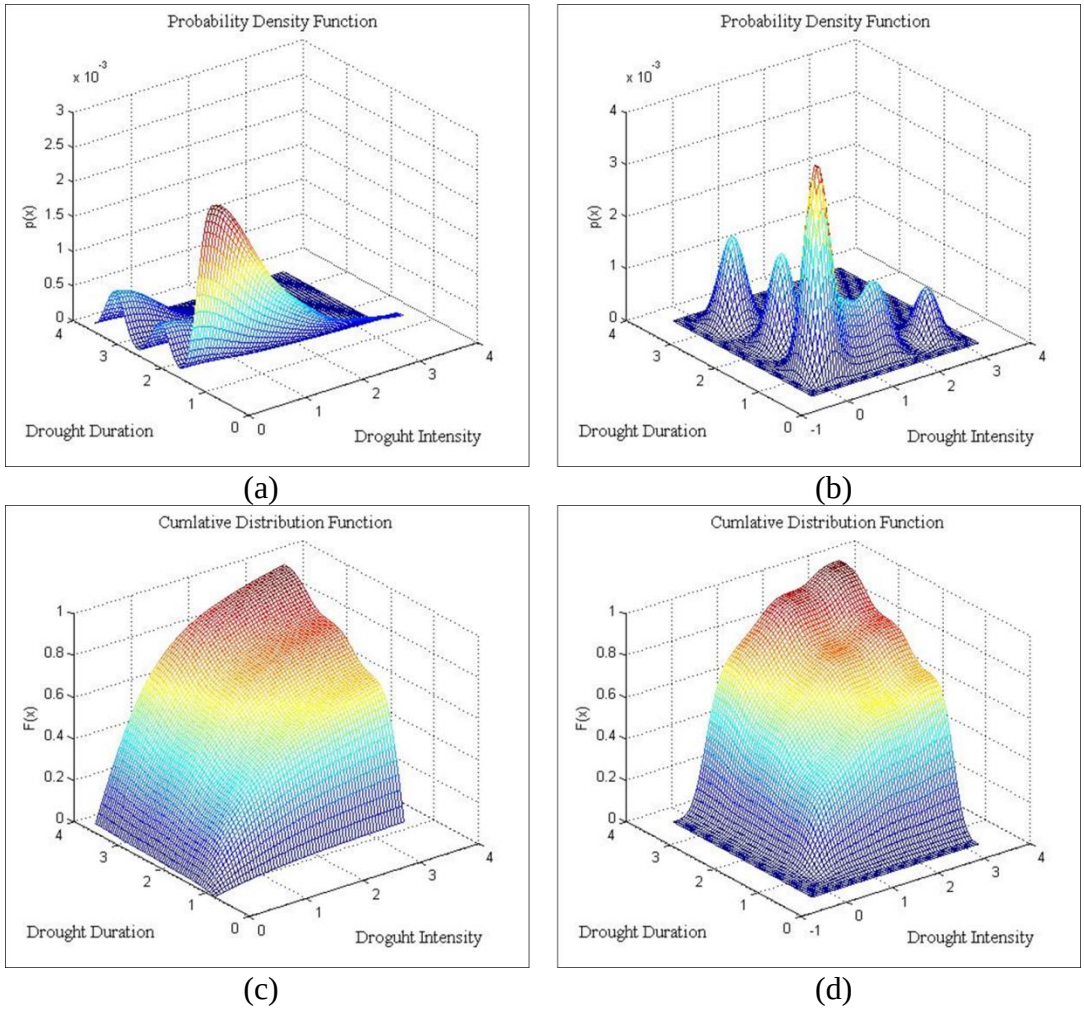

Figure 9-8 Weather station 54823 (a) DKDE estimated bivariate PDF of SPI based drought risk (PII-PV) (b) GKDE estimated bivariate PDF of SPI based drought risk (PII-PV) (c) DKDE estimated bivariate CDF of SPI based drought risk (PII-PV) (d) GKDE estimated bivariate CDF of SPI based drought risk (PII-PV)

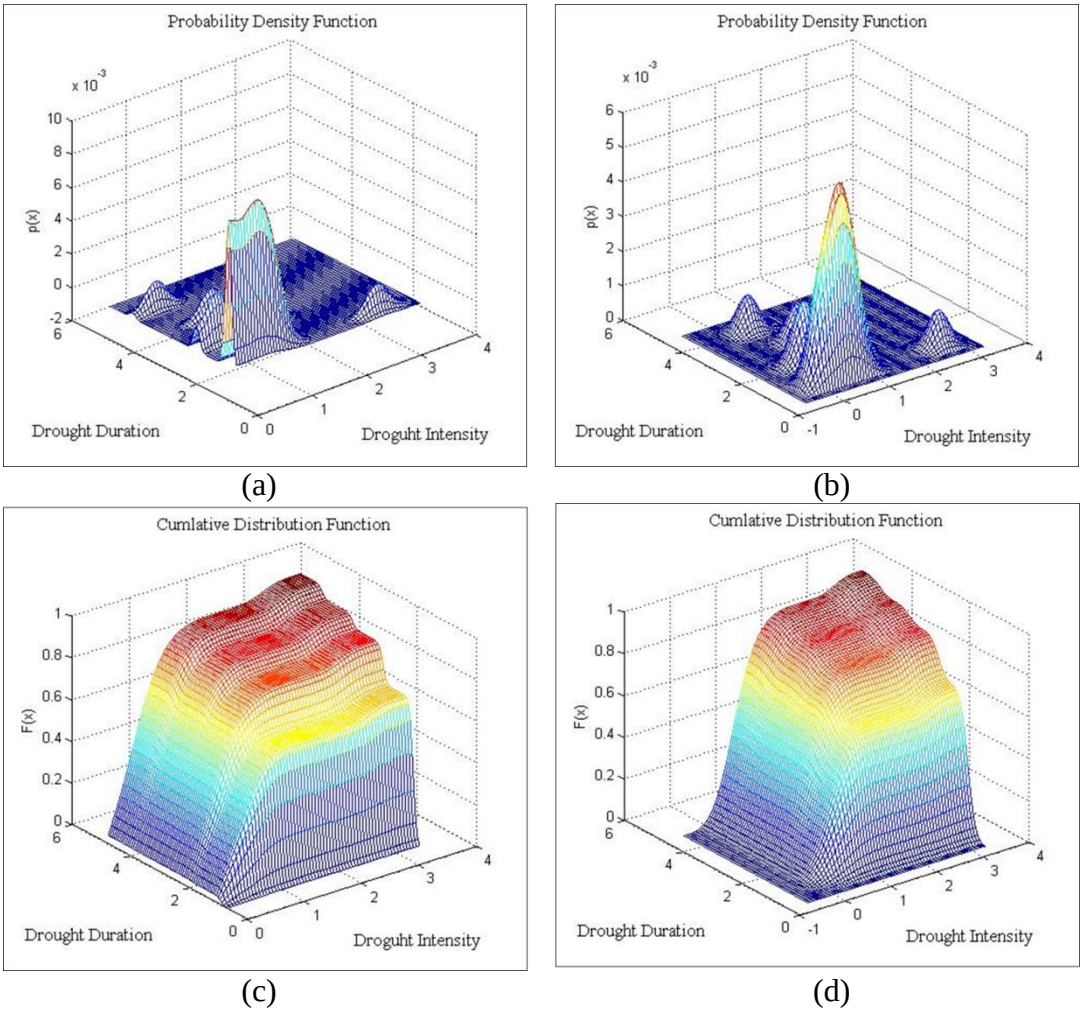

Figure 9-9 Weather station 54824 (a) DKDE estimated bivariate PDF of SPI based drought risk (PII-PV) (b) GKDE estimated bivariate PDF of SPI based drought risk (PII-PV) (c) DKDE estimated bivariate CDF of SPI based drought risk (PII-PV) (d) GKDE estimated bivariate CDF of SPI based drought risk (PII-PV)

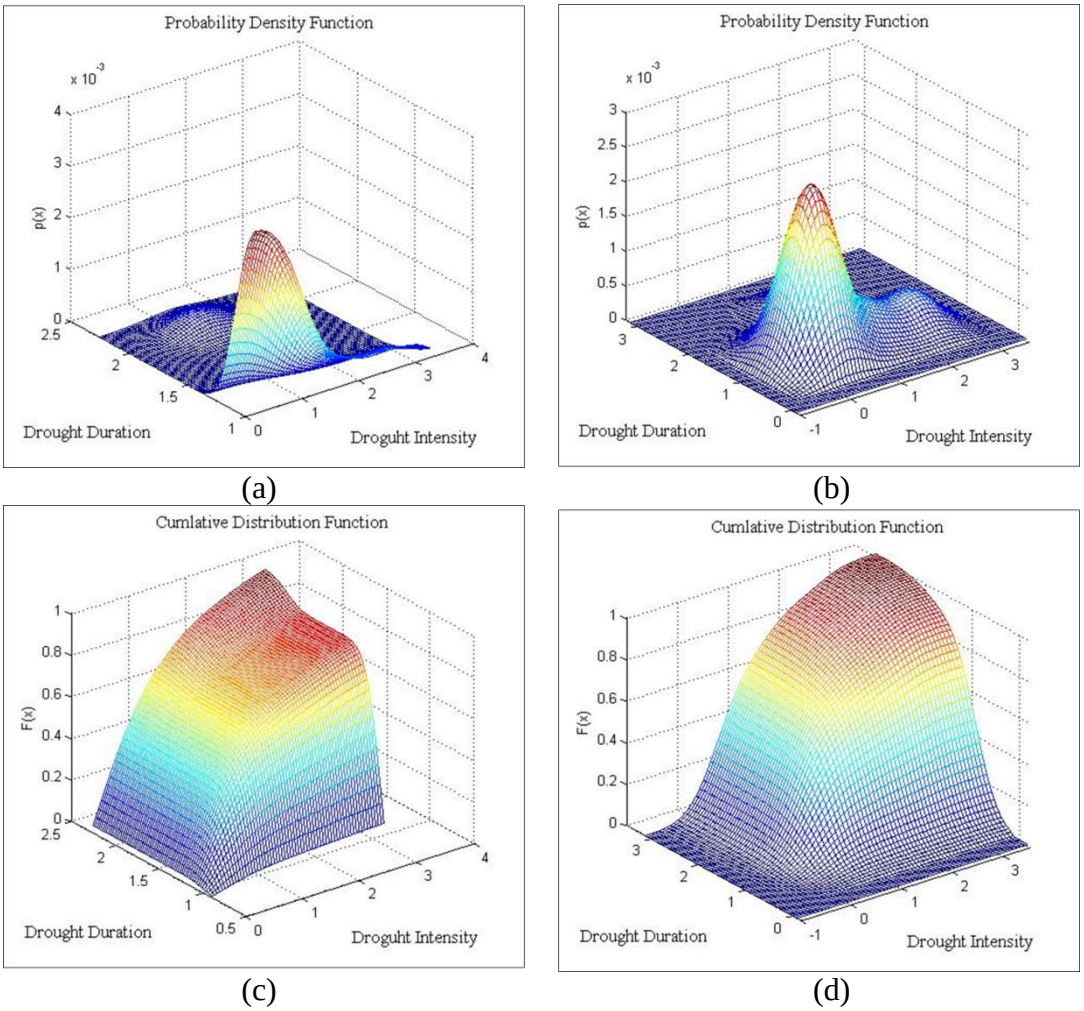

Figure 9-10 Weather station 54827 (a) DKDE estimated bivariate PDF of SPI based drought risk (PII-PV) (b) GKDE estimated bivariate PDF of SPI based drought risk (PII-PV) (c) DKDE estimated bivariate CDF of SPI based drought risk (PII-PV) (d) GKDE estimated bivariate CDF of SPI based drought risk (PII-PV)

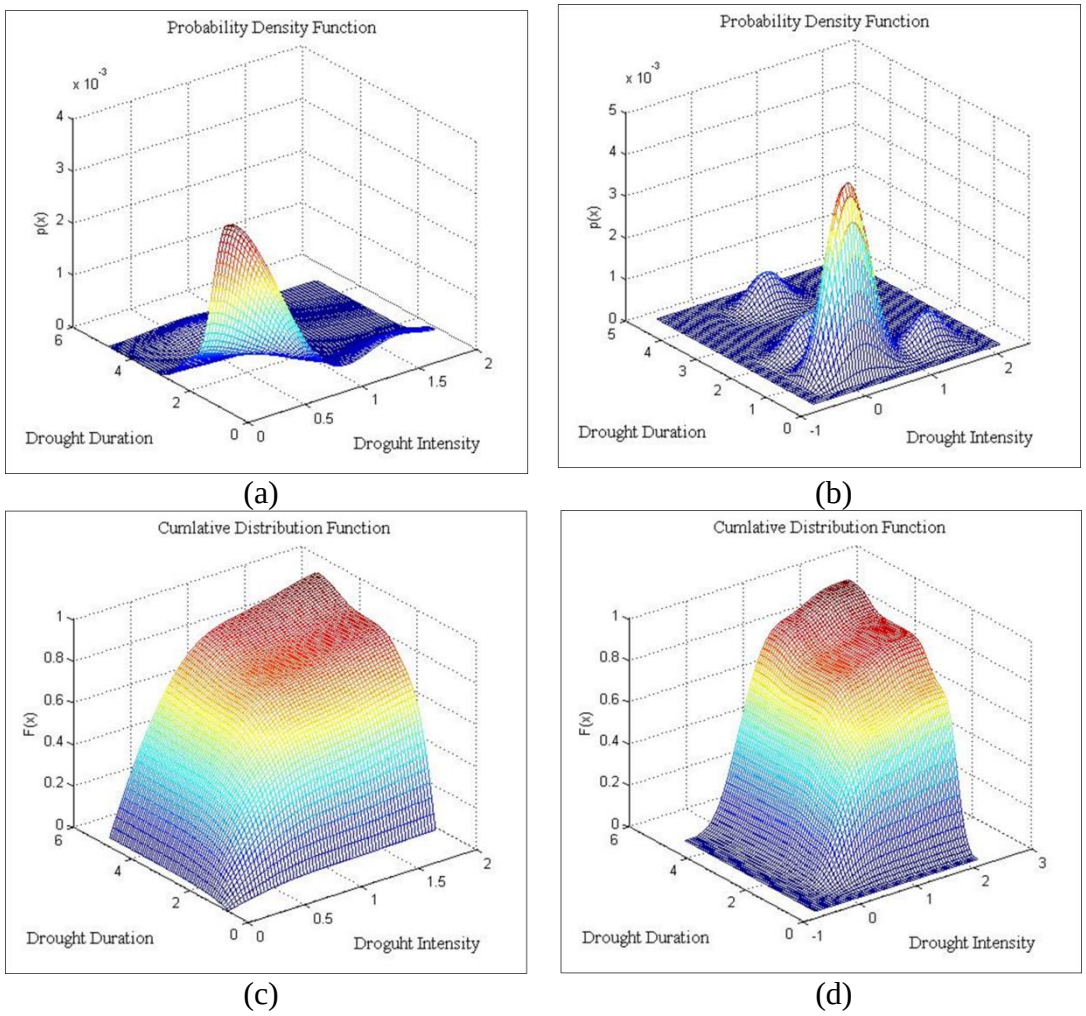

Figure 9-11 Weather station 54836 (a) DKDE estimated bivariate PDF of SPI based drought risk (PII-PV) (b) GKDE estimated bivariate PDF of SPI based drought risk (PII-PV) (c) DKDE estimated bivariate CDF of SPI based drought risk (PII-PV) (d) GKDE estimated bivariate CDF of SPI based drought risk (PII-PV)

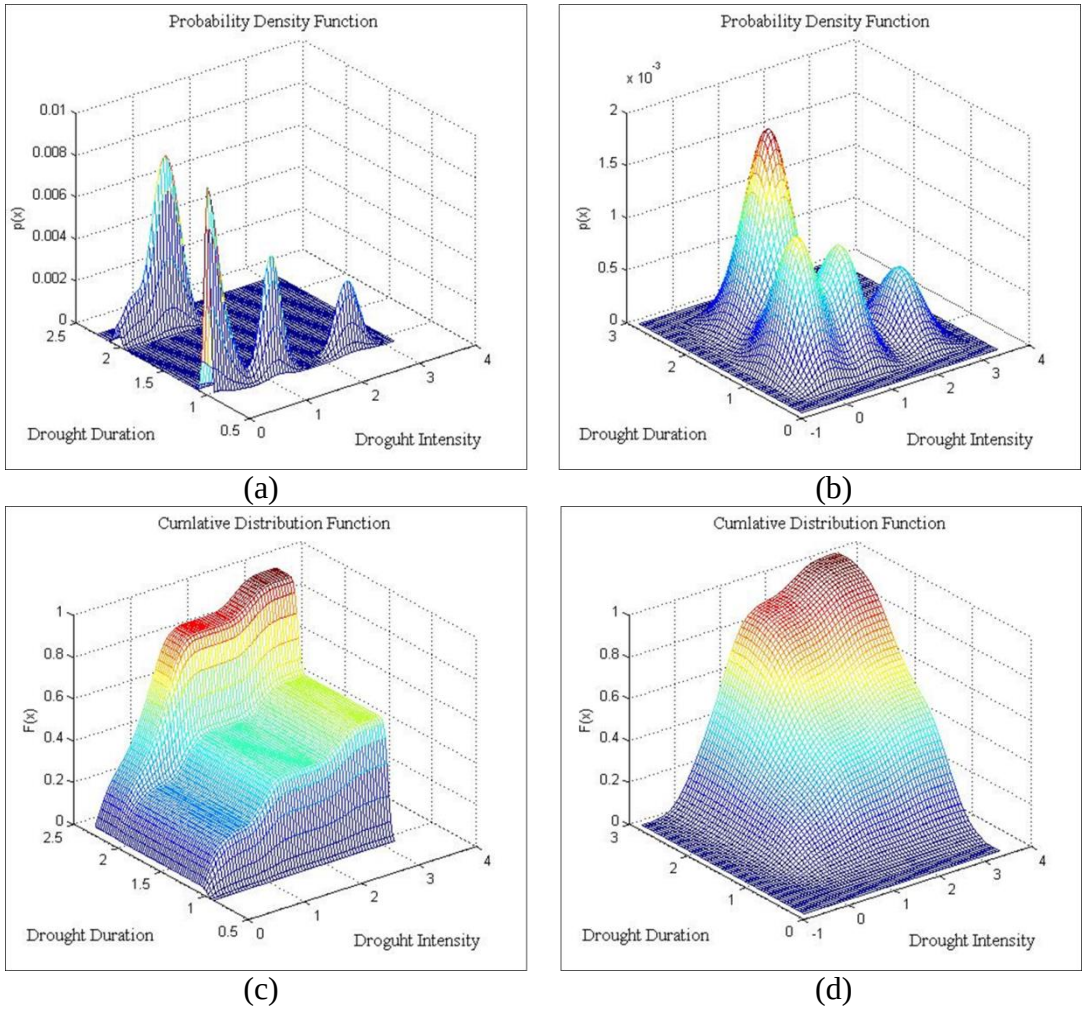

Figure 9-12 Weather station 54843 (a) DKDE estimated bivariate PDF of SPI based drought risk (PII-PV) (b) GKDE estimated bivariate PDF of SPI based drought risk (PII-PV) (c) DKDE estimated bivariate CDF of SPI based drought risk (PII-PV) (d) GKDE estimated bivariate CDF of SPI based drought risk (PII-PV)

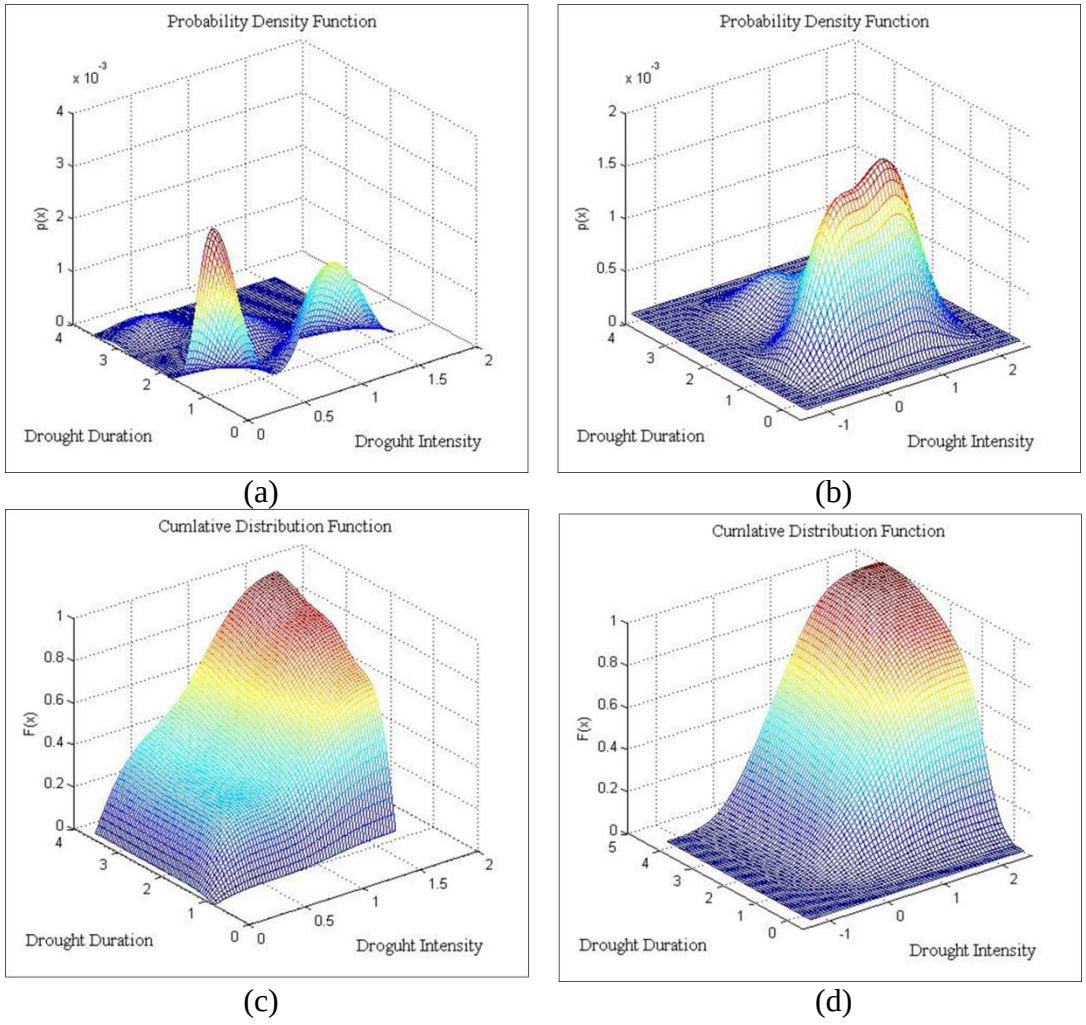

Figure 9-13 Weather station 54852 (a) DKDE estimated bivariate PDF of SPI based drought risk (PII-PV) (b) GKDE estimated bivariate PDF of SPI based drought risk (PII-PV) (c) DKDE estimated bivariate CDF of SPI based drought risk (PII-PV) (d) GKDE estimated bivariate CDF of SPI based drought risk (PII-PV)

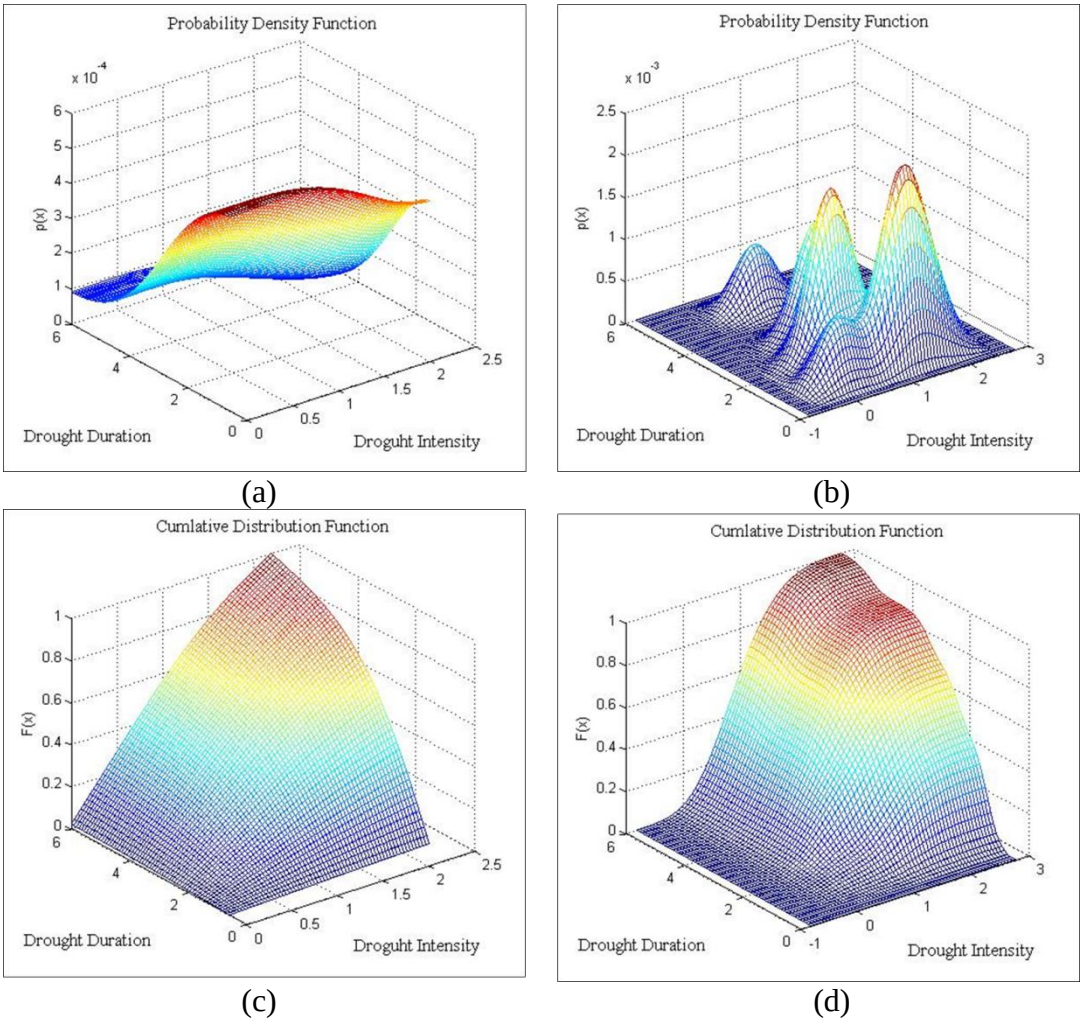

Figure 9-14 Weather station 548457 (a) DKDE estimated bivariate PDF of SPI based drought risk (PII-PV) (b) GKDE estimated bivariate PDF of SPI based drought risk (PII-PV) (c) DKDE estimated bivariate CDF of SPI based drought risk (PII-PV) (d) GKDE estimated bivariate CDF of SPI based drought risk (PII-PV)

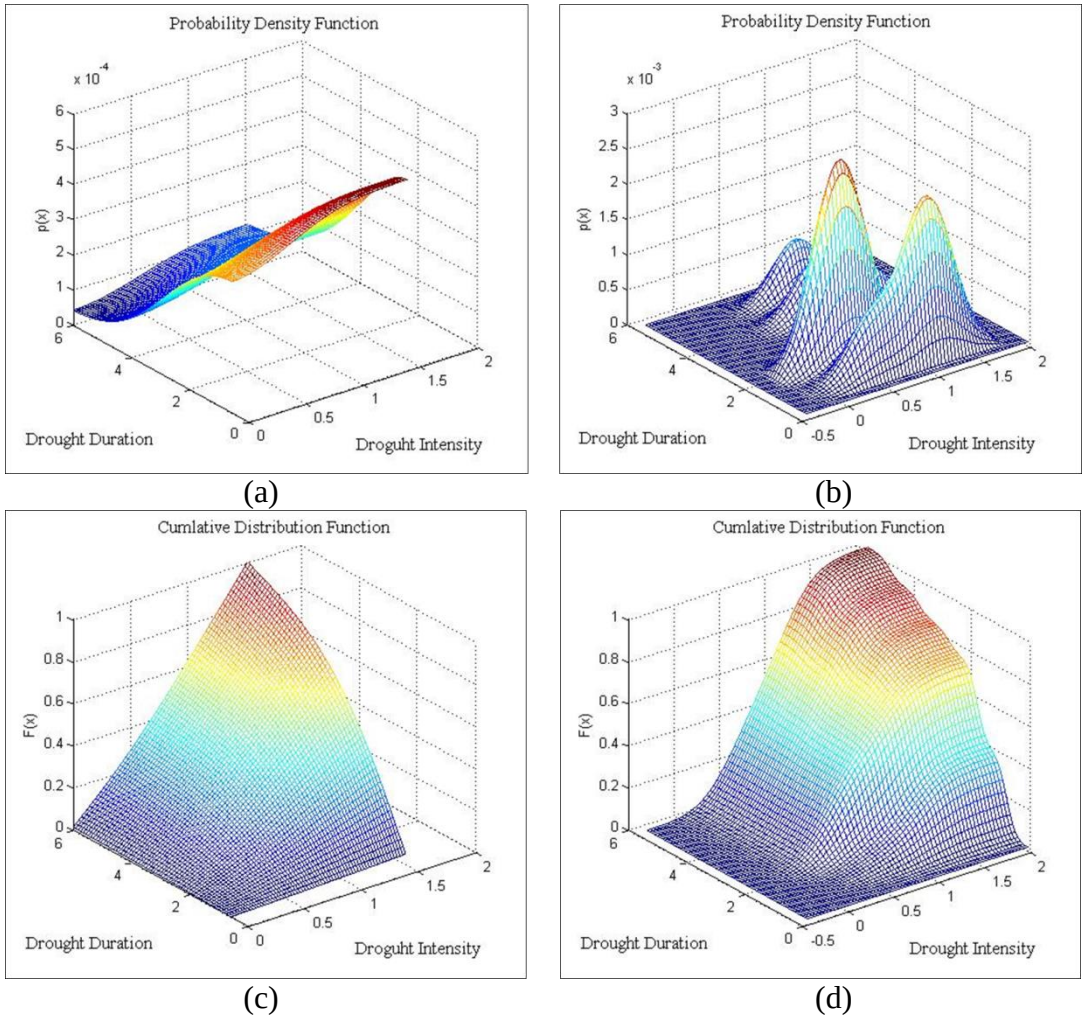

Figure 9-15 Weather station 54906 (a) DKDE estimated bivariate PDF of SPI based drought risk (PII-PV) (b) GKDE estimated bivariate PDF of SPI based drought risk (PII-PV) (c) DKDE estimated bivariate CDF of SPI based drought risk (PII-PV) (d) GKDE estimated bivariate CDF of SPI based drought risk (PII-PV)

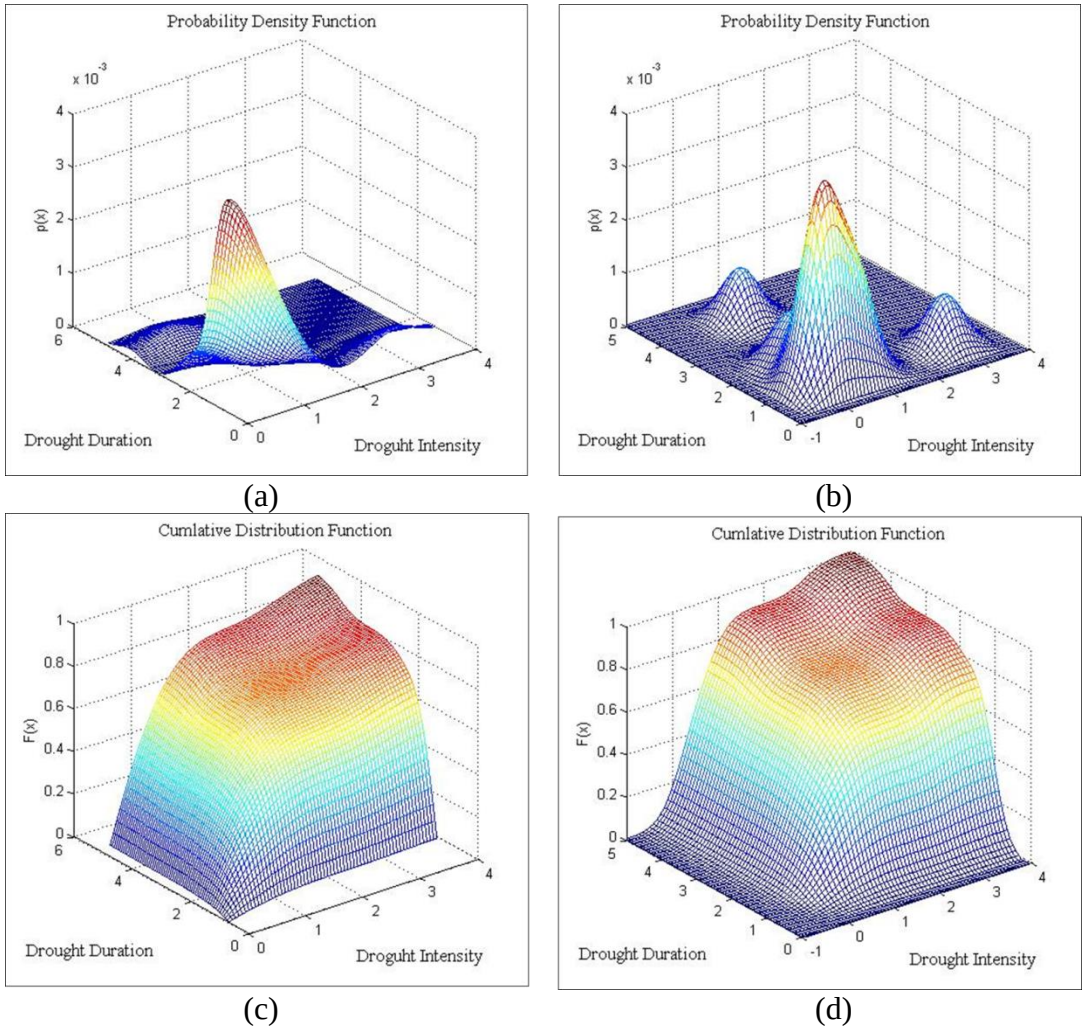

Figure 9-16 Weather station 54916 (a) DKDE estimated bivariate PDF of SPI based drought risk (PII-PV) (b) GKDE estimated bivariate PDF of SPI based drought risk (PII-PV) (c) DKDE estimated bivariate CDF of SPI based drought risk (PII-PV) (d) GKDE estimated bivariate CDF of SPI based drought risk (PII-PV)

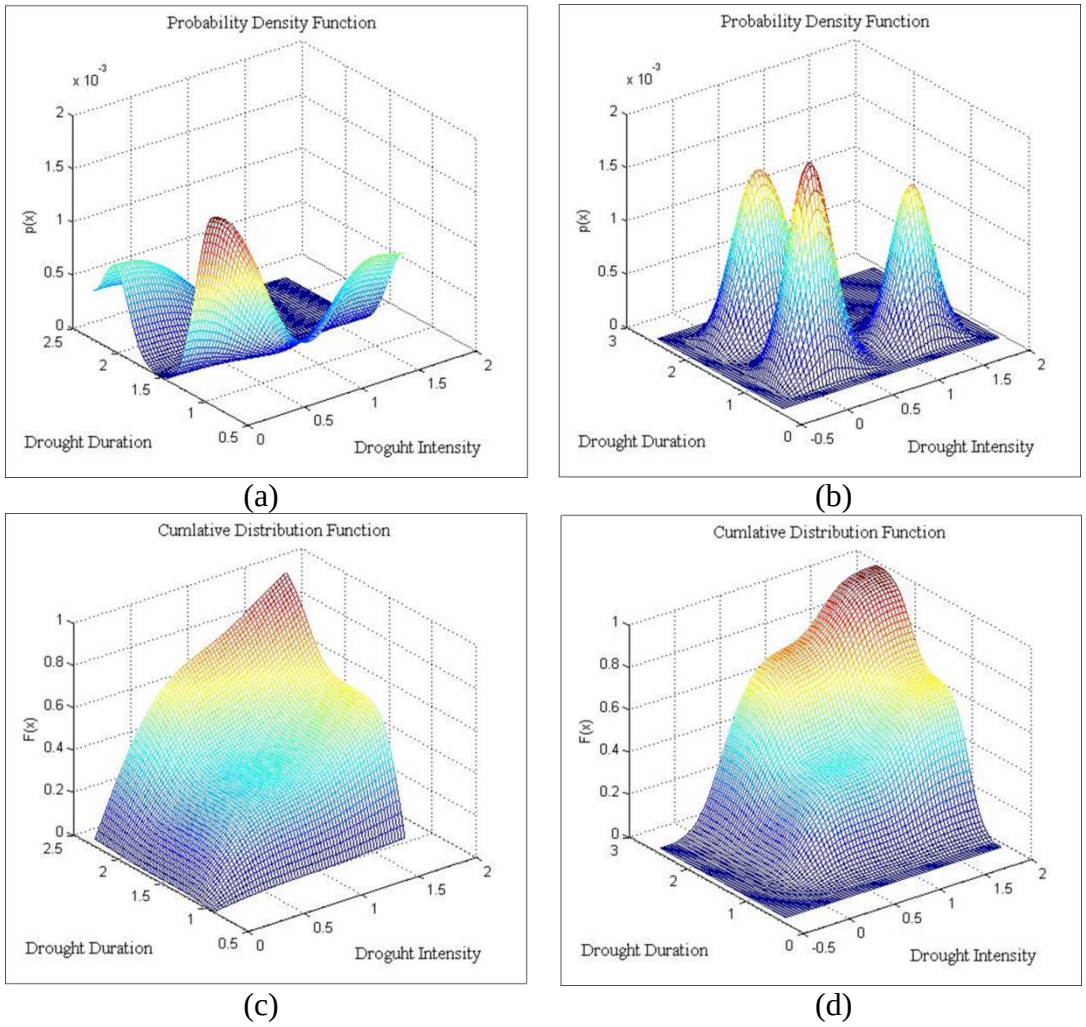

Figure 9-17 Weather station 54936 (a) DKDE estimated bivariate PDF of SPI based drought risk (PII-PV) (b) GKDE estimated bivariate PDF of SPI based drought risk (PII-PV) (c) DKDE estimated bivariate CDF of SPI based drought risk (PII-PV) for (d) GKDE estimated bivariate CDF of SPI based drought risk (PII-PV)

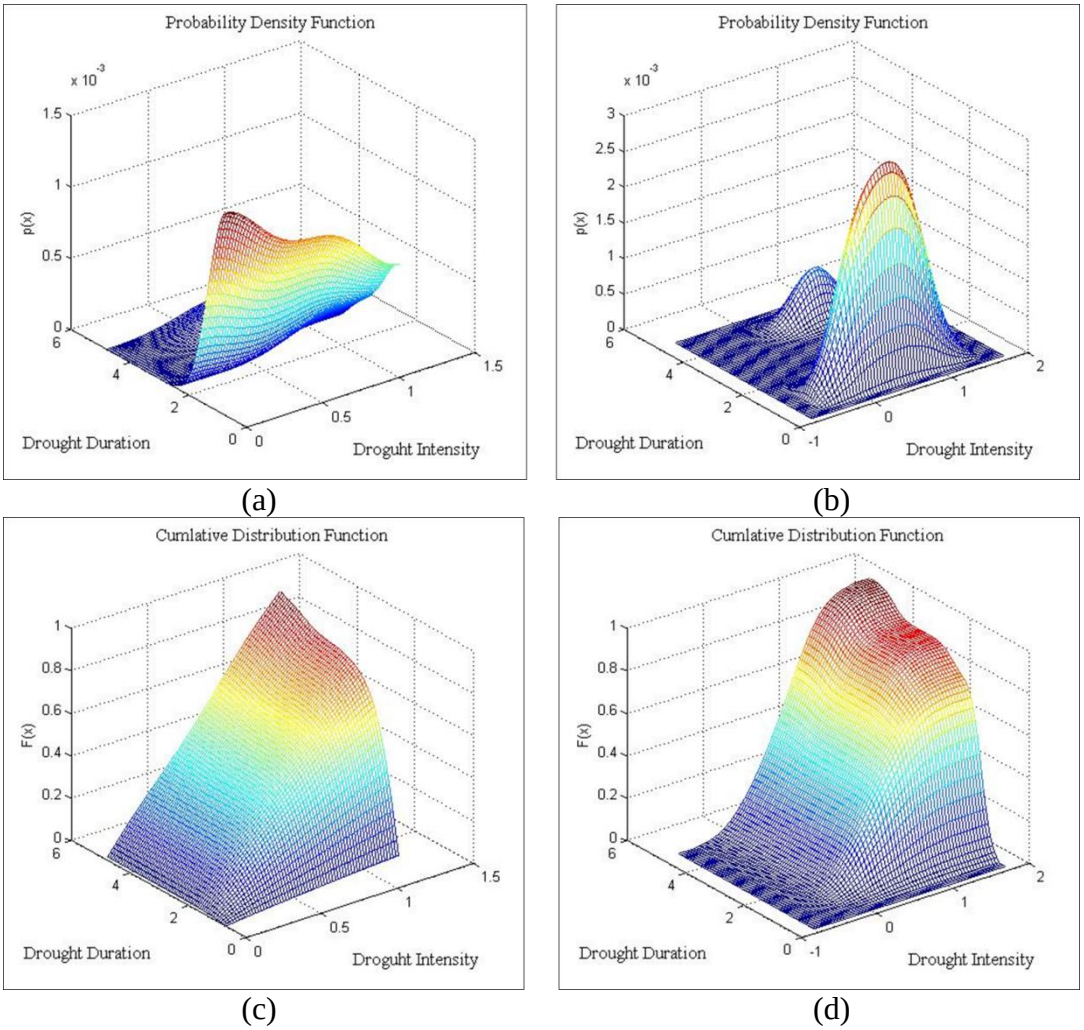

Figure 9-18 Weather station 54945 (a) DKDE estimated bivariate PDF of SPI based drought risk (PII-PV) (b) GKDE estimated bivariate PDF of SPI based drought risk (PII-PV) (c) DKDE estimated bivariate CDF of SPI based drought risk (PII-PV) (d) GKDE estimated bivariate CDF of SPI based drought risk (PII-PV)

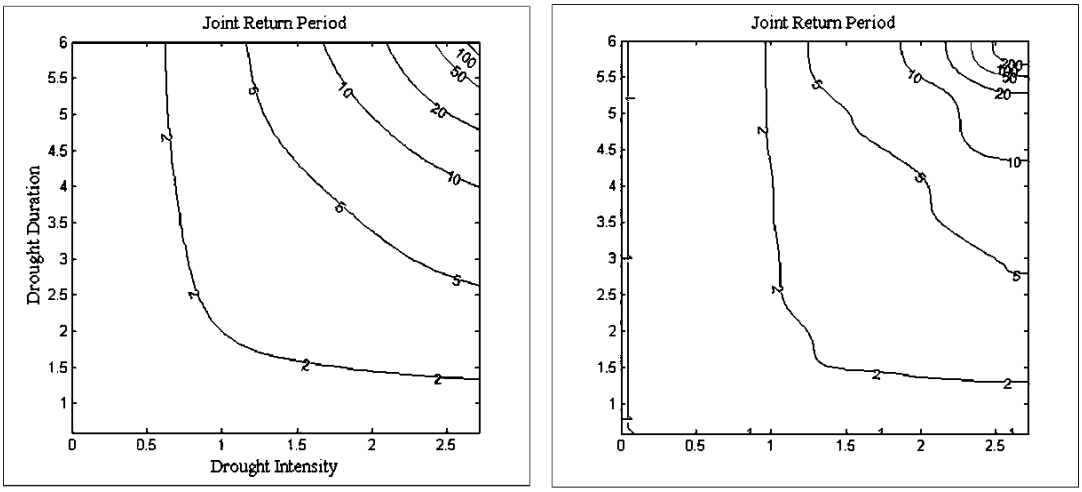

(a) (b)

Figure 9-19 Weather station 54725 (a) DKDE estimated Joint Return Period of SPI based drought risk (PII-PV) (b) GKDE estimated Joint Return Period of SPI based drought risk (PII-PV)

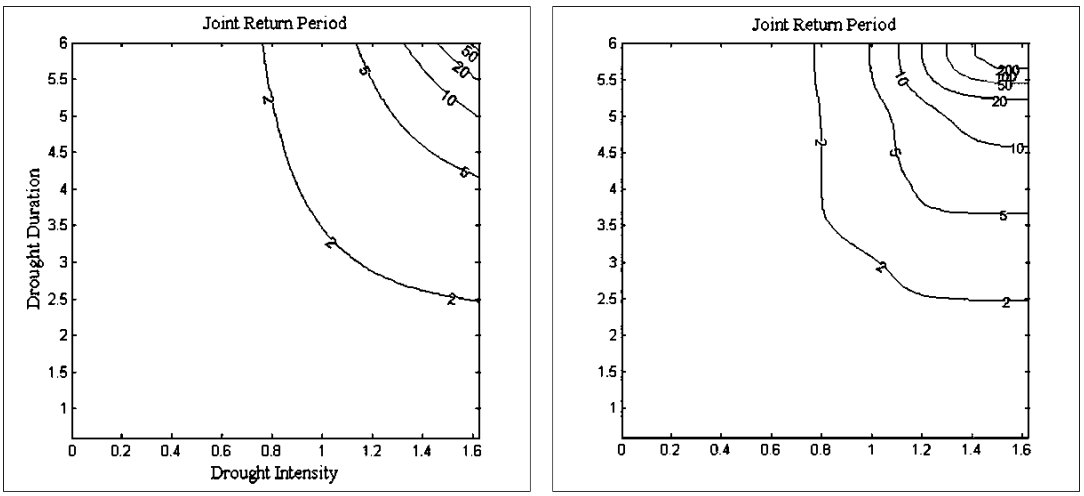

(a) (b)

Figure 9-20 Weather station 54736 (a) DKDE estimated Joint Return Period of SPI based drought risk (PII-PV) (b) GKDE estimated Joint Return Period of SPI based drought risk (PII-PV)

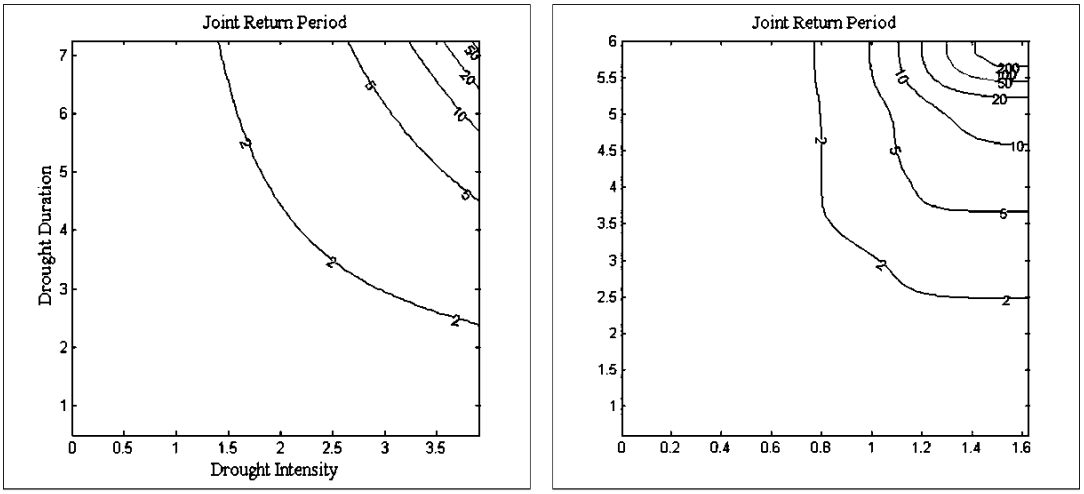

(a) (b)

Figure 9-21 Weather station 54741 (a) DKDE estimated Joint Return Period of SPI based drought risk (PII-PV) (b) GKDE estimated Joint Return Period of SPI based drought risk (PII-PV)

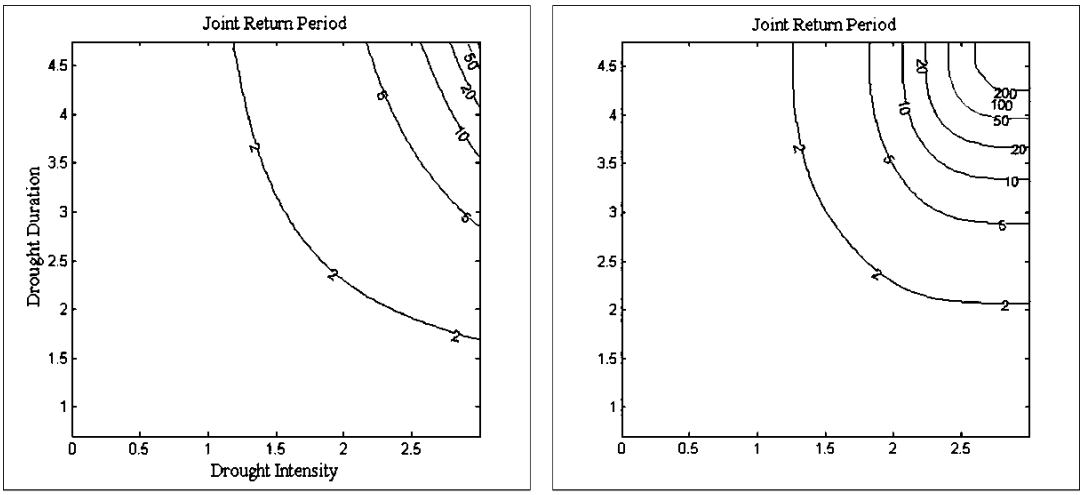

(a) (b)

Figure 9-22 Weather station 54753 (a) DKDE estimated Joint Return Period of SPI based drought risk (PII-PV) (b) GKDE estimated Joint Return Period of SPI based drought risk (PII-PV)

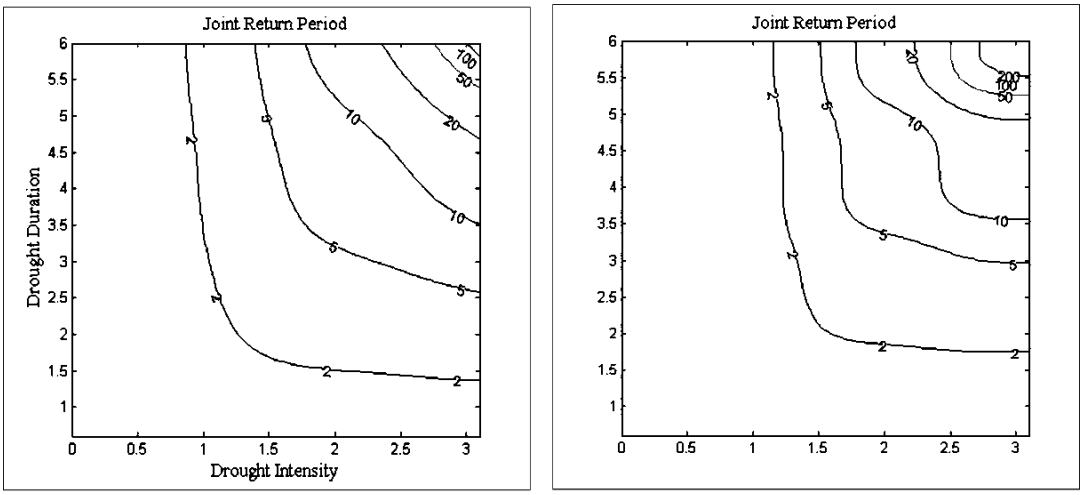

(a) (b)

Figure 9-23 Weather station 54764 (a) DKDE estimated Joint Return Period of SPI based drought risk (PII-PV) (b) GKDE estimated Joint Return Period of SPI based drought risk (PII-PV)

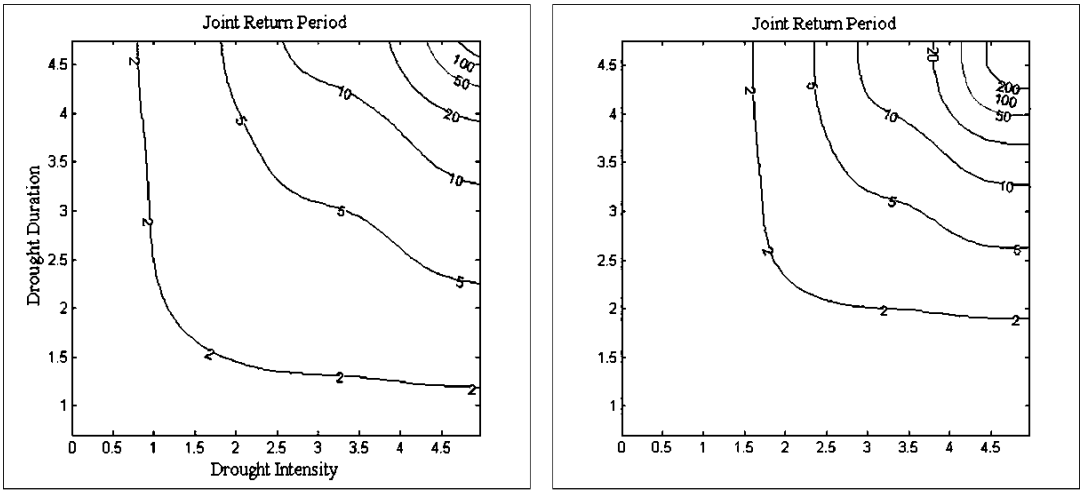

(a) (b)

Figure 9-24 weather station 54774 (a) DKDE estimated Joint Return Period of SPI based drought risk (PII-PV) (b) GKDE estimated Joint Return Period of SPI based drought risk (PII-PV)

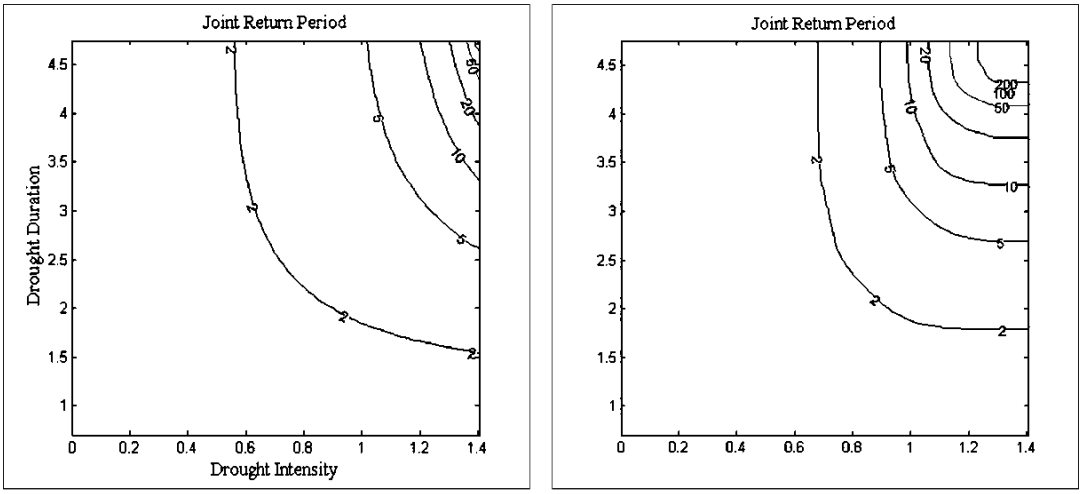

(a) (b)

Figure 9-25 Weather station 54776 (a) DKDE estimated Joint Return Period of SPI based drought risk (PII-PV) (b) GKDE estimated Joint Return Period of SPI based drought risk (PII-PV)

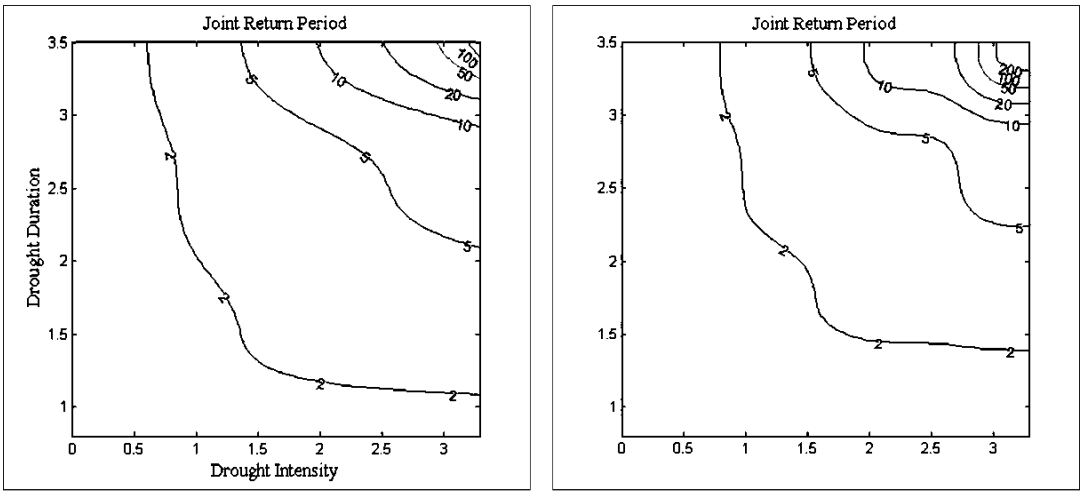

(a) (b)

Figure 9-26 Weather station 54823 (a) DKDE estimated Joint Return Period of SPI based drought risk (PII-PV) (b) GKDE estimated Joint Return Period of SPI based drought risk (PII-PV)

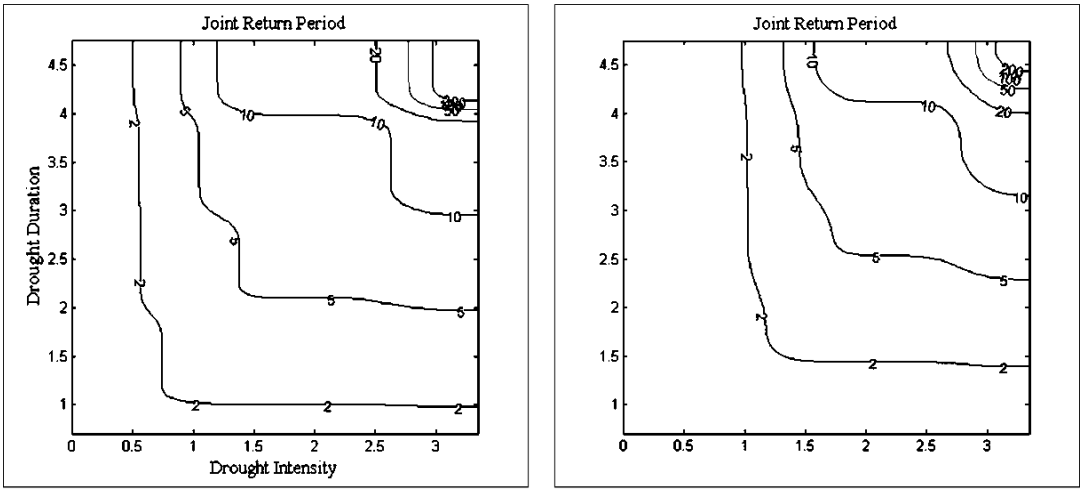

(a) (b)

Figure 9-27 Weather station 54824 (a) DKDE estimated Joint Return Period of SPI based drought risk (PII-PV) (b) GKDE estimated Joint Return Period of SPI based drought risk (PII-PV)

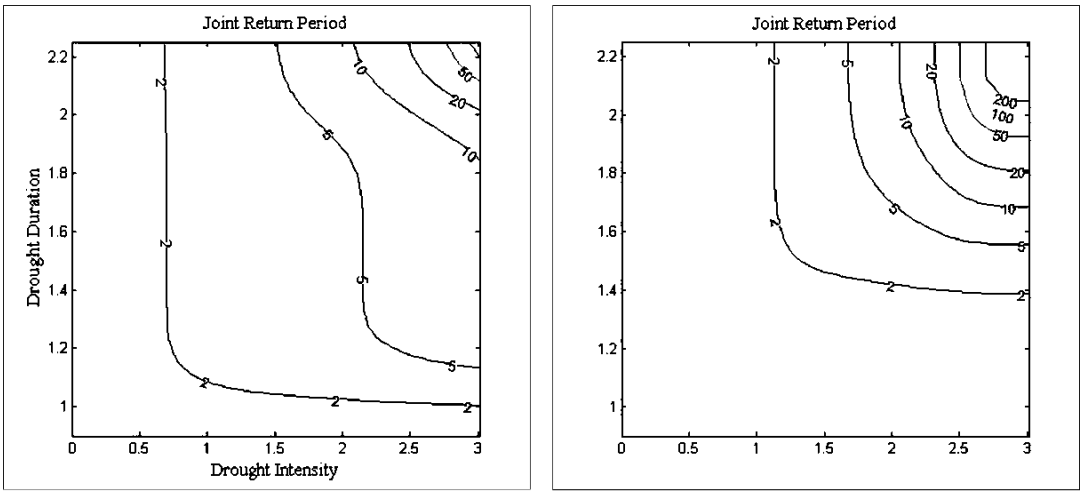

(a) (b)

Figure 9-28 Weather station 54827 (a) DKDE estimated Joint Return Period of SPI based drought risk (PII-PV) (b) GKDE estimated Joint Return Period of SPI based drought risk (PII-PV)

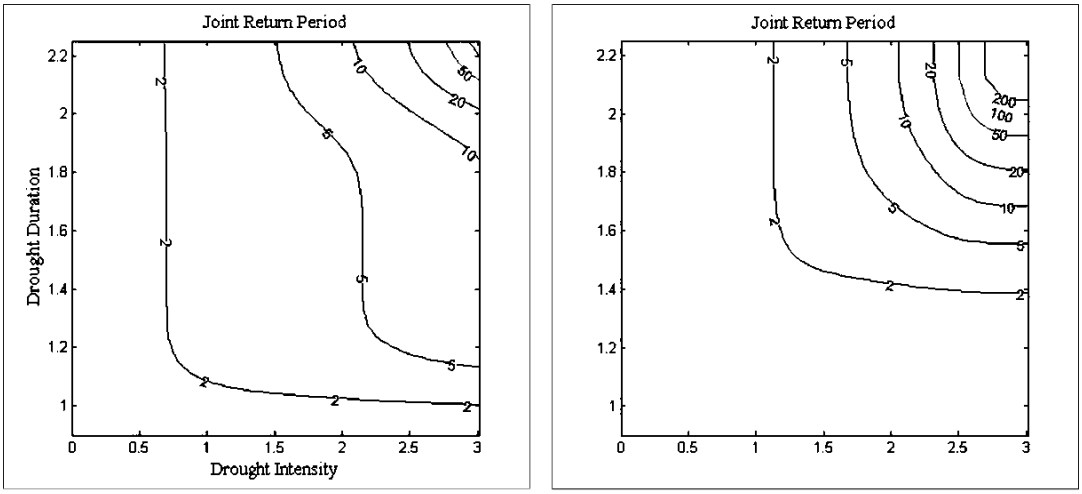

(a) (b)

Figure 9-29 Weather station 54836 (a) DKDE estimated Joint Return Period of SPI based drought risk (PII-PV) (b) GKDE estimated Joint Return Period of SPI based drought risk (PII-PV)

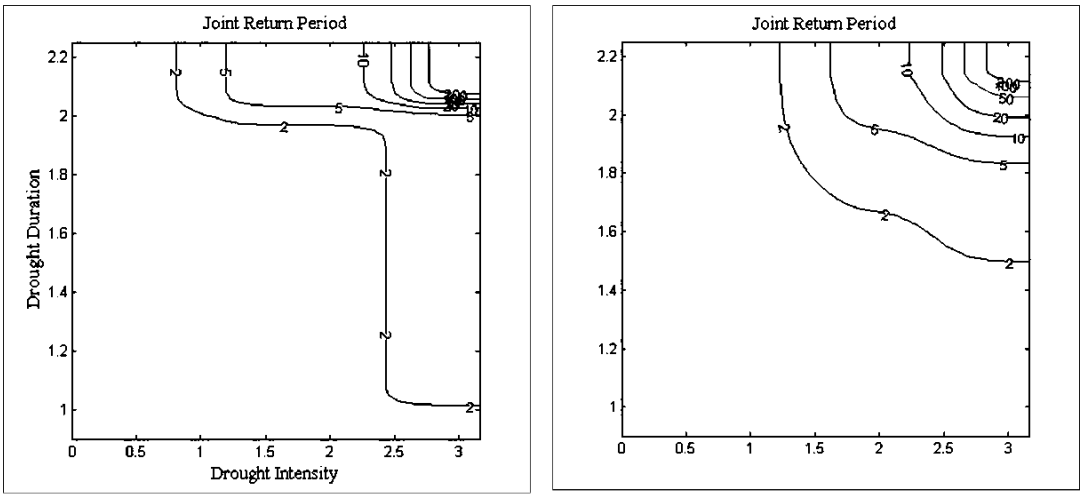

(a) (b)

Figure 9-30 Weather station 54843 (a) DKDE estimated Joint Return Period of SPI based drought risk (PII-PV) (b) GKDE estimated Joint Return Period of SPI based drought risk (PII-PV)

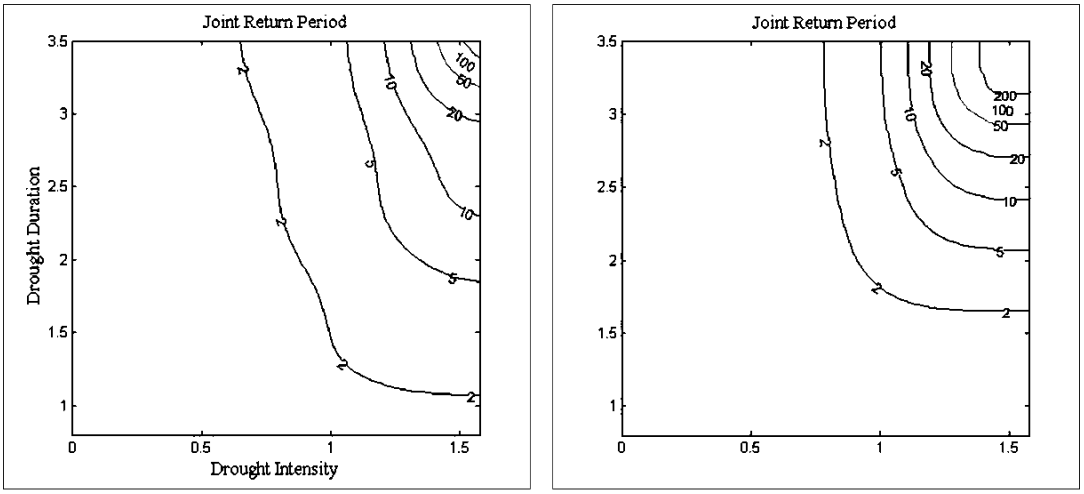

(a) (b)

Figure 9-31 Weather station 54852 (a) DKDE estimated Joint Return Period of SPI based drought risk (PII-PV) (b) GKDE estimated Joint Return Period of SPI based drought risk (PII-PV)

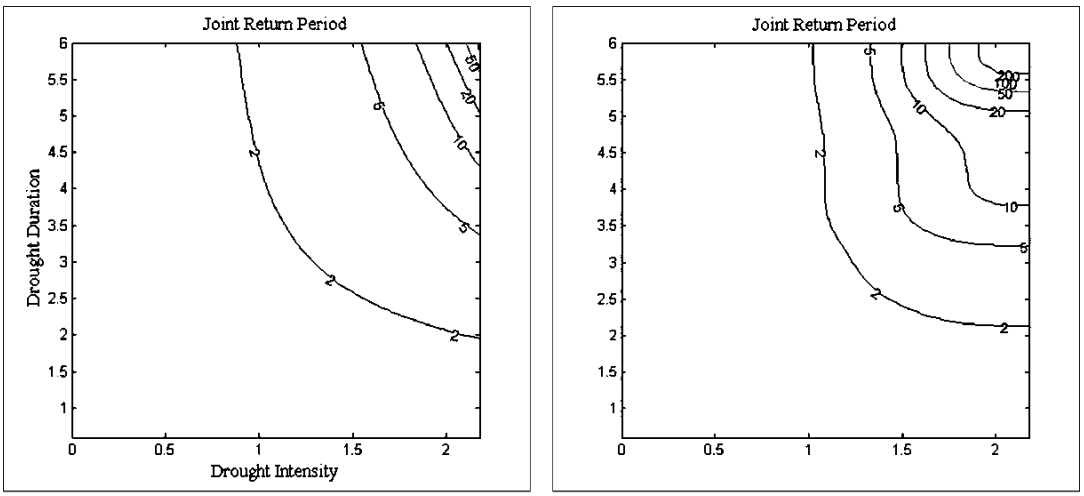

(a) (b)

Figure 9-32 Weather station 54857 (a) DKDE estimated Joint Return Period of SPI based drought risk (PII-PV) (b) GKDE estimated Joint Return Period of SPI based drought risk (PII-PV)

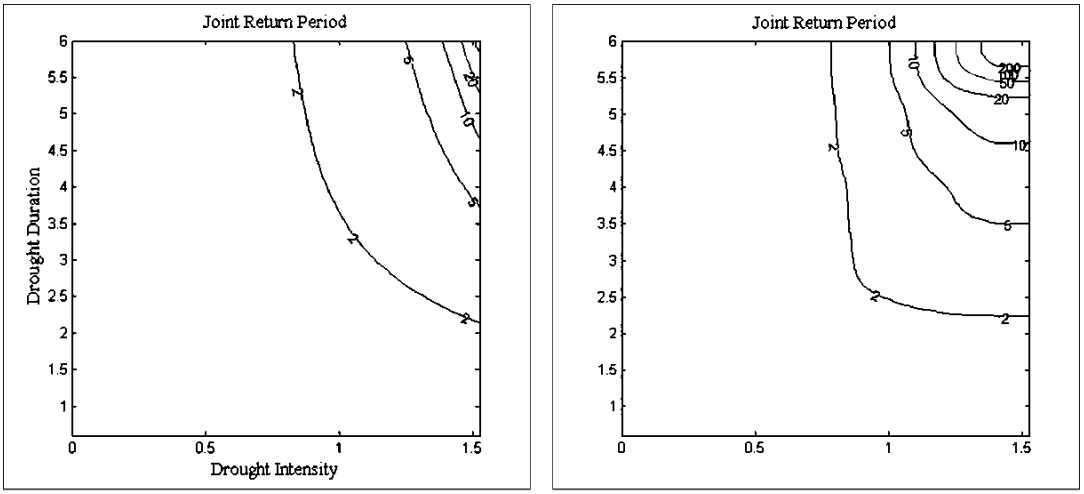

(a) (b)

Figure 9-33 Weather station 54906 (a) DKDE estimated Joint Return Period of SPI based drought risk (PII-PV) (b) GKDE estimated Joint Return Period of SPI based drought risk (PII-PV)

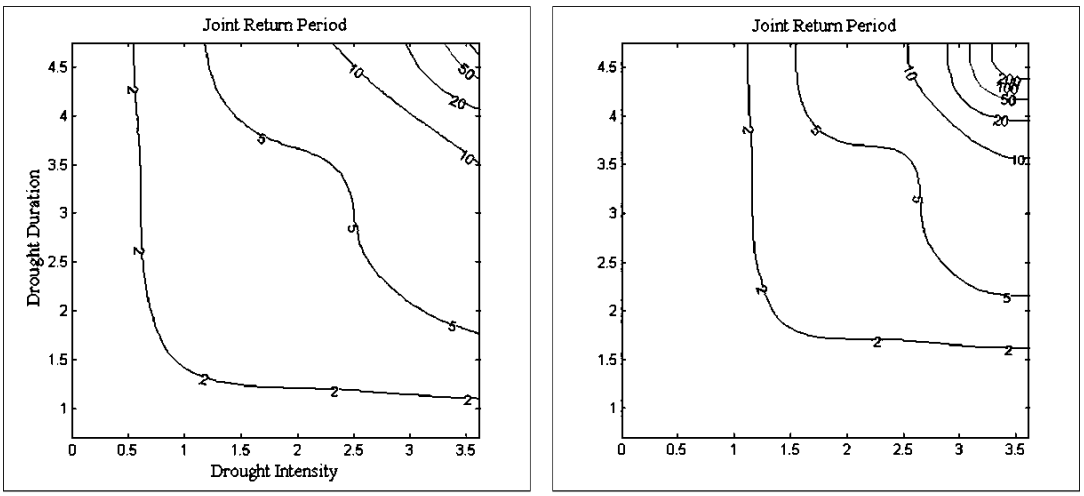

(a) (b)

Figure 9-34 Weather station 54916 (a) DKDE estimated Joint Return Period of SPI based drought risk (PII-PV) (b) GKDE estimated Joint Return Period of SPI based drought risk (PII-PV)

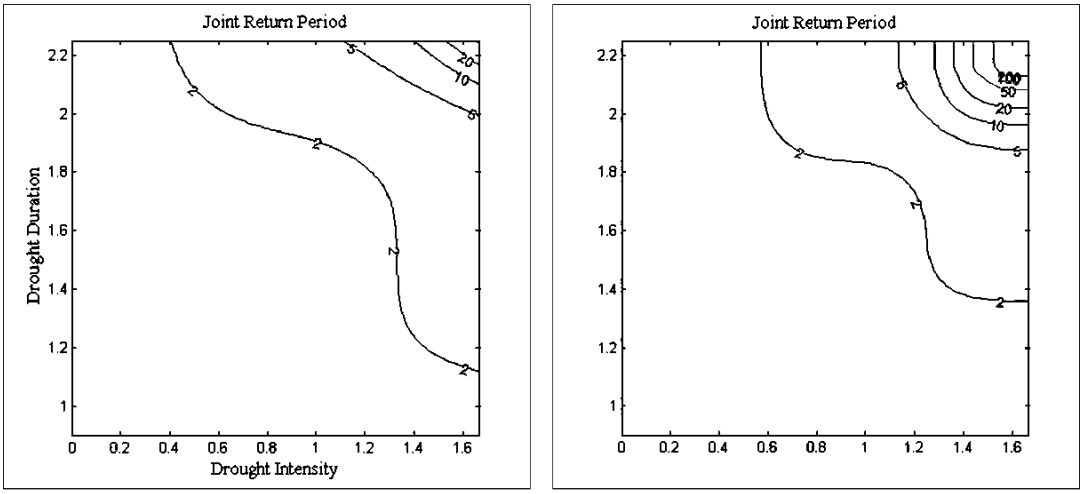

(a) (b)

Figure 9-35 Weather station 54936 (a) DKDE estimated Joint Return Period of SPI based drought risk (PII-PV) (b) GKDE estimated Joint Return Period of SPI based drought risk (PII-PV)

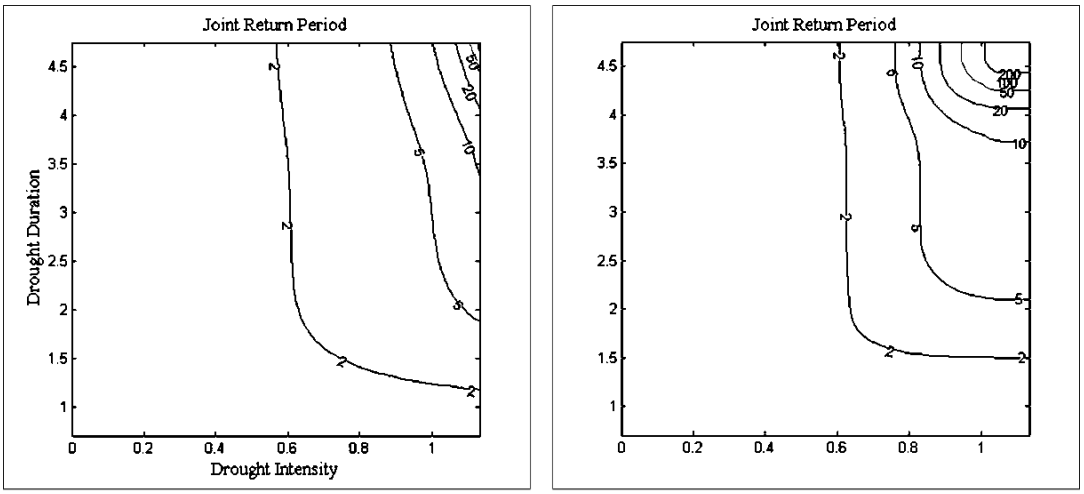

(a) (b)

Figure 9-36 Weather station 54945 (a) DKDE estimated Joint Return Period of SPI based drought risk (PII-PV) (b) GKDE estimated Joint Return Period of SPI based drought risk (PII-PV)

APPENDIX 2

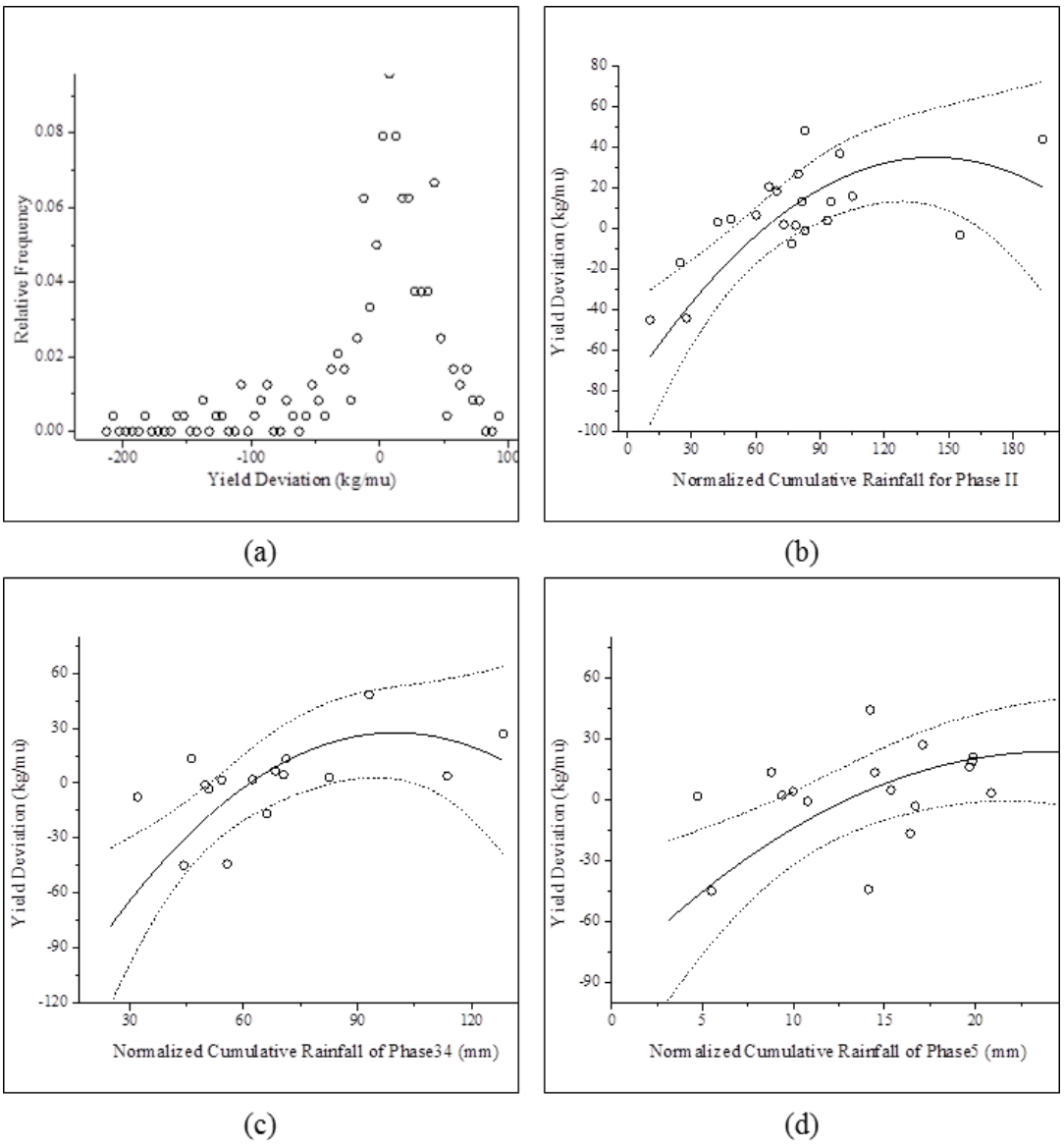

Figure 10-1 (a) Frequency analysis of historical yield redution in Feicheng county (b,c,d) 2nd order Polynomial curve fitting between yield reduction and weighted CR indices of PhaseII, Phase III & IV, Phase V in Feicheng county (dashed line is the 90% conference level line)

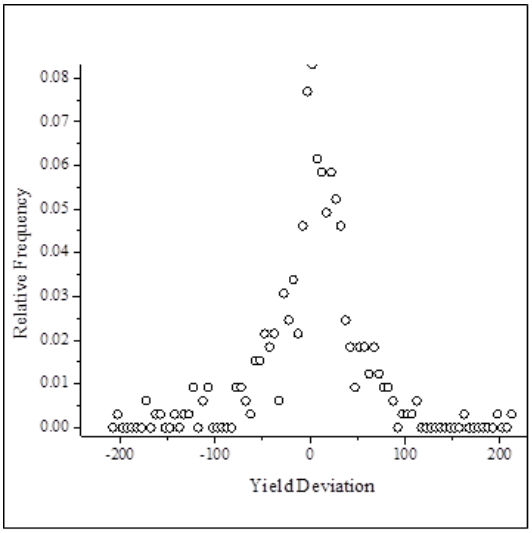
Relative Frequency
0.08
0.07
0.06
0.05
0.04
0.03
0.02
0.01
0.00
-200
-100
0
100
200
Yield Deviation

(a)

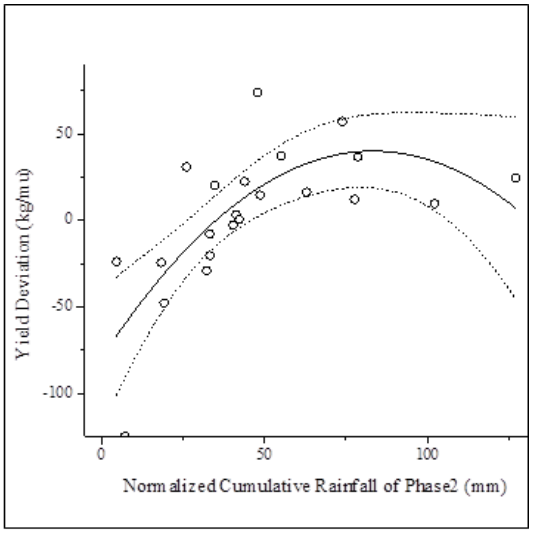
Yield Deviation (kg/mu)
50
0
-50
-100
0
50
100
Normalized Cumulative Rainfall of Phase2 (mm)

(b)

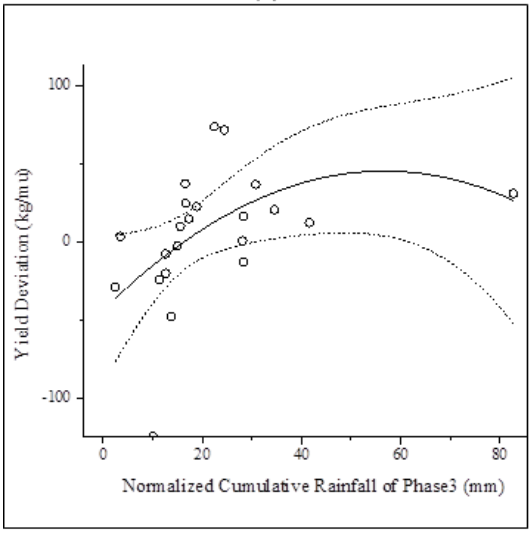
Yield Deviation (kg/mu)
100
0
-100
0
20
40
60
80
Normalized Cumulative Rainfall of Phase3 (mm)

(c)

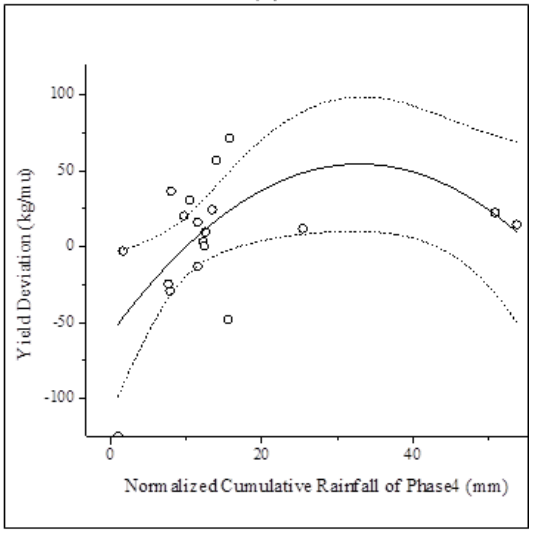
Yield Deviation (kg/mu)
100
50
0
-50
-100
0
20
40
Normalized Cumulative Rainfall of Phase4 (mm)

(d)

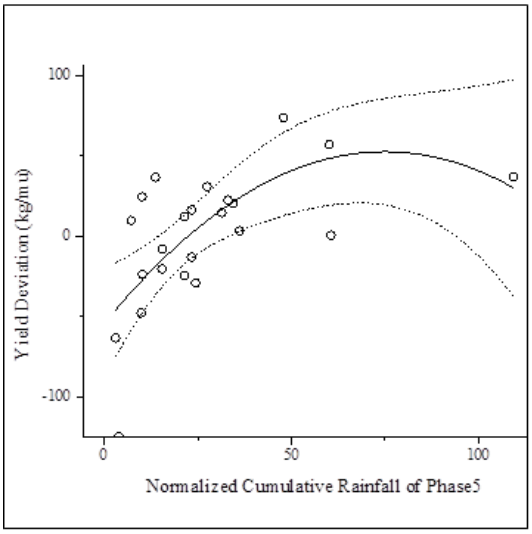
Yield Deviation (kg/mu)
100
0
-100
0
50
100
Normalized Cumulative Rainfall of Phase5

(e)

Figure 10-2 (a) Frequency analysis of historical yield redution in Xintai county (b,c,d) 2nd order Polynomial curve fitting between yield reduction and weighted CR indices of PhaseII, Phase III, Phase IV, Phase V in Xintai county (dashed line is the 90% conference level line)

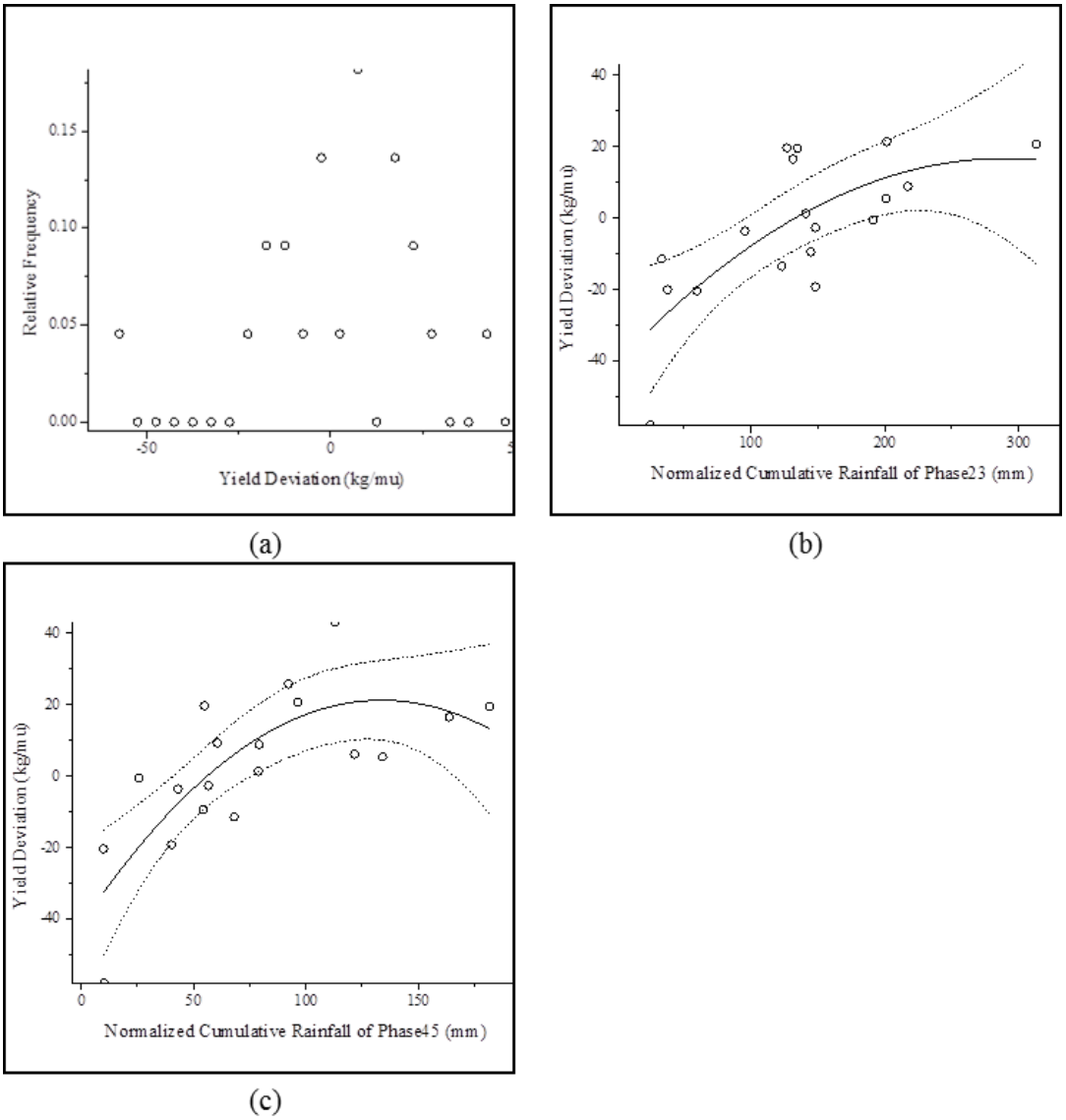

Figure 10-3 (a) Frequency analysis of historical yield redution in Ningyang county (b,c,d) 2nd order Polynomial curve fitting between yield reduction and weighted CR indices of PhaseII&III, Phase IV & V in Ningyang county (dashed line is the 90% conference level line)

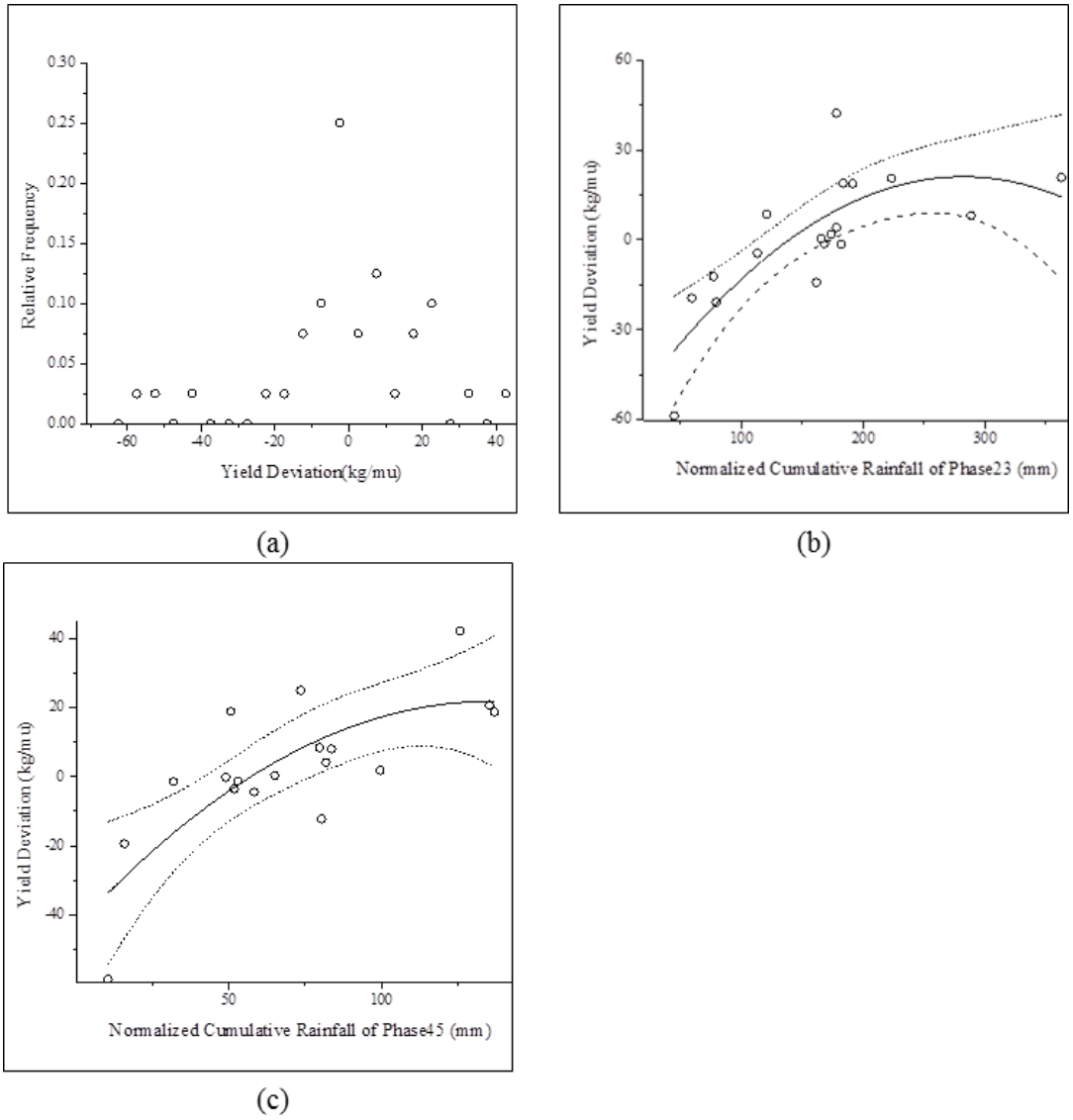

Figure 10-4 (a) Frequency analysis of historical yield redution in Ningyang county (b,c,d) 2nd order Polynomial curve fitting between yield reduction and weighted CR indices of PhaseII, Phase III & IV, Phase V in Ningyang county (dashed line is the 90% conference level line)

APPENDIX 3

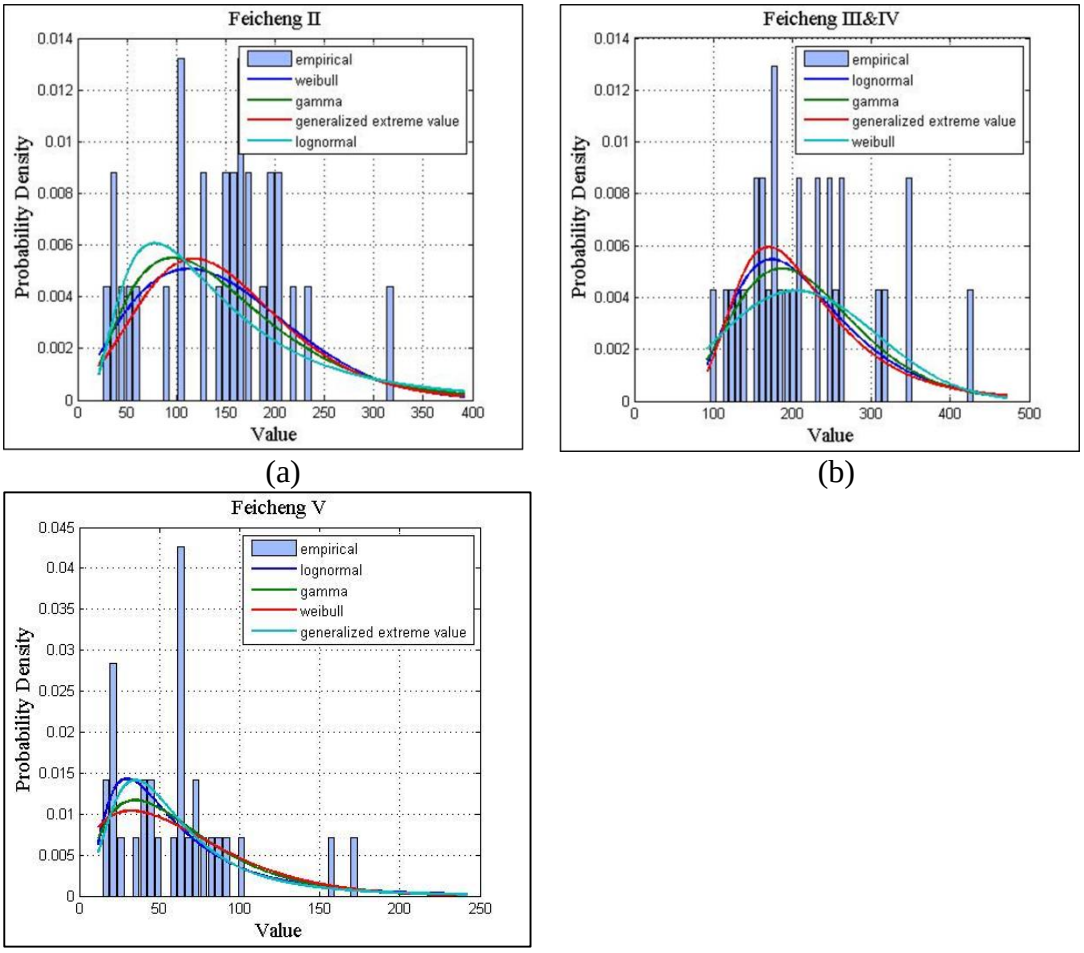

Figure 11-1 Comparison of PDF candidates (Lognormal, Gamma, Weibull and Generalized Extreme Value) for cumulative rainfall of Phase II (a), Phase III & IV (b) and Phase V (c) in Feicheng county

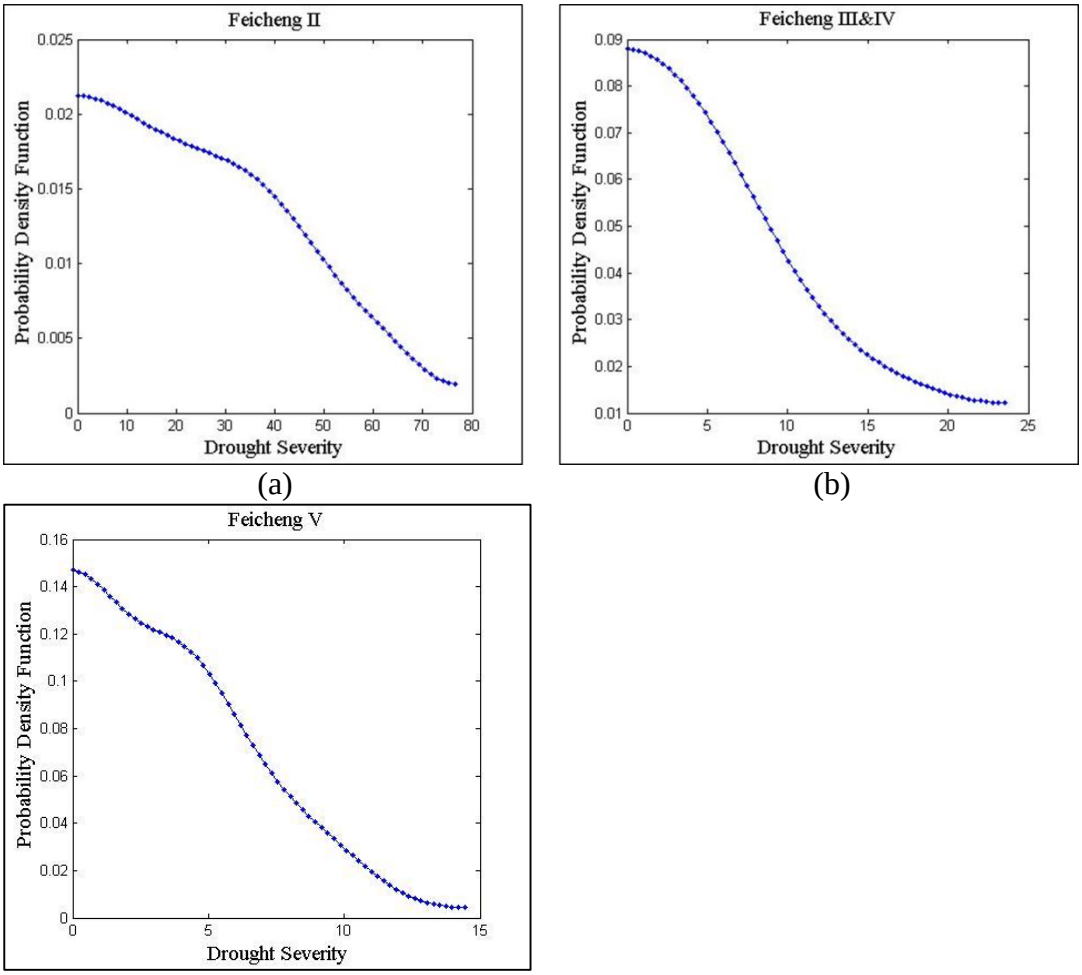

Figure 11-2 PDF of drought severity in Phase II (a), Phase III & IV (b) and Phase V (c) in Feicheng county, estimated by DKDE

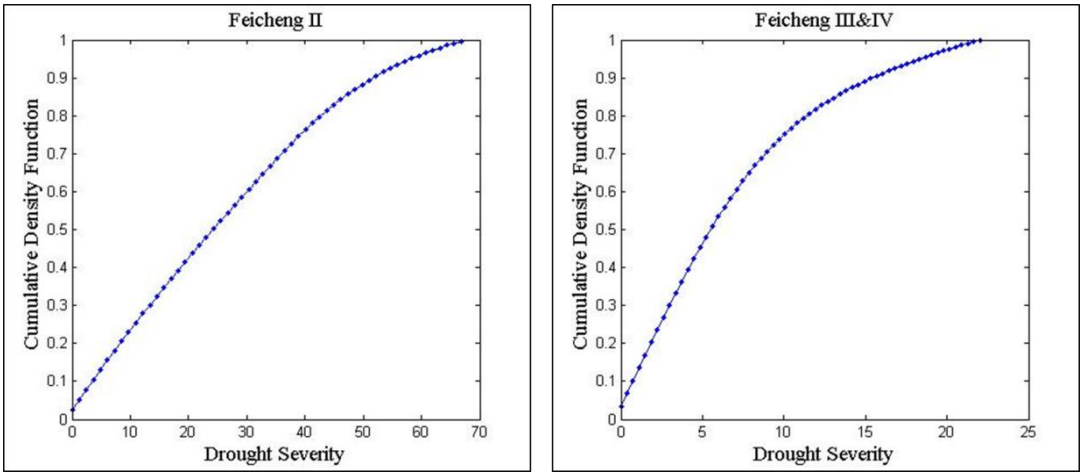

(a)

(b)

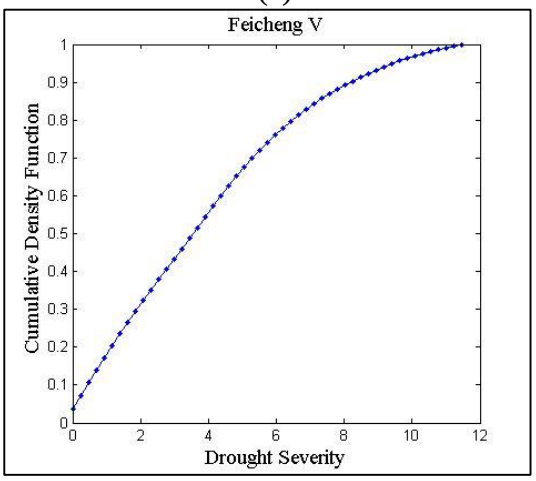

(c)

Figure 11-3 CDF of drought severity in Phase II (a), Phase III & IV (b) and Phase V (c) in Feicheng county, estimated by DKDE

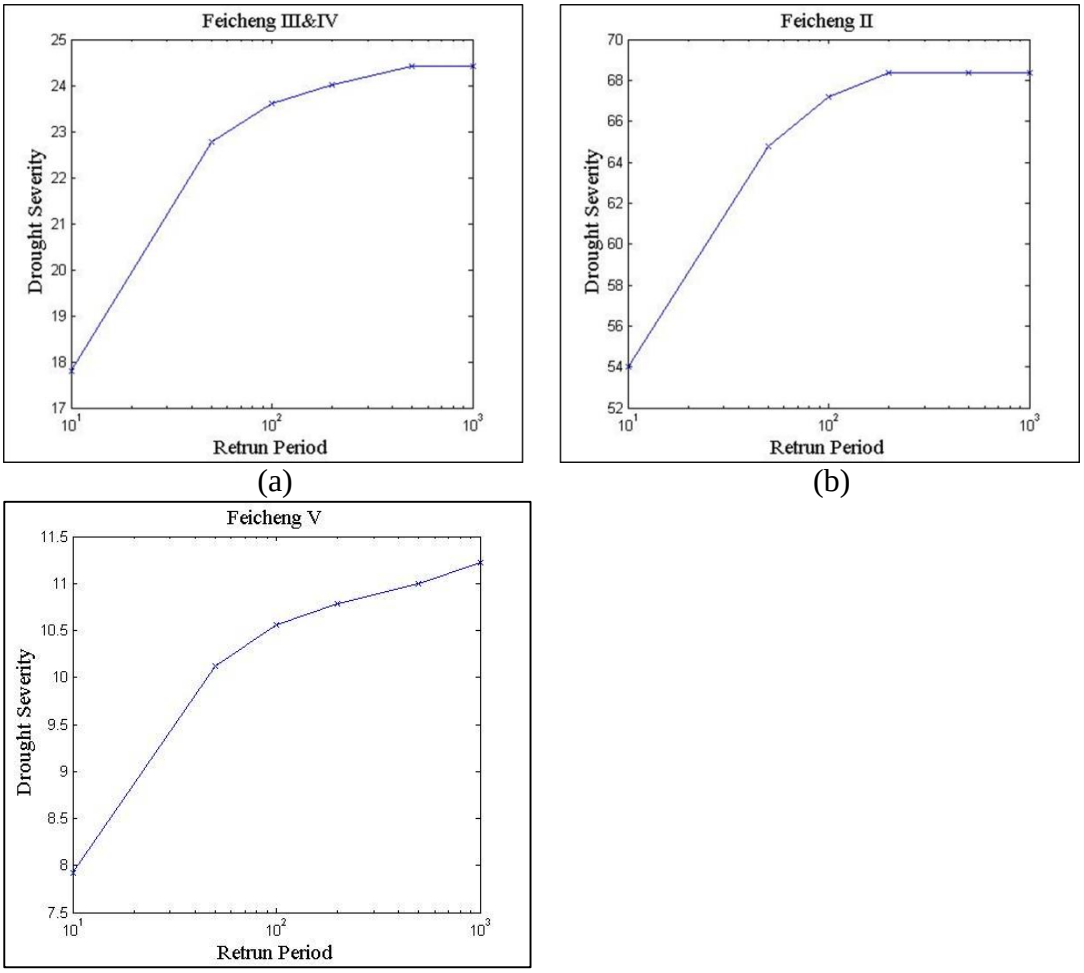

Figure 11-4 Drought severity return level (50 year, 100 year, 200 year, 500 year and 1000 year) of Phase II (a), Phase III & IV (b) and Phase V (c) in Feicheng county

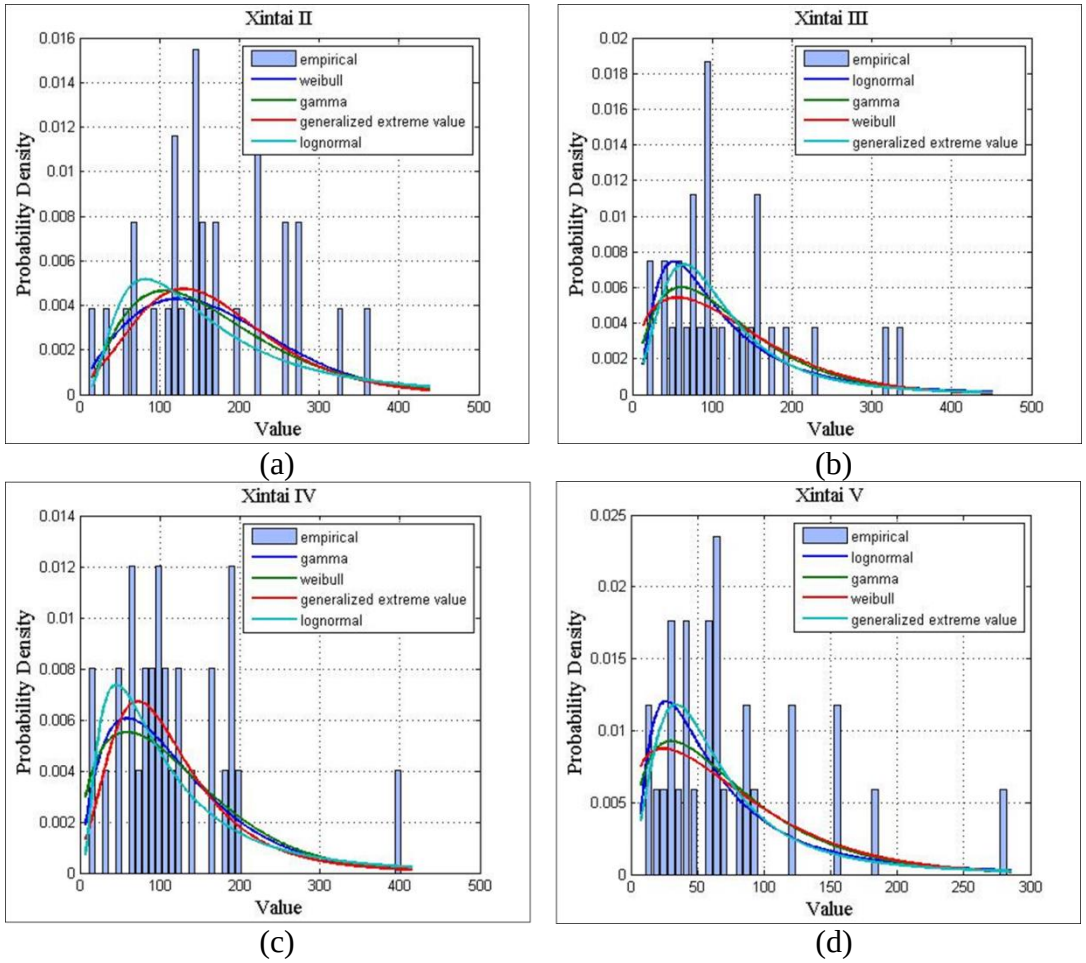

Figure 11-5 Comparison of PDF candidates (Lognormal, Gamma, Weibull and Generalized Extreme Value) for cumulative rainfall of Phase II (a), Phase III (b), Phase IV (c) and Phase V (d) in Xintai county

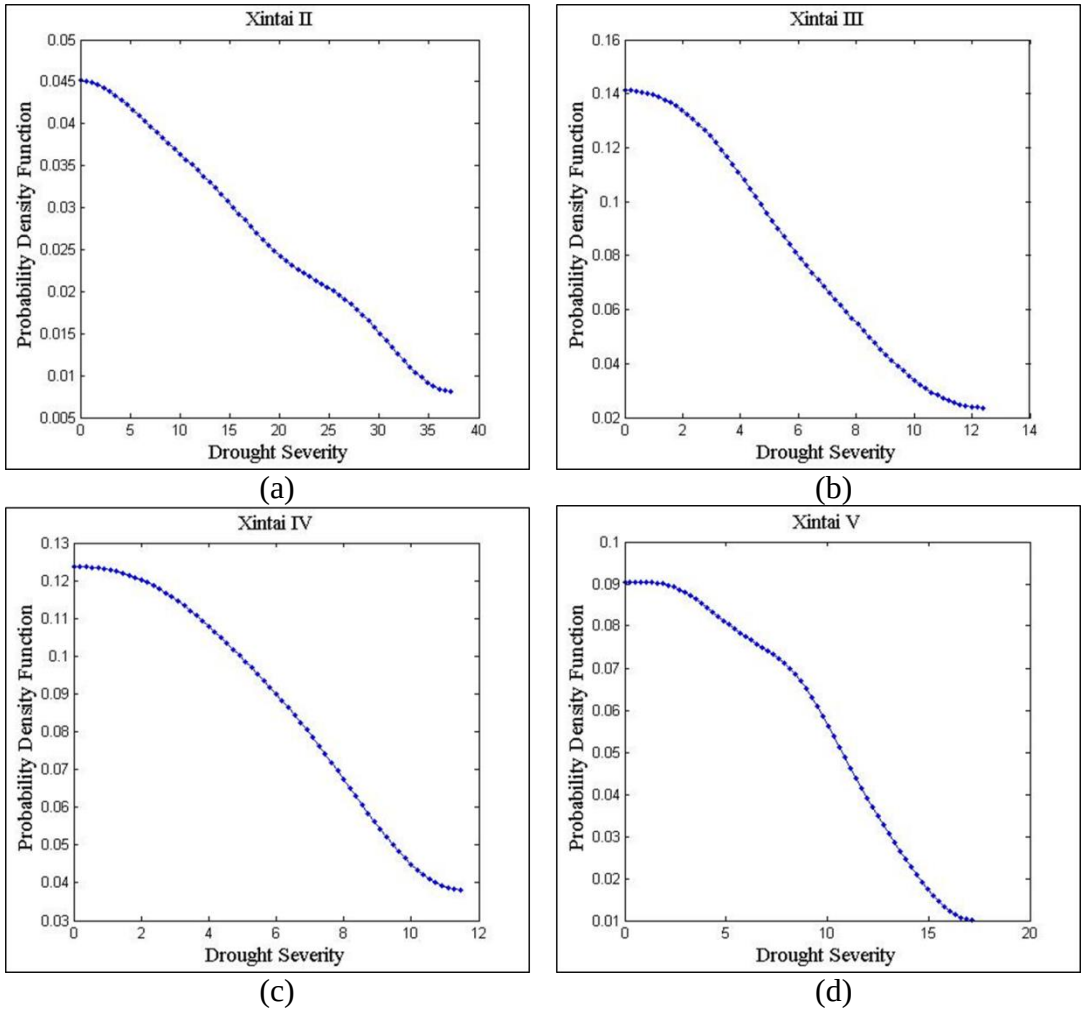

Figure 11-6 PDF of drought severity in Phase II (a), Phase III (b), Phase IV (c) and Phase V (d) in Xintai county, estimated by DKDE

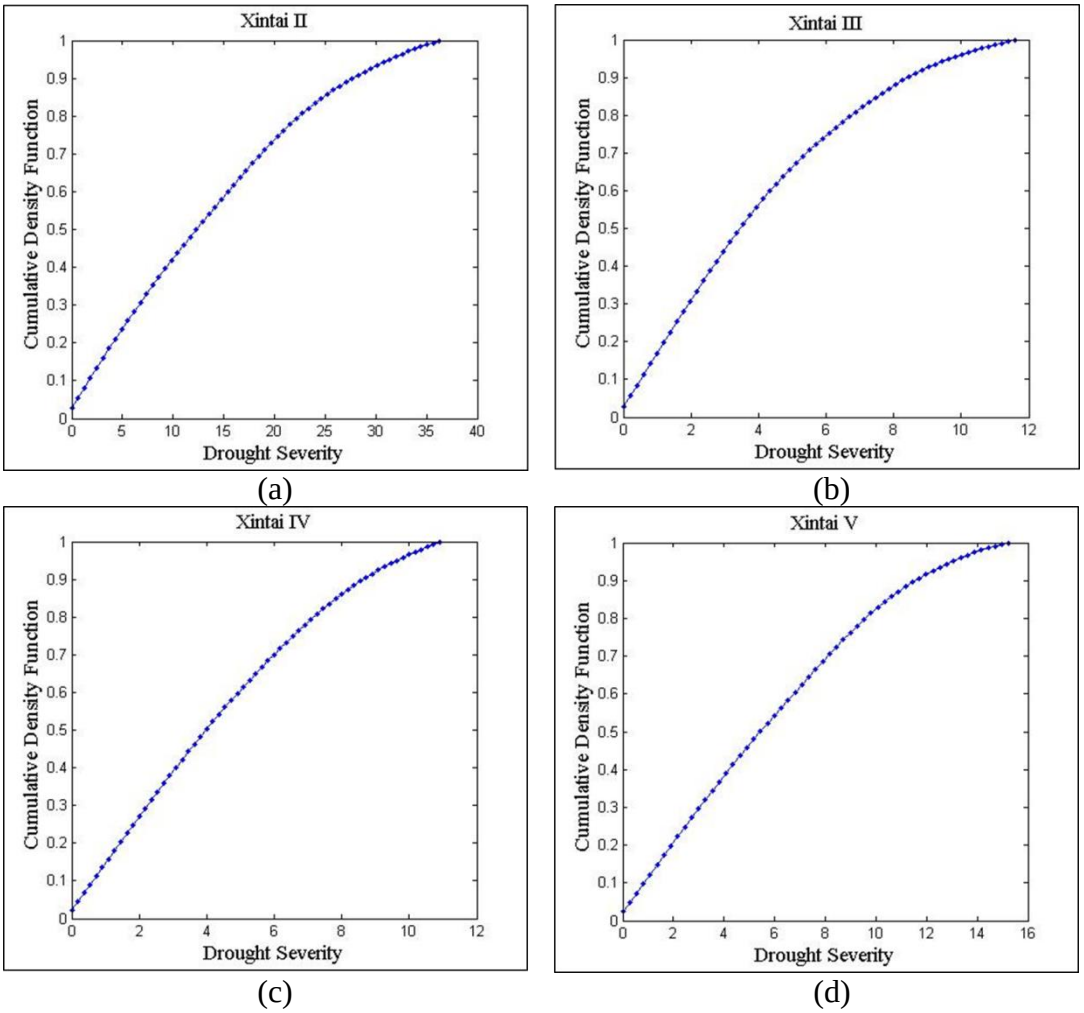

Figure 11-7 CDF of drought severity in Phase II (a), Phase III (b), Phase IV (c) and Phase V (d) in Xintai county, estimated by DKDE

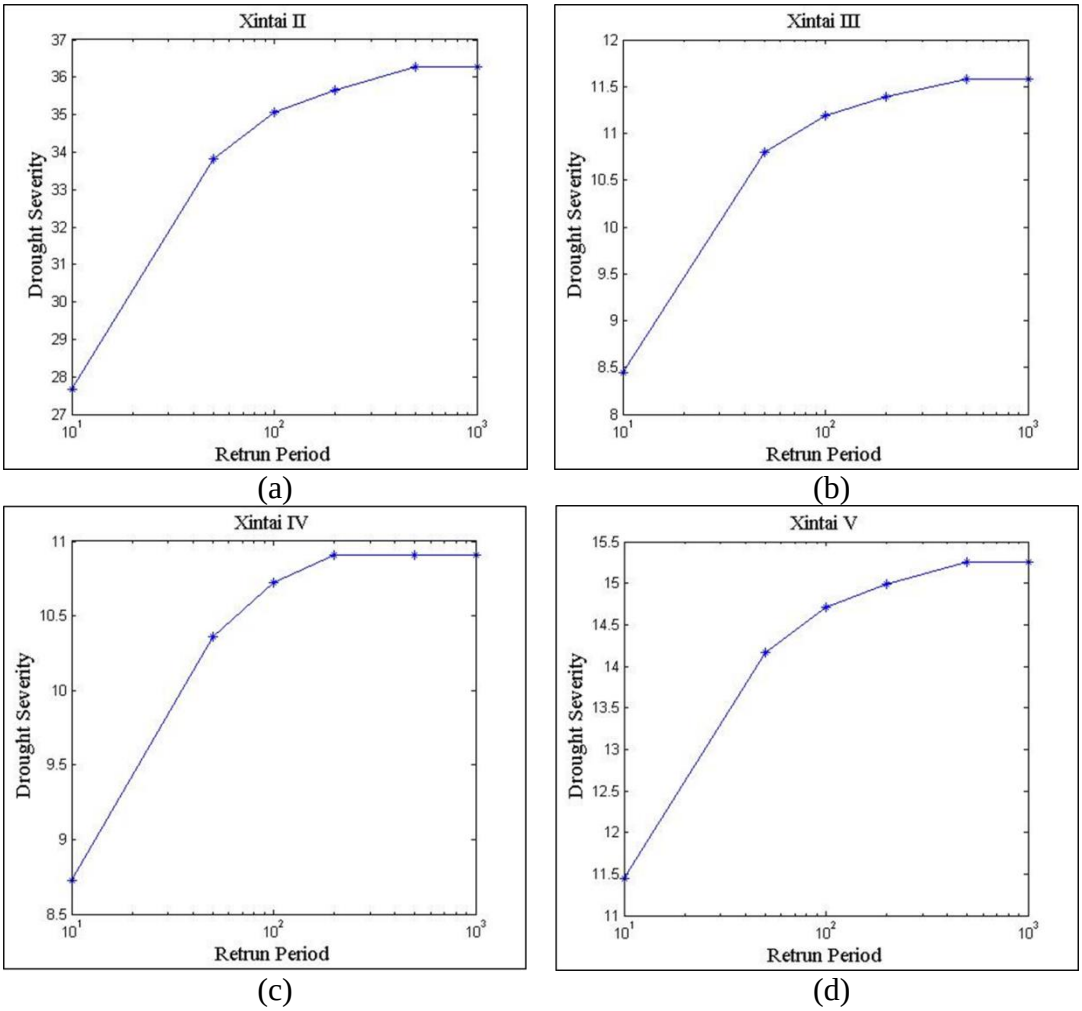

Figure 11-8 Drought severity return level (50 year, 100 year, 200 year, 500 year and 1000 year) of Phase II (a), Phase III (b), Phase IV (c) and Phase V (d) in Xintai county

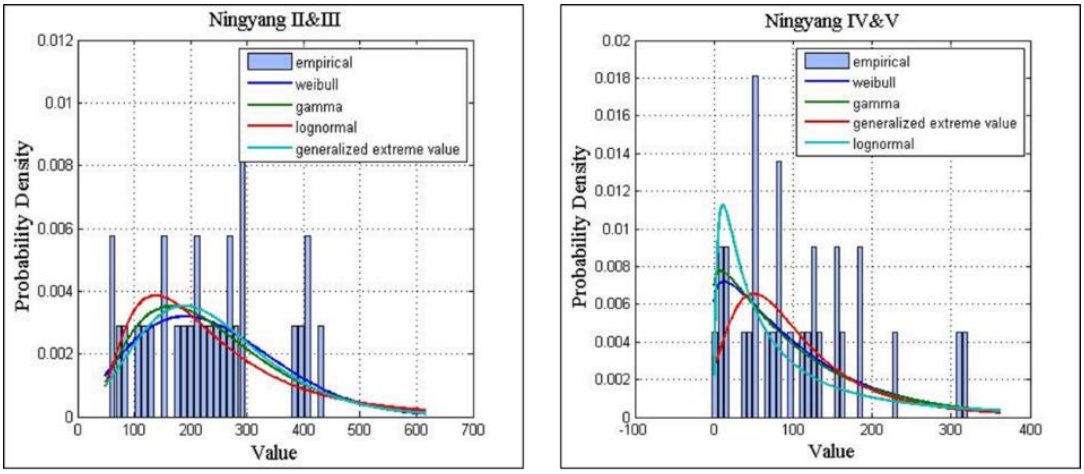

(a) (b)

Figure 11-9 Comparison of PDF candidates (Lognormal, Gamma, Weibull and Generalized Extreme Value) for cumulative rainfall of Phase II & III (a), Phase IV & V (b) in Ningyang county

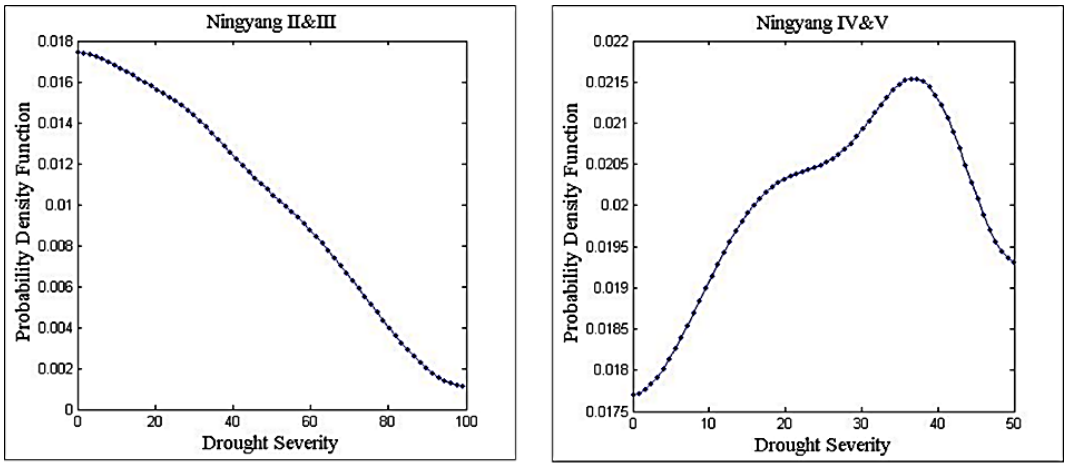

(a) (b)

Figure 11-10 PDF of drought severity in Phase II & III (a), Phase IV & V (b) in Ningyang county, estimated by DKDE

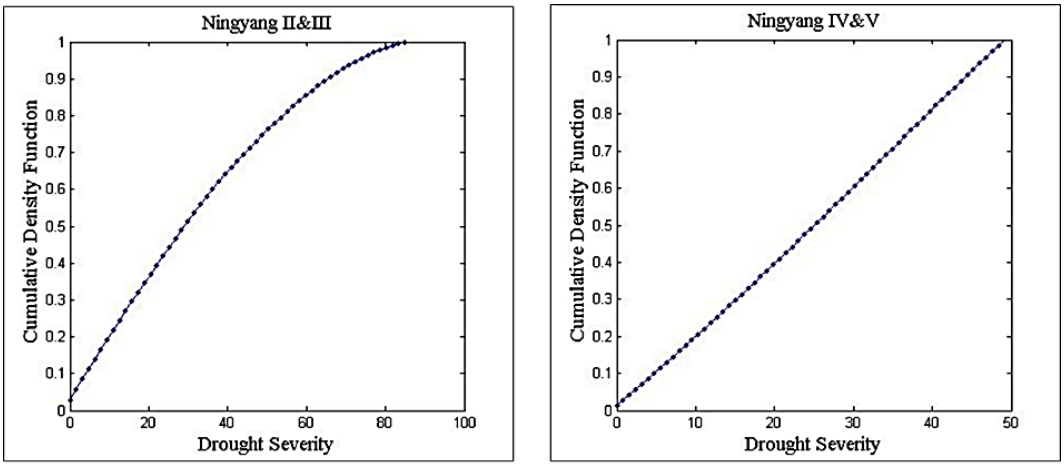

(a) (b)

Figure 11-11 CDF of drought severity in Phase II & III (a), Phase IV & V (b) in Ningyang county, estimated by DKDE

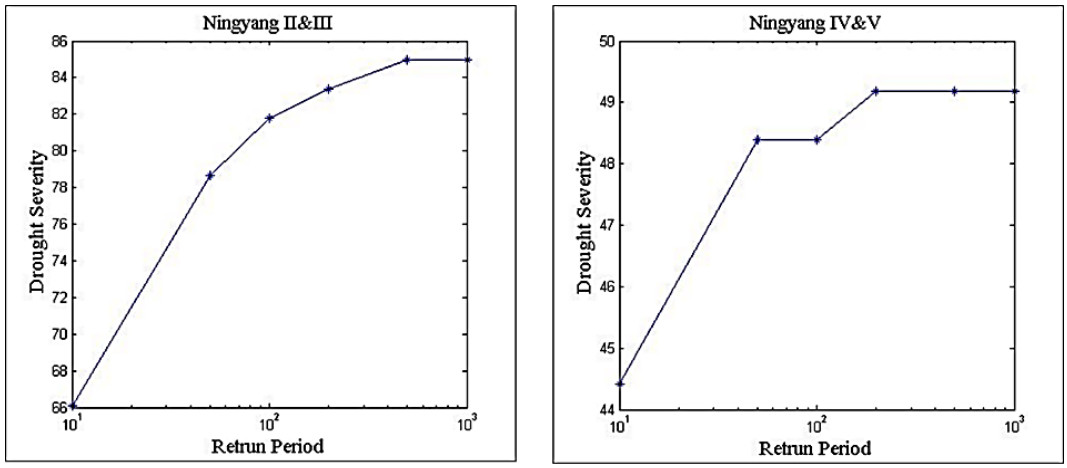

(a) (b)

Figure 11-12 Drought severity return level (50 year, 100 year, 200 year, 500 year and 1000 year) of Phase II & III (a), Phase IV & V (b) in Ningyang county

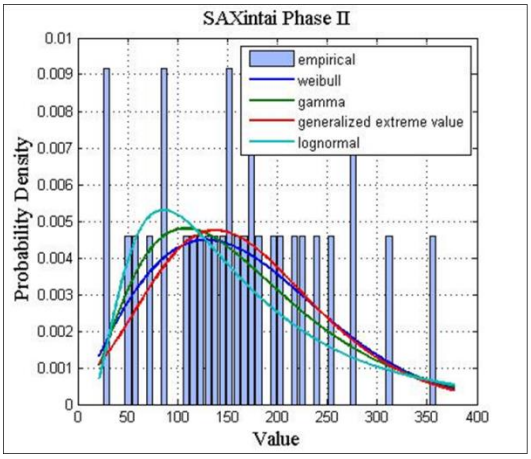

(a)

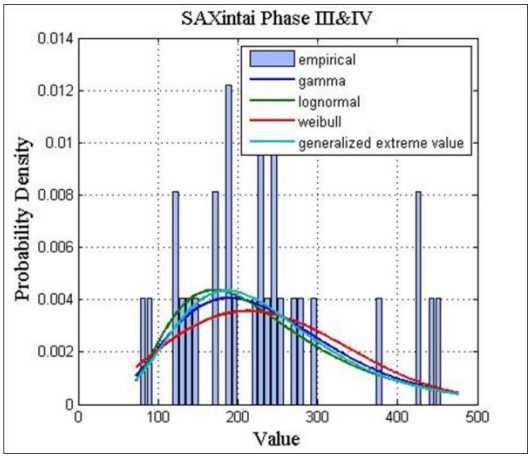

(b)

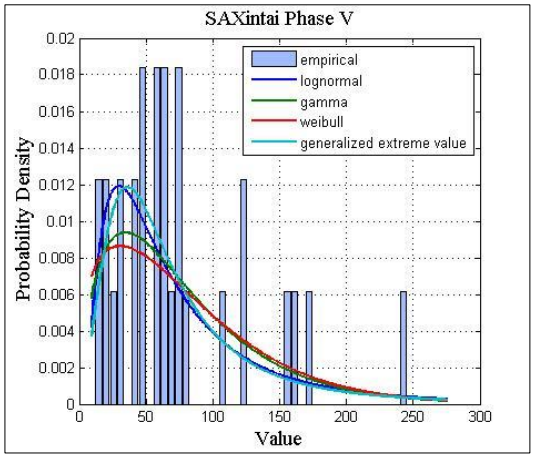

(c)

Figure 11-13 Comparison of PDF candidates (Lognormal, Gamma, Weibull and Generalized Extreme Value) for cumulative rainfall of Phase II (a), Phase III & IV (b) and Phase V (c) in SA-Xintai

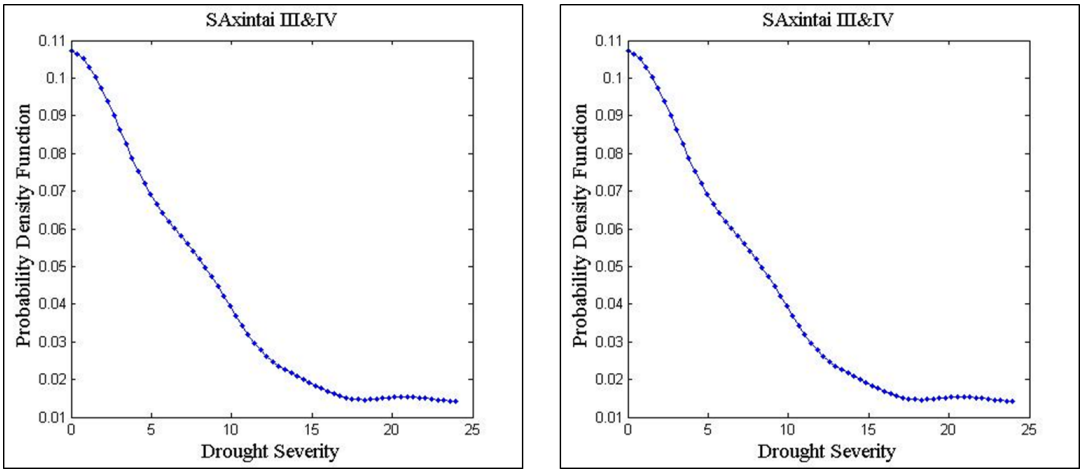

(a)

(b)

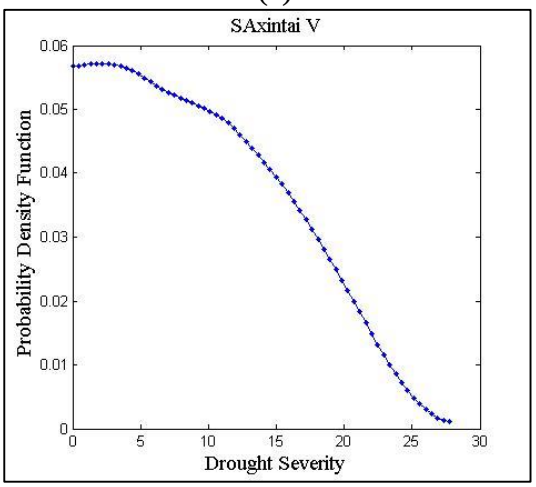

(c)

Figure 11-14 PDF of drought severity in Phase II (a), Phase III & IV (b) and Phase V (c) in SA-Xintai, estimated by DKDE

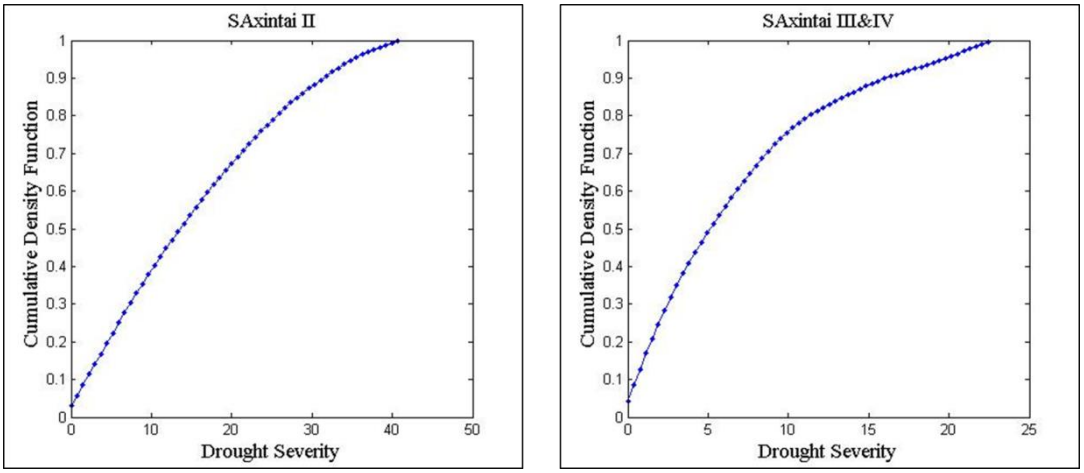

(a)

(b)

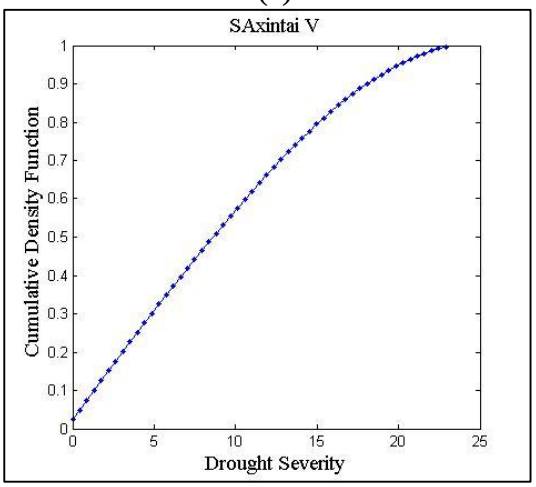

(c)

Figure 11-15 CDF of drought severity in Phase II (a), Phase III & IV (b) and Phase V (c) in SA-Xintai, estimated by DKDE

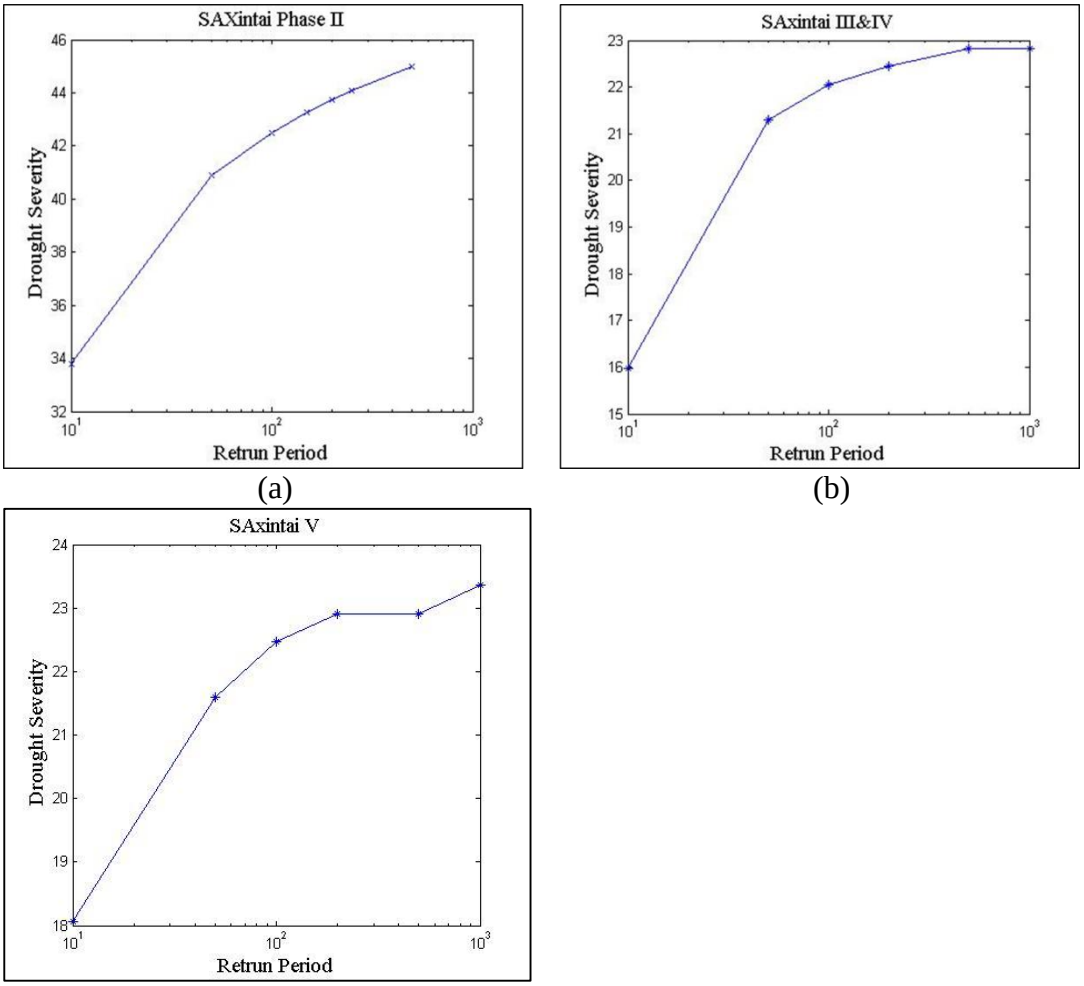

Figure 11-16 Drought severity return level (50 year, 100 year, 200 year, 500 year and 1000 year) of Phase II (a), Phase III & IV (b) and Phase V (c) in SA-Xintai

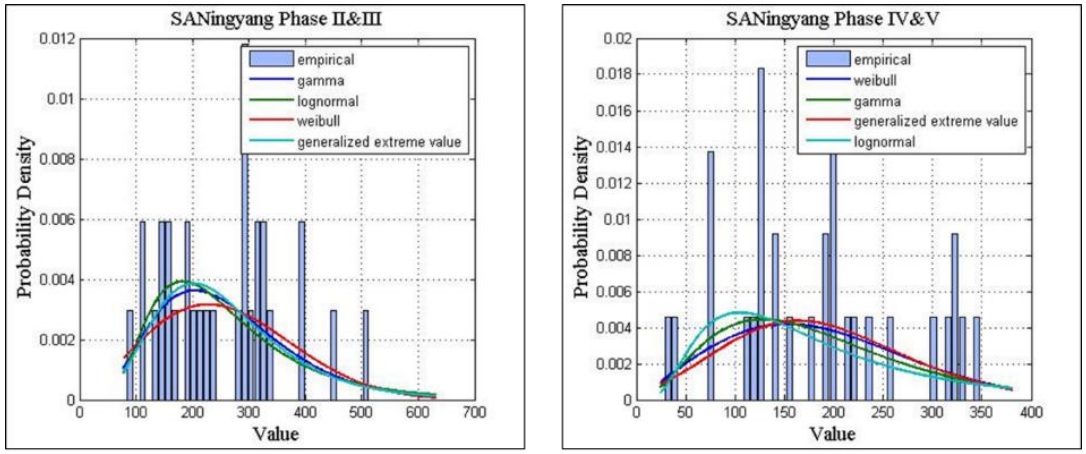

(a) (b)

Figure 11-17 Comparison of PDF candidates (Lognormal, Gamma, Weibull and Generalized Extreme Value) for cumulative rainfall of Phase II & III (a), Phase IV & V (b) in SA-Ningyang

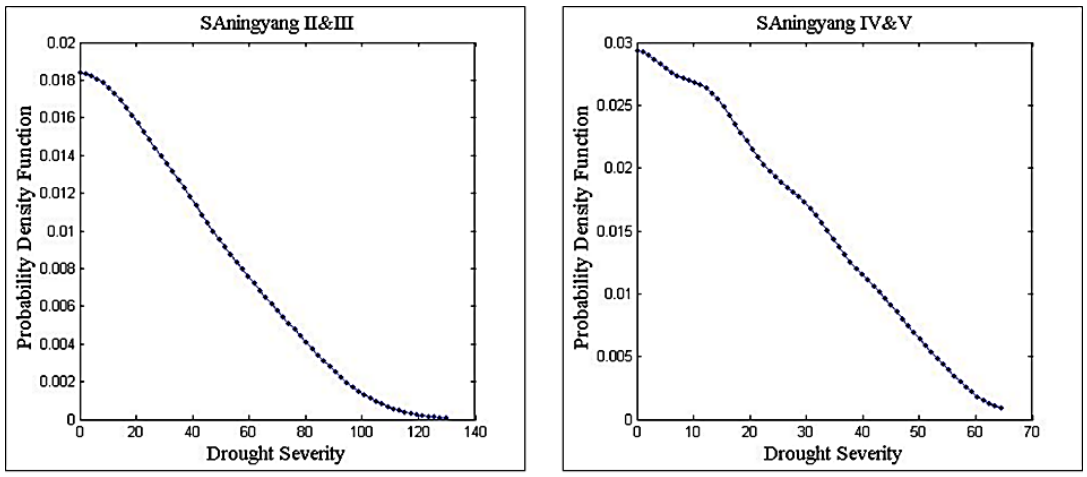

(a) (b)

Figure 11-18 PDF of drought severity in Phase II & III (a), Phase IV & V (b) in SA-Ningyang, estimated by DKDE

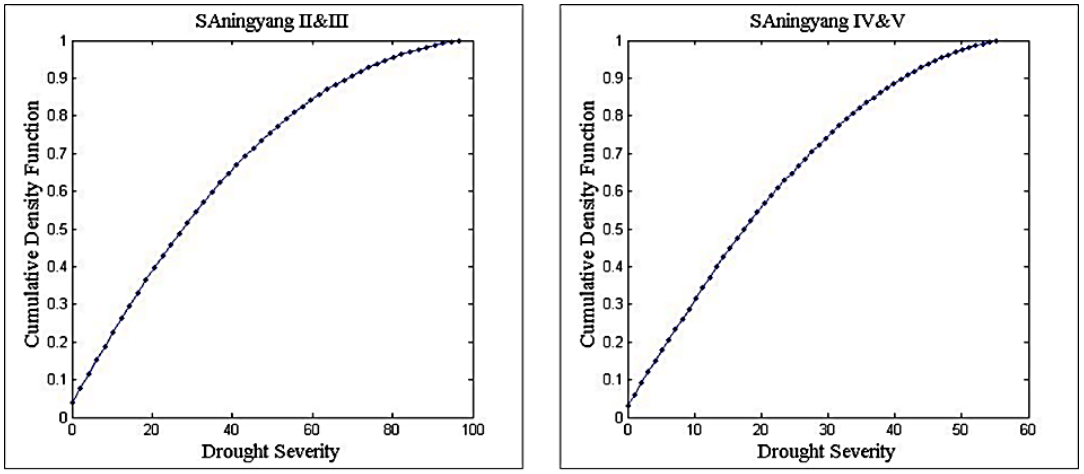

(a) (b)

Figure 11-19 CDF of drought severity in Phase II & III (a), Phase IV & V (b) in SA-Ningyang, estimated by DKDE

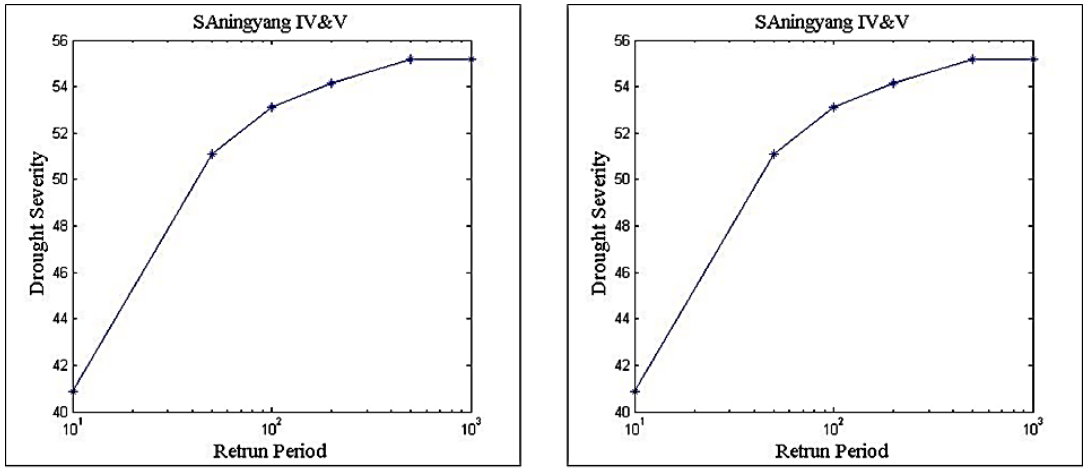

(a) (b)

Figure 11-20 Drought severity return level (50 year, 100 year, 200 year, 500 year and 1000 year) of Phase II & III (a), Phase IV & V (b) in SA-Ningyang

PUBLICATIONS

Conferences:

1. Chen Wen, Tiong Lee Kong and Roman Hohl (2013), "*Rainfall Index Insurance in Shandong, China*", International Conference on Southeast Asian Weather and Climate 2013, Nov 27-29, Chiang Mai, Thailand.
2. Chen Wen, Roman Hohl and Tiong Lee Kong (2014), "Feasibility Study of Rainfall Index Insurance in Shandong Province, China" International Conference on Regional Climate Adapted and Resilient towards Climate Adapted and Resilient Regions, Feb 24-25, Bremen, Germany, P19.
3. Chen Wen, Shao Zhe and Tiong Lee Kong (2014), "*Agriculture Drought Risk Management Through Index Insurance*" 4th Global Chinese Management Studies Conference, Oct 3-5, Singapore.

Journal papers:

1. Chen Wen, Roman Hohl and Tiong Lee Kong, *"Rainfall Index Insurance for Corn Farmers in Shandong based on High-resolution Weather and Yield Data"*. (Submitted to *Agricultural Finance Review*)
2. Chen Wen, Shao Zhe and Tiong Lee Kong, *"Exploration of Diffusion Kernel Density Estimation in Agricultural Drought Risk Analysis: A Case Study in Shandong, China"*. (Accepted as discussion paper by *Natural Hazards and Earth System Sciences*)